Научном већу Института за физику у Београду

Београд, 31. 01. 2019.

Предмет: Покретање поступка за избор у звање истраживач сарадник

Молим Научно веће Института за физику у Београду да покрене поступак за мој избор у звање истраживач сарадник.

Уз овај документ прилажем:

1. Мишљење руководиоца пројекта са предлогом комисије за избор у звање;
2. Стручну биографију;
3. Преглед научне активности;
4. Списак и копије објављених научних радова и других публикација;
5. Уверење о последњем овереном и уписаном семестру на докторским студијама
6. Фотокопију диплома са основних и мастер студија
7. Потврду о прихватању предлога теме докторске дисертације

С поштовањем,

Давид Кнежевић

Истраживач сарадник

____

Научном већу Института за физику у Београду

31. 01. 2019.

Предмет: Мишљење руководиоца пројекта о избору Давида Кнежевића у звање истраживач сарадник

Давид Кнежевић је запослен у Нискофонској лабораторији за нуклеарну физику на Институту за физику Београд и ангажован је на пројекту основних истраживања Министарства просвете, науке и технолошког развоја Републике Србије ОИ171002 под називом „Нуклеарне методе истраживања ретких догађаја и космичког зрачења". На поменутом пројекту ради на темама из физике неутрона и гама спектрометрије. С обзиром да испуњава све предвиђене услове у складу са Правилником о поступку, начину вредновања и квантитативном исказивању научноистраживачких резултата истраживача МПНТР, сагласан сам са покретањем поступка за избор Давида Кнежевића у звање истраживач сарадник.

За састав комисије за избор Давида Кнежевића у звање истраживач сарадник предлажем:

1. др Владимир Удовичић, виши научни сарадник, Институт за физику у Београду
2. др Александар Драгић, виши научни сарадник, Институт за физику у Београду
3. др Миодраг Крмар, редовни професор, Природно-математички факултет, Нови Сад

професор емеритус др Иштван Бикит

Руководилац пројекта ОИ171002

Потписано у Новом Саду 31.01.2019.

Биографија

Давид Кнежевић је рођен 03.06.1988. у Книну, република Хрватска. Основне академске студије физике је похађао на Природно-математичком факултету у Новом Саду (2007-2011) и завршио са просечном оценом 10. Мастер студије је завршио на истом факултету (2011-2012) са просеком 9,93 одбранивши мастер рад „Компаративна анализа симулиране и експерименталне ефикасности германијумског детектора“. 2012. уписује докторске акдаемске студије физике на истом факултету и тренутно се налази на трећој години студија (уписана четврти пут). У току је израда докторске дисертације под називом „Експериментално одређивање параметара нуклеарне структуре активационим техникама“ под менторством др Николе Јованчевића, доцента на природно-математичком факултету у Новом Саду. Од маја 2017. године Давид Кнежевић је запослен у Институту за физику у Београду као истраживач сарадник у Нискофонској лабораторији за нуклеарну физику Института за физику у Београду, у оквиру пројекта основних истраживања „Нуклеарне методе истраживања ретких догађаја и космичког зрачења“ (ОИ171002) Министарства просвете, науке и технолошког развоја Републике Србије, којим руководи проф. Емеритус др Иштван Бикит.

У току школске 2016/17, 2017/18 и 2018/19 године учествује у извођену наставе на Природно-математичком факултету Универзитета у Новом Саду, као сарадник у настави на предметима Савремена експериментална физика 3, увод у нуклеарну физику и виши курс нуклеарне физике. У току је завршетак рада на практикуму из области нуклеарне физике за студенте Природно-математичког факултета чији је коаутор. Практикум је добио позитивне рецензије и одобрен је.

До сада, Давид Кнежевић има три рада објављена у часопису категорије М21, два рада у часопису категорије М23, четири саопштења са међународних скупова штампана у целини (М33), један рад у часопису категорије М53 и два рада у зборнику радова са националног научног скупа објављена у целини (категорија М63).

Од учешћа на конференцијама, летњим школама и радионицама, издваја се:

1. Joint ICTP-IAEA School on “Nuclear Data Measurements for Science and Applications",19/10/2015 - 30/10/2015, Trieste, Italy.

2. 2015 Student Practice in JINR Fields of Research (3rd stage), 07/09/2015 - 25/09/2015, Dubna, Russia.

3. 9th International Physics Conference of the Balkan Physical Union – BPU9 , 24-27 August 2015 , Istanbul University , Istanbul , Turkey.

4. Scientific Workshop on Nuclear Fission dynamics and the Emission of Prompt Neutrons and Gamma Rays, 20-22 Jun 2017, Varna, Bulgaria.

Преглед научних активности

Током мастер студија, Давид Кнежевић се примарно бавио гама спектрометријом и германијумским детекторима, да би током докторских студија фокус био померен на примену знања стечених на мастер студијама на физику неутрона и физику језгра.

Под менторством доцента др Николе Јованчевића са Природно-математичког факултета у Новом Саду, рад Давида Кнежевића на докторским студија се фокусира примарно на двоструке гама каскаде настале након захвата термалних неутрона на језгрима. Предмет истраживања је одређивање параметара нуклеарне структуре као што су густина стања атомског језгра, функција јачине прелаза, шема енергетских нивоа и енергије гама зрачења. Одређивање параметара нуклеарне структуре је један од главних задатака у експерименталној нуклеарној физици на ниским енергијама. За ту сврху се користе различите методе од којих је једна од најважнијих детекција гама зрачења након деекситације побуђеног језгра насталог захватом неутрона на материјалу мете. На овај начин могу да се добију релевантне информације о испитиваном језгру. Проблем који се јавља приликом ових мерења је непостојање детектора чија би енергетска резолуција била мања од ширине енергетских нивоа атомског језгра. Такође, ови детектори би требали да имају и временску резолуцију која би била упоредива са временским интервалом гама прелаза. Због тога је развијена метода одређивања параметара нуклеарне структуре детекцијом двостепених гама каскада. Ова изузетно перспективна техника захтева даљи развој посебно у процесу обраде експерименталних података. Такође, захтевају се и нова мерења нуклида који до сада нису испитани овом методом.

Осим примарног тока истраживања, које је директно везано за докторат, Давид Кнежевић је радио и на новој техници одређивања неутронског спектра током нискофонских гама спектрометријских мерења. Ова нова техника се заснива на одређивању активности индуковане неутронским интеракцијама са германијумским детекторима. На основу одређене активности и познавања ефикасних пресека за детектоване неутронске нуклеарне реакције могуће је коришћењем метода деконволуције одредити неутронски спектар. Такође, учествовао је у раду на анализи могућности одређивања присуства неутрона у нискофонским Ge детекторским системима коришћењем детектованих интензитета гама пика од 595.8 keV, који може потицати и од интеракција брзих и спорих неутрона (путем ^{73}Ge(n,g)^{74}Ge и ^{74}Ge(n,n’)^{74}Ge реакција). Ово даје могућност да се флукс и спорих и брзих неутрона одреди само на основу детектованог интензитета овог једног пика.

Списак публикација Давида Кнежевића

Радови у врхунским међународним часописима (категорија М21):

1. **D. Knežević**, N. Jovančević, M. Krmar, J. Petrović, Modeling of neutron spectrum in the gamma spectroscopy measurements with Ge-detectors, Nuclear Instruments and Methods in Physics Research Section A, Volume 833, 23-26, 2016.

2. Anđelić B., **Knežević D.**, Jovančević N., Krmar M., Petrović J., Toth A., Medić Ž., Hansman J., Presence of neutrons in the low-level background environment estimated by the analysis of the 595.8 keV gamma peak, Nuclear Instruments and Methods in Physics Research Section A, Volume 852, 80-84, 2017.

3. I. Bikit, D. Mrdja, K. Bikit, S. Grujić, **D. Knežević**, S. Forkapić, U. Kozmidis-Luburić, Radon adsorption by zeolite, Radiation Measurements, Volume 72, January 2015, Pages 70-74, ISSN 1350-4487, http://dx.doi.org/10.1016/j.radmeas.2014.12.001

Радови у међународним часописима (категорија М23):

1. D. C. Vu, A. M. Sukhovoj, S. Zeinalov, N. Jovančević, **D. Knežević**, M. Krmar, A. Dragić, Representation of radiative strength functions within a practical model of cascade gamma decay, Physics of Atomic Nuclei, Vol. 80(2), 237-250, 2017.

2. K. Bikit, D. Mrđa, I. Bikit, J. Slivka, M. Veskovic, **D. Knežević**, Studies of the Low-energy Gamma Background, Physics Procedia, Volume 59, 2014, Pages 56-62, ISSN 1875-3892, http://dx.doi.org/10.1016/j.phpro.2014.10.009.

Саопштења са међународног скупа штампана у целини (категорија М33):

1. A. M. Sukhovoj, L. V. Mitsyna, Sh. Zeinalov, D. C. Vu, N. Jovančević, **D. Knežević**, M. Krmar, A. Dragić, Verification of the Partical Model of Cascade Gamma-Decay, XXIV Internation Seminar on Interaction of Neutrons with Nuclei, Proceeding of the International Conference, Dubna, ISBN 978-5-9530-0465-7, 122, 2016. **M33**

2. D.C. Vu, A.M. Sukhovoj, L. V. Misyna, Sh. Zeinalov, N. Jovančević, **D. Knežević**, M. Krmar, A. Dragić, Representation of the radiative strength function in the practical model of cascade gamma-deacay, XXIV Internation Seminar on Interaction of Neutrons with Nuclei, Proceeding of the International Conference, Dubna, ISBN 978-5-9530-0465-7, 134, 2016. **M33**

3. **D. Knežević**, N. Jovančević, M. Krmar, Estimation of neutron spectrum in the low-level gamma spectoscopy system using unfolding procedure, AIP Conference Proceedings, 1722, 030006, 2016. **M33**

4. **Knezevic, D.**, Jovancevic, N., Sukhovoj, A. M., Mitsyna, L. V., Krmar, M., Cong, V. D., ... & Dragic, A. (2018). Determination of the nuclear level densities and radiative strength function for 43 nuclei in the mass interval 28≤ A≤ 200. In EPJ Web of Conferences (Vol. 169, p. 00007). EDP Sciences. **M33**

Радови у научном часопису (категорија М53):

1. **Knezevic, D**., Jovancevic, N., Sukhovoj, A. M., & Mitsyna, L. V. (2018). Testing the modified dependence of the radiative strength function on different excitation energies in the light nucleus 28Al. Journal of Research in Physics, 39(1), 47-63.

Радови у зборнику радова са националног научног скупа објављени у целини (категорија М63):

1. Н. Јованчевић, **Д. Кнежевић**, М. Крмар, Ј. Николов, Н. Тодоровић, С. Илић, Утицај промена мионског флукса на ниво фонске активности у нискофонским гама спектрометријским мерењима, Зборник радова, XXIX Симпозијум ДЗЗСЦГ, Сребрно језеро, ИСБН 978-86-7306-144-3, 551, 2017.

2. Н. Јованчевић, **Д. Кнежевић**, М. Крмар, Ј. Николов, Н. Тодоровић, Ј. Петровић, Одређивање енергетског спектра неутрона присутног у гама спектрометријским мерењима са германијумским детекторима, Зборник радова, XXIX Симпозијум ДЗЗСЦГ, Сребрно језеро, ИСБН 978-86-7306-144-3, 558, 2017.

Estimation of neutron spectrum in the low-level gamma spectroscopy system using unfolding procedure

D. Knežević, N. Jovančević, and M. Krmar

Citation: AIP Conference Proceedings **1722**, 030006 (2016); doi: 10.1063/1.4944129
View online: http://dx.doi.org/10.1063/1.4944129
View Table of Contents: http://scitation.aip.org/content/aip/proceeding/aipcp/1722?ver=pdfcov
Published by the AIP Publishing

Estimation of Neutron Spectrum in the Low-level Gamma Spectroscopy System Using Unfolding Procedure

Knežević D.[1, a)], Jovančević N.[1] and Krmar M.[1]

[1]*University of Novi Sad, Faculty of Science, Department of Physics, Trg Dositeja Obradovića 3, 21000, Novi Sad, Serbia*

[a)] Corresponding author: david.knezevic@df.uns.ac.rs

Abstract. The radiation resulting from neutron interactions with Ge nuclei in active volume of HPGe detectors is one of the main concerns in low-level gamma spectroscopy measurements [1,2]. It is usually not possible to measure directly spectrum of neutrons which strike detector. This paper explore the possibility of estimation of neutron spectrum using measured activities of certain Ge(n,γ) and Ge(n,n') reactions (obtained from low-level gamma measurements), available ENDF cross section data and unfolding procedures. In this work HPGe detector with passive shield made from commercial low background lead was used for the measurement. The most important objective of this study was to reconstruct muon induced neutron spectrum created in the shield of the HPGe detector. MAXED [3] and GRAVEL [4] algorithms for neutron spectra unfolding were used. The results of those two algorithms were compared and we analyzed the sensitivity of the unfolding procedure to the various input parameters.

INTRODUCTION

This paper explores the possibility to use unfolding algorithms in order to calculate the neutron spectrum present in the HPGe detector system without measuring directly the neutron spectrum, but only using the neutron induced germanium gamma lines. Neutron induced processes are one of the main sources of background in gamma spectroscopy measurements. Neutrons are always present to some degree in gamma spectroscopy systems. Neutrons that create background in gamma spectroscopy systems originate from natural radioactivity of radionuclides from the detector system surroundings and from cosmic rays. Gamma activity is produced by neutron interaction with detector system materials. As one of the primary background sources, analysis of neutron induced gamma activity is of great importance in low-level gamma spectroscopy measurements. Main source of background inducing neutrons in low-level gamma spectroscopy measurements are cosmic muons.

We can calculate the activity of the reaction k using the equation:

$$A_k = \sum_i \sigma_{ik} \Phi_i \tag{1}$$

In the equation, σ_{ik} is the corresponding cross section and Φ_i is the neutron spectrum content in energy bin i. From eq. (1), the neutron fluence spectrum Φ_i can be determined by the unfolding procedure using cross sections and measured activities. For the unfolding procedure unfolding algorithms MAXED and GRAVEL were used. These techniques start with an initial default spectrum. A-priori information, necessary for the construction of the initial guess spectrum, can be obtained from the available experimental data concerning neutron production by muons in lead [5].

9th International Physics Conference of the Balkan Physical Union (BPU-9)
AIP Conf. Proc. 1722, 030006-1–030006-4; doi: 10.1063/1.4944129

MEASURED ACTIVITIES OF NEUTRON INDUCED GAMMA ACTIVITY

For the measurement of the activities of neutron induced gamma lines the HPGe detector from Canberra, serial number GX10021, was used. Detector is a coaxial n-type detector, with U-shaped cryostat configuration. Relative efficiency of the detector is 100%, and the active volume is 380 cm3. Detector is surrounded by passive lead shield, Canberra model 777B. Total mass of the shield is 1633 kg.

The experimental data was acquired by recording the background spectrum for 5886293 s (~68 days), in order to get the satisfying statistics of the detected gamma rays which are created due to interaction of neutrons with germanium nuclei inside the detector. In Table 1. the activities of the detected gamma peaks that were used in this paper are shown. Four inelastic scattering reactions of neutrons (dominant at high energies), and four radiative nautron capture reactions (dominant at low energies) were used.

TABLE 1. Activities of neutron induced reactions.

Reactions	Measured Activity [10^{-24}Bq/atom]
$^{72}Ge(n,\gamma)^{73m}Ge$	0.347(25)
$^{74}Ge(n,\gamma)^{75m}Ge$	0.322(25)
$^{70}Ge(n,\gamma)^{71m}Ge$	0.84(4)
$^{76}Ge(n,\gamma)^{77m}Ge$	2.5(4)
$^{76}Ge(n,n')\ ^{76}Ge$	5.7(5)
$^{74}Ge(n,n')\ ^{74}Ge$	6.83(20)
$^{72}Ge(n,n')\ ^{72}Ge$	1.44(5)
$^{70}Ge(n,n')\ ^{70}Ge$	2.49(24)

THE SPECTRUM UNFOLDING PROCEDURE

Maxed and Gravel

MAXED and GRAVEL are unfolding algorithms. Unfolding algorithms use measured gamma activity, response function (cross section) and a priori estimate of the spectrum in order to find the spectrum (in this case the neutron spectrum inside the active volume of HPGe detector).

GRAVEL is an iterative algorithm that uses an a priori estimate of spectrum to determine next iterative steps in order to get the solution spectrum, while MAXED uses the principle of maximum entropy, which chooses the final spectrum to be the one that requires the minimum of additional assumption (in a mathematical way) about the spectrum shape based on an a priori estimate of the spectrum.

Cross Sections Data

Cross section for the measured neutron induces reaction were taken from the ENDF database, from ENDF/B-VII.1 library. When extracting the data for usage in unfolding algorithms some approximations had to be made in order to optimize the number of data points, since large number of data points increases the complexity of the system of equation represented by eq. (1). For inelastic scattering cross sections there are no problems, since the cross section curves are fairly simple and can be desribed by a relatively small number of points (~100). Capture cross sections required different approach due to resonance region, where the cross section can change up to five orders of magnitude. To solve this, the average values of cross sections for data points inside the resonance region were calculated and used in unfolding algorithms.

A Priori Neutron Spectrum

A priori spectrum in unfolding methods is used as a starting point for unfolding algorithms in determination of the solution spectrum. Since most of the neutrons in our setup comes from muon interaction with lead shielding, for a priori spectrum we used the empirical equation [5] for the general spectrum shape of neutrons that originate from muon interaction with lead shielding. For neutrons with energies in 1-4 MeV, we used the equation:

$$\frac{dN(E)}{dE} \propto E^{5/11} e^{-E/\theta} \tag{2}$$

Where E is neutron energy, and θ is effective nuclear temperature and its value is 1.22 MeV. For neutron energies above 4 MeV, the equation takes the following form:

$$\frac{dN(E)}{dE} \propto e^{-E/E_d} \tag{3}$$

where E_d is the parameter that in the 4.5-10 MeV interval has the value of 8±1 MeV, and in the 10-50 MeV interval it has the value 8.6±0.5 MeV.

RESULTS

Figure 1. shows the obtained results. The left graph (a) shows the result obtained with GRAVEL and MAXED from the a priori spectrum. Above 1 MeV, both unfolding algorithms are in good agreement with the a priori estimate. Below 1 MeV, the results obtained by unfolding algorithms show disagreement with the a priori spectrum, and some data points differ by factor of 3. This disagreement is most probably due to the fact that the energy region below 1 MeV is not covered by the eq. (2). The lower part of the neutron energy curve was estimated simply by extending the eq. (2) below 1 MeV. Extended work on the energy region below 1 MeV should be done in order to improve the results, and can be used for the investigation of this energy region. The right graph (b) shows the sensitivity of unfolding algorithms (the results shown are for the GRAVEL unfolding algorithm only, since MAXED shown approximately the same behaviour) to the different binnings of the cross sections. The obtained results show that the bining can influence the results greatly, and this fact is clearly seen for the 0.4 MeV step where results are in clear disagreement with the a priori spectrum. Other two binnings show aproximately the same results. The stability of the solution for different binings should be tested in more detail.

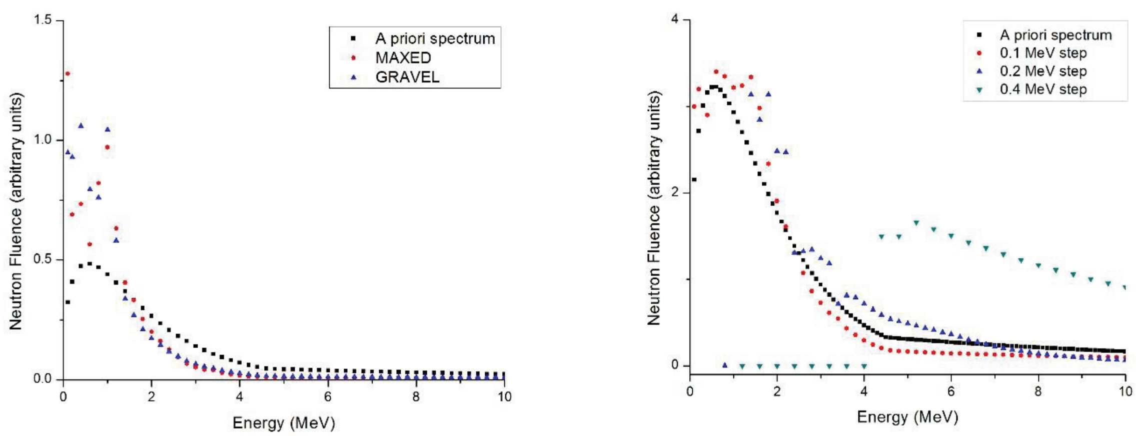

(a) (b)

FIGURE 1. The obtained results with MAXED and GRAVEL algorithms (a), and sensitivity of the solution spectrum to different binning of the cross sections for GRAVEL algorithm (the MAXED algorithm shown approximately the same behavior) (b). Since only the general shape of the spectrum is considered in this paper, the values of the data points were scaled differently in (a) and (b) in order to show the results more clearly.

CONCLUSION

In this paper, we explored the possibility of estimating the neutron spectrum inside the HPGe detector with unfolding algorithms using only neutron induced germanium gamma-lines. Obtained results show that this approach could be usefull for estimation of the neutron spectrum, and that further work should be done in this field, since it would be highly usefull to have the posibility to estimate the neutron spectrum for experiments in which the direct measurement of neutron spectrum is not possible.

For future work, there is a number of things to consider in order to improve the results. Better statistics of the measurement would reduce the errors of the measured activities, thus giving us greater confidence in obtained activities. Second thing to consider is the lower energy party (around and bellow the resonance region) of the a priori spectrum. Aditional information should be collected about the general shape of this part of neutron spectrum. Also, choise of data points from cross section inside the resonance region has to be optimized to represent the real shape as close as possible using as little data points as possible. Since above 10 MeV (n, 2n) and (n, 3n) reactions also contribute to the production of capture peaks, this should be included in the future work to see if the contribution of these reactions would alter the results. Efficiences used for the calculation of activities were calculated using Monte Carlo simulation. Precise dimensions of the detector are not well known, so additional uncertainties are introduced to the experiment. Future work will also include the usage of neutron induced lines in Ge from neutrons coming from Cf source. Since the spectrum of Cf is well known, the sensitivity of the unfolding methods to other unfolding parameters will be tested.

ACKNOWLEDGMENTS

The authors would like to thank the Serbian Ministry of Education, Science and Technological Development for the funding.

REFERENCES

1. N. Jovancevic, M. Krmar, D. Mrda, J. Slivka, I. Bikit, Nucl. Instr. and Meth. A, Volume 612, Issue 2, p. 303–308.
2. M. Krmar, J. Hansman, N. Jovančević, N.Lalović, J. Slivka, D. Joković, D. Maletić, Nucl. Instr. and Meth. A, Volume 709, p. 8-11.
3. M. Reginatto, P. Goldhagen, S. Neumann, Nucl. Instr. and Meth. A, Volume 476, p.242-246.
4. YongHao Chen, XiMeng Chen, JiaRong Lei, Li An, XiaoDong Zhang, JianXiong Shao, Pu Zheng, XinHua Wang, Science China Physics, Mechanics & Astronomy, Volume 57, Issue 10, p. 1885-1890.
5. W.U. Schröder, U. Jahnke, K.H. Lindenberger, G. Röschert, R. Engfer, H.K. Walter, “Spectra of Neutron from μ Capture Thallium, Lead and Bismuth”, Z.Phys. 268 (Springer-Verlag, 1974), p.p. 57-64

Nuclear Instruments and Methods in Physics Research A 852 (2017) 80–84

Contents lists available at ScienceDirect

Nuclear Instruments and Methods in Physics Research A

journal homepage: www.elsevier.com/locate/nima

Presence of neutrons in the low-level background environment estimated by the analysis of the 595.8 keV gamma peak

Brankica Anđelić, David Knežević, Nikola Jovančević, Miodrag Krmar, Jovana Petrović, Arpad Toth, Žarko Medić, Jan Hansman

Department of Physics, Faculty of Science, University of Novi Sad, Trg Dositeja Obradovica 3, 2100 Novi Sad, Serbia

A R T I C L E I N F O

Keywords:
Low-background gamma spectroscopy
Neutron capture
Inelastic scattering of neutrons
HPGe detector
Evaporated neutron spectra

A B S T R A C T

In order to explore possible improvements of the existing techniques developed to estimate the neutron fluence in low-background Ge-spectroscopy systems, gamma spectra were collected by a HPGe detector in the presence of the ^{252}Cf spontaneous fission neutron source. The spectra were taken with and without a Cd envelope on the detector dipstick, with different thicknesses of plastic used to slow down neutrons. We have analyzed the complex 595.8 keV gamma peak, as well as several more gamma peaks following the neutron interactions in the detector itself and surroundings materials. The investigation shows that some changes of the initial neutron spectra can be monitored by the analysis of the 595.8 keV gamma peak. We have found good agreement in the intensity changes between the long-tail component of the 595.8 keV and the 691 keV gamma peak (^{72}Ge(n,n′)^{72}Ge reaction), usually used for the estimation of the fast neutron fluence. Results also suggest that the thermal neutrons can have a stronger influence on creation of the Gaussian-like part of 595.8 keV peak, than on the 139 keV one following ^{74}Ge(n,γ)^{75m}Ge reaction and used in the standard methods (Škoro et al., 1992) [8] for determination of the thermal neutron flux.

1. Introduction

Reduction of different background effects induced by neutrons is very important in different types of low background gamma measurements, such as dark mater search experiments, rare nuclear events research or measurements of the low level environmental activity [1–7]. Consequently, efforts are made in order to improve methods that are used for estimation of the level of neutron presence in the Ge-spectroscopy systems during low-level background gamma measurements. [8–10]. Except for the low-background measurements, it is also important to know the background neutron contribution in different types of prompt neutron activation experiments [11].

Neutrons in the low-background gamma spectroscopy systems usually come from muon interactions, spontaneous fission of heavy elements and (α,n) reactions of α-emitters of the U- and Th-series with light elements in the surrounding rocks [12]. In the ground level laboratory, neutrons are mainly produced by muon capture in a lead shield of the gamma-ray spectroscopy systems [13]. There are a number of studies about the neutron induced activity during gamma spectroscopy measurements [8,13–17]. All of those analyses show that gamma peaks following neutron capture and scattering reactions with the detector itself (and surrounding materials) can give measurable contribution to the background spectra.

Peaks created in the neutron interactions with the detector and surroundings materials can be used for the determination of the neutron presence during gamma spectroscopy measurements. Methods for determination of the slow neutron flux, using intensity of the 139.9 keV gamma peak (following the ^{74}Ge(n,γ)^{75m}Ge reaction) and the intensity of the 691.0 keV gamma peak for fast neutrons (the ^{72}Ge(n,n′)^{72}Ge reaction), were proposed in Ref. [8]. However, results of the study [10] suggested that, alongside thermal neutron capture, excitation of the 139.9 keV level in ^{75m}Ge can also take place via some other mechanisms (for example, fast neutron interactions).

To investigate the possibility of using certain gamma peaks to estimate the presence of the neutrons, we performed measurements with the ^{252}Cf neutron source placed near the HPGe detector. The ^{252}Cf neutron energy spectrum is a standard evaporation spectrum. Its shape is very similar to the energy spectrum of background neutrons in deep underground laboratories, although in a sea level laboratory fast component of background neutron spectrum is not negligible [18–20]. In this work, investigation of the neutron induced gamma peaks in different neutron fluence was done by moderation of the original ^{252}Cf spontaneous fission neutron spectra with PVC plastic sheets. It was the easiest way to obtain different measurement conditions concerning the number of neutrons reaching the active volume of the HPGe detector. Different intensities of the neutron induced gamma peaks obtained in different measurements geometries (thickness of plastic sheets) were thereby analyzed.

Here, we have studied the possibility of using the 595.8 keV gamma peak for estimation of the neutron presence in the HPGe detector

http://dx.doi.org/10.1016/j.nima.2016.12.025
Received 4 July 2016; Received in revised form 17 November 2016; Accepted 14 December 2016
Available online 15 December 2016
0168-9002/

system. The gamma quanta, having the above-mentioned energy, can be emitted through the prompt de-excitation of the ^{74}Ge nuclei following two different processes: the neutron captures on the ^{73}Ge and the inelastic neutron scattering on the ^{74}Ge. The study [10] suggests that in the detected spectra a standard narrow Gaussian shape 595.8 keV gamma peak appears only when there is significant presence of the thermal neutrons. Fast neutrons will interact through inelastic scattering, producing a broad, long tail peak. The presence of this long tail peak is the underlying reason why the 595.8 keV gamma peak in collected gamma spectra has a characteristic structure, being a result of overlapping of a standard Gaussian shape peak, from the capture reaction, and a long tail peak following the neutron inelastic scattering on the Ge nuclei inside the detector. Therefore, in one relatively complex peak one can find the integral contribution of the thermal and also fast neutrons. For the analysis of the complex 595.8 keV gamma peak, the fitting procedure [3,21,22] was employed to differentiate between the contributions of the capture, on one hand, and the inelastic scattering on the other hand, to the overall peak intensity. A number of different gamma peaks were created in the interactions of Ge and surrounding materials with thermal neutrons, as well as in the interactions with fast neutrons. The intensities of those peaks depend on the measurement geometry (i.e. thickness of the plastic covering the neutron source). Obtained intensities of resolved components of the 595.8 keV gamma peak were compared with intensities of other gamma peaks to check whether they follow the same trends.

2. Experimental setup

The experimental setup was located in the low-background laboratory of the Department of Physics in Novi Sad (80 m amsl). The coaxial closed end HPGe detector with horizontal dipstick and a relative efficiency of 22.3 %, was used in the measurements. The HPGe is placed inside a cube chamber made of pre-World War II iron with a useful cube-shaped inner volume of 1 m^3. Iron walls are 25 cm thick and the total mass of the shield is approximately 20 tons [10,17].

Detector was exposed to the ^{252}Cf spontaneous fission neutrons. The source strength was 4.5×10^3 neutrons per second into 4π sr. The ^{252}Cf source was located in simple paraffin collimator. This was done to prevent some neutrons, which are not initially emitted in the direction of the detector, to reach active volume of the detector after scattering inside low-background iron chamber. The ^{252}Cf source was placed in a Marinelli container (inner diameter 10.6 cm, outer diameter 16.0 cm, height 20.5 cm, bottom thickness 3.0 cm) with wall thickness of 2 mm. The Marinelli container was filled with melted paraffin and located below the HPGe detector (Fig. 1). Some degree of neutron collimation was obtained in this geometry by 17.5 cm long paraffin tube in very

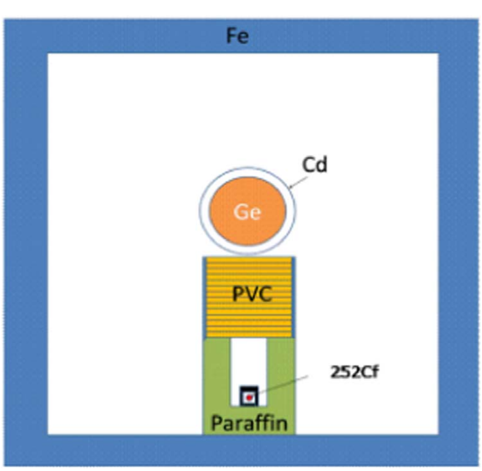

Fig. 1. Scheme of the experimental setup (not in scale).

narrow space of the low-background iron chamber. According to very simplified calculation based on measured values of the TVL for different light materials as paraffin or polyethylene [23], it was estimated that in the 3 cm thick walls of the Marinelli container about 50% of neutrons will be absorbed. To attenuate the gamma radiation of the accumulated fission products, the neutron source was placed in a 2 cm thick iron box. The measurements were carried out with different thicknesses of the PVC plates placed between the detector and the neutron source. The purpose of the PVC plates was to absorb and slow down neutrons. Thus, we obtained the simplest setup in which the detector was exposed to different neutron fluences. Six different thicknesses of the PVC plates (7 mm, 14 mm, 26 mm, 45 mm, 68 mm and 93 mm) were used. The measurements were performed for every thickness of the PVC plastic with and without the Cd envelope over the detector dipstick. Cadmium envelope served as an efficient absorber of the thermal neutrons. In this experimental configuration influence of the thermal neutrons was detected. The collection time for all spectra was approximately the same ~150,000 s.

3. Measurements and results

3.1. Rough insight in neutron fluence

Experimental setup presented in Fig. 1 was the simplest one which exposes the HPGe detector to different numbers of neutrons. It can be expected that the number (and energy spectra) of neutrons reaching detector is a result of a trade-off between thermalization and attenuation of neutrons. Intensities of several gamma lines emitted after neutron interactions in the surrounding materials can be used as a kind of an index showing how adding PVC attenuators can affect the number of neutrons striking active volume of the detector.

In the spectra recorded with the cadmium cap located around the detector dipstick, 651.1 keV and 558.4 keV peaks, following neutron capture on ^{113}Cd are detected. Detected intensity of both gamma lines following ^{113}Cd(n,γ)^{114}Cd reaction can be useful for a rough estimation of the slow neutron number at the very place of the active volume of the detector. Obtained values of the 558 keV and 651.3 keV gamma peaks intensities are presented in Fig. 2.

It can be seen that the count rates of the cadmium peaks do not change significantly with the thicknesses of the PVC plates. Measured intensities vary just up to 20% in the full range of the plastic thicknesses. The cross section for ^{113}Cd(n,γ)^{114}Cd reaction in the thermal region is a couple order of magnitude higher than the cross section in the resonant region. Thus, it can be expected that the results presented in Fig. 2 indicate, that the number of thermal neutrons does not changes significantly and the Ge crystal in the detector dipstick is exposed to thermal neutron fluence which is not dependent on thickness of the plastic attenuators. One possible explanation for a nearly constant number of thermal neutrons striking the detector, which should be verified, is that they result from a trade-off between two effects: the thermalization of fast neutrons and the neutron absorption. This can be found in detail for different moderator materials in the study Ref. [24].

In all recorded spectra, prominent 846.8 keV gamma peak was observed. The origin of this peak is the ^{56}Fe(n,n′) gamma reaction. This reaction took place in the walls of the iron shield. Considering that for an inelastic neutron scattering neutron energy should be higher than some threshold energy, the intensity of this peak could be a good indicator for monitoring the presence of fast neutrons. The detected intensity of the 846.8 keV ^{56}Fe(n,n′) peak measured for different thicknesses of the plastic plates is presented in Fig. 3. Count rates of this gamma peak decrease with the increase of the thickness of the PVC because of the slowing down of the neutrons in the PVC. It is evident that plastic PVC attenuators can reduce the number of fast neutrons. The change in the intensity of the 846.8 keV ^{56}Fe(n,n′) peak has the same trend in presence of the Cd layer since the interactions of slow

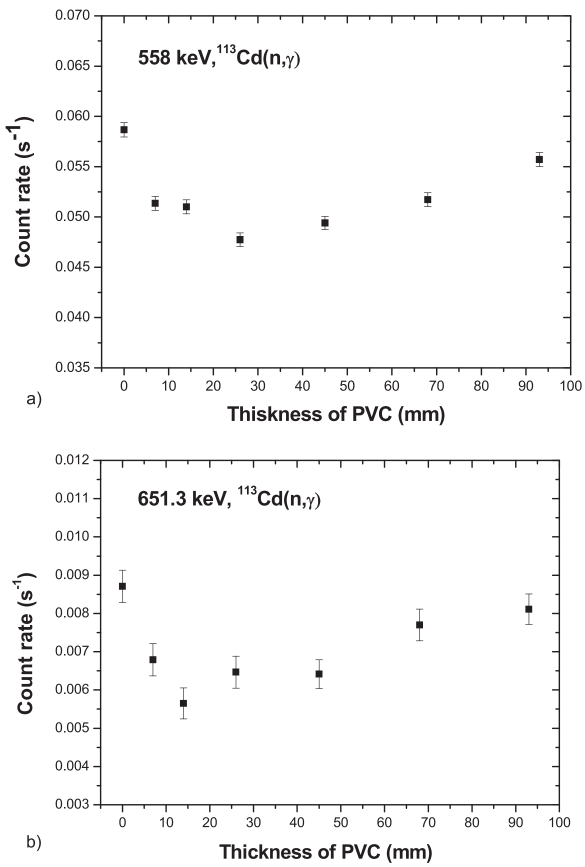

Fig. 2. Detected intensity of a) 558 keV and b) 651.3 keV for the ^{113}Cd(n.γ)^{114}Cd reaction.

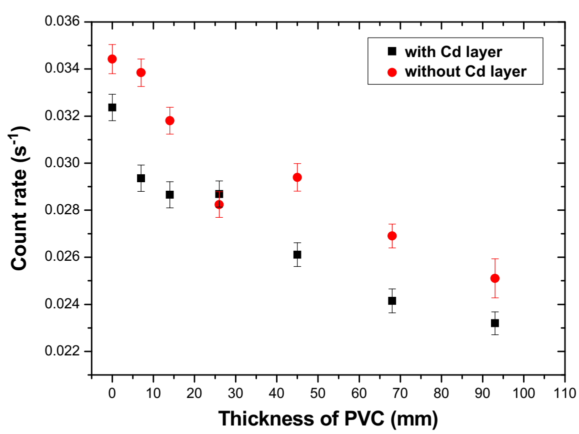

Fig. 3. Detected intensity of the 846.8 keV ^{56}Fe(n,n′) gamma peak for different thickness of PVC plastic with and without Cd layer around HPGe detector.

neutrons do not have an influence on the detection of this gamma peak.

We have to mention here that in our analysis we considered just the statistical uncertainty of detected gamma peaks. However, the jump in the count rate at 45 mm of PVC Fig. 6 can come from some systematic error. We do not have the possibility to repeat those measurements at the current time, but these results can be basis for future investigation.

3.2. Analysis of 595.8 keV gamma peak

The analysis of the 595.8 keV gamma peak was of particular interest in this work. As already noted, gamma quanta having this energy can be emitted thought a prompt de-excitation of the ^{74}Ge nuclei following two different processes: a) the slow neutron captures on the ^{73}Ge, b) the inelastic neutron scattering on the ^{74}Ge. Thus, this gamma peak, in collected gamma spectra, has a characteristic structure; due to the summation of a standard Gaussian shape peak from the capture reaction and a long tail peak following the neutron inelastic scattering on the Ge nuclei inside the detector. It is necessary to deconvolute this structure by a fitting procedure and to separate the contribution to the overall counts detected in interactions of slow and fast neutrons. Resolved intensities of the narrow Gaussian-shape and the long tail peaks obtained by the deconvolution of the 595.8 keV gamma peak can provide an insight into the presence of fast and slow neutrons in the area of the active volume of the Ge detector.

The most important problem which should be addressed in the deconvolution procedure is the overlapping of the Ge(n,γ) and Ge(n,n′) and interference of the background peaks. This particular issue arises from choosing the function for fitting the asymmetric peaks induced by fast neutrons. This problem was already discussed by other authors [3,22] and in our analysis the neutron induced peaks were fitted by the following function:

$$C(E) = a_0 ERFC\left[-\frac{(E-E_0)}{\sigma_0}\right]\cdot Exp\left[-\frac{(E-E_0)}{\Delta}\right] + \sum_{i=1}^{n} a_i \cdot Exp\left[-\frac{1}{2\sigma_i^2}(E-E_i)^2\right] + F \qquad (1)$$

where the first term corresponds to the Ge(n,n′) peak; in the second term, the expression inside the summation is a Gaussian function which corresponds to any symmetric gamma peak in the fitting region; the parameter F refers to the background (here to be a linear function). The Gaussian symmetric gamma peaks can be the Ge(n,γ) gamma peaks or any other gamma peak corresponding to the detection of some background gamma line. The parameters of the fit are: a_O, a_i, E_O, E_i, σ_O, σ_i and Δ. E_O and E_i and they correspond to the energy of the detected gamma peaks; a_O and a_i are the maximum amplitudes of those peaks. Parameters σ_O and σ_i should correspond to the energy resolution of the detector and they were determined by the peak full-width at half-maximum (FWHM). The characteristic of the exponential tail of Ge(n,n′) peaks is determined by the Δ parameter.

First step in the fitting procedure is to fix the level of the background continuum. It was shown in Ref. [3] that the quality of the results obtained by the fit of the Ge(n,n′) peaks depends on the energy region chosen for the fit. The next step was the variation of the fitting region for certain energy of the asymmetric peak. The energy region was varied between 30 keV and 40 keV. Different values of the level of the background continuum and energy region were used to get the fit which give the value of χ^2/NDF as close to 1 as possible. Furthermore, the uncertainties of fitting parameters were analyzed to get the optimal set of values. The gamma peaks were fitted by ROOT data analysis toolkit [25]. Fitting procedure was applied on the 691 keV ^{72}Ge(n,n′) gamma peak, which has the simplest structure, with one well developed peak (723.3 keV ^{154}Eu, product of ^{252}Cf fission, contained in sealed source). The result of the fit is depicted on Fig. 4.

The same technique was used for deconvolution of the 595.8 keV gamma peak. It can be seen in Fig. 5 that, in the observed energy region, except for the standard narrow ^{73}Ge(n,γ) and broad ^{74}Ge(n,n′) gamma lines, three additional background gamma peaks appeared (609.3 keV ^{214}Bi(U), 603 keV from fission product ^{154}Eu and 641 keV from fission product ^{145}Ba). The contribution of the background continuum, as well as the background gamma peaks, were subtracted and the intensities of ^{73}Ge(n,γ) and ^{74}Ge(n,n′) gamma peaks were obtained.

3.3. Ge(n,n′) component of the 595.8 keV gamma peak

The intensities of the ^{74}Ge(n,n′) component of the 595.8 keV gamma peaks, obtained after deconvolution are presented in Fig. 6. It can be seen that the intensity of the long tail 595.8 keV gamma peak,

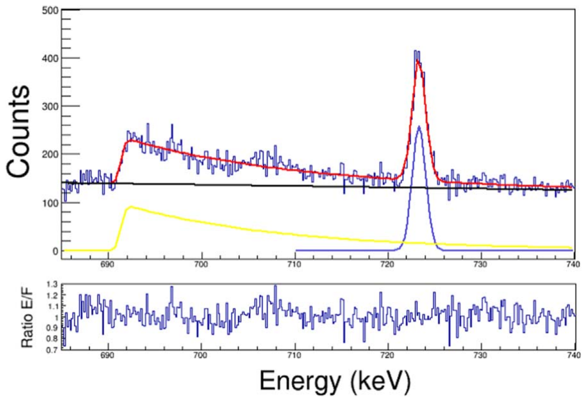

Fig. 4. The part of gamma spectrum in region around the 691 keV Ge(n,n′) gamma peak with the 7 mm of PVC between the Ge-detector and the ^{252}Cf source and the Cd envelope around detector. The lines show the fitting results for the ^{72}Ge(n,n′) and background peak (upper graph). Down graph – ratio of experimental spectra to fitting function.

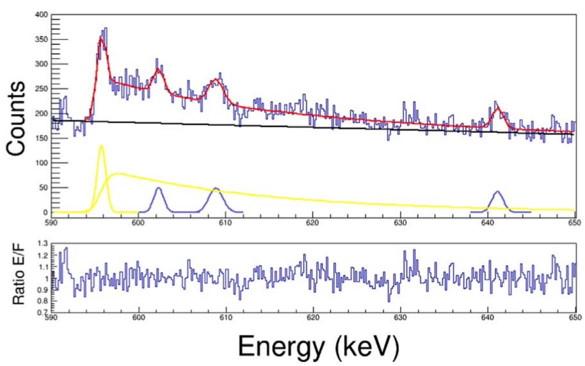

Fig. 5. The part of gamma spectrum in region around the 595.8 keV Ge(n,n′) gamma peak with 7 mm of PVC between the Ge-detector and the ^{252}Cf source. The lines show the fitting results for the ^{74}Ge(n,n′), ^{73}Ge(n,γ) and background peaks (upper graph). Down graph – ratio of experimental spectra to the fitting function.

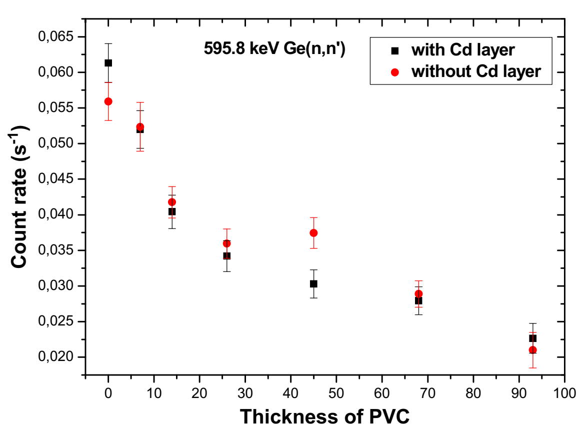

Fig. 6. Detected intensity of the 595.8 keV ^{74}Ge(n,n′) gamma peak for different thickness of PVC plastic with and without Cd layer around the HPGe detector.

measured for different thicknesses of the plastic plates located between the neutron source and the HPGe detector, has an apparent decreasing trend. As mentioned above, the same trend was observed in analysis of 846.8 keV ^{56}Fe(n,n′) gamma peak (Fig. 3). Considering that only fast neutrons can initiate the (n,n’) reaction, presence of the Cd envelope has no influence on the obtained intensities of the separated long tail peak.

To check the obtained results, comparison with the detected intensity of the 691 keV ^{72}Ge(n,n′) gamma peaks was performed. The intensity of the 691 keV gamma peak decreases with the increase of plastic thickness, as expected. There are no significant differences between the measurements done with and without the Cd envelope. Considering that the 691 keV gamma line was frequently used in estimation of the fast neutron fluence [8], let us consider whether it is possible to do the same using the long-tail component of the 595.8 keV gamma peak. Fig. 7 presents a scatter graph showing correlation between the intensities of the two mentioned peaks recorded in this experiment.

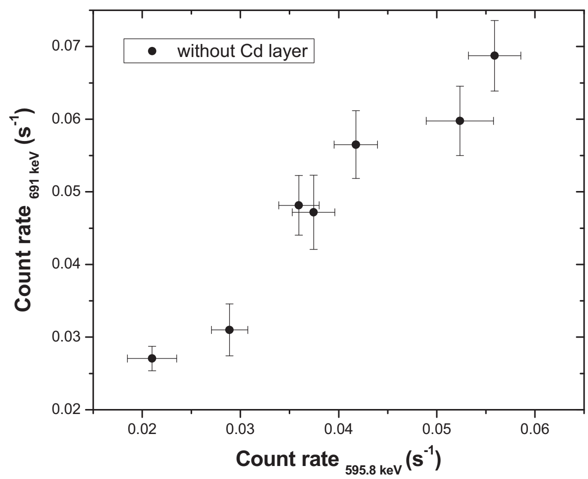

Fig. 7. Correlation between measured intensities of 691 keV and 595.8 keV peaks (without Cd layer around the HPGe detector).

The results in Fig. 7 shows strong linear correlation between the 595.8 keV ^{73}Ge(n,γ) and 691 keV ^{72}Ge(n,n′) gamma peaks with linear slope coefficient 1.24(4). This means that the 595.8 keV can be also used as a standard for the determination of the fast neutron fluence.

3.3.1. *Ge(n,γ) component of 595.8 keV gamma peak*

The intensity of the 595.8 keV ^{73}Ge(n,γ) gamma peak, obtained by deconvolution, has an almost constant value, not dependent on the plastic thickness (Fig. 8). The constant trend of the measured intensities, depicted in Fig. 8 can be expected considering the results obtained by the measurements of the cadmium gamma peaks (Fig. 2). It is evident that the simple experimental setup used in this experiment can provide different values of thermal neutron fluence at the very place of the detector dipstick.

Very similar results were obtained when the 139.9 keV line was used to estimate the thermal neutron fluence. Results are presented on Fig. 9.

Although experimental setup in this experiment did not allow us to provide different values of thermal neutron fluence at the place of the active volume of the HPGe detector to be able to compare neutron

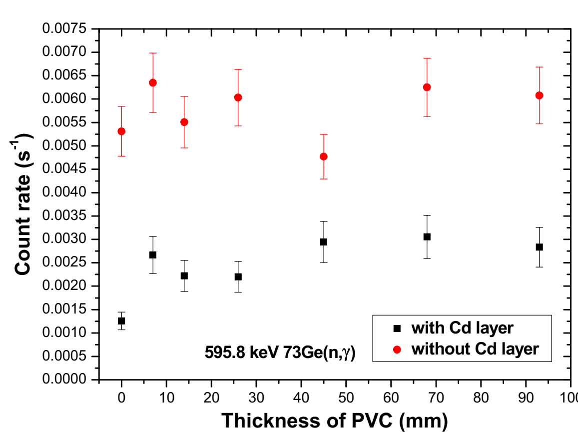

Fig. 8. Detected intensity of the 595.8 keV ^{73}Ge(n,γ) gamma peak for different thickness of PVC plastic with and without Cd layer around the HPGe detector.

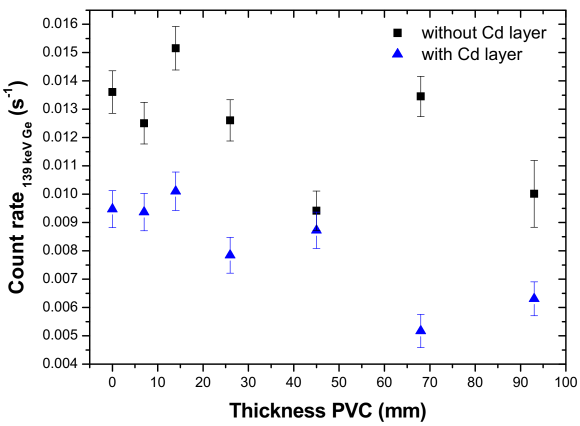

Fig. 9. Detected intensity of the 139.9 keV ^{74}Ge(n,γ) gamma peak for different thickness of PVC plastic with and without Cd layer around the HPGe detector.

fluence estimation by the 139.9 keV and the (n,γ) component of the 595.8 keV gamma peak, there is still one possible indicator. We have also calculated the ratio of contribution of thermal neutrons to detected intensity of Ge(n,γ) peaks using the following equation:

$$R(\%) = 100\% \cdot \left(1 - \frac{N_{withCd}}{N_{withoutCd}}\right) \tag{2}$$

where N_{withCd} and $N_{withoutCd}$ are the intensities of gamma peaks measured with and without Cd envelope respectively. The obtained mean radio R (for different thicknesses of PVC) for the 139.9 keV and 595.8 keV peak were 33(16)% and 57(12)%, respectively. This result can be a kind of an indication that the thermal neutrons have a stronger influence on creation of the 595.8 keV peak, than on the 139 keV one. Unfortunately, uncertainties are relatively large and for more exact confirmation that the 595.8 keV gamma line has some advantage over the 139.9 keV one, more investigations should be done.

4. Conclusions

In this work we have measured the gamma spectra using the low-background Ge-spectroscopy system in an iron shield, in the presence of the ^{252}Cf neutron source. A spontaneous fission neutron spectrum was moderated by PVC plastic plates placed between the HPGe detector and the neutron source. In our experimental setup it was possible to analyze several characteristic gamma peaks originating from the interactions of the neutrons with the isotopes of Ge and couple more surrounding materials. Special care was paid to the 595.8 keV peak because it contains records of simultaneous interaction of the thermal and fast neutrons with the Ge detector.

Preliminary results presented in this paper are quite encouraging: the 595.8 keV peak can be used in the estimation of the neutron fluence at the place of the active volume of the Ge detector. In the high energy region, above the threshold of the Ge(n,n′) nuclear reactions, very good coincidence between the long-tail component of the 595.8 keV and the 691 keV gamma peaks, usually used for the estimation of fast neutron fluence, was observed. Simple experimental setup unfortunately could not provide us with the variety of thermal neutron fluencies at the place of detector, however it was observed that even in these circumstances intensity of the sharp gamma peak at the beginning of the long-tail 595.8 keV peak, obtained in neutron capture process, shows a similar trend to the intensity of the 139.9 keV peak. Measured intensities of both mentioned peaks follow the same trends as the gamma peaks obtained in the ^{113}Cd(n,γ)^{114}Cd reaction. It can be expected that the (n,γ) part of the 595.8 keV peak has a potential to be used for estimation of the thermal neutron fluence.

Let us review some noticeable disadvantages and advantages of the method for estimation of neutron fluence based on the measurement of the 595.8 keV peak in gamma spectra. The structure of the 595.8 keV gamma peak is not simple and a sophisticated fit procedure has to be employed. However, the shapes of the sharp Gauss-like gamma lines and the long-tail peak are well known. Moreover, it was noticed that the intensity of the (n,γ) part of the 595.8 keV peak is about two times lower that intensity of the 139.9 keV gamma line, which could introduce some uncertainty, especially if the cases of low thermal neutron fluencies. Significant advantage of the suggested method based on the 595.8 keV gamma peak is the fact that both fast and slow neutron fluence can be determined using just one energy peak. For some rough estimation of thermal to fast neutron fluence ratio, not even the relative energy efficiency of detector needs to be calculated.

Considering that in our experiment no measurements in different fields of thermal neutrons were possible, it is valuable to repeat similar measurements in some other experimental setups. This is especially important in order to confirm the assumption that the intensity of the Gauss-like part of 595.8 keV gamma peak is less dependent on fast neutrons than the usually used 139.9 keV one.

References

[1] G. Heusser, Nucl. Instrum. Methods A 369 (1996) 539.
[2] R. Wordel, et al., Nucl. Instrum. Methods A 369 (1996) 557.
[3] E. Gete, et al., Nucl. Instrum. Methods A 388 (1997) 212.
[4] N. Jovancevic, M. Krmar, Phys. Procedia 31 (2012) 1–190.
[5] S. Croft, et al., Nucl. Instrum. Methods A 505 (2003) 536–539.
[6] Da Silva, et al., Nucl. Instrum. Methods Phys. Res. A 354 (1995) 553.
[7] Y. Feige, et al., J. Geophys. Res. 73 (1968) 3135–3142.
[8] G.P. Škoro, et al., Nucl. Instrum. Methods A 316 (1992) 333.
[9] N. Jovančević, M. Krmar, Appl. Radiat. Isot. 69 (2011) 629–635.
[10] N. Jovančević, et al., Nucl. Instrum. Methods A 612 (2009) 303–308.
[11] A. Dragić, et al., Phys. Procedia 59 (2014) 125.
[12] G. Heusser, Background in ionizing radiation detection, in: M. Garcia-Leon, R. Gracia-Tenorio (Eds.), Low-Level Measurements of Radioactivity in the Environment, Word Scientific, Singapore, 1994, pp. 69–112.
[13] G. Heusser, Annu. Rev. Nucl. Part Sci. 45 (1995) 543–590.
[14] M. Krmar, et al., Nucl. Instrum. Methods A 709 (2013) 8–11.
[15] M. Krmar, et al., Appl. Radiat. Isot. 70 (1) (2012) 269–273.
[16] S. Niese, Underground laboratories for low-level radioactivitymeasurements, in: P.P. Povinec (Ed.)Analysis of Environmental Radionuclides, Elsevier, Amserdam, 2008, pp. 209–239.
[17] I. Bikit, et al., Nucl. Instrum. Methods A 606 (2009) 495.
[18] C.W. Mannhart et al., 1989, IAEA Technical Report INDC(NDS)220/L, p.305, IAEA, Vienna.
[19] W.V. Schröder, et al., Z. Phys. 239 (1974) 57.
[20] The ENDF. Evaluated Nuclear Data File, ⟨https://www-nds.iaea.org/exfor/endf.htm⟩ (on 4/9/2016).
[21] G. Fehrenbacher, et al., Nucl. Instrum. Methods A 372 (1996) 239.
[22] T. Siiskonen, H. Toivonen, Nucl. Instrum. Methods A 540 (2005) 403.
[23] NCRP Report 79, Neutron contamination from medical electron accelerators (1984).
[24] Study of the optimal performance of a neutron activation analyisi facility based on a DD neutron Generator. In: Proceedings of Neutron Generators for Analytical Purposes, IAEA Radiation Technology Reports Series No. 1, Vienna (2012).
[25] ROOT cern, ⟨https://root.cern.ch⟩ (on 4/9/2016).

Nuclear Instruments and Methods in Physics Research A 833 (2016) 23–26

Contents lists available at ScienceDirect

Nuclear Instruments and Methods in Physics Research A

journal homepage: www.elsevier.com/locate/nima

Modeling of neutron spectrum in the gamma spectroscopy measurements with Ge-detectors

D. Knežević, N. Jovančević*, M. Krmar, J. Petrović

University of Novi Sad, Faculty of Sciences, Department of Physics, Trg Dositeja Obradovića 3, 21000 Novi Sad, Serbia

ARTICLE INFO

Article history:
Received 20 April 2016
Received in revised form
23 June 2016
Accepted 1 July 2016
Available online 1 July 2016

Keywords:
Gamma spectroscopy
Neutron spectra
Unfolding procedures
Ge - detectors

ABSTRACT

In this study, we present a novel approach for estimation of neutron spectra that are present during gamma spectroscopy measurements performed by a Ge detector. This method is based on the calculation of the neutron spectra by using an unfolding procedure, where the activity of the Ge isotopes, produced by the neutron reactions, and the available cross section data for those reactions are the input parameters. This new approach was tested by background gamma spectroscopy measurements with a HPGe detector. Obtained results show that this method can provide useful information about the neutron spectra at the position of the Ge detectors.

1. Introduction

Detectible gamma activity can be produced by neutron interactions with the Ge-detector itself and surrounding materials, via captures and scattering reactions [1]. As one of the primary background sources, analysis of neutron presence is of great importance in low-background experiments, as well as in different kinds of prompt neutron activation measurements [2]. Analysis of neutron interactions with the Ge–detector was the subject of numerous studies [1–16]. However, today still we are faced with an old issue - the determination of neutron spectra in the Ge-detector during gamma spectroscopy measurements [17–19]. Thus, we present here a novel approach in order to resolve this issue, that is based on very well known unfolding methods used in neutron activation analysis [20]. This approach is based on the fact that the activity induced by neutrons for the activated radionuclide, k, is proportional to the product of the cross-section for a production of certain radionuclide and the neutron fluence rate:

$$A_k = \sum_i \sigma_{ik} \cdot \Phi_i; \quad i = 1, 2..... c; \quad k = 1, 2.... m \tag{1}$$

where σ_{ik} are the corresponding cross section functions and Φ_i is the neutron fluence rate for a certain energy bin E_i. The index k runs over the number of used radionuclides, and m is the number of radionuclides. The maximum value for the index i, c, denotes the number of bins in the neutron spectra and the cross section function. From Eq. (1), the neutron spectra Φ_i can be determined by the unfolding procedure. In this approach we denote the activity of the Ge isotopes induced by different neutron reactions as A_k. For the reactions of interest, the available ENDF data cross section data, σ_{ik}, were used [21]. This method gives us the possibility to model neutron spectra at the position of the Ge-detector.

It should be emphasized that this approach is different from others applied in previous studies [17–19], which are based on the analysis of the detector response functions for certain neutron induced gamma peaks by Monte Carlo simulations.

In our present work, this new method was tested by modeling of the background neutron spectra during gamma spectroscopy measurements with the HPGe detector at our laboratory located at sea level [11,22]. Present neutrons are mostly created by muon captures on the Pb nuclei of the lead shield [11]. For the unfolding procedure the GRAVEL unfolding algorithm was used [23,24].

2. Measurements of neutron induced gamma activity

For the measurement of the neutron induced gamma activity, the HPGe detector from Canberra, serial number GX10021, was used. This detector is a coaxial n-type detector, with a U-shaped cryostat configuration. The relative efficiency of this detector is 100%, and the active volume is 380 cm^3. The detector is surrounded by a passive lead shield, Canberra model 777B., weighing 1633 kg and being 15 cm thick. The detector is located in the low background laboratory of the Faculty of Sciences in Novi Sad (80 m asl) [22].

The experimental data was acquired by recording the background spectrum during 5886293 s (∼68 days), in order to get

* Corresponding author.

http://dx.doi.org/10.1016/j.nima.2016.07.001
0168-9002/

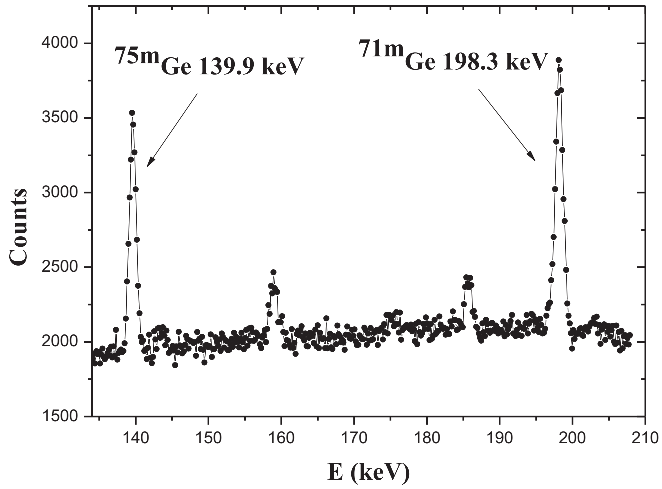

Fig. 1. Low energy part of the spectrum with the neutron induced Ge gamma peaks collected with the HPGe detector in the lead shield.

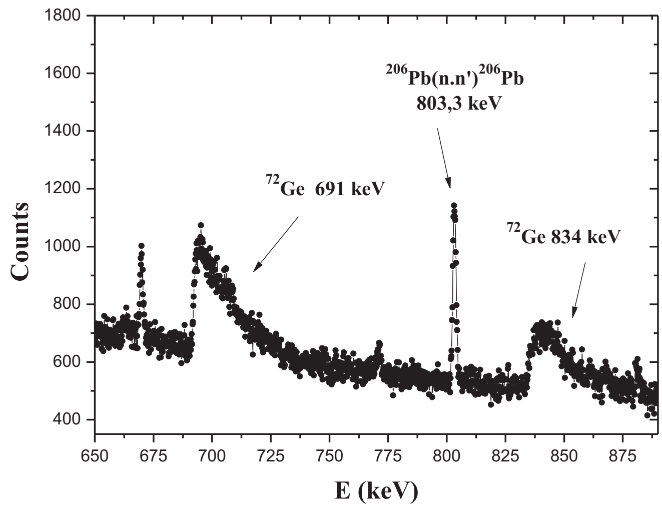

Fig. 2. The part of the spectrum with the neutron induced Ge(n,n') gamma peaks collected with the HPGe detector in the lead shield.

Table 1
General information about detected Ge-gamma peaks and corresponding values of the count rates.

Energy (keV)	Nuclide	Reactions	Count rates (s^{-1})
66.7	^{73m}Ge	^{72}Ge(n,γ)^{73m}Ge ^{74}Ge(n,2n)^{73m}Ge	2.10(12)
139.9	^{75m}Ge	^{74}Ge(n,γ)^{75m}Ge ^{76}Ge(n,2n)^{75m}Ge	1.77(11)
198.3	^{71m}Ge	^{70}Ge(n,γ)^{71m}Ge ^{72}Ge(n,2n)^{71m}Ge ^{73}Ge(n,3n)^{71m}Ge	2.43(11)
562.8	^{76}Ge	^{76}Ge(n,n') ^{76}Ge	2.51(22)
691.3	^{72}Ge	^{72}Ge(n,n') ^{72}Ge	6.67(21)

satisfying statistics of the detected gamma rays, which are created due to the interactions of neutrons with the germanium nuclei. On Figs. 1 and 2, parts of the collected spectrum with characteristic neutron induced gamma peaks are shown [11,25]. Identified Ge gamma peaks, their origin and intensities are presented in Table 1. The gamma peaks that have suitable detected statistic are chosen for the analysis [11,18].

The intensities of standard narrow Gaussian shape peaks (66.7 keV, 139 keV and 198.3 keV) were determined by the CANBERA softer GENIE2000. To obtain the intensity of the long tail asymmetric Ge(n,n') 562.8 keV and 691.0 keV peaks, their shape was fitted by the following function [4,25]:

$$C(E) = a_0 ERFC\left[-\frac{(E-E_0)}{\sigma_0}\right]\cdot Exp\left[-\frac{(E-E_0)}{\Delta}\right] + \sum_{i=1}^{n} a_i\cdot Exp\left[-\frac{1}{2\sigma_i^2}(E-E_i)^2\right] + F \quad (2)$$

In the equation above, the first term corresponds to the Ge(n,n') peak. In the second term, the expression inside the summation is a Gaussian function which corresponds to any symmetric gamma peak in the fitting region. Those peaks can be the Ge(n,γ) gamma peaks or any other gamma peaks corresponding to the background gamma lines. The parameter F refers to the background continuum which is assumed to be a linear function here. The parameters of the fit were: a_0, a_i, E_0, E_i, σ_0, σ_i and Δ. In this case E_0 and E_i correspond to the energies of the detected gamma peaks; a_0 and a_i are the maximum amplitudes of those peaks. Parameters σ_0 and σ_i were determined by the peak full-width at half-maximum (FWHM) and should correspond to the energy resolution of the detector. The Δ parameter determines the characteristic of the exponential tail of Ge(n,n') peaks.

First step in the fitting procedure was to fix the level of background continuum. It was shown in Ref. [4]. that the quality of the results obtained by the fit of Ge(n,n') peaks depends on the energy region chosen for the fit. The next step was to vary the fitting region for a chosen energy of the asymmetric peak between 30 keV and 40 keV. Different values of the level of background continuum and energy region were used to get the fit with the value of χ^2/NDF as close to unity as possible. Additionally, the errors of the fitting parameters were analyzed to get the optimal set values. The gamma peaks were fitted by the ROOT data analysis toolkit [31].

Based on detected gamma peak intensities, the activity for production of certain Ge isotopes per atom of natural germanium is calculated by [11,18]:

$$A_k = \frac{C\cdot M}{t\cdot p\cdot(\varepsilon+\alpha)\cdot m\cdot N_a} \quad (3)$$

where C is the detected number of counts for certain gamma peak, t is the measurement time, p is the gamma-ray emission probability [26], α is the conversion coefficient [27], ε is the full energy peak efficiency (calculated by the Geant4 toolkit [11,28]), M is the Ge molar mass, m is the mass of the Ge crystal and N_a is the Avogadro constant. Obtained values of activities, A_k are shown in Table 2.

3. Cross sections data

Cross sections for the Ge isotope production were obtained by summing the cross sections for different neutron reactions (as

Table 2
The activities, A_k, of Ge isotopes.

Ge isotope	A_k [10^{-24}Bq/atom]
^{71m}Ge	0.173(9)
^{73m}Ge	0.095(7)
^{75m}Ge	0.118(9)
^{72}Ge	0.398(13)
^{76}Ge	0.44(4)

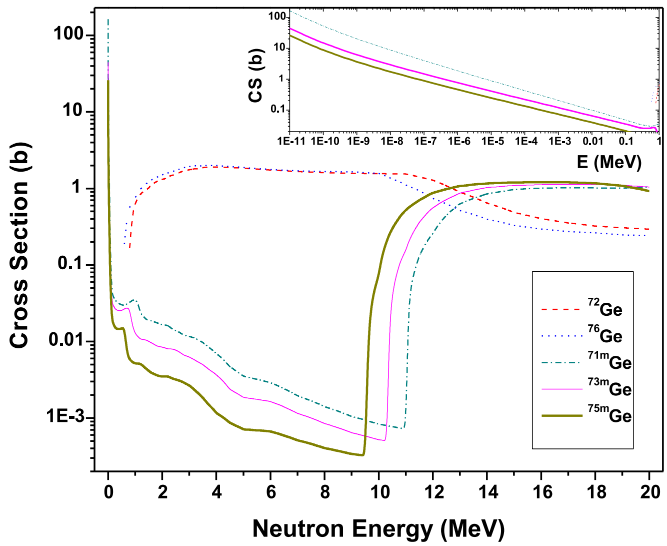

Fig. 3. The cross section functions for Ge isotopes production via neutron reactions (with magnified low energy region) [21].

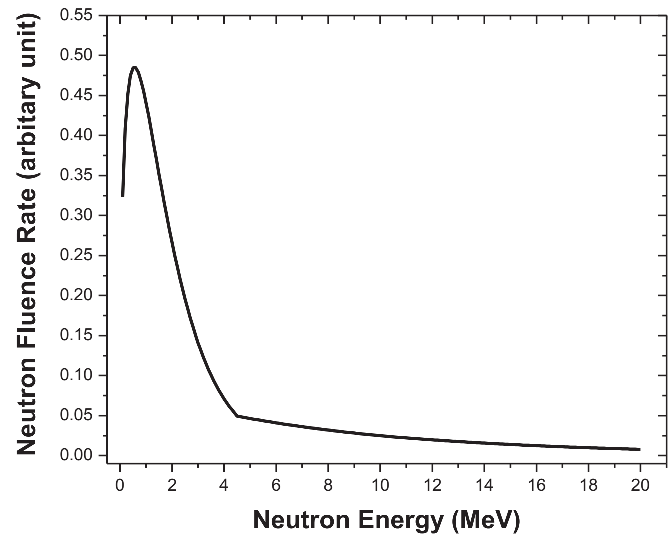

Fig. 4. Default neutron spectrum used in analysis [29].

listed in Table 1). The cross sections for neutron reactions were taken from the ENDF database, specifically from the ENDF/B-VII.1 library [21], as presented on Fig. 3. In order to be used in the unfolding algorithm, the cross section functions were divided into 200 energy bins. Since the cross section functions cover a fairly wide energy range, we have the possibility to determine the neutron spectrum up to 20 MeV.

3.1. A priori neutron spectrum

A priori spectrum in unfolding methods is used as a starting point for the unfolding algorithm in determination of the solution spectrum. The main sources of background neutrons are the spontaneous fission of U and Th, (α,n) nuclear reactions as well as cosmic rays [1]. At ground and shallow depth laboratories, most of the neutrons come from the muon interactions with high-Z shielding materials [11]. Having in mind this was also the case in our measurements,we used the empirical equation (available from the literature [29]) as an a priori spectrum for the general shape of neutrons spectrum. For neutron energies between 1 MeV and 4 MeV, the spectrum is well described by:

$$\frac{dN(E)}{dE} \propto E^{5/11} e^{-E/\theta} \tag{4}$$

where E is the neutron energy, and θ is the effective nuclear temperature and it's value is 1.22 MeV. For the neutron energies above 4 MeV, the spectrum takes the following form:

$$\frac{dN(E)}{dE} \propto e^{-E/E_d} \tag{5}$$

where E_d is the parameter that for the energy range 4.5–10 MeV has the value of 8 ± 1 MeV, and for the 10–50 MeV range it takes the value 8.6 ± 0.5 MeV. Our default spectrum is shown in Fig. 4.

4. Unfolding results

In this work, we used the GRAVEL algorithm for the unfolding procedures [24,29]. GRAVEL is an iterative unfolding algorithm that starts with a guess default function. In this technique, from the J-th iteration of the neutron fluence rate (Φ_i^J, for energy bin E_i) the next iteration, Φ_i^{J+1}, will be calculated by:

$$\Phi_i^{J+1} = \Phi_i^J \cdot f\left(A_k, \varepsilon_k, \sigma_{ki}, \Phi_i^J\right) \tag{6}$$

The function f is defined as follows:

$$f = \exp\left(\frac{\sum_k W_{ik}^J \log\left(\frac{A_k}{\sum_i \sigma_{ki} \Phi_i^J}\right)}{\sum_k W_{ik}^J}\right), \quad W_{ik}^J = \frac{\sigma_{ki} \cdot \Phi_i^J}{\sum_i \sigma_{ki} \cdot \Phi_i^J} \frac{A_k^2}{\varepsilon_k^2} \tag{7}$$

where W_{ik}^J is the weight factor, A_k is the measured activity, ε_k is the measurement uncertainty, and σ_{ki} is the cross section for production of k-th Ge isotope and energy bin E_i (Fig. 3). It should be noted that the standard sensitivity analysis and uncertainty propagation cannot be performed by the GRAVEL algorithm. However, the solution spectrum is always non-negative.

The unfolding was performed for 200 energy bins covering the energy range up to 20 MeV. After every integration the parameter χ^2 per degree of freedom n (equal to the number of used radionuclides) was calculated:

$$\chi^2/n = \frac{1}{n} \sum_k^n \frac{\left(\sum_i \sigma_{ki} \Phi_i - A_k\right)}{\varepsilon_k} \tag{8}$$

The iteration procedure is stopped when the solution leads to $\chi^2/n \approx 1$. The unfolding neutron spectrum function is given in Fig. 5, together with the default function.

In order to validate the obtained results, the activity (A_c) is calculated for both, default and final neutron spectrum functions, and compared with the measured data (A_m). In Table 3. the sums of squared values, S, are presented and defined by:

$$S = \frac{1}{(p-1)} \sum_{i=1}^{p} \left(\frac{A_{ci} - A_{mi}}{A_{mi}}\right)^2 \tag{9}$$

where p is the number of the Ge isotopes (in this case $p = 5$).

The results from Table 3. Show that the unfolding procedure converges to a better description of the measured activity data than the initial a priori neutron spectrum. There is an increase of the unfolding spectrum in the low energy range in comparison to the default spectrum. The reason behind this can be the change in energy of the neutron (emitted in muon capture process) through scattering in surrounding materials. In the region above 10 MeV, the determined spectrum function has higher values than the default function (Fig. 5) which can be used as a starting point for further investigations.

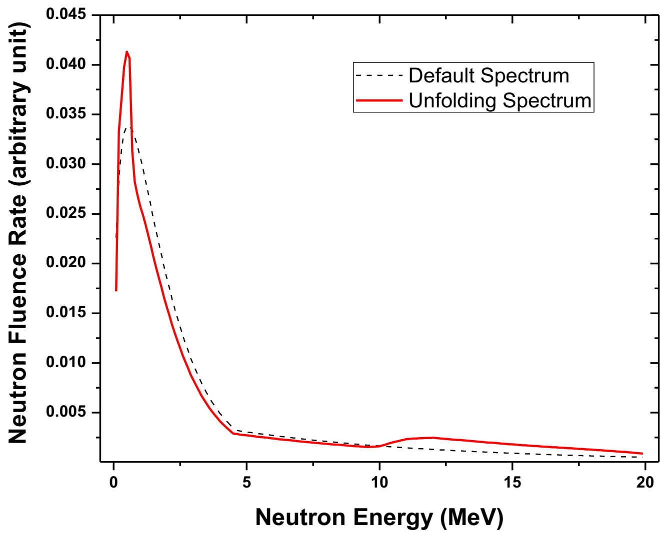

Fig. 5. The obtained unfolded neutron spectrum with GRAVEL algorithm compared with default one. The integral for both spectra is normalized to unity.

Table 3
Relations between calculated A_c and measured A_m activity.

Radionuclide	$\frac{A_c - A_m}{A_m}$ **default**	$\frac{A_c - A_m}{A_m}$ **final**
^{73m}Ge	−0.16197	0.07832
^{71m}Ge	0.04694	0.02852
^{75m}Ge	−0.42702	−0.15732
^{72}Ge	0.04293	0.00726
^{76}Ge	0.03737	0.02377
S	**0.053506**	**0.008079**

5. Conclusion

In this work, we have analyzed the possibility of estimating the neutron spectrum inside the HPGe detector with an unfolding procedure. This new approach was tested by modeling of the background neutron spectrum. The resulting unfolded spectrum (Fig. 5) describes the neutron presence in the low-background gamma spectroscopy system located in the laboratory at sea level in a satisfactory way.

The obtained results show that this technique could provide useful information about the neutron spectrum in measurements with the Ge – detectors. However, this measurement can also be a starting point for future studies. For future analyses there are a few things to consider in order to improve the results. Better statistics of the measurements would reduce the errors of the measured activities, thus giving us greater confidence in the obtained activities. We would also consider experiments with different neutron fields, such as the ^{252}Cf spontaneous fission neutron source. Future work will also include the usage of different unfolding algorithms, since other authors reported deviations between them [30]. In this work as a priory neutron spectrum we used compound function based on the available empirical data. As an alternative for default neutron spectrum simplified functions such as Maxwellian function, can be used. The choice of the a priory neutron spectrum function would depend on the characteristics of neutron fields, a feature that can also be studied in the future. After all of the improvements suggested above and after performing tests, this method could become a standard for the determination of the neutron spectra during gamma spectroscopy measurements with the Ge – detectors.

References

[1] G. Heusser, Nucl. Instrum. Methods Phys. Res. A 369 (1996) 539.
[2] A. Dragić, et al., Phys. Procedia 59 (2014) 125.
[3] R. Wordel, et al., Nucl. Instrum. Methods Phys. Res. A 369 (1996) 557.
[4] E. Gete, et al., Nucl. Instrum. Methods Phys. Res. A 388 (1997) 212.
[5] N. Jovančević, M. Krmar, Phys. Procedia 31 (2012) 93–98.
[6] S. Croft, et al., Nucl. Instrum. Methods Phys. Res. A 505 (2003) 536–539.
[7] Da Silva, et al., Nucl. Instrum. Methods Phys. Res. A 354 (1995) 553.
[8] Y. Feige, et al., J. Geophys. Res. 73 (1968) 3135–3142.
[9] G.P. Škoro, et al., Nucl. Instrum. Methods Phys. Res. A 316 (1992) 333.
[10] N. Jovančević, M. Krmar, Appl. Rad. Isot. 69 (2011) 629–635.
[11] N. Jovančević, et al., Nucl. Instrum. Methods Phys. Res. A 612 (2009) 303–308.
[12] G. Heusser, Background in ionizing radiation detection, in: M. Garcia-Leon, R. Gracia-Tenorio (Eds.), Low-Level Measurements of Radioactivity in the Environment, Word Scientific, Singapore, 1994, pp. 69–112.
[13] G. Heusser, Annu. Rev. Nucl. Part. Sci. 45 (1995) 543–590.
[14] M. Krmar, et al., Nucl. Instrum. Methods Phys. Res. A 70 (2013) 8–11.
[15] M. Krmar, et al., Appl. Rad. Isot. 70 (1) (2012) 269–273.
[16] S. Niese, Underground laboratories for low-level radioactivitymeasurements, in: P.P. Povinec (Ed.), Analysis of Environmental Radionuclides, Elsevier, Amserdam, 2008, pp. 209–239.
[17] C. Chund, Y.R. Chen, Nucl. Instrum. Methods Phys. Res. A 301 (1991) 328–336.
[18] J.E. Naye, Nucl. Instrum. Methods Phys. Res. A 368 (1996) 832–846.
[19] G. Fehrenbacher, et al., Nucl. Instrum. Methods Phys. Res. A 372 (1996) 239.
[20] A. Trkov, V. Radulović, J. Radioanal. Nucl. Chem. 304 (2015) 763–778.
[21] The ENDF, Evaluated Nuclear Data File, ⟨https://www-nds.iaea.org/exfor/endf.htm⟩.
[22] I. Bikit, et al., Nucl. Instrum. Methods Phys. Res. A 606 (2009) 495.
[23] M. Reginatto, et al., Health Phys. 77 (1999) 579.
[24] W. Goffe, Studies in Nonlinear Dynamics and Econometrics, Berkeley Electronic Press 1996, pp. 169–176.
[25] T. Siiskonen, H. Toivonen, Nucl. Instrum. Methods Phys. Res. A 540 (2005) 403.
[26] National Nuclear Data Center, Brookhaven National Laboratory, ⟨http://www.nndc.bnl.gov/⟩.
[27] LBNL Isotopes Project- LUNDS University, Nuclear Data Dissemination Homepage, ⟨http://ie.lbl.gov/toi.html⟩.
[28] S. Agostinell, et al., Nucl. Instrum. Methods Phys. Res. A 506 (2003) 250.
[29] W.V. Schröder, et al., Z. Phys. 239 (1974) 57.
[30] R. Behrens, JINST 4 P03027, 2009.
[31] ROOT cern, ⟨https://root.cern.ch⟩.

Radiation Measurements 72 (2015) 70–74

Contents lists available at ScienceDirect

Radiation Measurements

journal homepage: www.elsevier.com/locate/radmeas

Radon adsorption by zeolite

I. Bikit [a,*], D. Mrdja [a], K. Bikit [a], S. Grujic [b], D. Knezevic [a], S. Forkapic [a], U. Kozmidis-Luburic [b]

[a] *University of Novi Sad, Faculty of Sciences, Trg Dositeja Obradovica 4, 21000 Novi Sad, Serbia*
[b] *University of Novi Sad, Faculty of Technical Sciences, Trg Dositeja Obradovica 6, 21000 Novi Sad, Serbia*

HIGHLIGHTS

- Measurements of radon adsorption by various zeolite granulation are done.
- Adsorption coefficients for natural zeolite and activated charcoal are determined.
- The adsorption coefficients for activated charcoal and natural zeolite are compared.

ARTICLE INFO

Article history:
Received 4 September 2014
Received in revised form
26 November 2014
Accepted 1 December 2014
Available online 2 December 2014

Keywords:
Radon
Zeolite granulation
Adsorption coefficient

ABSTRACT

Due to well defined three dimensional nano- and micro-porous structure, one of the most important properties of zeolite is its surface adsorption capacity. Nevertheless, a natural zeolite adsorption capability of ^{222}Rn has not been thoroughly investigated. The objective of this paper is to review the research concerning the application of natural zeolite in ^{222}Rn adsorption. To achieve this goal the investigation based on measurements of radon adsorption by various zeolite granulation was done. Ball mill is used to achieve different granulations of zeolite in the range of μm–mm, whereas the particle size distributions are determined by particle size analyzer, Mastersizer 2000. The zeolite samples were exposed to elevated radon concentrations up to 1800 Bq/m^3 inside a closed chamber (volume $\approx 5.4 \times 10^{-3}$ m^3). The absorbed radon quantity was measured by high resolution gamma spectroscopy. The influence of particle size was measured and discussed. We found that the adsorption coefficients that were obtained in our experiment for natural zeolite samples for different granulations are similar to adsorbing coefficients for silica gel, but they are an order of magnitude lower than radon adsorbing coefficient for synthetic zeolite. The adsorption coefficient for activated charcoal derived in our experiment (≈ 3 m^3/kg) is in average 50 times higher comparing to the adsorption coefficients obtained for zeolite samples (0.038 m^3/kg–0.11 m^3/kg). All adsorbing coefficients are determined for very low relative humidity of air of about 7%, since our simple experimental setup did not allow possibility to change the relative humidity, or temperature. In addition, we explored the perturbation of radon concentration inside small-volume radon chamber caused by the presence of adsorbing sample and influence of this perturbation on obtained values of adsorbing coefficients.

1. Introduction

Due to the gaseous properties of radon, it is easily emanated from ground or building materials and it can reach high levels of activity in poorly ventilated buildings. Hence, the regular measurement of radon is necessary in order to control the radioactivity levels and take appropriate measures in case of elevated concentrations. Since the late 1980s the main method for short-term measurement of radon concentration indoors is usage of activated charcoal canisters. In the recent years there is an increase in number of studies oriented toward measurement of radon adsorption by alternative types of adsorbing material, and one of those materials is zeolite. It is a naturally occurring mineral group consisting of many different minerals, and it has special porous crystalline structure (Baerlocher et al., 2007). Zeolites can be adapted for a variety of uses, and its ability to adsorb radon should

* Corresponding author. University of Novi Sad, Faculty of Sciences, Department of Physics, Trg Dositeja Obradovica 4, 21000 Novi Sad, Serbia.
E-mail address: bikit@df.uns.ac.rs (I. Bikit).

http://dx.doi.org/10.1016/j.radmeas.2014.12.001
1350-4487/

be investigated in detail. Studies that measured adsorption of radon by zeolite have shown relatively good adsorbing properties of both, natural and synthetic zeolites (Mortazavi et al., 2009; Paschalides et al., 2010). However, their adsorption properties can vary greatly, due to the pore size distribution and composition of natural ores, as well as the degradation of adsorption characteristics over time due to sensitivity towards ionizing radiation in synthetic zeolites (Hedström et al., 2012). Few article reported data on the subject, although the ability of natural zeolites to adsorb radioisotopes is known; for example *Clinoptilolite* was used extensively in dealing with the effects of Chernobyl accident, while *Chabazite* has been used in the Three Mile Island clean-up (Dyer et al., 2000).

It should be also emphasized that removal of radon from indoor air by contacting the air with a silver-exchanged zeolite was patented (Patent US 7381244 B2).

2. Experiment

For radon adsorption measurements, we used highly porous natural zeolite material, produced by FiMö-Aquaristik GmbH, Germany. We used this material from original, hermetically closed fabric boxes, without its exposure to higher temperatures. Different granulations of this material are obtained by different times of milling (10, 20 and 40 min). Milling was performed in a planetary ball mill Fritsch Pulverisette 5. A hardened steel vial (250 cm^3 volume) and hardened steel balls (10 mm in diameter) were used. The mass of the milled sample was 50 g, and the angular velocity of the supporting disc and vial were 400 and 800 rpm, respectively. Particle size distribution was determined using a Malvern Mastersizer 2000 particle size analyzer capable of analyzing particles between 0.01 and 2000 μm. This analyzer records the light pattern scattered from a field of particles at different angles. The device then uses an analytical procedure to determine the particle size

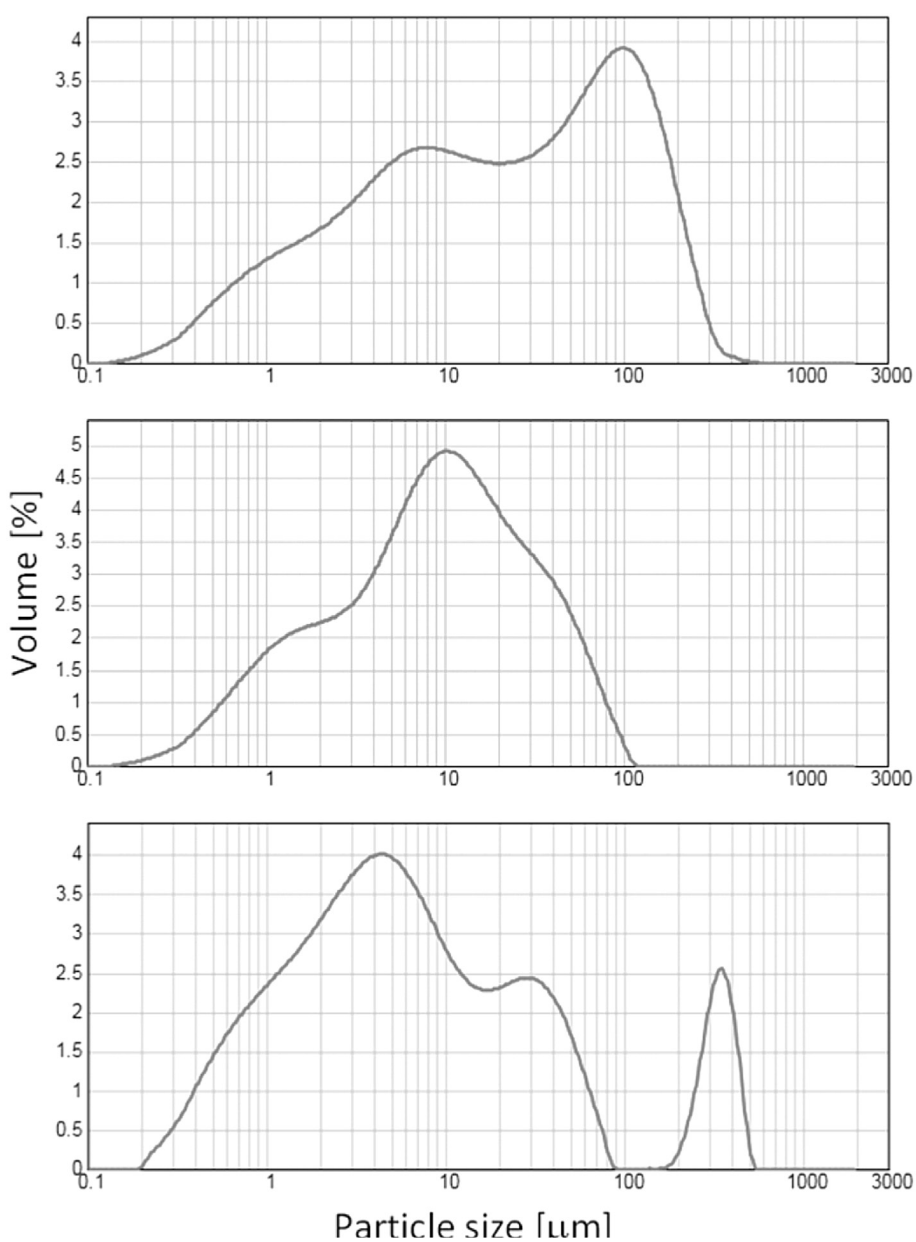

Fig. 1. Particle size distributions for different milling times (from top to bottom: 10 min, 20 min and 40 min).

distribution that created the patterns. The wavelengths of light used during measurement were 632.8 nm and 740 nm. The particle size distributions for different milling times are presented in Fig. 1.

The first measurement of radon adsorption was performed without milling of zeolite (i.e. with zeolite grain size 5–10 mm), and then pulverized samples were used. Only in the first measurement, together with zeolite sample, the activated charcoal canister was present. All the samples were placed in metal canisters that were opened during the exposure to radon within glass chamber and closed immediately after exposure to avoid changes in moisture content of the sample and, potentially more importantly, loss of adsorbed radon from the zeolite.

The experimental setup designed to test the radon adsorption by zeolite is presented in Fig. 2. Zeolite samples were exposed to radon concentrations of about 1400–1800 Bq/m^3, during 48 h for each sample, by placing them inside a chamber with thick glass walls, whose volume is $5.4 \cdot 10^{-3}$ m^3. The changes of radon concentration inside the chamber over time were continuously measured by alpha-spectrometer RAD7. Circulation of air at a rate of 0.5 l/min is provided thanks to the pump that is an integral component of the alpha-spectrometer, without mixing the air inside the chamber with the outside air. The air inside this closed system contained radon that emanated from the zirconium-oxide ($m = 0.9$ kg), containing Ra-226 radionuclide (4.10 ± 0.20 kBq/kg) which was placed at the chamber bottom. Humidity absorption was performed by passing the air through a column of calcium sulfate ($CaSO_4$). Each sample was also measured by low-level gamma spectrometry system before exposure to radon elevated concentrations and after exposure.

3. Results and discussion

The concentrations of radon depending on time inside the glass chamber, measured by alpha-spectrometer RAD7, during all exposures of zeolite samples to radon, are presented in Fig. 3. The detected decreases of radon concentrations after inserting the samples (zeolite + activated charcoal, or zeolite only) inside the glass chamber were not caused only due to radon adsorption, but also as a result of radon loss during the sample replacement. Our test by short opening of glass chamber showed that the estimated radon loss can reach up to 40%.

The results of gamma-spectrometry measurements, performed in order to precisely quantify the adsorption characteristics of various zeolite granulations, are presented in Table 1. Relative uncertainties of presented net intensities of 352 keV gamma ray line, associated with lead-214, a short-lived decay product associated with radon-222, expressed at 95% confidence level, are about 10%.

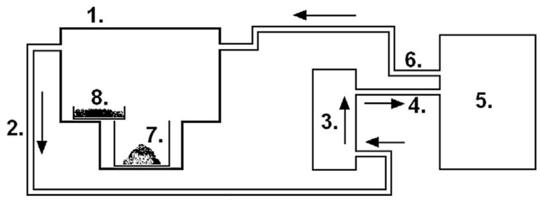

Fig. 2. The experimental setup designed to test the radon adsorption by zeolite 1. Chamber with thick glass walls, 2. Plastic tube, 3. Humidity absorber (CaSO4), 4. Input plastic tube, 5. Alpha spectrometer (RAD7), 6. Output plastic tube, 7. Zirconium-oxide containing Ra-226, 8. Zeolite. The direction in which the air moves through the closed system is labeled by arrows. The temperature of air and relative humidity were measured by devices that are integral parts of RAD7 device. However, in this experimental setup the temperature of the air and its relative humidity were not adjustable parameters.

From results presented in Fig. 3 and Table 1 it is obvious that radon adsorption by zeolite samples is much less efficient than by activated charcoal. This fact does not necessarily represents a disadvantage, especially in the case of high radon concentrations (500–1500 Bq/m^3) where zeolite can be used as an indicator of elevated indoor radon concentrations, which could be measured if zeolite adsorption coefficient is known. The granulation of zeolite samples doesn't significantly influence its radon adsorption characteristics. However, we found better adsorption by zeolite sample milled for 20 min, which can be attributed to the relatively uniform particle size distribution, with average value of 10 μm. In further investigations, the radon adsorption characteristics of zeolite for longer exposure times should be explored (in presented experiment, only one exposure interval of 48 h was used).

Although relatively simple, our experimental setup provided the possibility for estimation of adsorption coefficients of Rn-222 gas on activated charcoal, as well as on zeolite. This coefficient, k (m^3/kg), characterizes the capacity that sorbent material has in adsorbing of radon, and can be determined in the following way (López and Canoba, 2002):

$$k = Q/C,$$

where Q is radon activity adsorbed by unit of mass of sorbent material (Bq/kg), and C is concentration of Rn-222 in air during exposure of sorbent material (Bq/m^3). In our case the time interval of exposure to radon of activated charcoal and each zeolite sample was 48 h. The temperature of air inside the glass chamber was in interval (25–30) °C, while the relative humidity was about 7%.

Knowing the net intensity of 352 keV post-radon line for activated charcoal after exposure (Table 1), gamma emission probability for this line ($p_\gamma = 0.371$), and detection efficiency at this energy of our HPGe detector for cylindrical geometry of measured sample ($\varepsilon = (30 \pm 3) \times 10^{-3}$), we found $Q = 153 \pm 23$ Bq/kg for activated charcoal. As can be seen from Fig. 3 (time interval 2–3), the radon concentration inside glass chamber dropped quickly (within 1 h) in the presence of activated charcoal, reaching the constant level of $C = 50 \pm 6$ Bq/m^3 for next 48 h. From these values of Q and C, we found $k_{\text{activated charcoal}} = 3.1 \pm 0.6$ m^3/kg. This is in a relatively good agreement with previously reported values for adsorption coefficient of radon on activated charcoal at room temperature (2–6 m^3/kg, Cohen and Cohen, 1983; Ren and Lin, 1987, Scarpitta, 1995), although these reported values are related to higher relative humidity, which represent in a better way realistic indoor conditions.

Using similar procedure we found the corresponding value of $Q = 42 \pm 6$ Bq/kg for zeolite (40 min milling). However, the average radon concentration for 48 h exposure interval for this zeolite sample (time interval 6–7 in Fig. 3) was relatively high, $C = 1.10 \pm 0.09$ kBq/m^3, giving the corresponding value of $k_{\text{zeolite (40 min milling)}} = 0.038 \pm 0.006$ m^3/kg.

Based on values given in Table 1 and Fig. 3, the adsorption coefficients of zeolite samples with 20 min milling and 10 min milling are found to be 0.11 ± 0.021 m^3/kg and 0.046 ± 0.009 m^3/kg, respectively. The relative uncertainties of derived adsorption coefficients reach up to 20%.

The obtained values for adsorption coefficients of these zeolite samples with different granulations are 25–75 times lower than corresponding value of activated charcoal in our experiment. These values for zeolite samples are very similar to the adsorbing coefficients of radon previously reported for silica gel (0.022–0.065 m^3/kg) for relatively broad temperature range 5–35 °C (Ackley, 1975).

The possible disadvantage of our experiment is the use of a radon chamber with a very small volume (only 5.4 L), while the

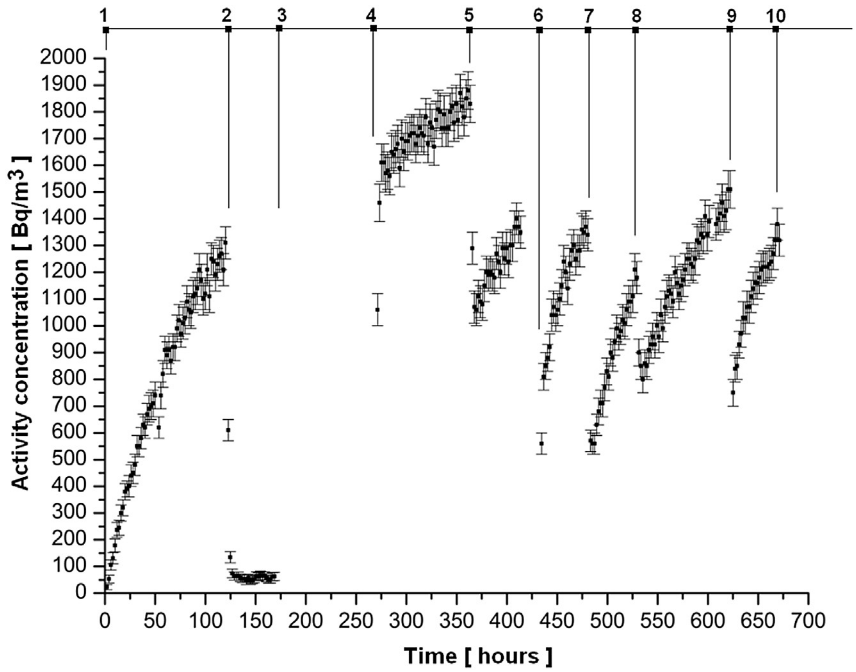

Fig. 3. Time dependence of radon concentration inside the glass chamber. Explanation for corresponding time intervals: 1–2 – only zirconium-oxide closed inside glass chamber; 2–3 – activated charcoal + zeolite, not milled (grain size 5–10 mm); 3–4 – without measurement (only zirconium-oxide closed inside glass chamber); 4–5 – only zirconium-oxide closed inside glass chamber; 5–6 – test of radon loss by short opening (5 s) of glass chamber; 6–7 – exposure of the finest zeolite fraction (40 min milling); 7–8 – exposure of zeolite fraction, 20 min milled; 8–9 – only zirconium-oxide closed inside glass chamber; 9–10 – exposure of zeolite fraction, 10 min milled. Error bars are presented for each single measurement.

Table 1
Gamma-spectrometry measurements of samples.

Sample	Intensity of post-radon 352 keV line **before** sample exposure to radon [c/(s kg)]	Intensity of post-radon 352 keV line **after** sample exposure to radon [c/(s kg)]	Net intensity of post-radon 352 keV line due to radon adsorption by sample [c/(s kg)]
Activated charcoal	–	1.87 ± 0.17	1.87 ± 0.17
Zeolite (not milled)	0.23 ± 0.02	0.78 ± 0.06	0.55 ± 0.06
Zeolite (40 min milling)	0.23 ± 0.02	0.70 ± 0.05	0.47 ± 0.05
Zeolite (20 min milling)	0.23 ± 0.02	1.18 ± 0.10	0.95 ± 0.10
Zeolite (10 min milling)	0.23 ± 0.02	0.75 ± 0.06	0.52 ± 0.06

equivalent air-volume of the activated charcoal canister (with a typical 70 g weight) is about 210 L (this directly follows from adsorption coefficient value of ≈ 3 m^3/kg, i.e. 0.07 kg $\times$ 3 m^3/kg $= 0.21$ m^3). This is strikingly apparent from Fig. 3 at the interval 2–3, where Rn-222 concentration dropped at very low level when active charcoal of 75 g was present. In principle, the sample to be exposed in the radon chamber should not affect the radon concentration of the chamber. However, we did not possess strong enough Ra-226 source to produce high Rn-222 concentration within a big volume. Thus, we repeated measurement by activated charcoal sample, but with mass of only 5 g (15 times lower mass than in previous measurement) in order to obtain value for adsorption coefficient under new conditions and compare it with previous value of ≈ 3 m^3/kg. Even with this mass, the equivalent air-volume of the activated charcoal (15 L) is still higher than volume of our radon camber, but we expected a smaller perturbation of radon concentration inside chamber. The use of activated charcoal sample with mass below 1 g (equivalent air-volume 3 L) would, on the other hand, increase the measurement uncertainty of intensity of 352 keV gamma line, necessary for final determination of adsorption coefficient.

The exposure time for this small activated charcoal sample within radon chamber was 48 h and radon concentration inside chamber registered by RAD7 device is presented in Fig. 4.

As can be seen from Fig. 4, we could not avoid the decrease of radon concentration within radon chamber, although in this measurement we reached average concentration of $C_1 = 370$ (15) Bq/m^3, which is about 7 times higher, than in first measurement with 75 g of activated charcoal. After exposure, using gamma spectrometry measurement, we found $Q_1 = 1.6 \pm 0.3$ kBq/kg for activated charcoal sample of 5 g mass. The obtained values C_1 and Q_1 imply the following value for adsorption coefficient of activated charcoal: $k = Q_1/C_1 = 4.3 \pm 0.8$ m^3/kg. This is about 40% higher than our first result for adsorption coefficient of activated charcoal, but it

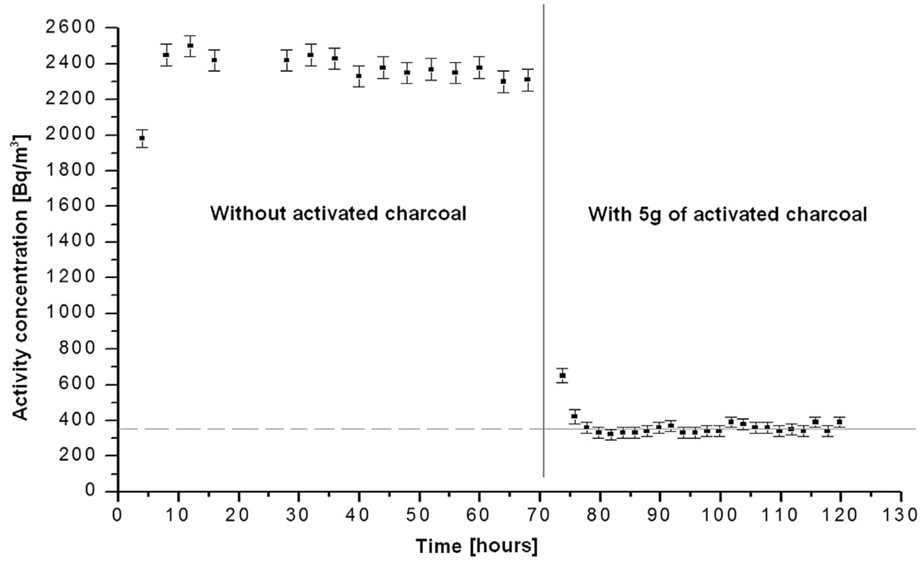

Fig. 4. Time dependence of radon concentration inside the glass chamber without activated charcoal, and with 5 g of activated charcoal sample inside the chamber.

shows relatively good consistency between obtained results for significantly different perturbations of initial radon concentration (both results are in agreement within measurement uncertainties). This further means that adsorption coefficients we obtained for natural zeolite samples are less influenced by radon perturbation effect inside radon chamber, since the magnitude of these perturbations were relatively small in comparison with perturbation caused by activated charcoal.

4. Conclusions

Our results suggest that zeolite, with some constrains, can be used both, to radon measurements (in the case of higher radon concentrations (Sextro, 1987; Ennemoser et al., 1993)) and radon suppression in the air of dwellings, especially having in mind inexpensiveness of the zeolite and its wide availability. However, the measurement of radon concentrations in the range 50–400 Bq/m^3 based on radon adsorption on natural zeolite, probably could not be possible (we estimated that the lowest measurable radon concentration is about 500 Bq/m^3). In addition, a huge amount of this material is required for reduction of indoor radon concentration, compared to activated charcoal.

For the optimal grain size of the zeolite sample (achieved by 20 min milling), the exposure of the zeolite to the average radon concentration of about 800 Bq/m^3, during 48 h, resulted in an activity increase of the 352 keV post-radon line of about 1 c s^{-1} kg^{-1} (35% nominal efficiency HPGe). The adsorption coefficients that were obtained in our experiment for natural zeolite samples (0.038 m^3/kg–0.11 m^3/kg) are comparable with adsorbing coefficients for silica gel, but they are an order of magnitude lower than radon adsorbing coefficient for 5A synthetic zeolite (Paschalides et al., 2010), and in average about 50 times lower than corresponding value that we found for activated charcoal ($\approx$3 m^3/kg). The standardization of zeolite for routine Rn-222 measurements (similar as the EPA procedure (EPA 520/5-87-005, 1987) for activated charcoal) needs more detailed studies.

Acknowledgments

The authors acknowledge the financial support of the Provincial Secretariat for Science and Technological Development within the project Development and application low-background alpha, beta spectroscopy for investigating of radionuclides in the nature, and Ministry of Education and Science of Serbia, within the projects Nuclear Methods Investigations of Rare Processes and Cosmic Rays No.171002 and Biosensing Technologies and Global System for Continuous Research and Integrated Management of ecosystems No.43002.

References

Ackley, R.D., 1975. Removal of Radon-220 from HTGR Fuel Reprocessing and Refabrication Off-Gas Streams by Adsorption (Based on a Literature Survey). Oak Ridge National Laboratory Libraries, p. 15. ORNL-TM-4883.
Baerlocher, Christian, McCusker, Lynne B., Olson, David H., 2007. Atlas of Zeolite Framework Types, sixth revised ed., ISBN 978-0-444-53064-6
Cohen, B.L., Cohen, E.S., 1983. Theory and practice of radon monitoring with charcoal adsorption. Health Phys. 45, 501–508.
Dyer, A., Las, T., Zubair, M., 2000. The use of natural zeolites for radioactive waste treatment: studies on leaching from zeolite/cement composites. J. Radioanal. Nucl. Chem. 243 (3), 839–841.
Ennemoser, O., et al., 1993. Unusually high indoor radon concentrations. Atmos. Environ. 27A (14), 2169–2172.
EPA 520/5-87-005, 1987. EERF Standard Operating Procedures for Rn-222 Measurement Using Charcoal Canisters.
Hedström, H., Foreman, M., Ekberg, C., Ramebäck, H., 2012. Radon capture with silver exchanged zeolites. Radiochim. Acta 100 (6), 395–399.
López, F.O., Canoba, A.C., 2002. ^{222}Rn gas diffusion and determination of its adsorption coefficient on activated charcoal. J. Radioanal. Nucl. Chem. 252 (3), 515–521.
Mortazavi, S.M.J., Mehdizadeh, S., Zehtabian, M., Sina, S., 2009. Development of an economical radon-resistant construction technique that is applicable in national radon-reduction programmes. Int. J. Low Radiat. 6 (2), 113–118.
Paschalides, J.S., Marinakis, G.S., Petropoulos, N.P., 2010. Passive, integrated measurement of radon using 5A synthetic zeolite and blue silica gel. Appl. Radiat. Isot. 68 (1), 155–163.
Ren, T., Lin, L., 1987. A passive integrating indoor radon detector with activated carbon. Radiat. Prot. Dosim. 19, 121–124.
Scarpitta, S.C., 1995. A theoretical model for ^{222}Rn adsorption on activated charcoal canisters in humid air based on Polanyi's potential theory. Health Phys. 68, 332–339.
Sextro, R.G., 1987. Understanding the origin of radon indoors - building a predictive capability. Atmos. Environ. 21 (2), 431–438.

Determination of the nuclear level densities and radiative strength function for 43 nuclei in the mass interval 28≤A≤200

Article *in* The European Physical Journal Conferences · January 2018

DOI: 10.1051/epjconf/201816900007

Determination of the nuclear level densities and radiative strength function for 43 nuclei in the mass interval 28≤A≤200

David Knezevic[1,5], *Nikola* Jovancevic[1,⋆], *Anatoly M.* Sukhovoj[2], *Ludmila V.* Mitsyna[2], *Miodrag* Krmar[1], *Vu D.* Cong[2], *Franz-Josef* Hambsch[4], *Stephan* Oberstedt[4], *Zsolt* Revay[3], *Christian* Stieghorst[3], and *Aleksandar* Dragic[5]

[1] *University of Novi Sad, Faculty of Science, Department of Physics, Trg Dositeja Obradovica 3, 21000 Novi Sad, Serbia*
[2] *Joint Institute for Nuclear Research, 141980 Moscow region, Dubna, Russia*
[3] *Technische Universität München, Forschungsneutronenquelle Heinz Maier-Leibnitz (FRM II), Lichtenbergstr. 1, 85747 Garching, Germany*
[4] *European Commission, Joint Research Centre, Directorate G – Nuclear Safety and Security, Unit G.2, Retieseweg 111, 2440 Geel, Belgium*
[5] *Institute of Physics Belgrade, Pregrevica 118, 11080 Zemun, Serbia*

Abstract. The determination of nuclear level densities and radiative strength functions is one of the most important tasks in low-energy nuclear physics. Accurate experimental values of these parameters are critical for the study of the fundamental properties of nuclear structure. The step-like structure in the dependence of the level densities ρ on the excitation energy of nuclei E_{ex} is observed in the two-step gamma cascade measurements for nuclei in the $28 \leq A \leq 200$ mass region. This characteristic structure can be explained only if a co-existence of quasi-particles and phonons, as well as their interaction in a nucleus, are taken into account in the process of gamma-decay. Here we present a new improvement to the Dubna practical model for the determination of nuclear level densities and radiative strength functions. The new practical model guarantees a good description of the available intensities of the two step gamma cascades, comparable to the experimental data accuracy.

1 Introduction

The development of theoretical models of nuclear structures requires a set of experimental information of the excited levels density, ρ, (with given quantum numbers) and of the values of the partial width (radiative strength function), Γ, of all possible decay channels. Correct interpretation of the dynamics of the nuclear transitions, in a broad variety from the simple low-lying levels (e.g., quasi-particle or phonon structure) to the very complex compound-states is possible by the theoretical calculations if those experimental data are available. One of the most suitable techniques for determination of required nuclear mater parameters (ρ and Γ) is the two-step gamma cascades methods based on measurement of gamma coincidences following neutron capture [1].

⋆e-mail: `nikola.jovancevic@df.uns.ac.rs`

Based on the experimental data collected by two-step gamma cascades experiment a model for description the gamma-decay of neutron resonance was developed at JINR, Dubna [2, 3]. In this model the level density ρ of quasi-particles in any nucleus is defined using the known model of n-quasi-particle levels. Here we presented the improved version of this model taking into account shell inhomogeneities of the single-particle level spectra and their influence on the functions: $\rho=\varphi(E_{ex})$ and $\Gamma=\psi(E_1)$, where E_{ex} is the excitation energy and E_1 is primary transition energy. The experimental results of two step gamma cascades intensity for 43 nuclei in the $28 \leq A \leq 200$ mass region were fitting by this model. This provide us possibility to extract parameters of nuclear structure such as breaking thresholds of the second and the third Cooper pairs, ratio of the collective level density to the total one or level parity.

2 Dubna two-step gamma cascades method

The two-step gamma-cascades method for obtaining information about the nuclear structure parameters following the thermal neutron captures was developed at FLNP, JINR, DUBNA [2, 3]. From amount of gamma-gamma coincidences the method allows to choose registration events of full energy of two-gamma transition cascade with a sufficiently low background. And the experimental intensity distributions of cascades to the final levels of compound-nucleus with excited energy below ~500–800 keV are obtained from these coincidences. Using the nuclear spectroscopy procedures allows decomposing the initial spectrum on primary and secondary transmission components of cascades with an acceptable uncertainty [2, 3].

The basic idea of this method comes from specific dependence of the two-step gamma- cascade intensity on the partial radiative width Γ and the density of excited levels:

$$I_{\gamma\gamma} = \sum_{\lambda,f}\sum_{i}\frac{\Gamma_{\lambda i}}{\Gamma_{\lambda}}\frac{\Gamma_{if}}{\Gamma_{i}} = \sum_{\lambda,f}\frac{\Gamma_{\lambda i}}{\langle\Gamma_{\lambda i}\rangle m_{\lambda i}}n_{\lambda i}\frac{\Gamma_{if}}{\left\langle\Gamma_{if}\right\rangle m_{if}} \tag{1}$$

where $\Gamma_{\lambda i}$ and Γ_{if} are the partial radiative widths corresponding to the primary and to the secondary transitions; $n_{\lambda i} = \rho\Delta E_i$ is the number of the excited intermediate levels in a certain interval of the excitation energy ΔE_i; $\langle\Gamma_{\lambda i}\rangle$ and $\langle\Gamma_{if}\rangle$ are the average values of the corresponding intervals of the nucleus excitation energy widths; $m_{\lambda i}$ and m_{if} are the number of levels in the same intervals. When this method was developed for the first time it was based on an interactive calculation. Using iterative process with "randomly" chosen functions ρ and Γ, it is possible to obtain the most probable values of level density and radiative width (or radiative strength function).

3 Model of the gamma-decay of neutron resonance

Here we present improved version of the model for the gamma-decay of neutron resonance [2] which can explain the experimental data based on combination of phenomenological and theoretical representations.

The level density, described by an expression for density ρ_l of Fermi levels, was taken from the model of density Ω_n of n-quasi-particle states [4]:

$$\rho_l = \frac{(2J+1)\exp\left(-(J+1/2)^2/2\sigma^2\right)}{2\sqrt{2\pi}\sigma^3}\cdot\Omega_n(E_{ex}), \Omega_n(E_{ex}) = \frac{g^n(E_{ex}-U_l)^{n-1}}{((n/2)!)^2(n-1)!} \tag{2}$$

Here J is the spin quantum number, $g = 6a/\pi^2$ is the density of the single-particle states near Fermi-surface, σ is the cut-off factor (a and σ values were taken from the back-shifted Fermi-gas model

[5]), and U_l, is the energy of the l-th Cooper pair breaking threshold. The effect of the collective enhancement was also included in this model by the coefficient C_{col} of the collective enhancement of the vibrational level density (or both vibrational and rotational ones for deformed nuclei). For a given excitation energy, E_{ex}, the phenomenological coefficient is determined by a theoretical description that can be found in Ref. [3]:

$$C_{coll} = A_l \exp(\sqrt{(E_{ex} - U_l)/E_\nu} - (E_{ex} - U_l)/E_\mu) + \beta \tag{3}$$

where A_l are parameters of density for the vibrational levels above the breaking point for each l-th Cooper pair, E_μ and E_ν determine the change in the nuclear entropy and the change of the quasi-particles excitation energies, respectively. Coefficients A_l for different pairs are fitted independently, as it was done in Ref. [2]. Coefficient β is used for a description of the rotation level density.

Radiative strength functions for $E1$- and $M1$-transitions are determined in this model by Ref. [6]:

$$\begin{aligned} k(E1, E_\gamma) + k(M1, E_\gamma) &= w \frac{1}{3\pi^2\hbar^2 c^2 A^{2/3}} \frac{\sigma_G \Gamma_G^2 (E_\gamma^2 + \kappa 4\pi^2 T^2)}{(E_\gamma^2 - E_G^2)^2 + E_\gamma^2 \Gamma_\gamma^2} + \\ &+ P\delta^- \exp(\alpha_p (E_\gamma - E_p)) + P\delta^+ \exp(\beta_p (E_p - E_\gamma)) \end{aligned} \tag{4}$$

with fitting normalization parameter w and coefficient κ; thermodynamic temperature T; the location of the center of the giant dipole resonance E_G, with width Γ_G and cross section σ_G in the maximum for each nucleus. For description of experimental data of Ref. [3] it is necessary to add one or several narrow peaks to the strength function is based on the data of Ref. [3]. The second summand of Eq. (5) corresponds to the left slope of the peak (energies below the maximum), and the third summand is the right slope (energies above the maximum). Position E_p in the energy scale, amplitudes $P\delta^+$ and $P\delta^-$ and slope parameters α_p and β_p are fitted for each peak independently. At $E_1 \approx B_n$ the fitted ratios Γ_{M1}/Γ_{E1} of $E1$- and $M1$-strength functions are normalized to known experimental values, and their sum Γ_λ is normalized to the total radiation width of the resonance.

The influence of the shell correction δE on the density of the quasi-particle levels were tested in this work. It was done by using the $a(A)$ value, which depends on the excitation energy, included linearly in the parameter of the single-particle density g (see Eq. (2)). For a nucleus with mass A and excitation energy E_{ex}, $a(A)$ is expressed, as [3]:

$$a(A) = \tilde{a}(1 + ((1 - exp(\gamma E_{ex}))\delta E / E_{ex})) \tag{5}$$

where asymptotic value is $\tilde{a} = 0.114 \cdot A + 0.162 \cdot A^{2/3}$ and $\gamma = 0.054$. The δE values slightly varied relative to their evaluations [3] in order to keep an average spacing between neutron resonances (see [2]).

In our model the set of common parameters for fitting (see Eqs. (2, 3)) were:

1) the break up thresholds energies U_l up to l=4,

2) the E_μ and E_ν parameters, which are common for all Cooper pairs

3) the mutually independent parameters A_l of the density of vibrational levels above the break up threshold U_l

4) the coefficients w, κ and β

5) the ratio r of negative parity and the total level density.

Those parameters were used for the description of the intensity $I_{\gamma\gamma}$ (E_1) for 43 nuclei, in the framework of the proposed model.

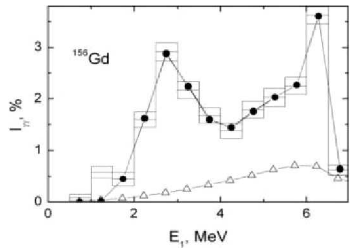

Figure 1. Histogram - experimental cascade intensity and its uncertainties for ^{156}Gd as function of primary cascade quanta E_1. Points - the best fit of the presented practical model; triangles - a calculation of $I_{\gamma\gamma}$ using models of Ref. [5, 6]. Recorded threshold for cascade gammas is $E_\gamma = 520$ keV.

a) **b)**

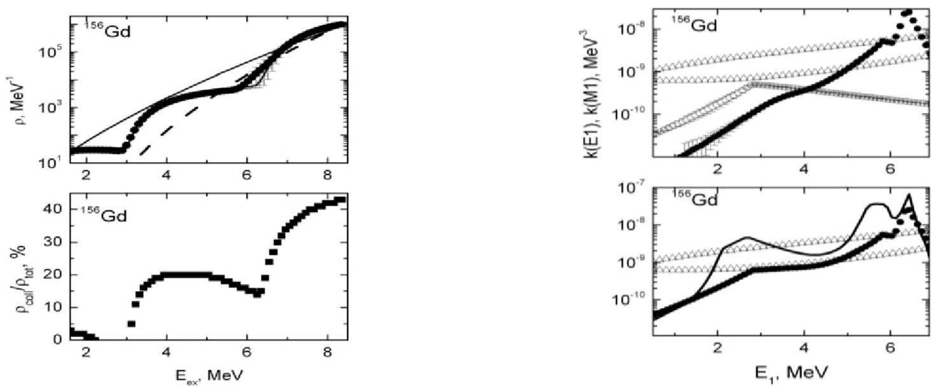

Figure 2. **a)** Level density of ^{156}Gd. *Top:* points are the best fit of level density (uncertainties – scatter of fits for different sets of initial parameters); dashed and solid lines are the level density calculated using the model of Ref. [5], with taking into account the shell correction δE (6) and without δE, correspondingly. *Bottom:* fitted ratio of density of collective levels to the total level density. **b)** Strength function for ^{156}Gd. *Top:* solid points are the best fit of the strength function of $E1$-transitions; open points are the best fit of the strength function of $M1$-transitions. *Bottom:* solid points are a sum of $E1$- and $M1$- strength functions; dash line is the sum of strength functions multiplied by $\rho_{\mathrm{mod}}/\rho_{\mathrm{exp}}$ ratio (Ref. [7]). Calculations using the model of Ref. [6] (lower triangles) and using the model of Ref. [8] (upper triangles) were fulfilled with $k(M1)$= const.

4 Results and discussion

A solution of the system of Eq. (1) is performed by the Monte-Carlo method. The nonlinearity of the strongly correlated equations of the system (1) produces an uncertainty of extracting the ρ and Γ parameters from $I_{\gamma\gamma}$ intensities.

Experimental data on $I_{\gamma\gamma}$ (E_1) are usually obtained with a small total uncertainty and averaged over 500 keV energy intervals. The results for ^{156}Gd are shown, in more detail, in Figs. 1–2. The best fits to $I_{\gamma\gamma}$ (E_1), as well as the fitted level densities and strength functions, are compared to corresponding values calculated using the statistical model. The results and corresponding calculations of level density and radiative strength function for the rest of the investigated nuclei will not be shown in

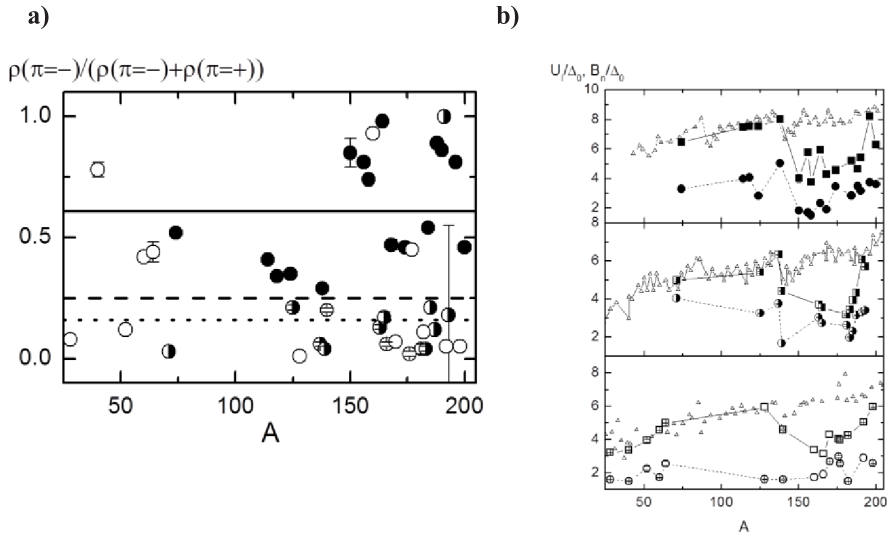

Figure 3. a) A-dependence of the ratios U_l/Δ_0, for the second (points) and the third (squares) Cooper pairs. Full points – even-even, half-open points are even-odd and open points are odd-odd compound nuclei. Triangles – the mass dependence of B_n/Δ_0 ratio. **B)** Mass dependence of the ratio of the level density with negative parity to the total level density at the upper energy border of the E_d and their averages for even-even nuclei (solid lines), even-odd (dashed lines) and odd-odd nuclei (dotted lines). Full points – even-even, half-open points – even-odd and open points – odd-odd compound nuclei.

this publication. However, we are presented here obtained results for some of parameters of nuclear structure.

One important parameter is the breaking thresholds for Cooper pairs. In the present analysis was confirmed the previous results about the connection between the shape of the investigated nucleus and the breaking thresholds. That was established for the first time in our prior analysis [3]. As the breaking thresholds differ for nuclei with various nucleon parities and depend on the average pairing energy (Δ_0) of the last nucleon, the mass dependencies for the ratios of the break up thresholds of the second and the third Cooper pairs to Δ_0, as well as the mass dependence of the binding energy to Δ_0, are presented in Fig. 3. As it can be seen in Fig. 3, there is a noticeable difference in U_2/Δ_0 and U_3/Δ_0 ratios for spherical and deformed nuclei in contrast to B_n/Δ_0.

In this work it was also obtained information about levels parity. For determination of the part $r = \rho(\pi-)/(\rho(\pi-) + \rho(\pi+))$ of levels $\rho(\pi-)$ with negative parity, a linear extrapolation for r value was applied in the $E_d \leq E_{ex} \leq B_n$ energy interval. At that, in the B_n point we use generally accepted assumption, that $\rho(\pi-) = 0.5(\rho(\pi-) + \rho(\pi+))$, and $\rho(\pi-)$ value in this energy point was fixed, and at the E_d energy the $\rho(\pi-)$ value varied.

The calculated ratios of density of the levels with negative parity to the total level density are shown in Fig. 3. The averages of these ratios are 0.61(22), 0.25(28) and 0.16(16) for even-even, even-odd and odd-odd nuclei, respectively (and for odd-even ^{177}Lu it is 0.65(1)). Hence, the behavior of the gamma-decay process is different for nuclei of various nucleon parities.

5 Conclusion

In this work we presented new variant of model for gamma decay of neutron resonance, taking into account shell inhomogeneities of the single-particle level spectra. We used this model for fitting the experimental intensity of two-step gamma cascades and to obtain information about parameters of nuclear structure.

The data on Cooper pair break-up energies, obtained with a high accuracy, are sufficient to conclude that the dynamics of interaction between superfluid and normal phases of a nucleus depends on its' shape. Our model allows for a separate determination of the density of vibrational levels between the breaking thresholds of the Cooper pairs.

Unfortunately, an existence of the sources of uncertainties of the sought ρ and Γ functions is a fundamental problem, and it is inevitable for any nuclear model used for experimental data analysis and for predictions of the spectra and cross sections. There are also fluctuations of the intensities of gamma-transitions in different nuclei, which has a contribution to the systematical error. Nevertheless, the practical model showed one possibility to describe the data of the two-step experiments with the accuracy that exceeds the statistical one.

For future development of reliable model of cascade gamma decay new experimental data are necessary. Because of that, ^{108}Ag, ^{110}Ag, ^{104}Rh and ^{56}Mn nuclei will be investigated by two step gamma cascade method.

References

[1] V.G. Soloviev, Nuclear Physics A **586**(2), 265 (1995)
[2] A.M. Sukhovoj, Phys. Atom. Nucl. **78**, 230 (2015)
[3] A.M. Sukhovoj, L.V. Mitsyna, N. Jovancevic, Phys. Atom. Nucl. **79**, 313 (2016)
[4] V.M. Strutinsky, in Proceedings of the International Congress on Nuclear Physics, Paris, France, p. 617 (1958)
[5] W. Dilg, W. Schantl, H. Vonach, and M. Uhl, Nucl. Phys. A **217**, 269 (1973)
[6] S.G. Kadmenskij, V.P. Markushev and W.I. Furman, Sov. J. Nucl. Phys. **37**, 165 (1983)
[7] N. Jovancevic, A.M. Sukhovoj, W.I. Furman, and V.A. Khitrov, in Proceedings of XX ISINN, Preprint E3-2013-22, p. 157 (Dubna, 2013); `http://isinn.jinr.ru/past-isinns.html`
[8] P. Axel, Phys. Rev. **126**, 671 (1962)

ISINN-24

Neutron Spectroscopy, Nuclear Structure, Related Topics

Chinese Spallation Neutron Source

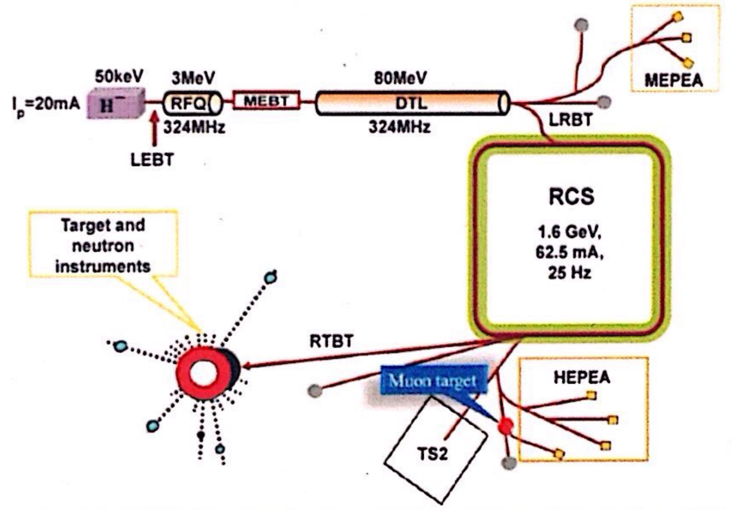

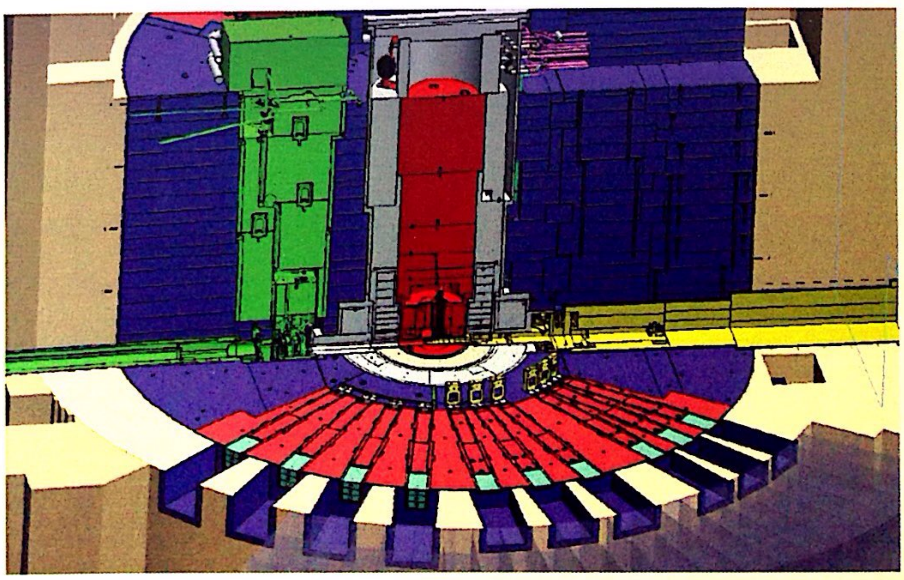

Dubna 2017

Joint Institute for Nuclear Research

FUNDAMENTAL INTERACTIONS & NEUTRONS, NUCLEAR STRUCTURE, ULTRACOLD NEUTRONS, RELATED TOPICS

XXIV International Seminar on Interaction of Neutrons with Nuclei

Dubna, Russia, May 24–27, 2016

Proceedings of the Seminar

Dubna • 2017

УДК 539.125.5(042)
ББК 22.383.2я431+22.383.5я431+22.383.25я431
F97

Organizing Committee

W. I. Furman (*co-chairman*), V. N. Shvetsov (*co-chairman*),
E. V. Lychagin (*scientific secretary*), Yu. N. Kopatch,
P. V. Sedyshev, L. V. Mitsyna, M. V. Frontasyeva

Secretariat: T. S. Donskova (*seminar co-ordinator*),
N. A. Malysheva, T. L. Pikelner

The contributions are reproduced directly from the originals presented by the Organizing Committee.

Fundamental Interactions & Neutrons, Nuclear Structure, Ultracold Neutrons, Related
F97 Topics: Proceedings of the XXIV International Seminar on Interaction of Neutrons with Nuclei (Dubna, Russia, May 24–27, 2016). — Dubna: JINR, 2017. — 442 p.
ISBN 978-5-9530-0465-7

This collection of papers reflects the present state of neutron-aided investigations of the properties of the nucleus, including fundamental symmetries, properties of the neutron itself, neutron-excited reactions, and the parameters of the nucleus that determine the reaction cross section, as well as the latest theoretical development of all these problems. The works on experimental investigations in the physics of fission by neutrons of various energies are presented in great detail. The current state of experiments on the physics of ultracold neutrons and facilities to obtain them is described at length. The status achieved by now of the latest (from the viewpoint of technique) experiments and environment studies is covered as well.

Фундаментальные взаимодействия и нейтроны, структура ядра, ультрахолодные нейтроны, связанные темы: Труды XXIV Международного семинара по взаимодействию нейтронов с ядрами (Дубна, Россия, 24–27 мая 2016 г.). — Дубна: ОИЯИ, 2017. — 442 с.
ISBN 978-5-9530-0465-7

В сборнике представлено современное состояние исследований свойств ядра с помощью нейтронов: фундаментальных симметрий и свойств самого нейтрона, возбуждаемых им реакций и параметров ядра, определяющих их сечения, а также последние теоретические разработки всех этих вопросов. Очень детально представлены работы по всем аспектам, связанным с экспериментальными исследованиями физики деления ядра нейтронами различных энергий. Достаточно полно описано современное состояние экспериментов по физике ультрахолодных нейтронов и установок для их получения, а также достигнутый к настоящему времени статус методически новейших экспериментов и результаты экологических исследований.

УДК 539.125.5(042)
ББК 22.383.2я431+22.383.5я431+22.383.25я431

ISBN 978-5-9530-0465-7

Nuclear Structure, Nuclear Data

Reactions with Fast Neutrons

Verification of the Practical Model of Cascade Gamma-Decay

Sukhovoj A.M.[1], Mitsyna L.V.[1], Zeinalov Sh.[1], Vu D.C.[1,2],
Jovancevic N.[3], Knezevic D.[3], Krmar M.[3], Dragic A.[4]

[1]*Joint Institute for Nuclear Research, Dubna, 141980, Russia*
[2]*Vietnam Academy of Science and Technology Institute of Physics, Hanoi, Vietnam*
[3]*University of Novi Sad, Facility of Science, Department of Physics, Novi Sad, Serbia*
[4]*Institute of Physics, Belgrade, Serbia*

Abstract

To determine simultaneously both the level density ρ and the partial widths Γ of nuclear reaction products is possible only by fitting the intensities of the cascades between fixed initial, any intermediate and some final levels. Experimental total gamma-spectra with their calculations by the practical model of the gamma-decay were compared. Verification of ρ and Γ values obtained earlier and evaluation of the achieved accuracy of the practical model were done. Determined using the practical model ρ and Γ systematic uncertainties led to a conclusion that the calculated accuracy of spectra of products from any nuclear reaction will be several percents.

Introduction

An adequate and correct mathematical model of nucleus is need for understanding and subsequent prediction of the nuclear-physical parameters for any nuclei. The basis of this model is experimental determination of both the excited level density ρ and the widths Γ of partial processes of excitation and decay of any given level. In the case if the space D_λ between excited levels is less than detector resolution FWHM only an average of ρ and Γ parameters may be determined.

Excitation energy E_{ex} determines unambiguously and simultaneously both the level density and the strength functions $k=\Gamma/(A^{2/3}\cdot E_\gamma^3\cdot D_\lambda)$ for any nucleus with A mass number and energy E_γ for emitted gamma-rays below neutron binding energy B_n. It means that level density and partial radiative widths (or corresponding strength functions k) must be determined simultaneously from the system of equations, which connects experimental data with the sought parameters of $\rho=f(q_1, q_2,...)$ and $k=\varphi(p_1, p_2,...)$ functional dependencies.

With regard to ordinary spectra of emission of reaction products and reaction cross sections at any energy E_{ex} they are determined by the ρ and Γ product normalized on a constant. As a strong correlation of ρ and Γ is inevitable in this case, the simultaneous determination of these values is impossible without using any subjective assumptions or untested hypothesis. Correspondingly, calculation of cross sections of nucleon reactions gives an addition to an uncertainty connected with errors of emission widths for nucleon products.

All experimental information about nuclear structure is determined only by shapes of ρ and Γ dependencies on energy. And low count of ρ and Γ absolute values measured in several energy points is not enough to understand all nucleus properties. Measuring the intensities of any two-step cascades between compound-state and some group of the low-lying nuclear levels allows to determine shapes both of level density dependence on the excitation energy and of average dependence of decay widths of intermediate levels on energy of emitted products at the compound-state decay. Now it was done in Dubna for 43 nuclei in the mass region $28 \leq A \leq 200$ for a measured part of intensities of primary gamma-transitions of two-step cascades [1, 2].

Experimental data on Fermi- and Bose-system interaction

Experimental research of the dynamics of interaction of Fermi- and Bose-states of nuclear matter allows to obtain a new fundamentally information about this nuclear process, so properties of nucleus and of macro systems (as objects for this process investigation) differ in principle. For example, to date in Dubna the unique information is obtained [3, 4] about possible dependency of breaking thresholds of some Cooper pairs of nucleons on the nuclear shape, what is presented in Fig. 1. It is found that the region of deformed nuclei at A>150 the second and the third breaking pairs thresholds are smaller than these thresholds for spherical nuclei. To observe something like that in a superconducting macro system of electron gas is impossible, at least, in the absence of a technique of production of special nanosystem contained combinations of linear nano objects (type of conductor/inculator).

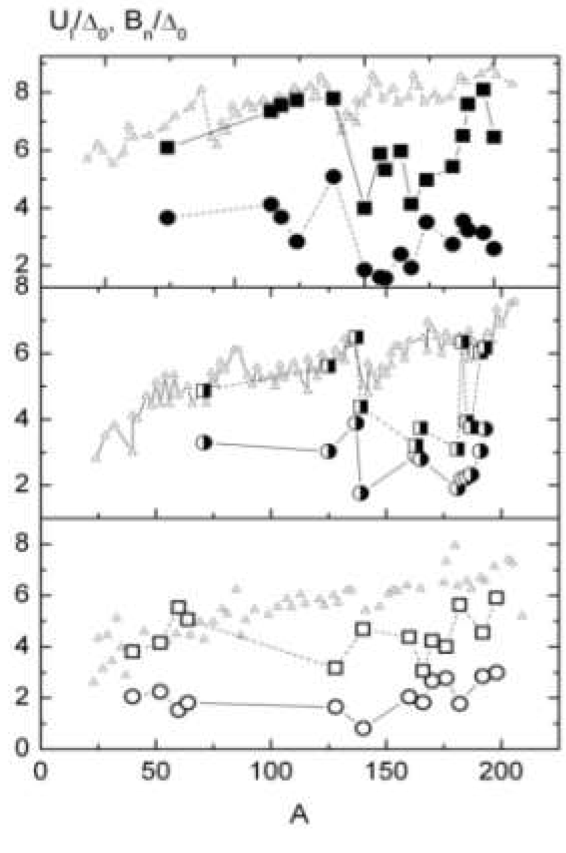

Fig.1. Mass dependencies of ratios of breaking thresholds U_l for the second (points) and the third (squares) Cooper pairs to the approximated average pairing energy Δ_0 for even-even compound nuclei (upper part), for even-odd nuclei (in the middle) and for odd-odd compound nuclei (bottom part). Triangles are known mass dependencies of B_n/Δ_0.

The intensities $I_{\gamma\gamma}(E_1)$ of two-step cascades between neutron resonance (or another compound-state) λ and some group of low-lying nuclear levels f through any intermediate levels i for a fixed energy E_1 of primary transition are written by a system of equations of type:

$$I_{\gamma\gamma}(E_1) = \sum_{\lambda,f}\sum_{i}\frac{\Gamma_{\lambda i}}{\Gamma_{\lambda}}\frac{\Gamma_{if}}{\Gamma_{i}} = \sum_{\lambda,f}\frac{\Gamma_{\lambda i}}{<\Gamma_{\lambda i}> m_{\lambda i}} n_{\lambda i}\frac{\Gamma_{if}}{<\Gamma_{if}> m_{if}}, \quad (1)$$

where $m_{\lambda i}$ is a number of levels of excited primary gamma-transitions in intervals from the energy of initial level λ to an energy of intermediate level i, m_{if} is a number of levels of excited secondary transitions in intervals from the energy of intermediate level i to energy of the final level f, $n_{\lambda i}$ is a number of intermediate cascade levels in a set of small energy intervals. From the system (1), which connects an unknown level number n (or m) and unknown partial widths, a set of p and q parameters of the model functions $\rho=f(p_1, p_2, ..)$ and $\Gamma=\varphi(q_1,q_2,..)$ with some uncertainty is determined.

The experimental spectrum of the two-step cascade intensity is a sum of infinite set of possible pairs of mirror-symmetrical distributions. Ignoring this circumstance [5, 6] distorts entirely a picture of investigated process [7, 8]. Actually, using nuclear-spectroscopy methods the experimental spectra of cascades between initial and finite levels may be factorized on two mirror-symmetrical distributions as functions of energy of primary and secondary quanta of the cascades [9] with an acceptable systematic error. In a case of approximation of pure experimental spectra [5, 6] (without an execution of above-mentioned procedure) a likelihood function values can't give a reliable result for desired ρ and Γ values.

A necessary condition for determination of reliable ρ and Γ functions is an existence of the experimental data on branching coefficients of partial radiative widths of decay of all possible levels i onto limited group of final low-lying levels. In other words, the experiment is needed for recording all possible cascades connected known initial level λ of the nucleus and finite level f through any intermediate levels i. The required result can be obtained only if to take into account Boson part of nuclear excitations and theoretical (or phenomenological) assumptions of ρ and Γ functions for describing the intensity distributions of all primary quanta of cascades and branching coefficients $B_r(E_2)$ for any secondary quanta. There is a nonrecoverable systematic error of nuclear parameters determined such a way. This error causes are experimental systematic errors and mismatch of models for ρ and Γ to their obtained distributions.

We used the model [10] with varied weight and thermodynamic temperature, which gives a possibility for initialization of Γ functions in a wide range of their initial values. For ρ initialization both the function [12] elaborated for a growing number of quasi-particles of a level density and some phenomenological assumptions [13] were used. Besides, inasmuch as experimental spectra of two-step cascades are measured only for some part of intensities of primary gamma-transitions, an uncertainty of the best ρ and Γ fits gives an addition to inevitable systematic uncertainty.

In spite of the fact that an inevitable systematic uncertainty exists, the calculation results are good enough. To evaluate a quality of the ρ and Γ obtained data is possible by comparison of experimental and calculated gamma-spectra (Fig. 2–6).

Features of the total gamma-spectra at thermal neutron capture

Assumed by us normalization of total gamma-spectrum satisfies the condition $\Sigma I_\gamma E_\gamma = B_n$, where I_γ is an intensity, E_γ is a gamma-quantum energy, and B_n is a neutron binding energy. Consequently, a sum of all possible cascades with any quanta multiplicity doesn't depend on ρ and Γ function types. For determination of shapes of ρ and Γ functions it is need to use only individual cascades ($I_\gamma E_\gamma = \varphi(E_\gamma)$ dependencies). For example, strength function increasing for a part of cascades (Fig.2) is obligatory accompanied by a change both level density and strength functions for the rest cascades.

A distortion of information extracted from the comparison of experimental spectrum with a calculated one is caused by a difference of shapes of these spectra only. And valid information can be obtained if to compare the experiment with two or more calculated spectra. It was done by developed in Dubna practical model of cascade gamma-decay with different representations for the radiative strength functions and for coefficient of vibrational level density enhancement. Two of these representations with various shapes of several (not more than four) local peaks in the functional dependencies on energy of *E*1- and *M*1-primarily transitions of two-step cascades are presented below.

In a framework of quasi-particle model of nucleus authors of [14] calculated a shape of fragmentation of strength of one-particle states at their different deviation from Fermi-surface. Calculated fragmentation sufficiently depended on energies of initial quasi-particle state and of photon excitation. A practical result of these calculations is asymmetry of distribution of strength of fragmented state. If to suppose that local peaks in cascade gamma-spectra (Fig. 2) appear in consequence of defined process we could wait that these peaks are asymmetric. We described each of them by a simple analytical function and added several peaks to a smooth energy dependency expected on a base of modified model [10] for both mutlipolarities with varied thermodynamic temperature *T* and normalization parameter *w*:

$$k(E1,E_\gamma),k(M1,E_\gamma) = w\frac{1}{3\pi^2\hbar^2c^2A^{2/3}}\frac{\sigma_G\Gamma_G^2(E_\gamma^2+\kappa 4\pi^2T^2)}{(E_\gamma^2-E_G^2)^2+E_G^2\Gamma_G^2} + \text{ several local peaks.} \quad (2)$$

Here E_G , Γ_G and σ_G are location of the center, width and cross section in maximum of giant dipole resonance, correspondingly.

In the first variant of calculations each of the local peaks was described as:

$$P\delta^-\exp(\alpha_p(E_\gamma-E_p))+P\delta^+\exp(\beta_p(E_p-E_\gamma)), \quad (3)$$

where the first summand is a left slope of peak (energies below maximum) and the second summand is a right slope (energies above maximum). Position E_p, amplitude *P* and slope parameters α_p, δ– and β_p, δ+ for each peak are determined independently.

In the second case each of the local peaks was described by asymmetric Lorentzian curve:

$$k = W_i\frac{(E_\gamma^2+(\alpha_i(E_i-E_\gamma)/E_\gamma))\Gamma_i^2}{(E_\gamma^2-E_i^2)^2+E_\gamma^2\Gamma_i^2}. \quad (4)$$

Parameters for each *i*-th peak are similar to ones in model [KMF]: center position E_i, width Γ_i, amplitude W_i and asymmetry parameter $\alpha_i \sim T^2$. Expression $\alpha_i(E_i-E_\gamma)/E_\gamma$ grows with increasing B_n–E_i value from zero in the center of peak to maximum at B_n energy and decreases at excitation energy fall. Peaks of *E*1- and *M*1-strength functions are presented by the same expressions.

In Fig. 2 the experimental intensities of two-step cascades and their best fits for 12 nuclei are compared. A quality of measured intensity fitting (χ^2) for all nuclei in cases of (3) and (4) peak shapes is practically the same what gave a possibility to test surely the obtained ρ and Γ values for the total gamma-spectra calculation. If ρ and Γ functions from the statistical model of nucleus are used in calculations there is a mismatch what is seen also in Fig.2. At upper row of Figs. 3–6 the best fits of densities for intermediate cascade levels are presented.

Fractures of level density curves for spherical nuclei correspond to breaking thresholds of the second Cooper pairs, and fitted breaking thresholds of the third pair for these nuclei are near or above neutron binding energy. For deformed and transition nuclei the breaking thresholds of the fourth pair were found also near B_n.

Calculated total gamma-spectra

The fitted data for two chosen forms (2, 3) of the local peaks of strength functions are shown in Figs. 3–6. Fitted ρ values were compared with calculated ones from back shifted Fermi-gas model [11] and from model with taking into account an influence of shell inhomogeneities on a density of single-particle states near Fermi surface [13]. And sums of the strength functions of *E*1- and *M*1-transitions and calculated total gamma-spectra (for 10 nuclei – at capture of thermal neutrons [15]; and for ^{198}Au, ^{128}I [16] – at capture of fast neutrons) are also shown in Figs. 3–6.

For any cascade quantum a fixed threshold 520 keV was chosen because of too complex shape of annihilation line 511 keV and too small cascade primary transition intensities E_1<511 keV. So an intensity of the total experimental gamma-spectrum was compared with a calculated one in $0.52 < E_\gamma < B_n - E_d$ interval of gamma-quanta energy only.

In all cases the total calculated and experimental gamma-spectra were normalized on a sum of $I_\gamma E_\gamma$ products. For a model variant (2) two calculation results of total gamma-spectra were presented in Figs. 3–6. Calculations were done with and without a compensation of local reduction of level density taken into account [1– 4] by corresponding coefficient of increasing of strength functions:

$$M=\rho_{mod}/\rho_{exp} , \qquad (5)$$

where ρ_{exp} is a level density obtained from experimental data, and ρ_{mod} is level density from Fermi-gas model. The level densities and radiative strength functions obtained from theoretical representations of statistical model of nucleus and ones calculated using presented model are compared in Figs. 3–6.

Results of all fittings shown in Figs. 3–6 indicate unambiguously that level density and radiative strength functions for correct calculations of any nuclear-physical parameters had to take into account effects of nucleon pairing and existence of the levels with sizeable vibrational components of wave-functions near neutron binding energy and, most likely, at higher energies.

In the Table there are ratios $2(I_{exp}-I_{cal})^2/(I_{exp}+I_{cal})$ of total gamma-spectra intensities in percents for 12 chosen nuclei. In I and II columns are the calculations with use of peak shapes (3) of strengths functions, and calculations in III and IV columns were done using peak shapes (4). In calculations presented in I and III columns it was supposed that level densities and strength functions are independent (M=1), and in calculations from II and IV columns a compensation (5) was taken into account.

Table 2. $2(S_{exp}-S_{cal})^2/(S_{exp}+S_{cal})$ ratios of total gamma-spectra

Nucleus	I	II	III	IV
^{60}Co	36	34	22	20
^{114}Cd	26	28	24	26
^{128}I	15	9	15	9
^{150}Sm	20	24	17	9.5
^{156}Gd	15	15	19	19
^{158}Gd	20	20	20	20
^{168}Er	32	34	11	17
^{182}Ta	13	16	17	14
^{192}Ir	18	13	26	11
^{196}Pt	22	16	22	15
^{198}Au	20	17	15	8
^{200}Hg	34	28	30	30

Comparing the data of calculations presented in the Table we can do a following resume.

1) The main features of total gamma-spectra (at E_γ =2–3 MeV and some below the neutron binding energy) are reproduced by calculations accurately enough.
2) Description of the local peaks in radiative strength functions by two exponents (3) gives greater distortion between calculated and experimental total gamma-spectra than Lorentzian description (4).
3) In many ways an existence of distortion is caused by insufficient statistical accuracy of data on intensities of measured cascades (changes of level density and radiative strength functions are noticeable if χ^2 of the data from Fig. 2 vary within a few percents). If to use Monte-Carlo method for the system (1) solving the likelihood function always has the same inaccuracy.
4) Practically it is not possible to describe sums of radiative strength functions with a maximal accuracy by smooth functional dependencies because there are peaks caused by influence of structure of wave-functions of nuclear fragmented state on matrix elements of all cascade transitions. There is no any reason of an absence of similar dependence in cascades with multiplicity of 3 quanta or more. This proposition means that to describe exactly a total gamma-spectrum only by nuclear parameters obtained from $I_{\gamma\gamma}$ fittings (Fig.2) is unachievable.
5) An evaluation of systematic errors of calculated total gamma-spectra allows to wait an accuracy of the practical model of some percents for calculating the spectra of nuclear reaction products. It may be achieved if a statistic accuracy of an experiment on cascade intensity measuring will be, at least, 3–10 times more than now. In order to increase the practical model accuracy it is need also to develop a theoretical model of vibrational level density with taking into account both sequential breaking of Cooper pairs of neutrons and protons (an appearance of mixed neutron-proton pairs may be possible at some excitation energies also) and corresponding change of quasi-particle level density.

Conclusion

A comparison of results obtained in different variants of Dubna model with an available set of experimental $I_{\gamma\gamma}$ data shows that determination of breaking threshold of the second Cooper nucleon pair was done with an excellent accuracy. It isn't possible to determine from the $I_{\gamma\gamma}$ data the breaking threshold of the first Cooper pair because density of low-lying levels is small. But it is need to take its existence into account in $I_{\gamma\gamma}$ analysis so the condition of equality of fitted and experimental level densities had to be kept in the point E_d of transition from discrete individual levels to a range of unresolved ones.

An uncertainty of the breaking threshold determination for each consequent pair grows because number of quasi-particles (and an appropriate derivative $d\rho/dE_{ex}$ [Str]) quickly increase. In addition, an increase of correlation between the breaking threshold of consequent Cooper pairs and a coefficient of vibrational level density inhancement may give the similar effect.

An existence of the sources of uncertainties of the sought ρ and Γ functions is a fundamental problem and it is inevitable for any nuclear model used for experimental data analysis and for prediction of spectra and cross sections.

References

[1] A.M. Sukhovoj, Phys. Atom. Nucl. **78,** 230 (2015).

[2] L.V. Mitsyna, A.M. Sukhovoj, in *Proceedings of XXII International Seminar on Interaction of Neutrons with Nuclei*, *Dubna, May 2014,* Preprint № E3-2015-13 (Dubna, 2015), p. 245; http://isinn.jinr.ru/past-isinns.html.

[3] A.M. Sukhovoj, L.V. Mitsyna, and N. Jovancevich, Phys. Atom. Nucl. **79,** 313 (2016).

[4] L.V. Mitsyna, A.M. Sukhovoj, in *Proceedings of XXIII International Seminar on Interaction of Neutrons with Nuclei*, *Dubna, May 2015,* Preprint № E3-2016-12 (Dubna, 2015), p. 299; http://isinn.jinr.ru/past-isinns.html.

[5] M. Krticka et al., Phys. Rev., C. **77**, 054319(2008).

[6] A. Voinov et al., Phys. Rev., C. **81**, 054607(2010).

[7] A.M. Sukhovoj, V.A. Khitrov, Phys. At. Nucl., **72**, 1426(2009)

[8] A.M. Sukhovoj, and V.A. Khitrov, in *Proceedings of XVIII International Seminar on Interaction of Neutrons with Nuclei*, *Dubna, May 2002,* Preprint № E3-2011-26 (Dubna, 2011), p. 180; http://isinn.jinr.ru/past-isinns.html.

[9] S.T. Boneva, A.M. Sukhovoj, V.A. Khitrov, and A.V. Voinov, Nucl. Phys. **589**, 293 (1995).

[10] S.G. Kadmensky, V.P. Markushev and W.I. Furman, Sov. J. Nucl. Phys. **37,** 165 (1983).

[11] W. Dilg, W. Schantl, H. Vonach, and M. Uhl, Nucl. Phys. A **217**, 269 (1973).

[12] V.M. Strutinsky, in *Proceedings of the International Congress on Nuclear Physics, Paris, France, 1958*, p. 617.

[13] V. Ignatyuk, Report INDC-233(L), IAEA (Vienna, 1985).

[14] L.A. Malov and V.G. Soloviev, Sov. J. Nucl. Phys. **26,** 384 (1977).

[15] L.V. Groshev et al., Nuc. Data Table, 5 (1-20) 1968.

[16] J. Voignier., S. Joly, G. Greinier, Nucl. Sci. Eng., 93(1986) 43.

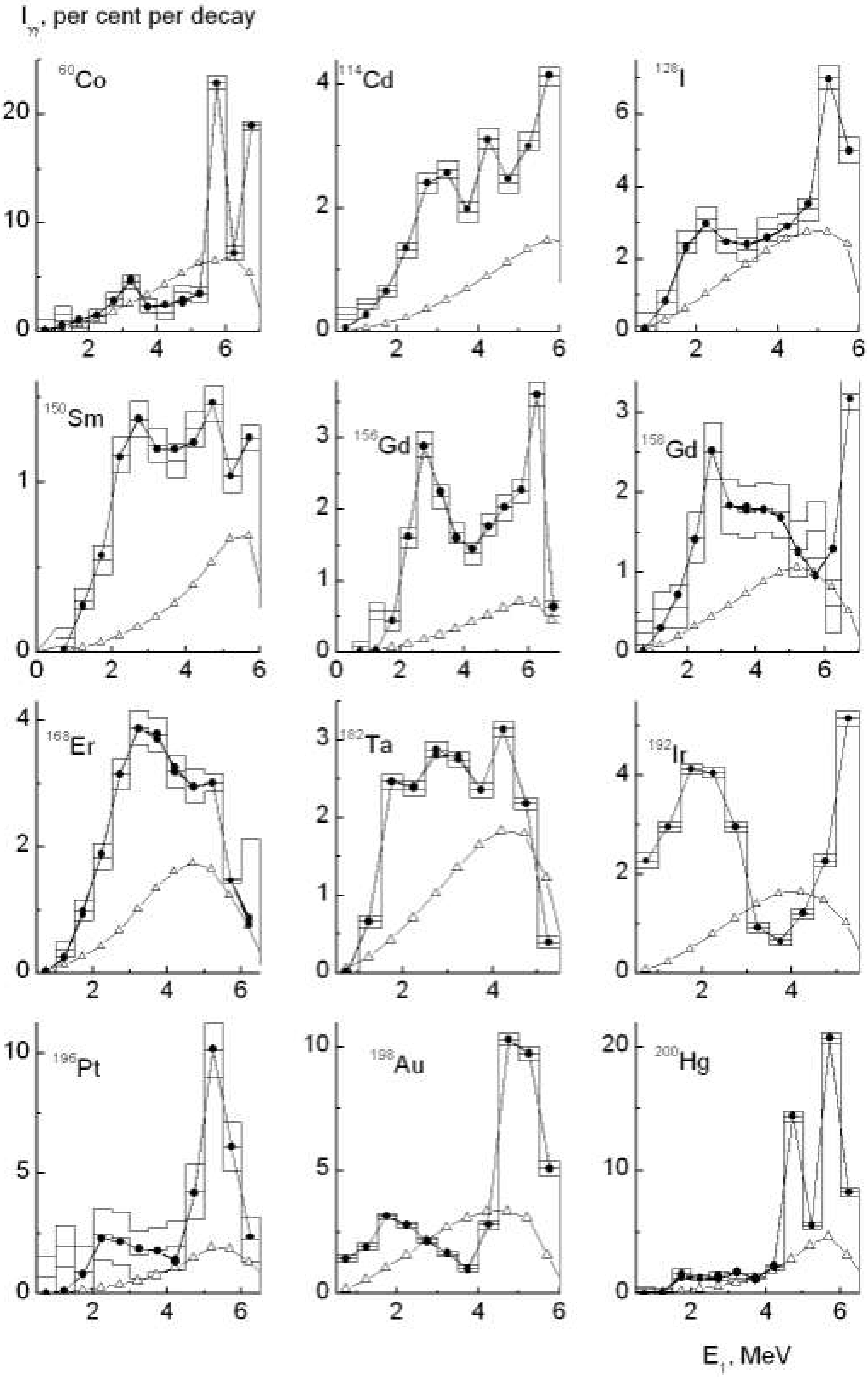

Fig.2. Fitting the experimental intensities $I_{\gamma\gamma}$ for investigated nuclei. Histogram is experiment with its errors, black points are the best fitted values, triangles are calculations by models [10, 11].

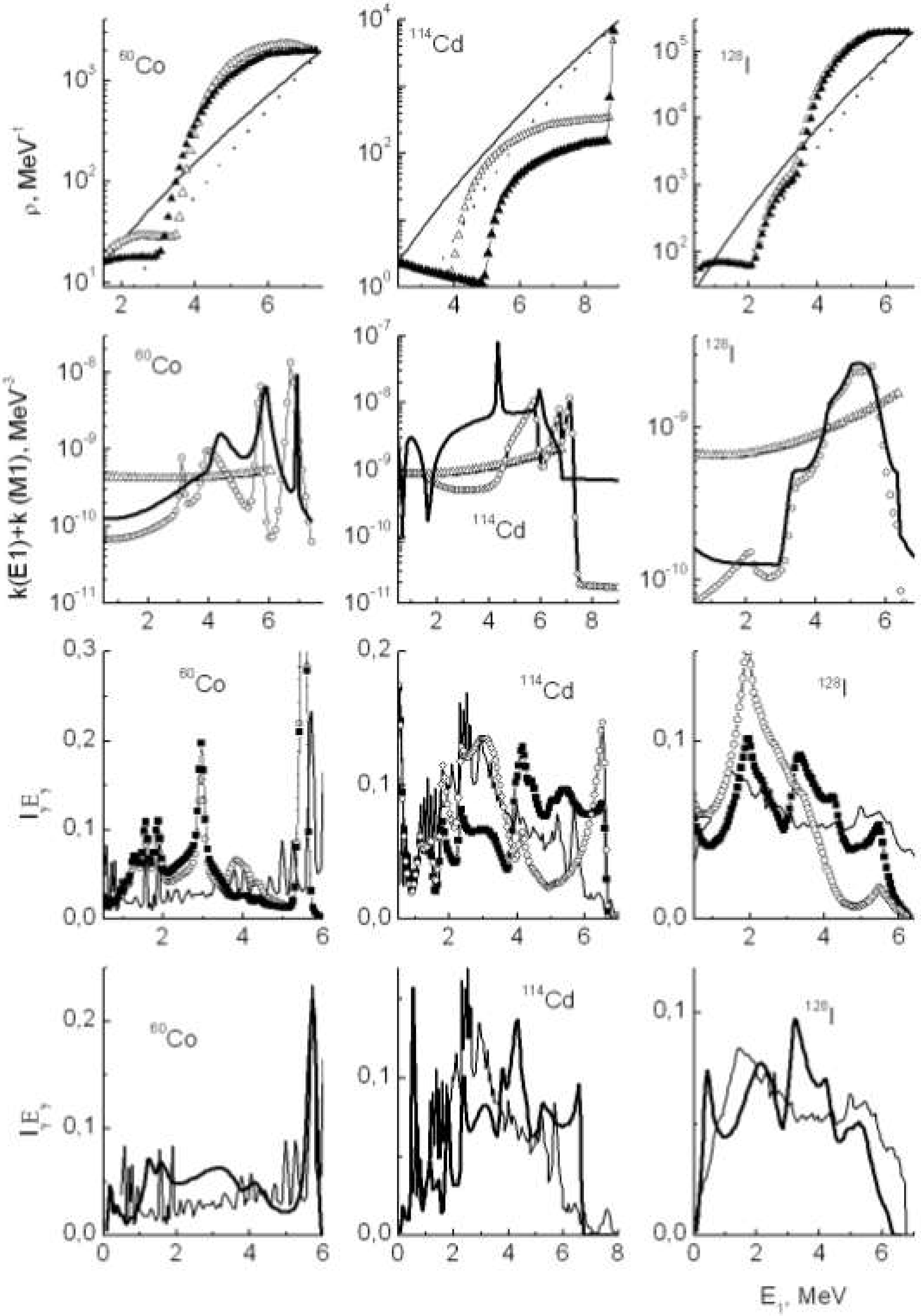

Fig.3. Upper row: level densities calculated with use of function (3) (open triangles), with function (4) (black triangles), and model calculations (solid line – model [11], dashed line – model [13]). Second row: strength functions with local peaks described by exponents (3) (open points), by asymmetric Lorentzian curve (4) (black points), and calculation by model [10] in a sum with k(M1)=const (triangles). Third row: the best fits of the total gamma spectra if local peaks described as (3) (open points) and as (4) (squares), and experimental one (bottom line). Down row: the total gamma spectra calculated using function (4) and condition (5) (bold solid line) and experimental one (solid line).

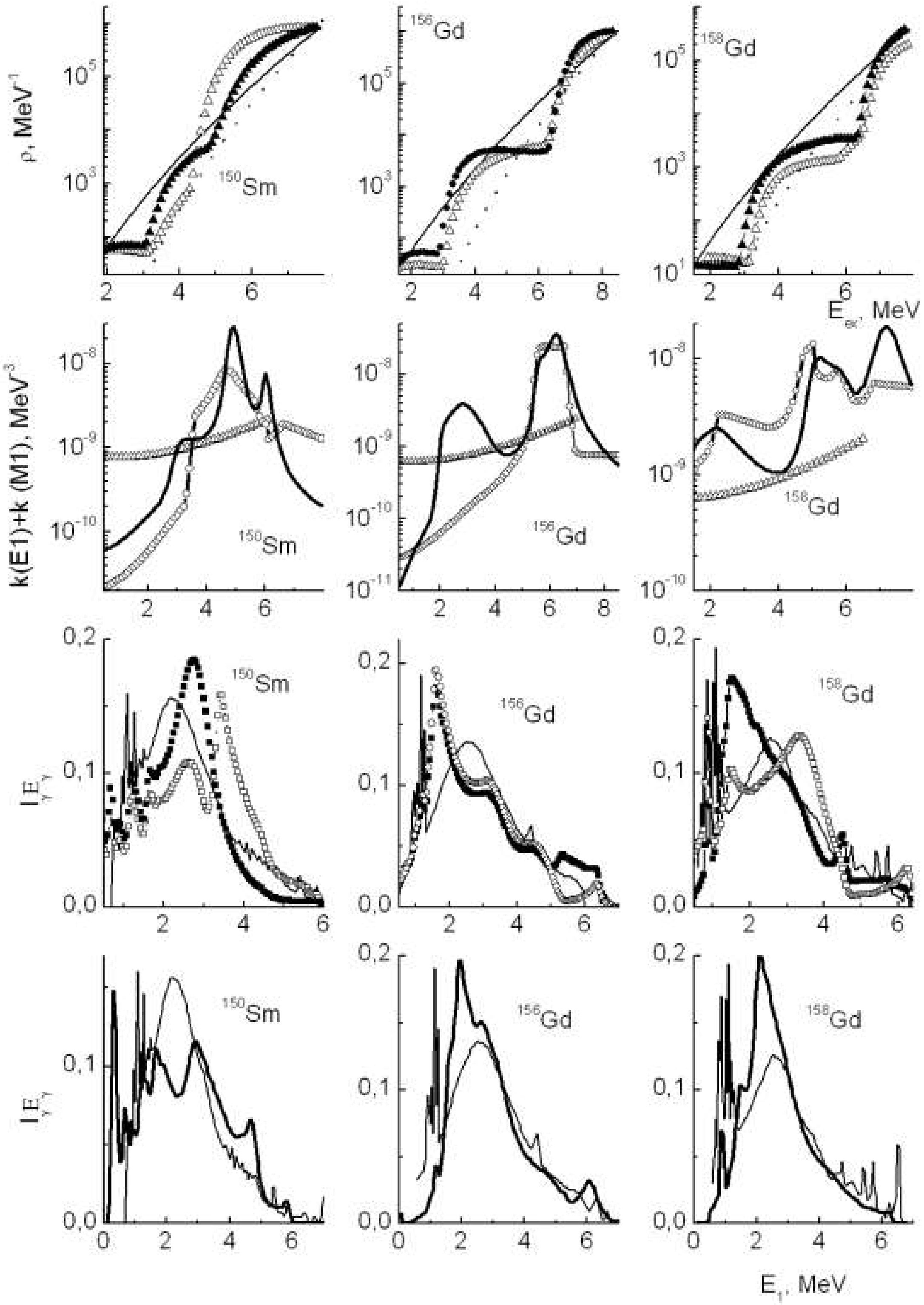

Fig. 4. The same as in Fig.3 for ^{150}Sm and ^{156,158}Gd.

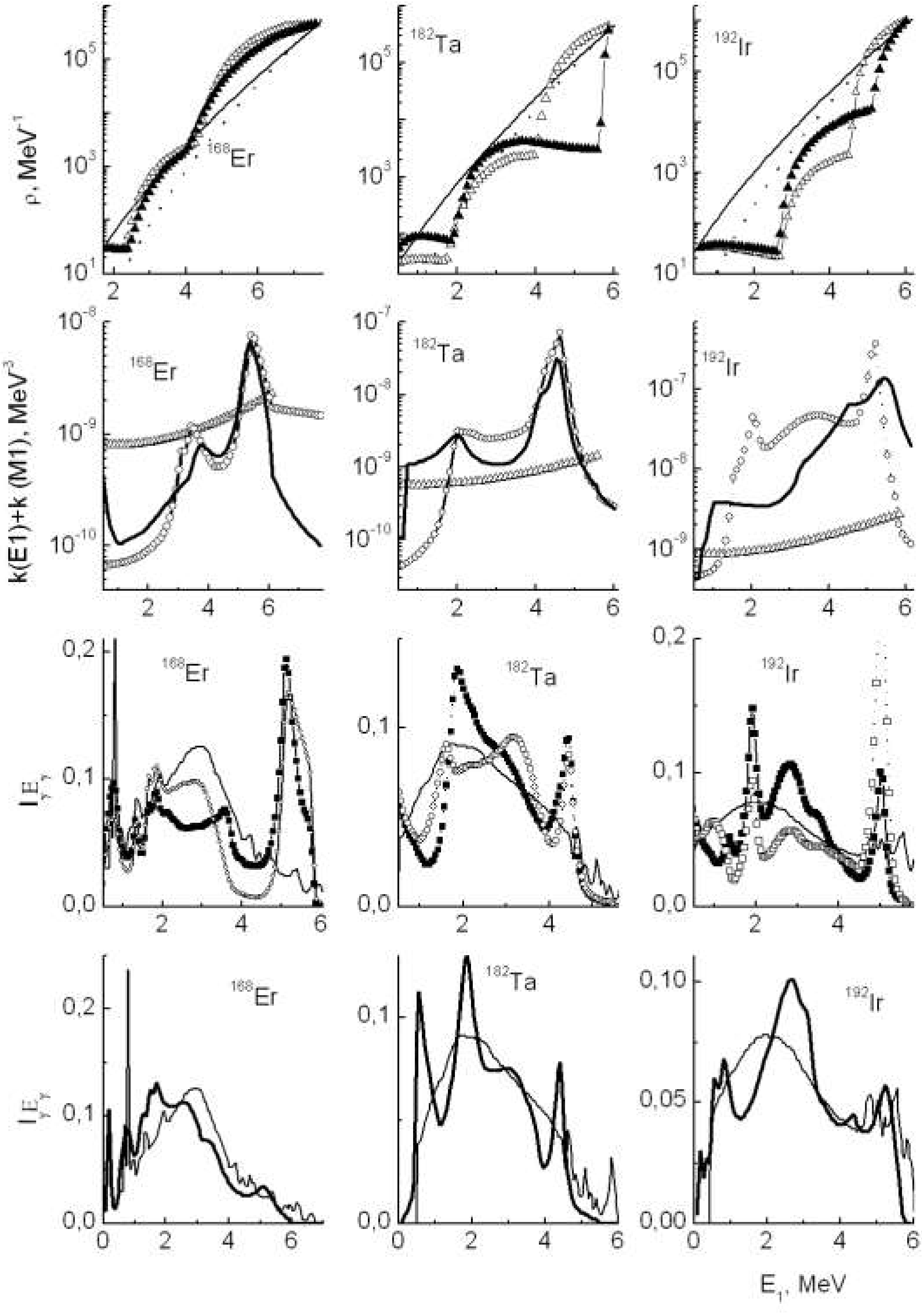

Fig. 5. The same as in Fig. 3 for ^{168}Er, ^{182}Ta, and ^{192}Ir.

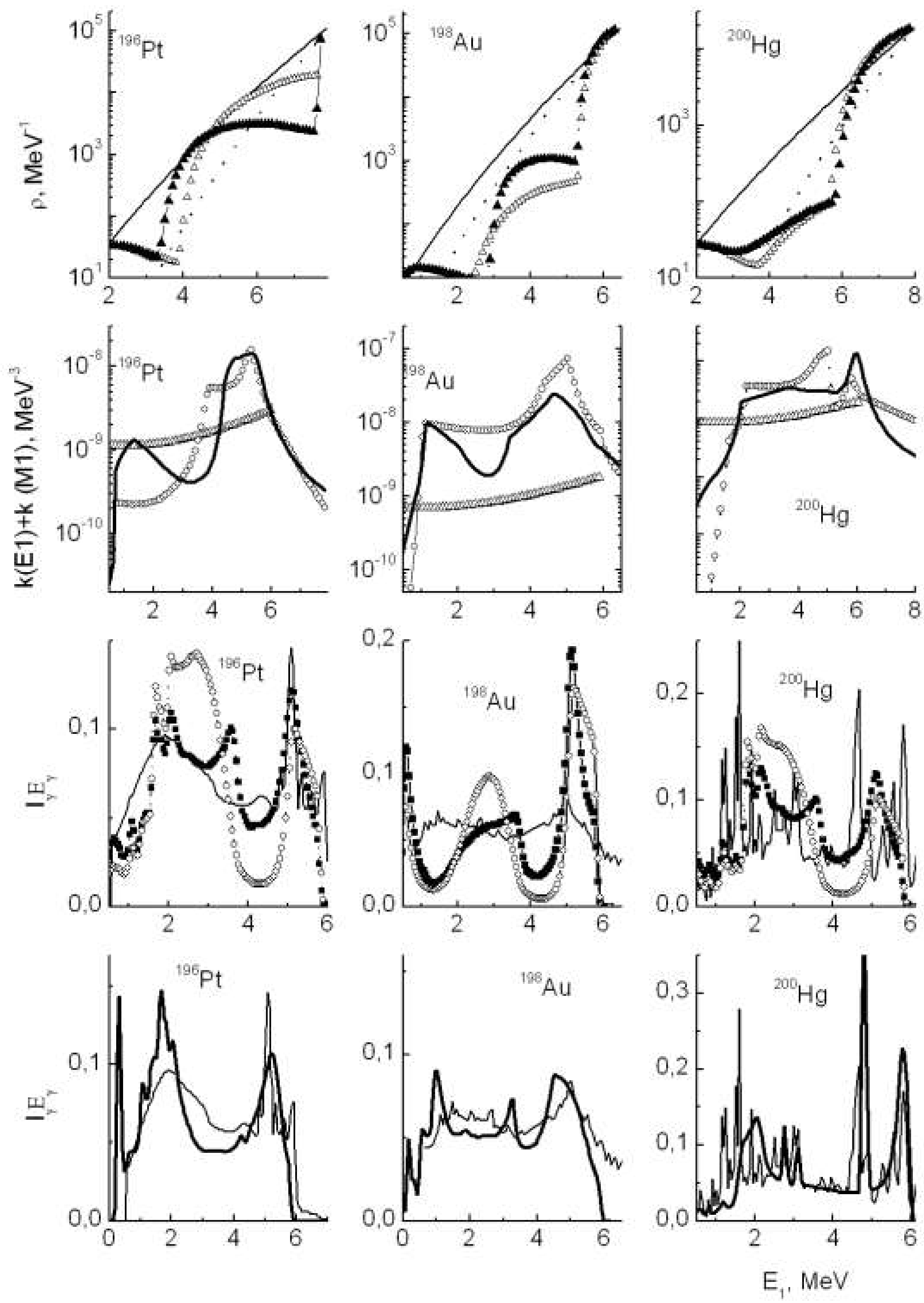

Fig. 6. The same as in Fig. 3 for ^{196}Pt, ^{198}Au, and ^{200}Hg.

Representation of the Radiative Strength Functions in the Practical Model of Cascade Gamma-Decay

Vu D.C.[1,3], Sukhovoj A.M.[1], Mitsyna L.V.[1], Zeinalov Sh.[1], Jovancevic N.[2], Knezevic D.[2], Krmar M.[2], Dragic A.[4]

[1]*Joint Institute for Nuclear Research, Dubna, 141980, Russia*
[2]*University of Novi Sad, Facility of Science, Department of Physics, Novi Sad, Serbia*
[3]*Vietnam Academy of Science and Technology Institute of Physics, Hanoi, Vietnam*
[4] *Institute of Physics, Belgrade, Serbia*

Abstract

The developed in Dubna practical model of the cascade gamma-decay of neutron resonance allows one, from the fitted intensities of the two-step cascades, to obtain parameters both of level density and of partial widths of emission of nuclear reaction products. In the presented variant of the model a part of phenomenological representations is minimized. Analysis of new results confirms the previous finding that dynamics of interaction between Fermi- and Bose-nuclear states depends on the form of the nucleus. It also follows from the ratios of densities of vibrational and quasi-particle levels that this interaction exists near binding neutron energy and probably differs for nuclei with varied parities of nucleons.

Introduction

Parameters of the cascade gamma-decay of any high-lying nuclear level (see Figs. 1–3) at any excitation energy are determined only by the level density ρ and by the partial widths Γ of dipole electrical and magnet transitions. Cascade intensity with pure quadrupole transitions is negligible at the nuclear excitation energy of more than a few MeV. For levels excited by primary transitions interval of spins is $\Delta J \leq 4$ for any parity.

Investigation of the process of gamma-decay is interesting most of all for analysis of interaction dynamics of fermion and boson states of nuclear matter. Valid information is need also for describing the process of fission more correctly. According to [1], energy is divided between excited fission fragments dependent on their level densities. As it is seen in Figs. 4–6, level densities calculated using available models [2] differ greatly from the modern experimental data.

Ordinary gamma-spectra and reaction cross sections depend on a $\rho\times\Gamma$ product and this fact completely cuts out a possibility of simultaneous determination of ρ and Γ valid values using such kind of data. This possibility is realized only in experiments on studying the cascade intensities of two sequential gamma-transitions. Two-step experiments can decrease a total error of determined ρ and Γ functions up to several dozens of percents as the intensities of two-step cascades include all information about energy of two gamma-transitions and any triplets of fixed nuclear levels.

As it is impossible to resolve all individual levels and to determine probabilities of transitions between them by available now spectrometers, information on superfluidity can be obtained from indirect experiments only. At that, both level density ρ and partial widths Γ in any nucleus are fitting functions with a minimal as far as possible number of parameters.

1. Possibility of up-to-date experiment and its model representation

The intensities $I_{\gamma\gamma}(E_1)$ of two-step cascades between neutron resonance (or another compound-state) λ and some group of low-lying nuclear levels f through any intermediate levels i for a fixed energy E_1 of primary transition are written by a system of equations of type:

$$I_{\gamma\gamma}(E_1) = \sum_{\lambda,f} \sum_{i} \frac{\Gamma_{\lambda i}}{\Gamma_\lambda} \frac{\Gamma_{if}}{\Gamma_i} = \sum_{\lambda,f} \frac{\Gamma_{\lambda i}}{<\Gamma_{\lambda i}> m_{\lambda i}} n_{\lambda i} \frac{\Gamma_{if}}{<\Gamma_{if}> m_{if}}, \quad (1)$$

where $m_{\lambda i}$ is a number of levels of excited primary γ-transitions in intervals from the energy of initial level λ to the energy of intermediate level i, m_{if} is a number of levels excited secondary transitions in intervals from the energy of intermediate level i to energy of the final level f, $n_{\lambda i}$ is a number of intermediate cascade levels in small energy intervals. From the system (1), which connects an unknown level number n (or m) and unknown partial widths, a set of p and q parameters of the model functions $\rho=f(p_1, p_2,...)$ and $\Gamma=\varphi(q_1,q_2,\dots)$ with some uncertainty is determined. The uncertainty is caused by a distortion of available theoretical representations and experimental results. Previous analysis [3] showed that a strong connection between ρ and Γ values in narrow intervals of excitation energies can be included in the model (1). In such a way from two-step cascades it is possible to determine simultaneously parameters of specified ρ and Γ functions at any densities of λ and i levels.

Analysis of the cascade intensities [4, 5] for nuclei of the region 28 ≤ A ≤ 200 showed that obtained level densities cannot be described with the experimental accuracy by models, which ignore influence of boson-states of nuclear matter on ρ function.

The Dubna model is free from using any hypothesis untested by experiment (for example, Porter-Thomas hypothesis [6] about emission widths of nuclear reaction products, hypothesis of Axel-Brink [7, 8] about independency of Γvalues on energy of excited level or Bohr-Mottelson hypothesis [9] about validation of the optical model used for determination of emission probability for nucleon products of reaction). The basis of our model of the cascade gamma-decay of nuclear compound-states with excitation energies $E_{ex} \approx 5$–10 MeV is the model of n-quasi-particle levels, balance of entropy and energy of quasi-particle levels [2, 10, 11] and tested model-phenomenological representations about form of energy dependency of radiative strength functions.

A systematic error in any procedure for ρ and Γ determination is always caused by large coefficients of error transfer of measured spectrum δS or cross section δσ of reaction onto errors of δρ and δΓ sought parameters. The error value strongly grows at increment of energy of decaying level. It is possible to evaluate this error and to choose a direction for correction of model representation about ρ and Γ only if to compare different model representations of $\rho=f(p_1,p_2, ..)$ and $\Gamma=\varphi(q_1,q_2, \dots)$ functions. For example, comparing a few variants of the practical model [3, 5, 12, 13] we discovered that rate of density change for vibrational levels (given in [12, 13] phenomenologically) is partially or completely determined [5] by pairing energy Δ for the last nucleon in nucleus. Therefore, in proposed variant of our practical model in the coefficient C_{coll} of collective level density increasing [5, 11] E_μ and E_ν parameters (changes of rates of nuclear entropy and of energy of quasi-particle states, correspondingly) are replaced by united fitting parameter E_u. Thus, C_{coll} coefficient was used in a form

$$C_{coll} = A_l \exp(\sqrt{(E_{ex} - U_l)/E_u} - (E_{ex} - U_l)/E_u) + \beta, \tag{2}$$

where A_l are fitting parameters of vibrational level density above breaking point of each l-th Cooper pair, and U_l are energies of the corresponding breaking thresholds. Parameter $\beta \geq 1$ can differ from 1 for deformed nuclei.

An influence of the shell inhomogeneities of a single-particle spectrum [2, 11] on a parameter defining a dependence of level density on excitation energy

$$a(A, E_{ex}) = \tilde{a}\,(1+((1-\exp(\gamma\, E_{ex}))\, \delta E/E_{ex})) \tag{3}$$

(and at the same time on $g=6a/\pi^2$ parameter of density of n-quasi-particle levels near Fermi-surface [11]) was also taken into account. An asymptotic value $\tilde{a} = 0.114A + 0.162A^{2/3}$ and coefficient $\gamma = 0.054$ were taken from [11]. A shell correction δE calculated from the data of mass defect in a liquid-drop nuclear model [2] was lightly changed to keep an average distance D_λ between resonances of the tested nucleus.

2. Energy dependence of the strength functions

In the model of the cascade gamma-decay for any excited levels and energies of emitted quantum, the form of energy dependence for partial radiative widths must be specified with a good accuracy.

On a base of available models for nucleus of A mass a strength function is determined as $k = \Gamma/(A^{2/3} E_\gamma^3 D_\lambda)$, where E_γ is an energy of the gamma-transition. An absolute value of sum of radiative widths for primary $E1$- and $M1$-transitions of cascades (total radiative width) is usually obtained from measured cross sections of the reaction. The expected form of this sum may be found using phenomenological representations or extrapolation of any models to $E_d < E_{ex} < B_n$ region of excitation (E_d is a point of transition from a set of known levels [14] to a concept of level density function, and B_n is a neutron binding energy in a nucleus).

The main summand of the functions $k(E1,E_\gamma)$ and $k(M1,E_\gamma)$ may be presented as a distribution of strength functions from models type of [15] with additional varied parameters. Variation of these parameters gives a set of functions of $E1$- and $M1$-transitions with a wide area of possible values (as it was done in [12, 13]).

It was experimentally established [16] that an addition to $k(E1,E_\gamma)+k(M1,E_\gamma)$ energy dependence of several peaks ensures a fine description of the cascade intensities. Form of these additional peaks may be found only by empiric way. For example, a description of each of them by two exponents (as in [5, 12]) is convenient to solve a system of nonlinear equations (1), although exponents are not used in theoretical models [2].

Usually for describing a form of peaks of $E1$- and $M1$-strength functions Breit–Wigner or Lorentz distributions are exploited. Asymmetrical Breit-Wigner function is used in theoretical analysis of fragmentation of quasi-particle states at varied locations relative to Fermi-surface [17]. However, variety of results is a trouble for a direct usage of these theoretical representations.

It turned out that application of an asymmetrical Lorentzian curve for description of peaks of the strength functions is simpler. Local peaks of $E1$- and $M1$-strength functions are written by an expression:

$$k = W_i \frac{(E_\gamma^2 + (\alpha_i (E_\gamma - E_i)/E_\gamma))\Gamma_i^2}{(E_\gamma^2 - E_i^2)^2 + E_\gamma^2 \Gamma_i^2}. \quad (4)$$

Lorentzian curve parameters for each i-th peak are similar to the model [15]: location of the peak center E_i, width Γ_i, amplitude W_i, and asymmetry parameter $\alpha_i \sim T^2$ (T is a nuclear thermodynamic temperature). Parameter $\alpha_i(E_\gamma - E_i)/E_\gamma$ grows linearly when an excitation energy increases (from zero in the center of peak to maximum at B_n), and it decreases if neutron excitation energy reduces.

An essential problem of using Lorentzian curve at fitting is a strong degradation of a convergence of iteration process. As all parameters of (4) are fitted, the possibility of unlimited Γ_i decreasing appears in some fitting paths.

A necessity of phenomenological accounting an influence of sharp local change of level density on the strength functions was discovered already at model-free determination of random functions ρ and Γ [18]. A required correction was done with the help of multiplication of fitted strength functions by ratio

$$M = \rho_{mod}/\rho_{exp}, \quad (5)$$

where ρ_{exp} is the best fit for a given iteration, ρ_{mod} is a smooth model functional described both density of neutron resonances and cumulative sum of known levels with E_{ex} below E_d. For ρ_{mod} determination the back shifted Fermi-gas model was chosen. In a given variant of analysis a limitation $1 \le \rho_{mod}/\rho_{exp} \le 10$ [12] was used. Sums of dipole strength functions with taking into account of such correction and without it are presented in Figs.7–9.

3. Results

An ambiguity of the system (1) solving appears because of both a strong nonlinearity of the sought functions ρ and Γ and their anti-correlation. There is a noticeable probability of falling into a false minimum of χ^2 what can lead to an essential systematic error of ρ and Γ values. It is possible to evaluate and minimize this uncertainty only if to compare results of different variants of the practical model with various functional ρ and Γ dependences.

A comparison of the results of a given model variant with previous ones showed that a good accuracy is achieved in describing a density of intermediate levels of cascades. The most distortion of density values were found only for ^{137}Ba and ^{182}Ta. At that, for ^{137}Ba the previous variant of fitting [5] most likely gives a large uncertainty. And breaking thresholds of the second and the third pairs for ^{182}Ta in presented variant are 1.6 and 5.8 MeV, but in [5] they are 1.6 and 4.0 MeV, respectively. It means that obtained data on the level density even at the worst case of ^{182}Ta give a picture where principle errors are caused only by ambiguity of the up-to-date representations about gamma-decay process.

A larger accuracy and adequacy of the results would be achieved if not less than ≈ 99% of intensity of primary transitions is separated in experiment from all gamma-cascades of compound-state decay. But a comparison of the breaking thresholds for 3 – 4 Cooper pairs determined from (1) using different functional ρ and Γ dependencies showed that a reliable information about the most probable level density and the strength functions of dipole gamma-transitions can be extracted even from a convolution of spectrum of primary products of decay of compound-state and dependency of gamma-transitions branches coefficients on energy of intermediate level. The obtained results in the last variants of the practical model vary very weakly.

The level densities from back shifted Fermi-gas model [19] and from model with taking into account shell inhomogeneities of single-particle spectrum [11] are presented in Figs. 4–6. It is seen that the second model describes a $d\rho/dE_{ex}$ derivative with a better accuracy than [19] model does. But the level densities calculated using [2] models strongly differ from ones extracted from (1).

In all realized variants of the practical model [5, 18, 20–22] at step-by-step reduction of number of fitted parameters a fitting accuracy is kept, and so description of $I_{\gamma\gamma}$ spectra in presented paper is practically the same as ones in [12, 13].

The radiative strength functions of $E1$- and $M1$-transitions and their sums presented in Figs. 7–9 and Figs. 10–12, respectively, have no principal distortions with ones published earlier. But a problem of unambiguous description for observed local peaks of electric and magnetic strength functions remains valid (using exponents [5] or modified Lorentzian curve (4) for this purpose gives closely χ^2).

It is need to append that the data of Figs. 7–12 do not demand to include to strength functions any additional "pygmy-resonances". For a total interpretation of the gamma-decay process theoretical representations (about co-existing quasi-particle levels with vibrational ones and about fragmentation of all nuclear states at E_{ex} growing) are quite enough.

For many nuclei (Figs. 10–12) "plateau" in sum of strength functions of $E1$- and $M1$-transitions coincides with a sum of calculated values from [15] and $k(M1)$ value ($k(M1) = const$) normalized by $k(M1)/k(E1)$ experimental ratio. An essential decrease of $k(M1)+k(E1)$ sum for small energies of gamma-transitions is observed for all tested variants of functional dependences of strength functions. But an existence of asymptotical zero of sums of strength functions does not follow from Dubna model results. At that, a noticeable increase in strength functions of $E1$- or $M1$-transition near B_n and above this energy can be observed at sufficiently high energies of fragmented quasi-particle state. It means that radiative strength functions are not just an extrapolation of giant resonances (it contradicts the Axel-Brink hypothesis [7, 8] used earlier for gamma-spectra calculations).

In Fig.13, mass dependences of breaking thresholds of the second and the third Cooper pairs are presented. As these values differ for nuclei with various nucleon parities and depend on an average pairing energy Δ_0 they are shown separately and compared with B_n/Δ_0 (much as in [5]). It follows from this comparison that dependency of breaking thresholds of pairs on form of strength function is weak and real correlation between ρ and Γ values is insignificant in experiments on the two-step cascade recording.

In Fig.14, the fits of E_u parameter are shown. Jnt can see practically complete coincidence of E_u fits with Δ_0 value for $\approx$ 30 nuclei. Causes of E_u scatter for the rest nuclei may be

- errors of normalization of experimental intensities of two-step cascades,
- unaccounted in model [12] possibility of breaking proton pairs together or instead of neutron pairs,
- inaccuracy of phenomenological part of the model,
- variability of Δ_0 experimental values [23].

One cannot exclude also a possibility of various ratios of components of quasi-particle and phonon types in wave-function of resonance determined a capture cross section of thermal neutrons by any stable (or long-living) nucleus-target. In the up-to-date models [2], a total level density is equal to sum of densities of quasi-particle levels and collective ones. In Fig.15, the ratios of collective (practically vibrational only) level density to the total density are presented. Near B_n these ratios are very similar for nuclei with any nucleon parity, but at E_d energy they are noticeable less for even-even nuclei than for even-odd and odd-odd ones.

All tested variants of Dubna model do not give reasons to suppose an existence of drastic changes of nuclear structure in $E_{ex} = B_n$ energy point. Therefore, the data of Fig.15 allow to believe that neutron resonances can keep a different type of structure (with a dominance of quasi-particle or phonon components) of wave-functions and that they belong to some various distributions of reduced neutron resonance widths and total radiative ones.

In [24], an approximation of reduced neutron widths and total radiative widths of neutron resonances was done. At analysis it is supposed that experimental set of these widths is represented by a sum of distributions (from 1 to 4) with varied widths and positions of maximums of neutron amplitudes. For total radiative widths in nuclei with a number of resonances ≥ 170 average parts of two the most intensive distributions are 44 and 34% of overall distribution of total radiative widths (it is close to 40%-part of vibrational levels).

Thus, two completely independent methodically experiments show that structure of the wave-functions differs for contiguous levels in a wide range of stable nuclei-targets up to B_n energy (and even at some higher energies).

The existence of non-principal distortion between the values of $E1$- and $M1$-strength functions (Fig. 10–12) and results of [5] are caused most likely by different degree of influence on χ^2 of various energy dependences (forms) of partial widths for peaks (4) at energy region of small functional values. At that, form variations for sums of $E1$- and $M1$-strength functions (Figs. 7–9) observed in different nuclei can be interpreted as existence of levels of various structures at excitation energy of 5–10 MeV.

Conclusions

Direct experimental information on dynamics of breaking 3 – 4 Cooper pairs of nucleons has been obtained. Systematic uncertainty of determination of breaking thresholds is not more than ~ 1 MeV for a majority of available studied nuclei.

The data extracted with the use of

1. model of *n*-quasi-particle level density [10] for description of sequential 3 – 4 Cooper pair breaking at energies below 5–10 MeV from Fermi-surface,
2. phenomenological representations (2) about energy dependence of density of vibrational levels at the same energy range,
3. and composition of phenomenological and/or theoretical representations about form of energy dependences of widths of gamma-quanta emission

allow us to suppose that dynamics of interaction between fermion and boson states of nuclear matter depends on the form and parity of nucleon number of studied nucleus.

References

[1] K.H. Schmidt and B. Jurado, Phys. Rev. C **92**, 014607 (2011).

[2] *Reference Input Parameter Library RIPL-2, Handbook for calculations of nuclear reaction data*, IAEA-TECDOC (2002).

[3] N. Jovancevich, A.M. Sukhovoj, W.I. Furman, and V.A. Khitrov, in *Proceedings of XX International Seminar on Interaction of Neutrons with Nuclei*, *Dubna, May 2012,* Preprint № E3-2013-22 (Dubna, 2013), p. 157; http://isinn.jinr.ru/past-isinns.html.

[4] Sukhovoj A.M., Mitsyna L.V., Jovancevic N. in *Proceedings of XXIII International Seminar on Interaction of Neutrons with Nuclei, Dubna, May 25-29,2015, JINR,* Preprint № E3-2016-12 (Dubna, 2016), p.299.
[5] A.M. Sukhovoj, L.V. Mitsyna, N. Jovancevich, Phys. Atom. Nucl. **79,** 153(2016).
[6] C.F. Porter and R.G. Thomas, Phys. Rev. **104**, 483 (1956).
[7] P. Axel, Phys. Rev. **126,** 671 (1962).
[8] D.M. Brink, Ph. D. Thesis (Oxford University, 1955).
[9] *A. Bohr, and B.R. Mottelson, Nuclear Structure, Vol. 1 (W.A. Benjamin, New York;* Amsterdam, 1969).
[10] V.M. Strutinsky, in *Proceedings of the International Congress on Nuclear Physics, Paris, France, 1958*, p. 617.
[11] V. Ignatyuk, Report INDC-233(L), IAEA (Vienna, 1985).
[12] A.M. Sukhovoj, Phys. Atom. Nucl. **78,** 230 (2015).
[13] L.V. Mitsyna, A.M. Sukhovoj, in *Proceedings of XXII International Seminar on Interaction of Neutrons with Nuclei*, *Dubna, May 2014,* Preprint № E3-2015-13 (Dubna, 2015), p. 245; http://isinn.jinr.ru/past-isinns.html.
[14] http://www-nds.iaea.org/ENDSF.
[15] S.G. Kadmensky, V.P. Markushev, and W.I. Furman, Sov. J. Nucl. Phys. **37,** 165 (1983).
[16] A.M. Sukhovoj, W.I. Furman, V.A. Khitrov, Phys. At. Nucl., **71**, 982(2008).
[17] L.A. Malov and V.G. Soloviev, Sov. J. Nucl. Phys. **26,** 384 (1977).
[18] E.V. Vasilieva, A.M. Sukhovoj, and V.A. Khitrov, Phys. Atom. Nucl. **64,** 153 (2001).
[19] W. Dilg, W. Schantl, H. Vonach, and M. Uhl, Nucl. Phys. A **217**, 269 (1973).
[20] A.M. Sukhovoj and V.A. Khitrov, Preprint No. E3-2005-196, JINR (Dubna, 2005).
[21] A.M. Sukhovoj and V.A. Khitrov, Phys. Part. Nucl. **36,** 359(2005).
[22] A.M. Sukhovoj and V.A. Khitrov, Phys. Part. Nucl. **37,** 899(2006).
[23] V.A. Kravtsov, Atomic Masses and Binding energy of Nuclei (Atomizdat, Moscow, 1965) [in Russian].
[24] A.M. Sukhovoj and V.A. Khitrov, Phys. Atom. Nucl. **76,** 68 (2015).

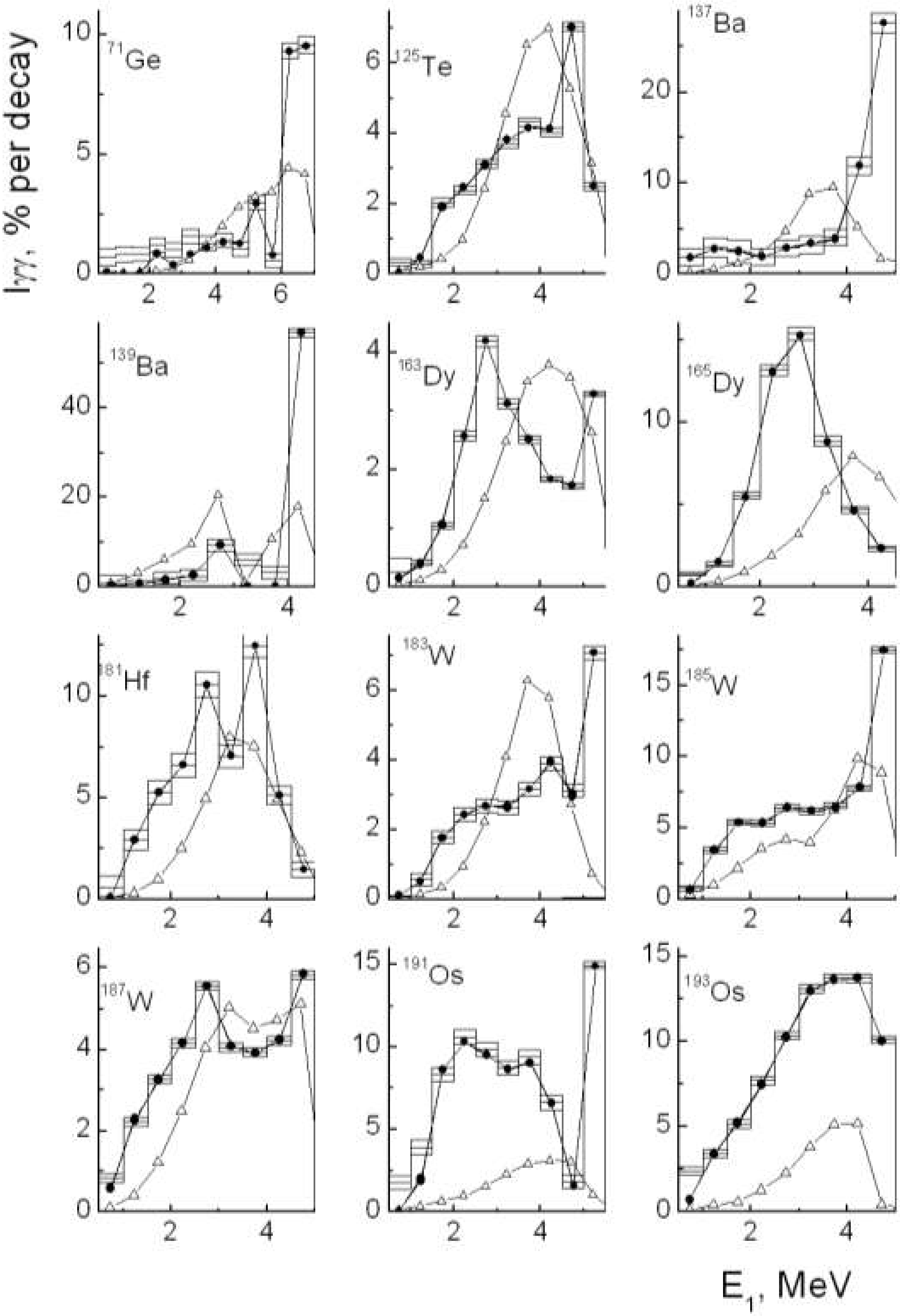

Fig. 1. Dependencies of the experimental intensities (histogram with experimental errors) and their best approximations (points) on the energy of primary transition. Triangles are the results of calculations based on statistical model.

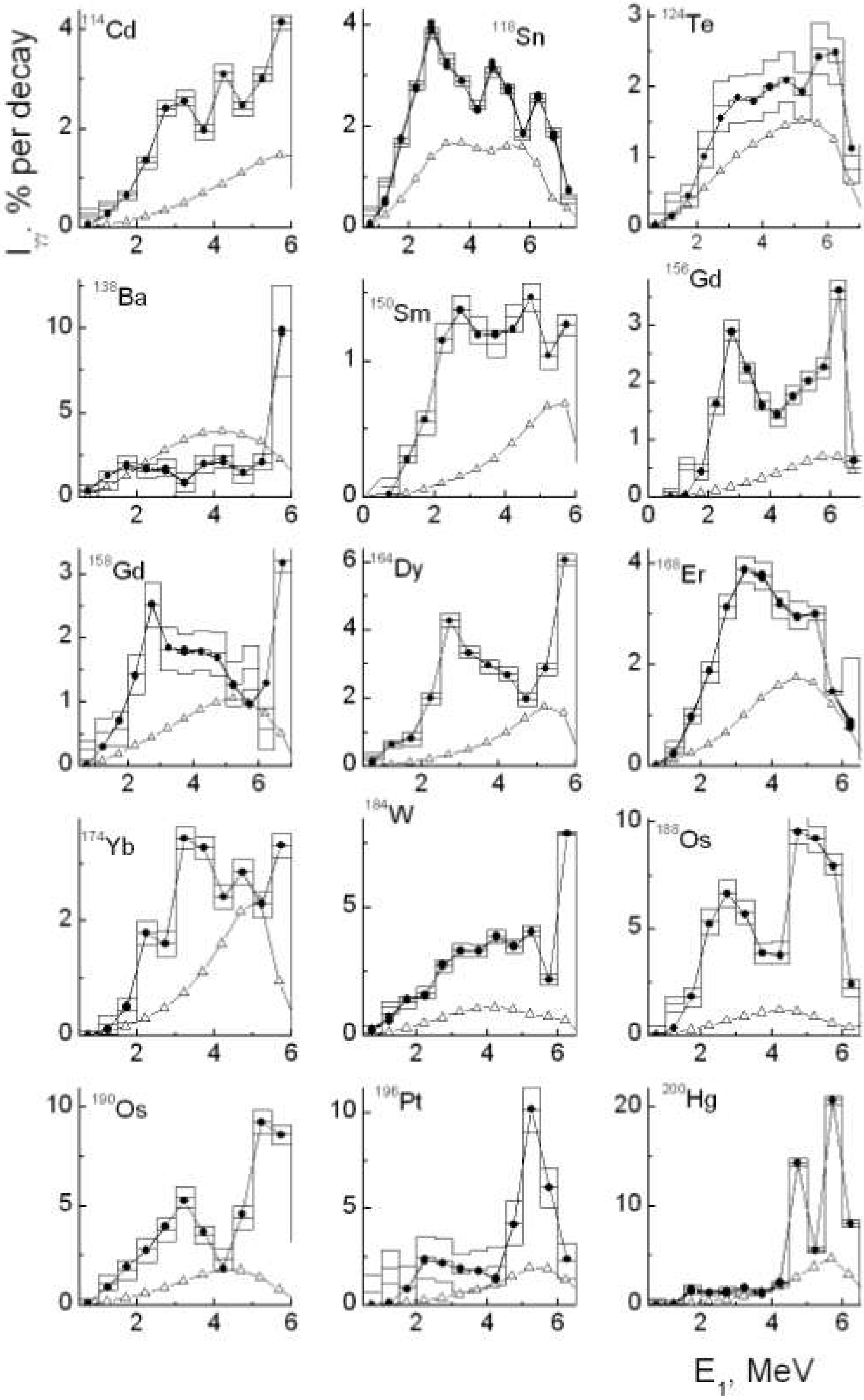

Fig. 2. The same (as fig. 1) for in for even-even nuclei.

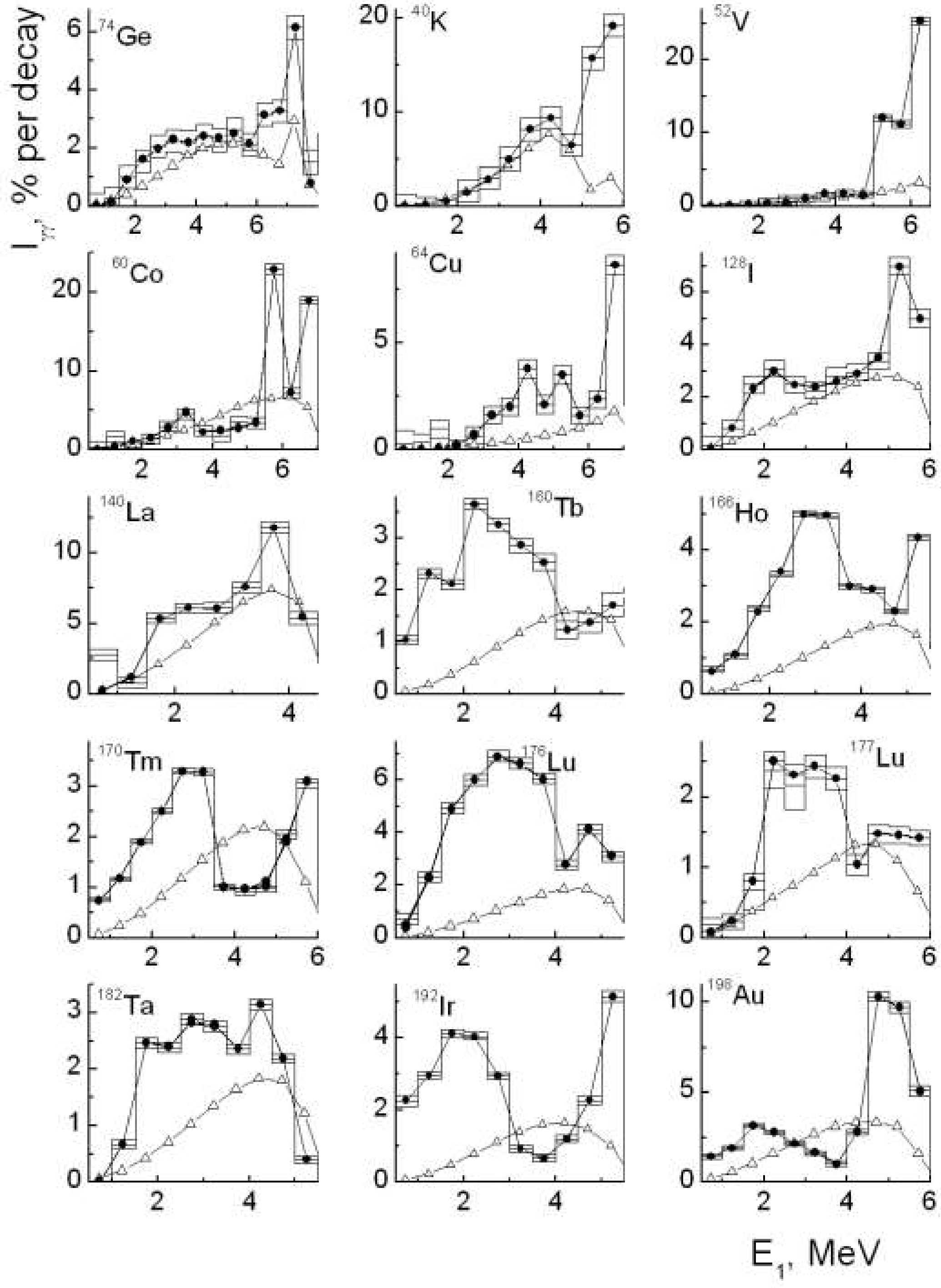

Fig. 3. The same (as fig. 1) for ^{74}Ge, ^{177}Lu and odd-odd nuclei.

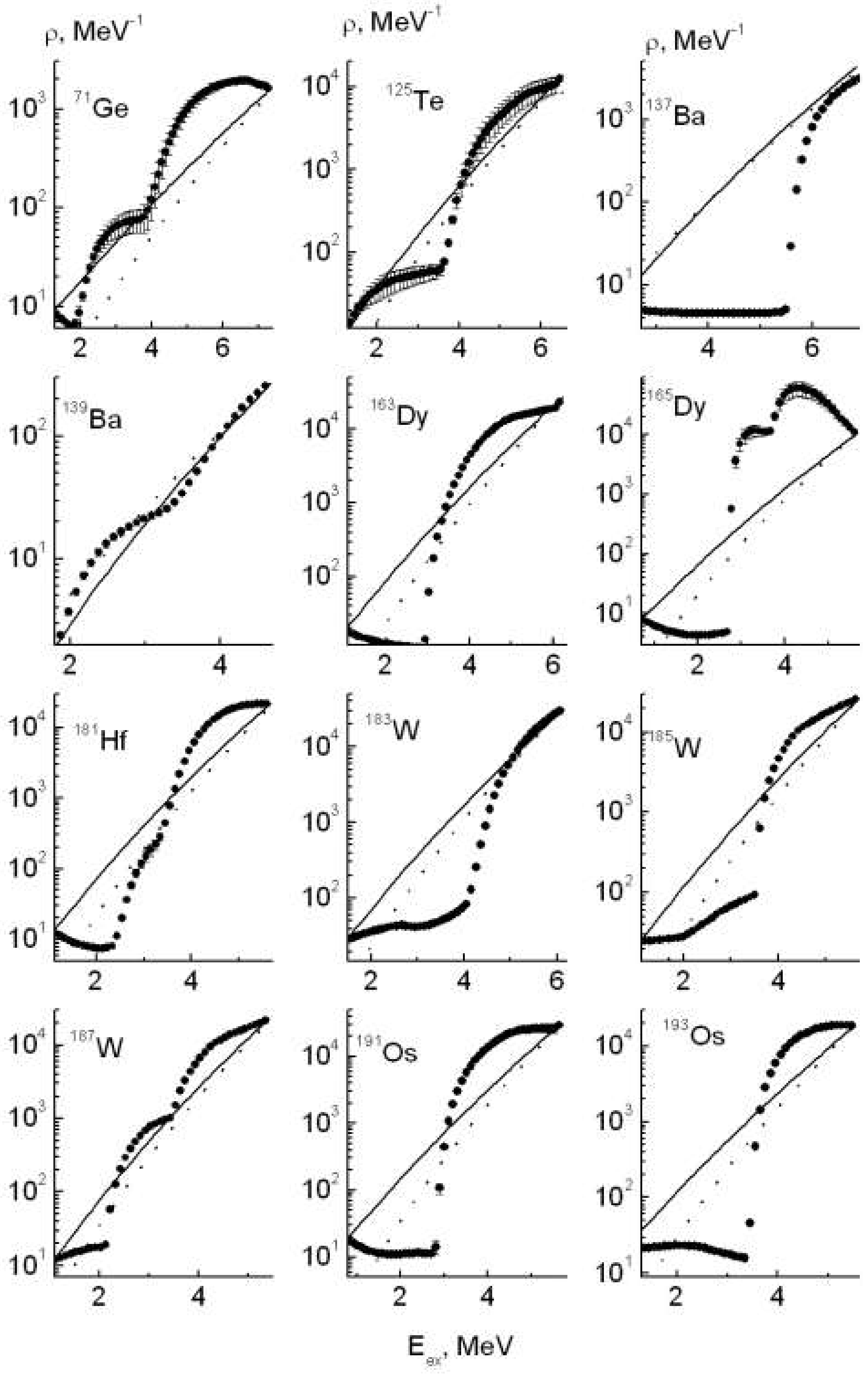

Fig. 4. Average densities of intermediate levels of two-step cascades (points with errors) for even-odd nuclei (fits of the smallest χ^2) depending on the excitation energy. Lines are the data of [19], dotted lines are calculations by model taken into account shell inhomogeneities of single-particle spectrum [11].

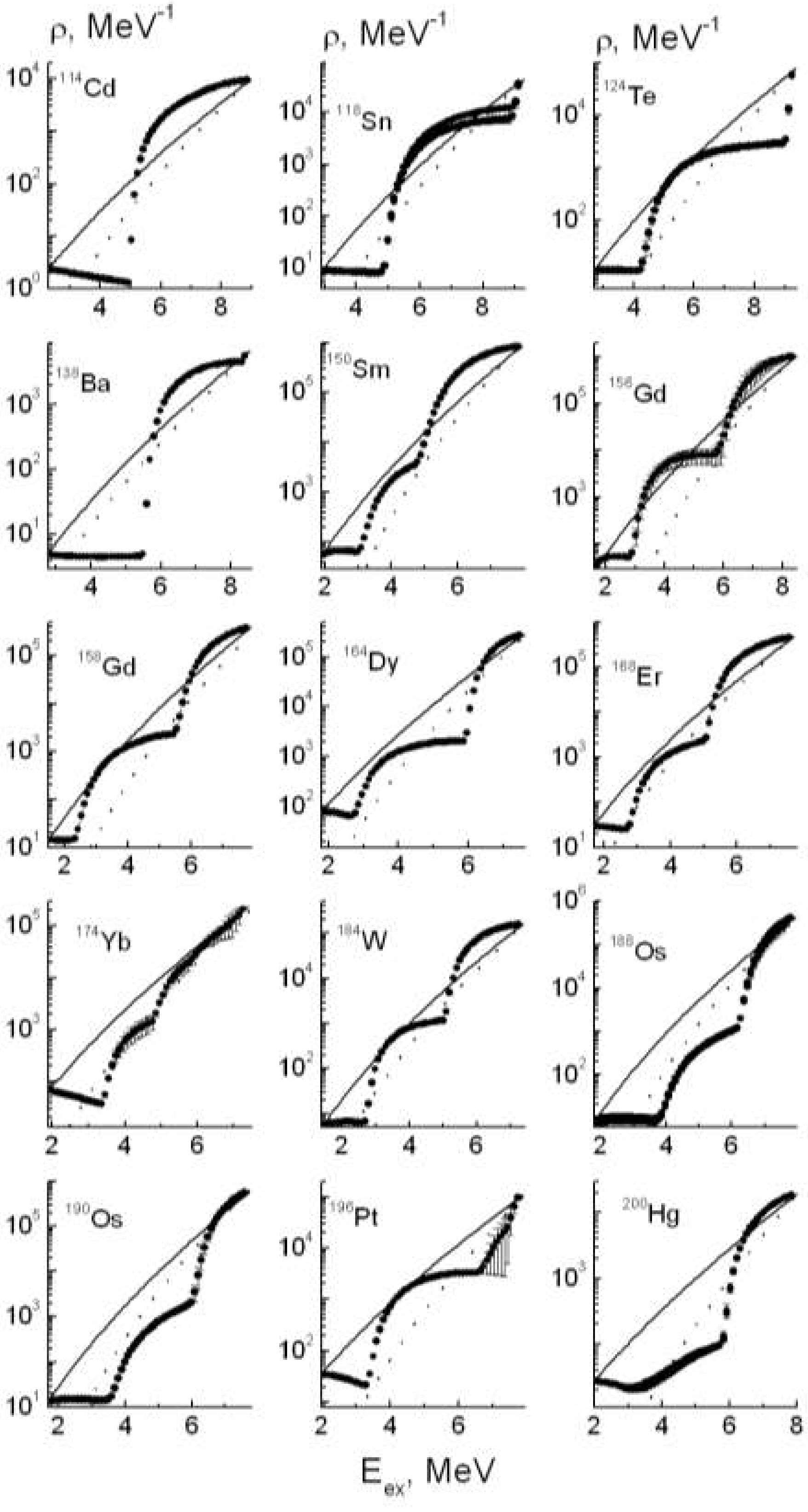

Fig. 5. The same (as fig. 4) for in for even-even nuclei.

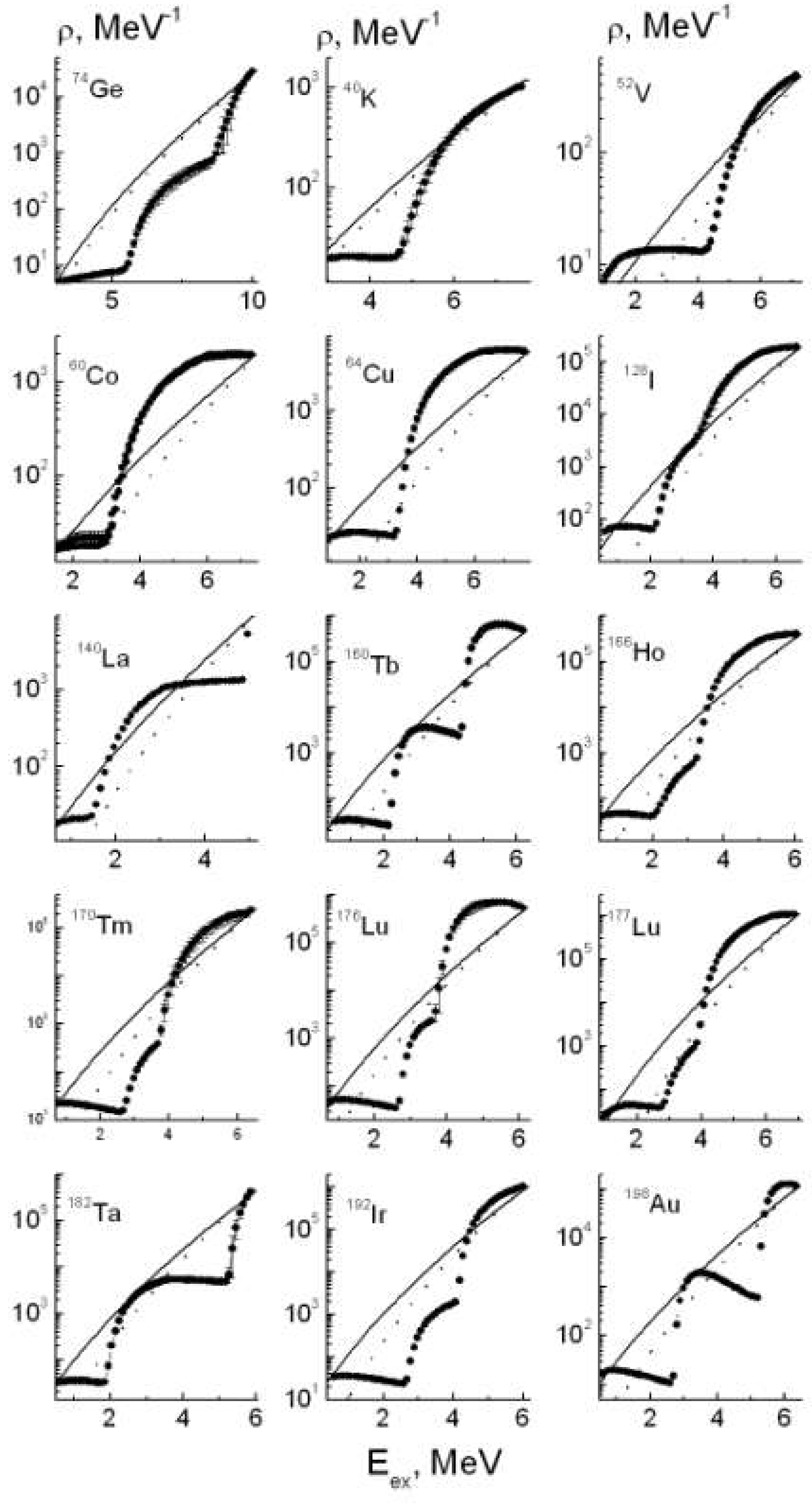

Fig. 6. The same (as fig. 4) for ^{74}Ge, ^{177}Lu and odd-odd nuclei.

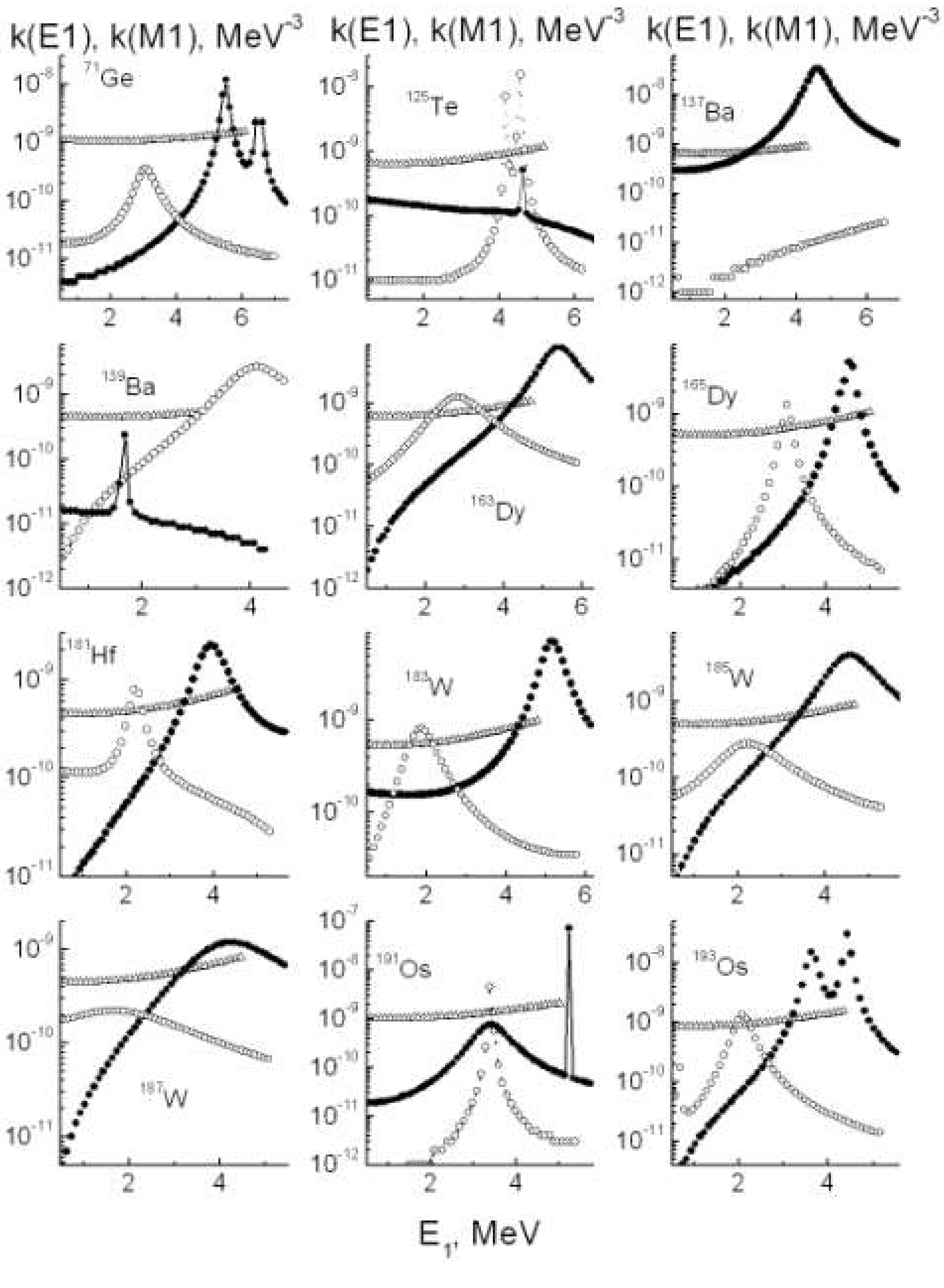

Fig.7. Strength functions of *E*1-transitions (black points) and of *M*1-transitions (open points) for even-odd nuclei. Triangles are calculations by model [KMF] adding $k(M1)$=const in $0 < E_1 \leq B_n - E_d$ energy range.

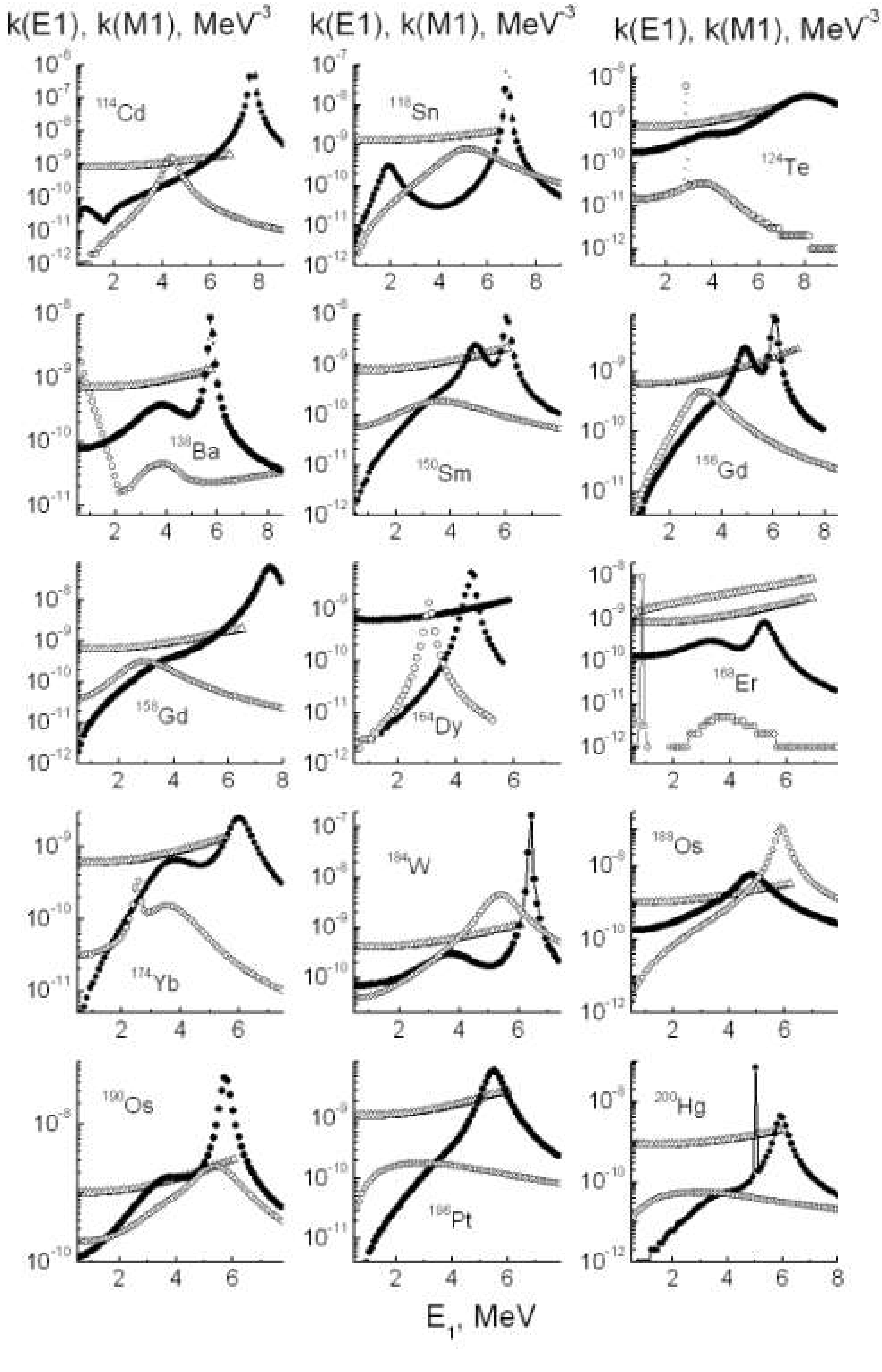

Fig. 8. The same (as fig. 7) for even-even nuclei.

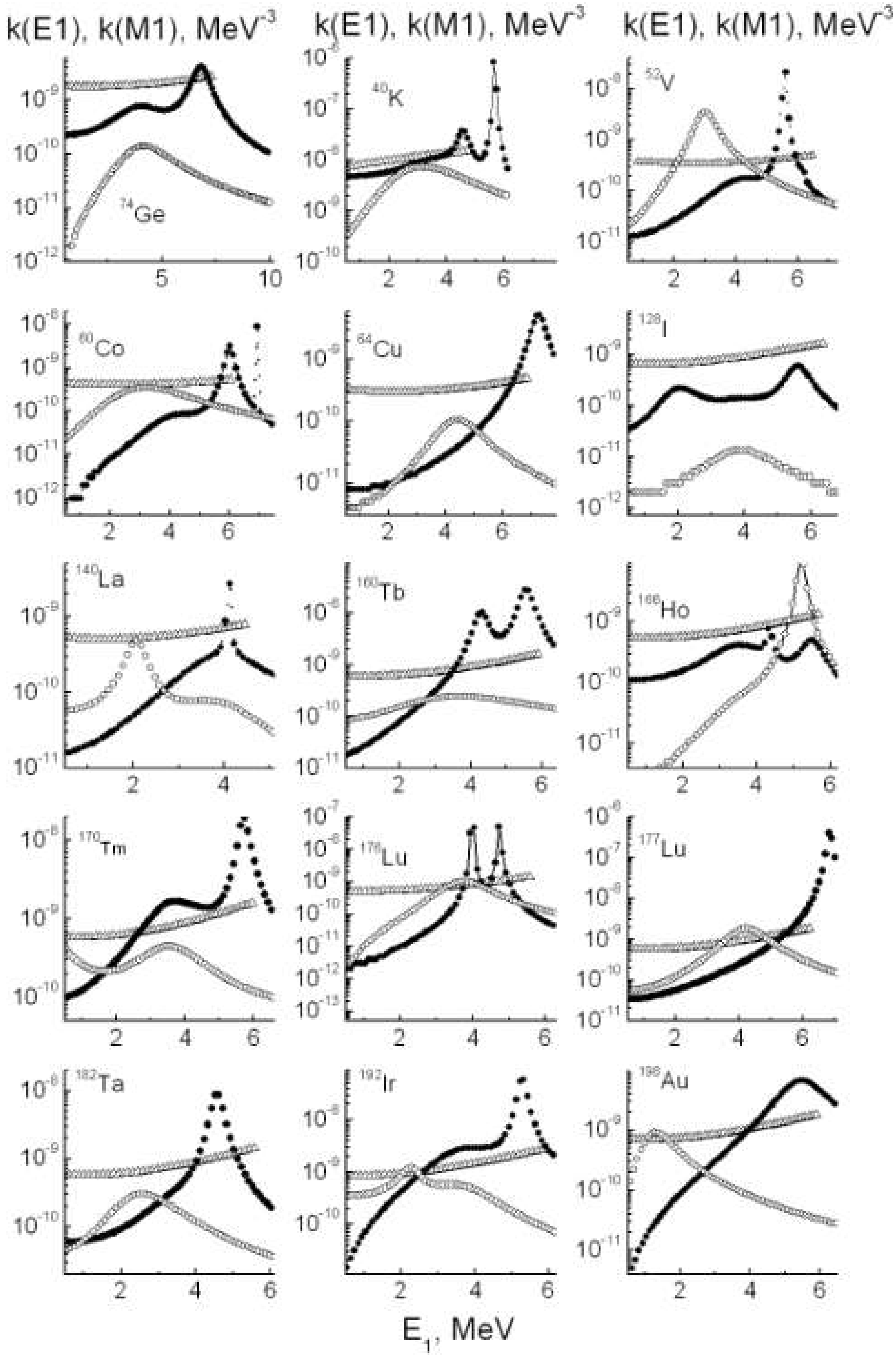

Fig. 9. The same (as fig. 7) for ^{74}Ge, ^{177}Lu and odd-odd nuclei.

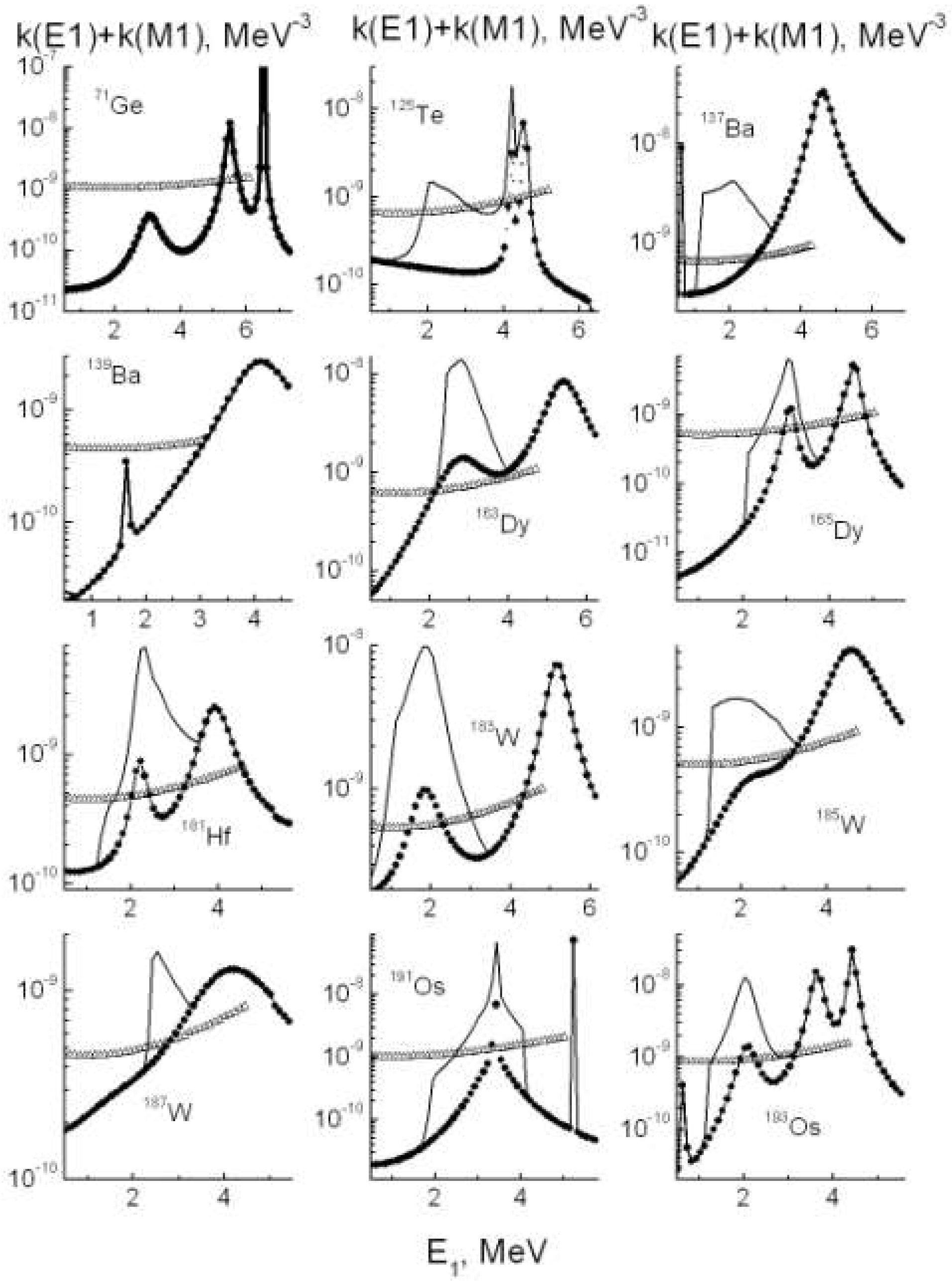

Fig. 10. Sums of strength functions of *E*1- and *M*1-transitions (black points) for even-odd nuclei depending on the energy of primary transition. Lines are fits with taking into account the correction (5). Triangles are calculations by model [15] adding *k*(*M*1)=const for $0 < E_1 \leq B_n – E_d$ energy range.

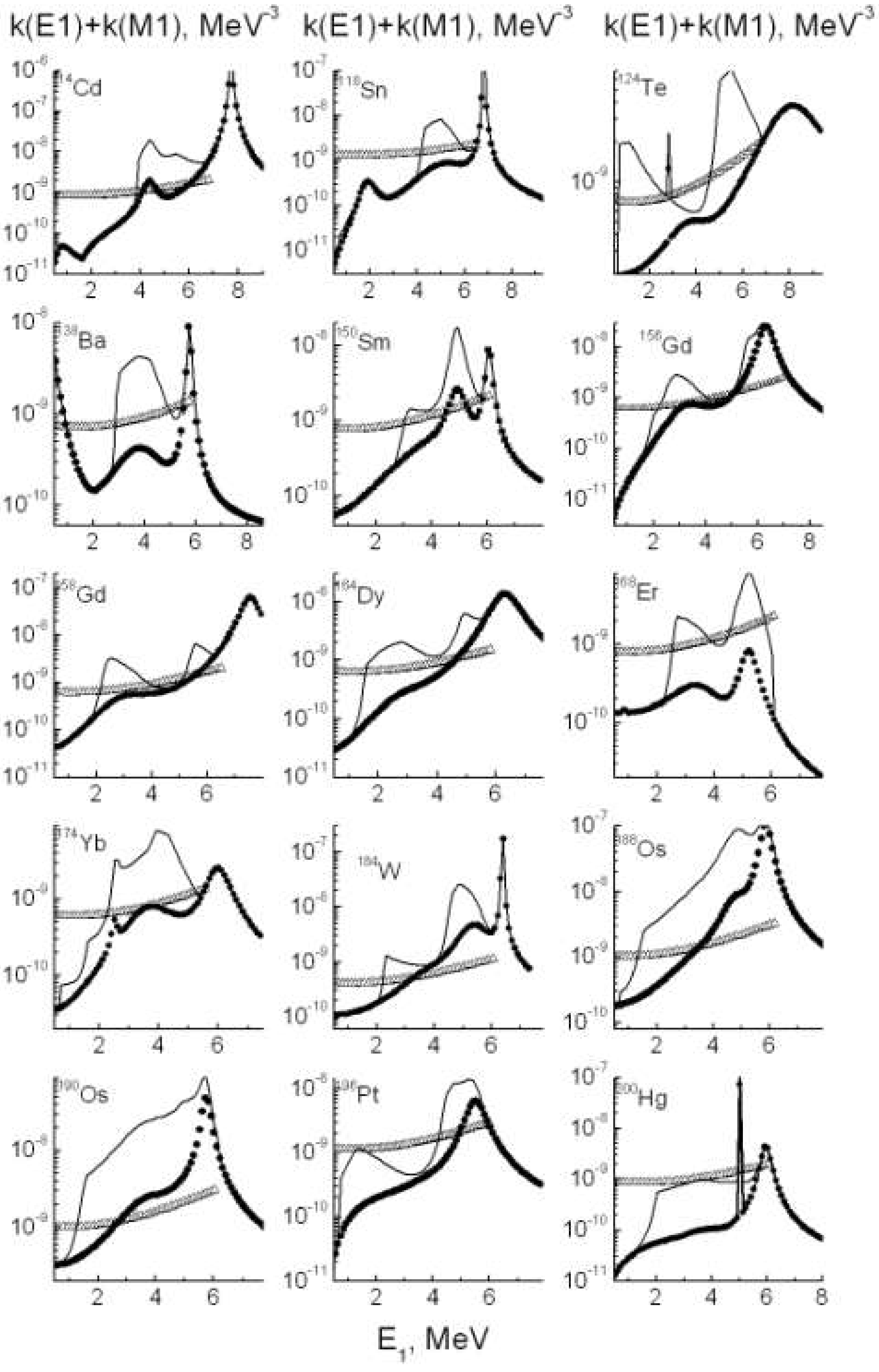

Fig. 11. The same (as fig. 10) for ^{74}Ge, ^{177}Lu and odd-odd nuclei.

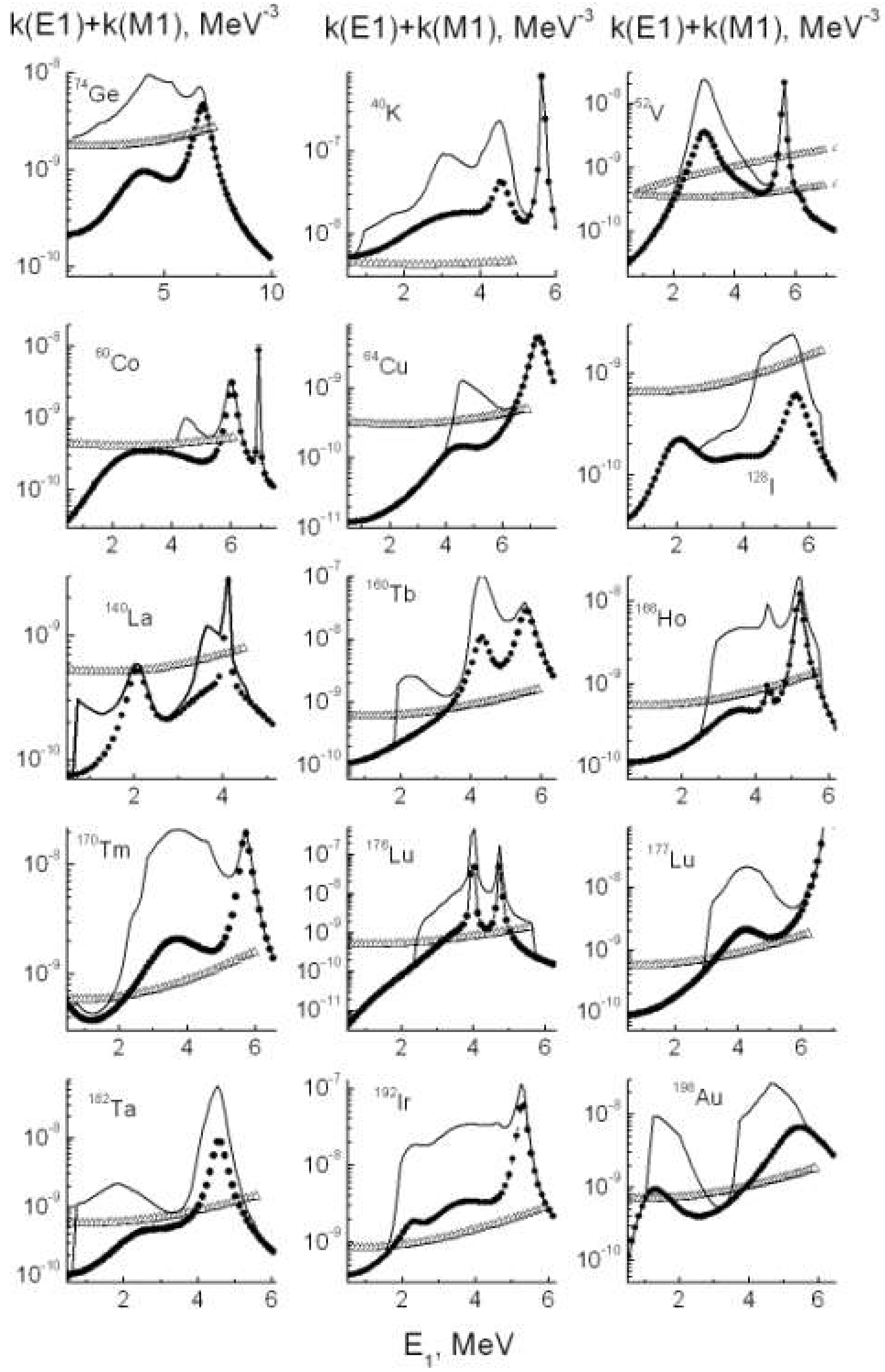

Fig. 12. The same (as fig. 7) for ^{74}Ge, ^{177}Lu and odd-odd nuclei.

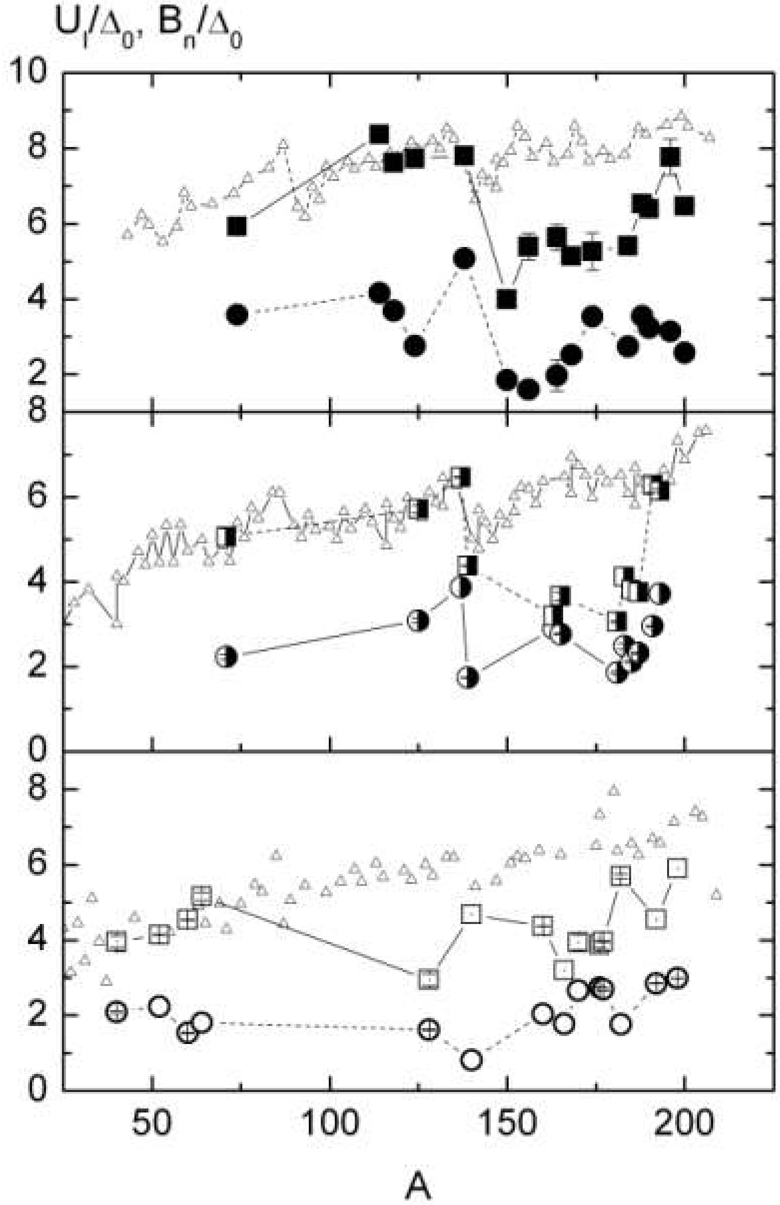

Fig. 13. Mass dependencies of breaking thresholds of the second (points) and of the third (squares) Cooper pairs. Black points – even-even nuclei, half-open points – even-odd nuclei, open points – odd-odd compound- nuclei. Triangles are mass dependencies of B_n/Δ_0.

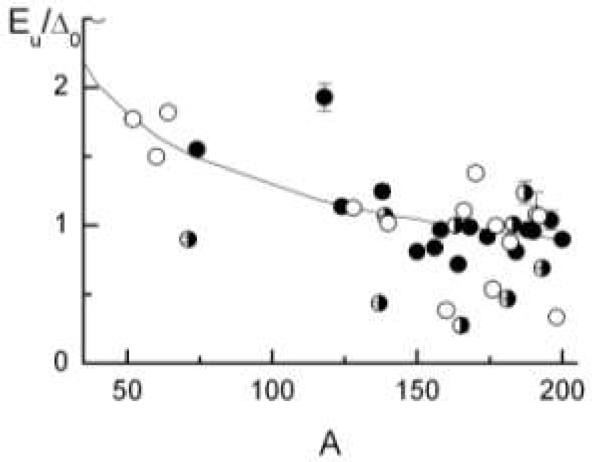

Fig. 14. Dependencies of E_u parameter (2) on nuclear mass A. Black points – even-even nuclei, half-open points – even-odd nuclei, open points – odd-odd compound-nuclei.

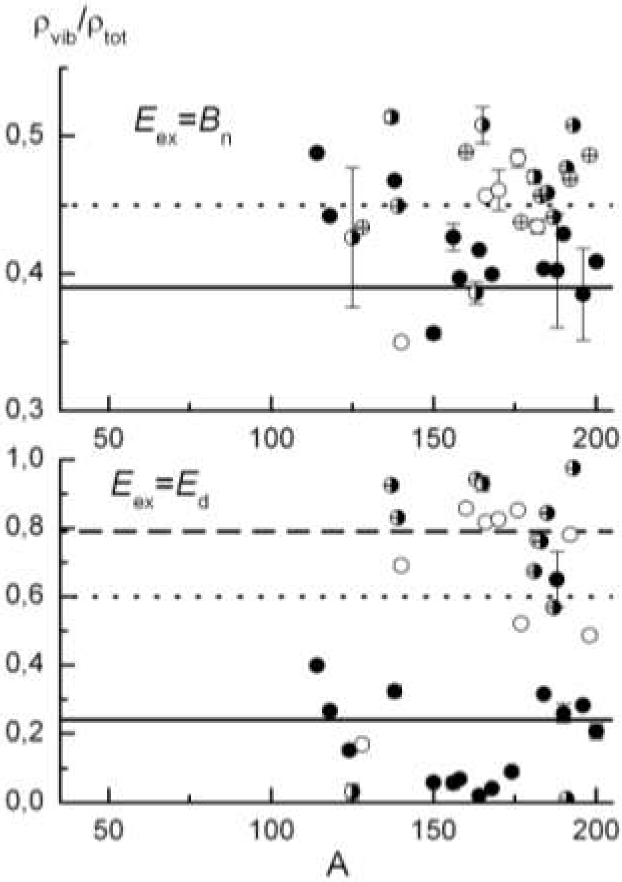

Fig. 15. Mass dependencies of the ration of vibrational level density to the total one near B_n energy (upper picture) and for E_d energy point (bottom picture). Lines – the average of these ratios for even-even nuclei, dashed lines – for even-odd nuclei and dot lines – for odd-odd nuclei.

ДРУШТВО ЗА ЗАШТИТУ ОД ЗРАЧЕЊА
СРБИЈЕ И ЦРНЕ ГОРЕ

ЗБОРНИК
РАДОВА

XXIX СИМПОЗИЈУМ ДЗЗСЦГ
Сребрно језеро
27- 29. септембар 2017. године

Београд
2017. године

SOCIETY FOR RADIATION PROTECTION OF SERBIA AND MONTENEGRO

PROCEEDINGS

XXIX SYMPOSIUM DZZSCG
Srebrno jezero
27- 29. September 2017

Belgrade
2017

ЗБОРНИК РАДОВА

XXIX СИМПОЗИЈУМ ДЗЗСЦГ
27-29.09.2017.

Издавачи:
Институт за нуклеарне науке „Винча“
Друштво за заштиту од зрачења Србије и Црне Горе

За извршног издавача:
Др Борислав Грубор

Уредници:
Др Јелена Станковић Петровић
Др Гордана Пантелић

ISBN 978-86-7306-144-3

Техничка обрада:
Јелена Станковић Петровић, Гордана Пантелић

Штампа:
Институт за нуклеарне науке ”Винча”, Мике Петровића Аласа 12-14, 11351 Винча, Београд, Србија

Тираж:
150 примерака

Година издања:
Септембар 2017.

XXIX СИМПОЗИЈУМ ДРУШТВА
ЗА ЗАШТИТУ ОД ЗРАЧЕЊА
СРБИЈЕ И ЦРНЕ ГОРЕ
Сребрно језеро, од 27.09. до 29.09.2017. године

Организатори:

ДРУШТВО ЗА ЗАШТИТУ ОД ЗРАЧЕЊА СРБИЈЕ И ЦРНЕ ГОРЕ

ИНСТИТУТ ЗА НУКЛЕАРНЕ НАУКЕ „ВИНЧА“
Лабораторија за заштиту од зрачења и заштиту животне средине „Заштита“

Организацију су помогли:

Институт за нуклеарне науке „Винча“, Лабораторија за заштиту од зрачења и заштиту животне средине

Излагачи:

Canberra Packard Central Europe GmbH.
Wienersiedlung 6
2432 SCHWADORF, Austria
Phone: +43 (0)2230 3700-0
Fax: +43 (0)2230 3700-15
Web: http://www.cpce.net/

LKB Vertriebs GmbH, Представништво Београд
Цвијићева 115
11120 Београд, Србија
Тел: +381 (0)11 676 6711
Факс: +381 (0)11 675 9419
Веб: *www.lkb.eu*

ТИМ Цо.
Јована Рајића 5ц
11000 Београд,
Тел: +381 11 2836-786, 2836-787
Факс: +381 11 2833-342
Веб: *http://www.timco.rs/*

Овај Зборник је збирка радова саопштених на XXIX Симпозијуму Друштва за заштиту од зрачења Србије и Црне Горе који је одржан од 27. до 29.09.2017. године на Сребрном језеру. Радови су разврстани по секцијама. Мада су сви радови у Зборнику рецензирани од стране Редакционог одбора, за све изнесене тврдње и резултате одговорни су сами аутори.
Југословенско друштво за заштиту од зрачења основано је 1963. године у Порторожу, а од 2005. године носи име Друштво за заштиту од зрачења Србије и Црне Горе.
Ове године Дрштво обележава 54 године организоване заштите од зрачења на простору бивше Југославије. Симпозијум Друштва за заштиту од зрачења Србије и Црне Горе је јединствена прилика да кроз стручни програм предочимо напредак у области заштите од зрачења, анализирамо досадашње резултате и актуелна дешавања, разменимо искуства са колегама из земље и региона, али и да сретнемо старе и упознамо нове пријатеље.
Организациони одбор се захваљује ауторима и коауторима научних и стручних радова на доприносу и уложеном труду. Посебно се захваљујемо спонзорима који су помогли одржавања Симпозијума.

Организациони одбор

CIP - Каталогизација у публикацији
Народна библиотека Србије, Београд

502:504.5]:539.16(082)(0.034.2)
614.875/.876(082)(0.034.2)
539.16.04(082)(0.034.2)
539.1.074/.08(082)(0.034.2)
577.1:539.1(082)(0.034.2)

ДРУШТВО за заштиту од зрачења Србије и Црне Горе (Београд). Симпозијум (29 ; 2017 ; Сребрно језеро)

Зборник радова [Електронски извор] / XXIX симпозијум ДЗЗСЦГ [Друштва за заштиту од зрачења Србије и Црне Горе], Сребрно језеро 27- 29. септембар 2017. године ; [организатори] Друштво за заштиту од зрачења Србије и Црне Горе [и Институт за нуклеарне науке "Винча", Лабораторија за заштиту од зрачења и заштиту животне средине Заштита ; уредници Јелена Станковић Петровић, Гордана Пантелић]. - Београд : Институт за нуклеарне науке "Винча" : Друштво за заштиту од зрачења Србије и Црне Горе, 2017 (Београд ; Институт за нуклеарне науке "Винча"). - 1 USB флеш меморија : текст ; 2 x 2 x 14 cm (у задњем делу оловке)

Системски захтеви: Нису наведени. - Насл. са насловне стране документа. - Радови на срп. и енгл. језику. - Текст ћир. и лат. - Тираж 150. -
Библиографија уз већину радова. - Abstracts. - Регистар.

ISBN 978-86-7306-144-3
а) Заштита од јонизујућег зрачења - Зборници b) Животна средина - Загађење радиоактивним материјама - Зборници c) Радиоактивно зрачење - Штетно дејство - Зборници d) Нејонизујуће зрачење - Штетно дејство - Зборници e) Радиобиологија - Зборници f) Дозиметри - Зборници
COBISS.SR-ID 245691404

UTICAJ PROMENA MIONSKOG FLUKSA NA NIVO FONSKE AKTIVNOSTI U NISKOFONSKIM GAMA SPEKTROMETRIJSKIM MERENJIMA

Nikola JOVANČEVIĆ[1], David KNEŽEVIĆ[1], Miodrag KRMAR[1], Jovana NIKOLOV[1], Nataša TODOROVIĆ[1], Strahinja ILIĆ[2]
1) Univerzitet u Novom Sad, Prirodno-matematički fakultet, Departman za fiziku, Novi Sad, Republika Srbija, nikola.jovancevic@df.uns.ac.rs
2) Fakultet tehničkih nauka, Novi Sad, Republika Srbija

SADRŽAJ

Mioni predstavljaju glavnu komponentu kosmičkog zračenja na nivou mora, zbog čega su značajan izvor fonske aktivnosti u gama spektrometrijskim merenjima. Fonsku aktivnost mioni mogu produkovati interakcijama sa detektorom i okolnim materijalima. Tom prilikom nastali neutroni daju takođe značajan doprinos vrednosti fonske gama aktivnosti. U ovom radu su predstavljeni rezultati merenja korišćenjem HPGe detektora sa gvozdenom i olovnom pasivnom zaštitom u dva okruženja, kada je iznad detektora bila prisutna različita debljina pokrovnog betonskog sloja. Monitoring prisustva miona je vršen korišćenjem plastičnog scintilacionog detektora. Određene su vrednosti inteziteta gama pikova koji se javljaju usled neutronskih reakcija i upoređeni su sa promenom prisustva miona u okruženju detektora. Dobijeni rezultati mogu poslužiti za unapređenje projektovanja zaštita prilikom niskofonskih gama spektrometrijskih merenja.

1. UVOD

Mioni su jedna od glavnih komponenata kosmičkog zračenja na nivou mora [1]. Putem različitih interakcija oni daju bitan dobrinos odbroju fonskog zračenja u različitim niskofonskim gama spektroskopskim merenjima [2-6]. Jedan od načina na koji mioni utiču na detekciju fonskih događaja je njihova interakcija sa detektorom i okolnim materijalima, prvenstveno materijalima zaštite detektora. Tom prilikom pre svega putem zahvata miona na materijalima velike gustine i visokog rednog broja može doći do produkcije neutrona [6-8]. Na ovaj način kreirani neutroni interaguju sa detektorom i okolnim materijalima. Ove interakcije se pre svega odvijaju putem zahvata neutrona i njihovog rasejanja. To dovodi do toga da se u snimljenim gama spektrima detektuju gama pikovi koji prate deekscitaciju jezgara pobuđenih u ovim procesima [9,10]. Detekcija ovih događaja je često neželjena tokom različitih gama spektroskopskih merenja. Zbog toga je od važnosti analizirati kako se gama aktivnost uzrokovana interakcijama fonskog neutronskog spektra menja u zavisnosti od promene prisustva miona u okruženju detektora [11-17]. Treba napomenuti da se doprinos miona fonskom zračenju otklanja izgradnjom dubokih podzemnih laboratorija ili korišćenjem različitih aktivnih zaštita [18, 19]. Međutim, u ovom radu biće razmatran ovaj doprinos u nadzemnim laboratorijama sa malom debljinom pokrovnog sloja.

Da bi se analizirala korelacija između prisustva miona i gama aktivnosti indukovane neutronskim interakcijama u ovom radu su vršena merenja sa dva HPGe detektora koja su bila prisutna u dva različita okruženja. U prvom slučaju iznad detektora je bio tanji pokrovni sloj u vidu jedne betonske ploče, dok je u drugom slučaju debljina pokrovnog

sloja bila četiri betonske ploče. Monitoring prisustva miona je izvršen merenjima pomoću plastičnog scintilacionog detektora. Treba napomenuti i da su HPGe detektori imali dve različite zaštite, olovnu i gvozdenu, te je na taj način analiziran i uticaj promene mionskog fluksa na produkciju neutrona u ovim materijalima.
Snimljeni gama spektri su analizirani i utvrđeni su intenziteti gama pikova koji potiču od neutronskih reakcija i njihova promena je upoređena sa varijacijama prisustva miona u okruženju detektora. Ovakva analiza može poslužiti za buduće projektovanje i izgradnju niskofonskih gama spektroskopskih laboratorija.

2. EKSPERIMENTALNA POSTAVKA I MERENJA

Gama spektrometrijska merenja su izvršena na Departmanu za fiziku, PMF, Novi Sad. Tom prilikom su korišćena dva germanijumska poluprovodnička detektora (HPGe) [10, 12, 14].
Prvi detektorski sistem se sastojao od HPGe detektora proizvođača Canberra. Detektor je koaksijalni n-tima, sa U-tipom kriostatske konfiguracije. Relativna efikasnost ovoga detektora je 100 % i aktivna zapremina mu je 380 cm^3. Detektor je postavljen u kućište sa prednjim prozorom od karbon fibera visoke čistoće sa debljinom od 0.89 mm, što omogućava visoku efikasnost za detekciju zračenja i sa energijama manjim od 20 keV. Detektor se nalazio u pasivnoj zaštiti izrađenoj od olova (Canberra model 777B). Ukupna masa zaštite je 1633 kg. Debljina zaštite je 15 cm s tim što je 125 cm spoljašnjeg sloja zaštite izgrađeno od običnog niskoaktivnog olova a unutrašnji sloj od 25 cm je od posebno namenjenog olova koje sadrži koncentraciju aktivnosti ^{210}Pb od 20 Bq/kg. Zaštita takođe sadrži i sloj bakra debljine 1.5 mm i kalaja debljine 1 mm [10].
Drugi detektorski sitem je HPGe detektor relativne efikasnost 22.3% i zapremine 119 cm^3 (Canberra model G.C.2525-7600). Detektor je bio smešten u gvozdenoj zaštiti zidova debljine 25 cm i mase od oko 20 tona [10]. Zaštita je proizvedena od gvožđa izlivenog pre Drugog svetskog rata zbog čega ne sadrži radioaktivnu kontaminaciju prouzrokovanu nuklearnim probama i havarijama na nuklearnim postrojenjima. Gvozdena zaštita je oblika kocke i ima korisnu zapreminu od oko 1 m^3 što omogućava postavljanje u zaštitu detektora zajedno sa Djuardovim sudom.
Monitoring prisustva miona je vršen korišćenjem plastičnog scintilatora. Ovaj detektor je dimenzija 50cm·50cm·5cm. Prozvođač detektora je Sconix Holland BV a tip detektora je R500*50 N 500/2P+VD 10-E2-X. Ova vrsta detektora je prvenstveno namenjena za izgradnju aktivnih zaštita germanijumskih detektora prilikom niskofonskih gama spektrometrijskih merenja.
Merenja u ovom radu sa dva germanijumska sistema i detektorom za praćenje prisustva miona su vršena na dve lokacije. Na prvoj lokaciji debljina pokrovnog sloja je bila od jedne betonske ploče debljine oko 20 cm dok je na drugoj lokaciji debljina pokrovnog sloja bila četiri betonske ploče (oko 80 cm). Mogućnost za ova merenja se javila usled preseljenja Laboratorije za gama spektroskopiju na Departmanu za fiziku u Novom Sadu. Na ovaj način je bilo moguće izvršiti analizu promene prisustva miona u dva različita okruženja i takođe analizirati promene u snimljenim gama spektrima.
Za potrebnu analizu su izvršena snimanja vremenski dugih fonskih spektara sa vremenom merenja od 252237 s do 2473816 s. Takođe na obe lokacije su vršena merenja i sa scintilacionim detektorom pri čemu su vremena merenja bila oko 2 h. To vreme merenja je bilo dovoljno da prikupljen broj događaja bude zadovoljavajući za statističku analizu podataka.

3. REZULTATI

Na slici 1 prikazani su snimljeni spektri sa scintilacionim detektorom na dve lokacije. U spektrima se uočava karakterističan pik od interakcije miona sa detektorom. Određen je ukupan odbroj ispod mionskog pika i vrednosti za dva data merenja su upoređene. Dobijeni rezultati si prikazani u tabeli 1.

Svi snimljeni gama spektri sa germanijumskim detektorima su analizirani pri čemu je posebna pažnja posvećena analizi broja detektovanih gama kvanata koji se javljaju usled interakcija neutrona sa germanijumom. Posebno su zanimljiva dva gama pika. Prvi od njih je sa energijom od 139,9 keV i prati zahvat neutrona na izotopu germanijuma ^{74}Ge (^{74}Ge(n,γ)^{75m}Ge) [2]. Ovaj gama pik se standardno koristi za određivanje prisustva sporih neutrona u niskofonskim spektrometrijskim sistemima sa Ge detektorima. Na slici 3 su prikazani delovi snimljenih spektara sa uočljivim pikom energije od 139,9 keV. Drugi gama pik čiji je intenzitet analiziran, prikazan na slici 2, ima energiju od 691 keV i detektuje se usled neelastičnog rasejanja neutrona na izotopu germanijuma ^{72}Ge (^{72}Ge(n,n')^{72}Ge) [2]. Ovaj gama pik se standarno koristi kao indikator prisustva brzih neutrona u samom germanijumskom detektoru.

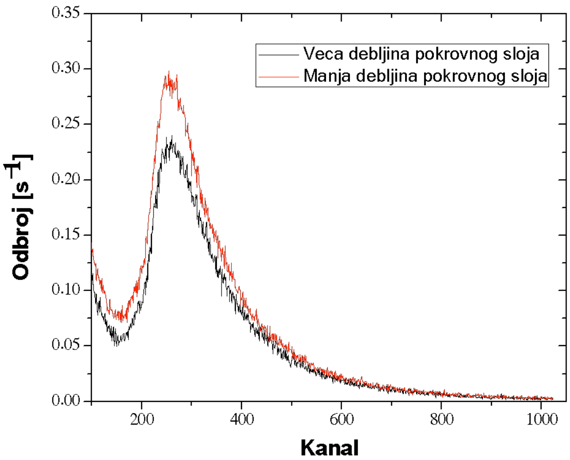

Slika 1. Snimljeni spektri sa scintilacionim detektorom na dve različite lokacije sa uočljivim pikom koji potiče od detekcije miona

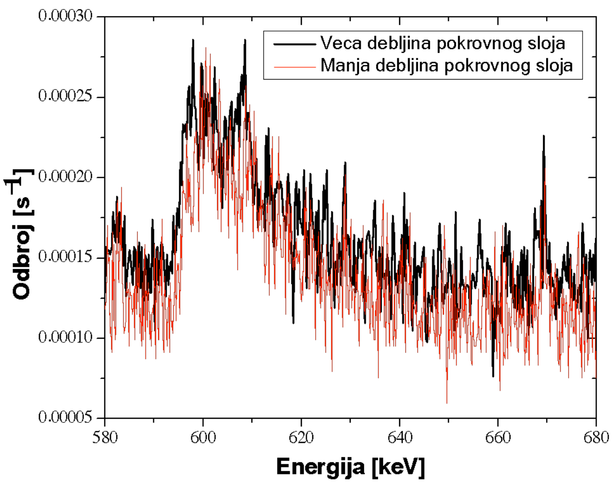

Slika 2. Deo snimljenih spektara sa HPGe detektorom u olovnoj zaštiti sa uočljivim gama pikom od 691 keV koji prati reakciju ^{72}Ge(n,n')^{72}Ge

Intenziteti ovih pikova su određeni i upoređeni su njihovi odnosi za oba HPGe detektora na dve merne lokacije. Rezultati su prikazani u tabeli 1.

Za analizu prisustva brzih neutrona u gvozdenoj zaštiti posebno može poslužiti gama pik energije od 846,8 keV koji prati reakciju $^{56}Fe(n,n')^{56}Fe$. Zbog toga su i intenziteti ovoga pika analizirani i predstavljeni u tabeli 1, dok je deo spektra koji sadrži ovaj pik prikazan na slici 4.

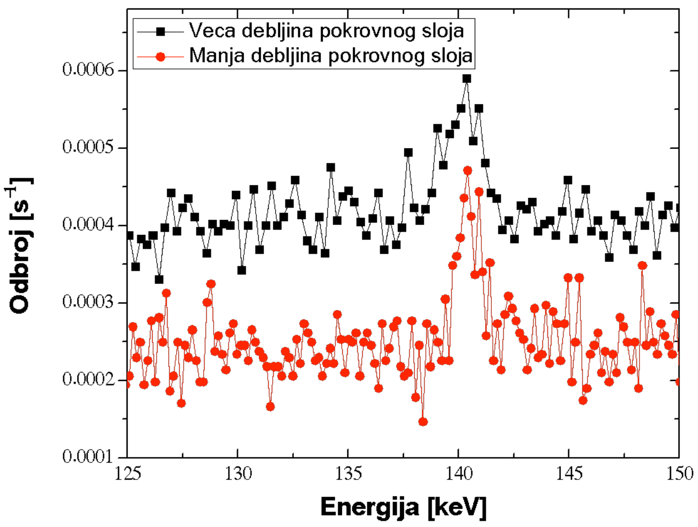

Slika 3. Deo snimljenih spektara sa HPGe detektorom u olovnoj zaštiti sa uočljivim gama pikom od 139 keV koji prati reakciju $^{74}Ge(n,\gamma)^{75m}Ge$

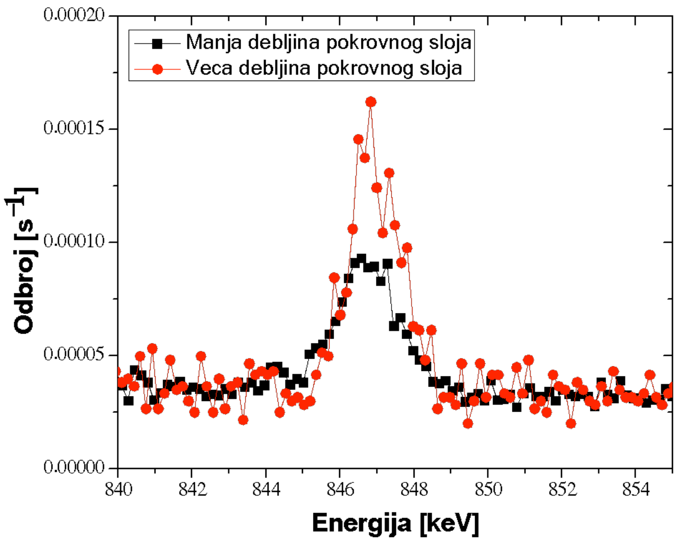

Slika 4. Deo snimljenih spektara sa HPGe detektorom u gvozdenoj zaštiti sa uočljivim gama pikom od 846.8 keV koji prati reakciju $^{56}Fe(n,n')^{56}Fe$

Tabela 1. Detektovani intenziteti i odnosi gama pikova koji potiču od neutronskih interakcija sa Ge detektorom i detektovani intenziteti mionskih događaja. Pozicija 1 - manja debljina pokrovnog sloja, Pozicija 2 - veća debljina pokrovnog sloja

	Pozicija 1	**Pozicija 2**	I_1/I_2
	$I_1[s^{-1}]$	$I_2[s^{-1}]$	
Odbroj mionskih događaja	56,51(28)	46,63(23)	1,212(8)
139,9 keV $^{72}Ge(n,\gamma)^{73}Ge$ **HPGe sa Pb zaštitom**	0,00128(7)	0,00088(5)	1,47(11)
139,9 keV $^{72}Ge(n,\gamma)^{73}Ge$ **HPGe sa Fe zaštitom**	0,00134(5)	0,000618(16)	2,18(8)
691 keV $^{74}Ge(n,n')^{74}Ge$ **HPGe sa Pb zaštitom**	0,00463(14)	0,00338(9)	1,37(5)
691 keV $^{74}Ge(n,n')^{74}Ge$ **HPGe sa Fe zaštitom**	0,0008(1)	Nije detektovano	**-**
846,8 keV $^{56}Fe(n,n')^{56}Fe$	0,00119(4)	0,000710(17)	1,69(7)

4. DISKUSIJA I ZAKLJUČAK

U ovom radu analiziran je uticaj promene prisustva miona na fonske događaje generisane neutronskim reakcijama sa germanijumskim detektorima u olovnoj i gvozdenoj zaštiti. Monitoring mionskog fluksa sa scintilacionim detektorom je pokazao da je na lokaciji sa manjim pokrovnim slojem prisutan oko 20% veći broj miona. Što je i očekivan rezultat usled veće atenuacije miona u većoj debljini materijala.

Rezulatati pokazuju da smanjenje broja miona prati i smanjenje broja detektovanih odbroja u gama pikovima koji potiču od neutronskih reakcija. To je posledica manje produkcije neutrona u materijalu zaštite detektora usled manjeg broja miona koji stižu do detektora u slučaju veće debljine pokrovnog sloja. Međutim, smanjenje broja neutrona je različito za detektore sa olovnom i gvozdenom zaštitom. Uočava se da je promena broja neutrona mnogo manja u olovnoj nego u gvozdenoj zaštiti (tabela 1). Smanjenje broja sporih neutrona (poređenje intenziteta gama linije od 139,9 keV) je u olovu oko 47% dok je u gvožđu značajno veće, čak više od dva puta. Isti trend se zapaža i za brze neutrone (gama linija od 691 keV). Broj brzih neutrona procenjen na osnovu neutronskih interakcija sa Ge je za oko 40% veći u slučaju manje debljine pokrovnog sloja. U slučaju Ge detektora u gvozdenoj zaštiti gama pik od 691 keV nije detektovan i neophodno je izvršiti fonsko merenje sa većim periodom merenja da bi se mogao utvrditi intenzitet ovoga pika. Odnosi detektovanih intenziteta gama pika od 846 keV upućuju na smanjenje broja brzih neutrona od oko 70% u gvozdenoj zaštiti.

Ovde prikazani rezultati će biti osnova za dalju analizu uticaja promene mionskog fluksa na produkciju neutrona u različitim materijalima koji su prisutni u okruženju germanijumskih detektora tokom niskofonskih gama spektrosopskih merenja. Ova analiza takođe može pružiti i informacije značajne za buduće projektovanje i izgradnju niskofonskih laboratorija za gama spektrometriju.

5. LITERATURA

[1] In: Povinec, P.P. (Ed.), Analysis of Environmental Radionuclides. Elsevier, Amserdam, pp. 209–239. S. Niese, 2008. Underground laboratories for low-level radioactivity measurements.

[2] G.P. Škoro et al., Environmental neutrons as seen by a germanium gamma-ray spectrometer, Nucl. Instr. and Meth. A 316 (1992) 333-336.

[3] G. Fehrenbacher et al., Fast neutron detection with germanium detectors: computation of response functions for the 692 keV inelastic scattering peak, Nucl. Instr. and Meth. A 372 (1996) 239-245.

[4] G. Heusser, Cosmic ray interaction study in low-level Ge spectrometry, Nucl. Instr. And Meth. A 369 (1996) 539-543.

[5] R. Wordel et al., Study of neutron and muon background in low-level germanium gamma-ray spectrometry, Nucl. Instr. And Meth. A 369 (1996) 557-562.

[6] W.V. Scroder et al, Z. Phys. 239 (1974) 57.

[7] E. Gete et al., Neutron-induced peaks in Ge detectors from evaporation neutrons, Nucl. Instr. And Meth. A 388 (1997) 212-219.

[8] T. Siiskonen and H. Toivonen, A model for fitting peaks induced by fast neutrons in an HPGe detector, Nucl. Instr. And Meth. A 540 (2005) 403-411.

[9] M. Krmar et al., A method to estimate a contribution of Ge(n,n′) reaction to the low-energy part of gamma spectra of HPGe detectors, Nucl. Instr. And Meth. A 709, (2013) 8-11.

[10] N. Jovancevic and M. Krmar, Analysis of Neutron Induced Gamma Activity in Lowbackground Ge – Spectroscopy Systems, Physics Procedia, 31, (2012) 93-98.

[11] M. Krmar et al., Measurement of ^{56}Fe activity produced in inelastic scattering of neutrons created by cosmic muons in an iron shield, Applied Radiation and Isotope, 70(1), (2012), 269-273.

[12] N. Jovančević and M. Krmar, Neutrons in the low-background Ge-detector vicinity estimated from different activation reactions, Applied Radiation and Isotopes, 69, (2011), 629-635.

[13] N. Jovančević et al., Neutron induced background gamma activity in low-level Ge-spectroscopy systems, Nucl. Instr. And Meth. A 612, (2009), 303-308.

[14] I. Bikit et al., Production of X-rays by cosmic-ray muons in heavily shielded gamma-ray spectrometers, Nucl. Instrum. Methods A 606, (2009), 495-500.

[15] S. Croft et al., The specific total and coincidence cosmic-ray-induced neutron production rates in materials, Nucl. Instrum. Methods A 505, (2003), 536–539.

[16] Da Silva et al., Neutron background for a dark matter experiment at a shallow depth site, Nucl. Instrum. Methods Phys. Res. A 354, (1995), 553-559.

[17] Y. Feige et al., Production rates of neutrons in soils due to natural radioactivity, J. Geophys. Res. 73, (1968), 3135–3142.

[18] G. Heusser, 1994. Background in ionizing radiation detection. In: Garcia-Leon, M., Gracia-Tenorio, R. (Eds.), Low-Level Measurements of Radioactivity in the Environment. Word Scientific, Singapore, pp. 69–112.

[19] G. Heusser, Low-radioactivity background techniques, Annu. Rev. Nucl. Part. Sci. 45, (1995), 543–590.

INFULECE OF MUON FLUX VARIATIONS TO LEVEL OF BACKGROUND ACTIVITY DURING LOW-BACKGROUND GAMMA SPECTROMETRIC MEASUREMENTS

Nikola JOVANČEVIĆ[1], David KNEŽEVIĆ[1], Miodrag KRMAR[1], Jovana NIKOLOV[1], Nataša TODOROVIĆ[1], Strahinja ILIĆ[2]

1) University of Novi Sad, Faculty of Scinece, Department of Physics, Novi Sad, Republic of Serbia, nikola.jovancevic@df.uns.ac.rs

2) Faculty of Technical Sciences, Novi Sad, Republic of Serbia

ABSTRACT

Muons are one of the main components of cosmic radiation on the sea level and there are significant source background activities during gamma spectroscopic measurements. Background activity can be produced by muon interactions with detector and surrounding materials. On this way created neutrons also have high influence on detection of background events. In this work there are presented the results of measurements by use of HPGe detectors with iron and lead shields. The detectors were located in two different environments where the different thicknesses of covering concrete layer were present. The monitoring of muons presence was done by measurements with plastic scintillation detector. The levels of neutron induced gamma activates were determinated and compared with changing of muon flux in detectors environment. The results can be used for improving of new detector shield in gamma spectrometry measurements.

ODREĐIVANJE ENERGETSKOG SPEKTRA NEUTRONA PRISUTNOG U GAMA SPEKTROMETRIJSKIM MERENJIMA SA GERMANIJUMSKIM DETEKTORIMA

Nikola JOVANČEVIĆ[1], David KNEŽEVIĆ[1,2], Miodrag KRMAR[1], Jovana NIKOLOV[1], Nataša TODOROVIĆ[1], Jovana PETROVIĆ[1]

1) Univerzitet u Novom Sadu,Prirodno-matematički fakultet,Departman za fiziku, Novi Sad, Republika Srbija, nikola.jovancevic@df.uns.ac.rs

2) Institut za fiziku, Univerzitet u Beogradu, Republika Srbija

SADRŽAJ

Određivanje prisustva neutrona tokom niskofonskih gama spektrometrijskih merenja je od posebne važnosti. Zbog toga je u ovom radu analiziran način određivanja energetskog spektra neutrona prisutnog u merenjima sa HPGe detektorima. Ovaj metod se zasniva na korišćenju metoda dekonvolucije. Za to je neophodno poznavati gama aktivnost indukovanu neutronskim reakcijama sa različitim izotopima germanijuma kao i efikasne preseke za date neutronske reakcije. Ovaj pristup je testiran merenjima sa fisionim izvorom neutrona ^{252}Cf koji je bio postavljen u blizini HPGe detektora. Dobijeni rezultati pokazuju da ovaj metod moze pružiti pouzdane podatke o obliku energetskog spektra neutrona tokom gama spektrometrijskih merenja.

1. UVOD

Neutronske reakcije sa Ge-detektorom i okolnim materijalima mogu da proizvedu merljivu gama aktivnost putem reakcija zahvata i rasejanja [1]. Kako su neutroni jedan od primarnih izvora fona u gama spektrometriji, analiziranje neutronskog prisustva je od velikog značaja u niskofonskim eksperimentima, kao i u različitim promptnim neutronsko aktivacionim eksperimentima [2]. Analiza neutronskih interakcija, shodno tome, je bila predmet mnogih istraživanja [1-10]. Međutim, i dalje ostaje problem određivanja neutronskog spektra u Ge-detektoru tokom gama spektrometrijskih merenja [11-13]. U prethodnim istraživanjima koristili smo proceduru dekonvolucije za procenu neutronskog spektra koji potiče od kosmičkog zračenja u germanijumskom detektoru [14]. Ova procedura polazi od početnog (pretpostavljenog) spektra, koji se određuje na osnovu eksperimentalno ili teorijski određenih dostupnih podataka. Postupak dekonvolucije modifikuje početni spektar tako da se dobije najbolje slaganje između izmerenih vrednosti gama aktivnosti (u našem slučaju germanijumskih izotopa nakon interakcije sa neutronima) i izračunatih vrednosti gama aktivnosti korišćenjem dekonvolucijom dobijenog neutronskog spektra i dostupnih podataka za efikasne preseke za nuklearne reakcije koje su od interesa. Ovaj metod bi trebao da bude univerzalan i primenjiv u svim merenjima kada su u okruženju germanijumskih detektora prisutni neutroni, kao na primer u slučaju promptnih neutronskih aktivacionih merenja. U ovom radu smo uporedili izmerene aktivnosti germanijumskih izotopa i uporedili ih sa vrednostima dobijenim računom, pri čemu je kao izvor neutrona korišćen ^{252}Cf.

Poređenje ovih vrednosti je neophodno da bi se dobio preliminarni rezultat koji će se koristiti u postupku dekonvolucije za dobijanje neutronskog spektra prilikom merenja sa fisionim izvorom neutrona ^{252}Cf [15, 16]. Poređenjem izračunatih i izmerenih vrednosti gama aktivnosti moguće je doći do informacija koje će poboljšati početni spektar koji se onda može koristiti za procedure dekonvolucije.

2. EKSPERIMENTALNA POSTAVKA

Merenje je izvršeno u Laboratoriji za gama spektroskopiju, Katedre za nuklearnu fiziku, u okviru Departmana za fiziku, Prirodno-matematičkog fakulteta u Novom Sadu. Za merenje gama aktivnosti indukovane neutronima, korišćen je HPGe detektor proizvođača Canberra, serijskog broja G.C.2520-7600. Detektor je n-tipa, relativne efikasnosti 22.3% i aktivne zapremine 119 cm^3. Detektor se tokom merenja nalazio unutar gvozdene zaštite zapremine 1 m^3 sa zidovima debljine 25 cm i mase oko 20 t.
Izvor neutrona u ovom eksperimentu je bio, kao što je ranije pomenuto, ^{252}Cf aktivnosti $4{,}5 \cdot 10^3$ n/s u 4π sr. ^{252}Cf ima dva moguća kanala raspada: alfa raspad (96,9%) i spontanu fisiju (3,2%). Period poluraspada za spontanu fisiju je $T_{1/2}$=2,645 godina i prilikom svake spontane fisije emituje se u proseku 3,77 neutrona.

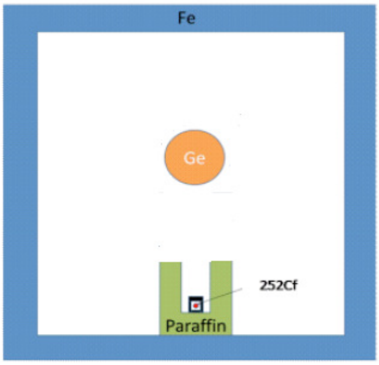

Slika 1. Šematski prikaz eksperimenta

^{252}Cf se nalazio u Marineli posudi obloženoj parafinom sa svih strane osim sa strane koja je usmerena ka HPGe detektoru, kao što je prikazano na slici 1. Kako bi se apsorbovalo gama zračenje koje potiče od raspada fisionih potomaka nakupljenih u ^{252}Cf, izvor je prekriven gvozdenom pločicom debljine 8 mm. Merenje je trajalo 151367 s, što je omogućilo zadovoljavajuću statistiku detektovanih gama kvanata nastalih prilikom interakcije neutrona sa jezgrima germanijuma.

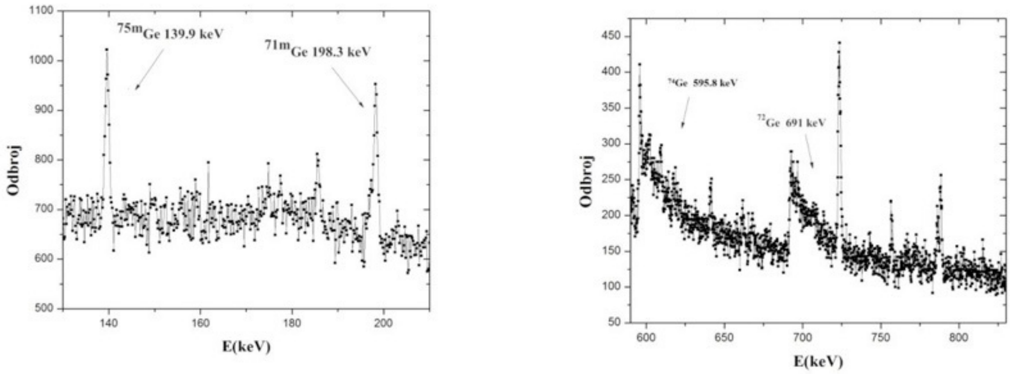

Slika 2. Delovi spektra sa detektovanim neutronima indukovanim gama pikovima koji potiču od (n,γ) reakcija (leva slika) i (n,n') reakcija (desno)

3. REZULTATI

3.1. DETEKTOVANE AKTIVNOSTI

Na slici 2 prikazani su delovi spektra sa karakterističnim gama pikovima koji potiču od neutronskih interakcija sa izotopima germanijuma [9, 17]. Identifikovane gama linije, njihovo poreklo i intenziteti su prikazani u tabeli 1. Od svih detektovanih linija izabrane su one sa najboljom statistikom [9]. Za intenzitete standardnih spektroskopskih pikova Gausovskog oblika (139 keV ^{74}Ge(n,γ)^{75m}Ge i 198 keV ^{70}Ge(n,γ)^{71m}Ge) korišćen je programski paket GENIE2000. Intenzitet asimetričnih (n,n') gama pikova (691,0 keV ^{72}Ge(n,n')^{72}Ge i 595,8 ^{74}Ge(n,n')^{74}Ge), određen je korišćenjem funkcije za fitovanje [4,17]:

$$C(E) = a_0 ERFC\left[-\frac{E\text{-}E_0}{\sigma_0}\right] \cdot Exp\left[-\frac{E\text{-}E_0}{\Delta}\right] + \sum_{i=1}^{n} a_i \cdot Exp\left[-\frac{1}{2\sigma_i^2}(E\text{-}E_i)^2\right] + F \quad (1)$$

Tabela 1. Opšte informacije o detektovanim gama linijama i odgovarajućim vrednostima intenziteta

Energija [keV]	Nuklid	Reakcije	Intenzitet [s^{-1}]
139,9	^{75m}Ge	^{74}Ge(n,γ)^{75m}Ge ^{76}Ge(n,2n)^{75m}Ge	0,0136(8)
198,3	^{71m}Ge	^{70}Ge(n,γ)^{71m}Ge ^{72}Ge(n,2n)^{71m}Ge	0,0159(8)
595,8	^{74}Ge	^{74}Ge(n,n')^{74}Ge	0,0559(27)
691,3	^{72}Ge	^{72}Ge(n,n')^{72}Ge	0,068(5)

U jednačini (1), prvi član opisuje oblik Ge(n,n') gama pika. U drugom članu, izraz unutar sume je Gausova funkcija koja odgovara simetričnim gama linijama u regionu koji se fituje. Ove linije mogu biti Ge(n,γ) gama linije ili bilo koje druge linije koje pripadaju fonu. Parametar F označava fonski kontinuum za koji se prilikom fitovanja pretpostavlja da je linearna funkcija. Parametri fita su a_0, a_i , E_0, E_i, σ_0 , σ_i i Δ. U ovom slučaju E_0 i E_i predstavljaju energije detektovanih gama linija; a_0 i a_i su maksimalne amplitude ovih linija. Parametri σ_0 i σ_i su određeni širinom linije na polovini maksimuma i odgovaraju energetskoj rezoluciji detektora. Parametar Δ određuje karakteristike eksponencijalnog repa Ge(n,n') linija. Varijacijom parametara fita linija i fona, kao i varijacijom energetskog opsega unutar kojeg je izvršeno fitovanje dobijeni su optimalni rezultati [4]. Za fitovanje je korišćen ROOT softver za analizu podataka [18]. Pomoću ovog fita obrađen je i intenzitet gama pika germanijuma energije od 595,8 keV-a koji nastaje i usled (n,γ) i (n,n') reakcija, tj. interakcijama i sporih i brzih neutrona. Ovo je omogućilo razdvajanje ove linije za potrebe analize na simetričnu gama liniju koja potiče od zahvata i asimetričnu gama liniju koja potiče od neelastičnog rasejanja [19].
Nakon određivanja intenziteta gama linija od interesa, saturacione aktivnosti određenih germanijumskih izotopa po atomu prirodnog germanijuma su izračunate kao [9, 12]:

$$A_k = \frac{C \cdot M}{t \cdot p \cdot (\varepsilon + \alpha) \cdot m \cdot N_a} \quad (2)$$

gde C predstavlja detektovani odbroj gama linije, t je vreme merenja, p je verovatnoća emisije gama linije, α je konverzioni koeficijent, ε je efikasnost u piku pune absorpcije (izračunata pomoću GEANT4 softverskog paketa), M je molarna masa germanijuma, m je masa germanijumskog kristala i N_a Avogadrova konstanta. Aktivnosti dobijene korišćenjem jednačine (2), A_k, su prikazane u tabeli 2.

3.2. RAČUNATE AKTIVNOSTI

Metod za računanje aktivnosti germanijumskih izotopa se zasniva na činjenici da je neutronima indukovana aktivnost za aktivirani radionuklid, k, proporcionalna proizvodu efikasnog preseka za proizvodnju određenog radionuklida i neutronskog fluksa [20]:

$$A_k = \sum_i \sigma_{ik} \Phi_i \; ; \; i = 1, 2, 3 \ldots c; \quad k = 1, 2, 3 \ldots . m \tag{3}$$

gde su σ_{ik} odgovarajuće funkcije efikasnog preseka, a Φ_i je neutronski fluks za energijski prozor E_i . Indeks k prolazi kroz brojeve korišćenih radionuklida, a m predstavlja ukupan broj radionuklida. Maksimalna vrednost indeksa i, c, označava broj energijskih prozora u neutronskom spektru i funkciji efikasnog preseka. Iz jednačine (3), moguće je proceniti očekivane vrednosti za aktivnosti germanijumskih izotopa. U ovom radu, aktivnosti od interesa, A_k, predstavljaju aktivnosti izotopa germanijuma koje su indukovane različitim neutronskim reakcijama. Vrednosti σ_{ik} za reakcije od interesa su preuzete iz ENDF baze podataka za efikasne preseke, preciznije iz ENDF/B-VII.1 biblioteke [21], kao što je prikazano na slici 3.

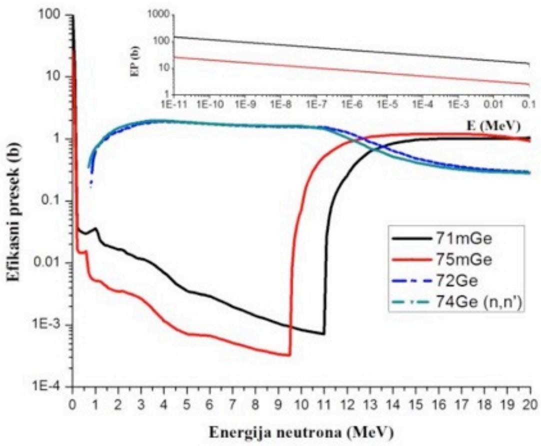

Slika 3. Funkcije efikasnih preseka za proizvodnju Ge izotopa putem neutronskih reakcija (sa uvećanim niskoenergetskim delom)

Za neutronski spektar je korišćen spektar ^{252}Cf čiji je oblik dobro poznat, bez ikakvih modifikacija njegovog oblika, iako je realno za očekivati da je u našoj eksperimentalnoj postavci spektar neutrona u detektoru drugačiji od spektra koji emituje izvor. Ovo je urađeno upravo iz razloga da bi se poređenjem merenih i izračunatih vrednosti aktivnosti izotopa germanijuma moglo zaključiti kakve modifikacije treba izvršiti nad spektrom ^{252}Cf tako da on realnije opisuje spektar neutrona unutar samog detektora. Vrednosti ovako dobijenih aktivnosti su prikazani u tabeli 2. Treba napomenuti da je prilikom izračunavanja aktivnosti izotopa germanijuma korišćen faktor normiranja koji treba da omogući poređenje izmerenih i izračunatih vrednosti jer je prilikom računanja ukupan fluks neutrona normiran na jediničnu vrednost.

4. DISKUSIJA I ZAKLJUČAK

U tabeli 2 prikazane su izmerene i izračunate aktivnosti, kao i njihovi odnosi. Uočava se da se za izotope germanijuma ^{71m}Ge i ^{72}Ge izračunate vrednosti relativno dobro slažu sa izmerenim vrednostima, dok su kod ^{74}Ge i ^{75m}Ge izmerene vrednosti veće oko 2,5 i 4 puta od izračunatih, respektivno. Odstupanja računatih i izmerenih vrednosti za izotop ^{75m}Ge upućuju na mogućnost značajnijeg uticaja interakcija brzih neutrona na intenzitet gama pika od 139,9 keV, što je i bio predmet naše prethodne studije [19]. Neslaganje izmerenih i računatih vrednosti za ^{74}Ge moze biti objašnjeno značajnijim doprinosom ^{73}Ge(n,γ)^{74}Ge detektovanom odbroju gama pika energije od 595,8 keV. Ova odstupanja postavljaju i pitanje validnosti dostupnih efikasnih preseka za korišćene neutronske reakcije.
Ovde prikazani rezultati upućuju na to da promptni fisioni neutronski spektar ^{252}Cf ne može na najbolji način objasniti prisutan spektar neutrona tokom izvršenog merenja. To može biti posledica usporavanja i termalizacije neutrona u materijalima prisutnim u okruženju detektora. Takođe, za dalju analizu neophodno je u račun uključiti i druge neutronske reakcije sa izotopima germanijuma i izvršiti proveru validnosti dostupnih podataka za efikasne preseke za interakciju neutrona sa jezgrima germanijuma.

Tabela 2. Intenziteti, izmerene i računate aktivnosti za reakcije od interesa, kao i odnosi izmerenih i računatih vrednosti

Izotop	Izmerena aktivnost [10^{-26} Bq]	Računata aktivnost [10^{-26} Bq]	Odnos aktivnosti (I/R)
^{71m}Ge	0,506(27)	0,63	0,80
^{72}Ge	1,31(9)	1,57	0,83
^{74}Ge	7,1(3)	1,74	4,08
^{75m}Ge	0,288(16)	0,112	2,57

5. LITERATURA

[1] G. Heusser, Nucl. Instrum. Methods Phys. Res. A 369 (1996) 539.
[2] A. Dragić, et al., Phys. Procedia 59 (2014) 125.
[3] R. Wordel, et al., Nucl. Instrum. Methods Phys. Res. A 369 (1996) 557.
[4] E. Gete, et al., Nucl. Instrum. Methods Phys. Res. A 388 (1997) 212.
[5] N. Jovančević, M. Krmar, Phys. Procedia 31 (2012) 93–98.
[6] Y. Feige, et al., J. Geophys. Res. 73 (1968) 3135–3142.
[7] G.P. Škoro, et al., Nucl. Instrum. Methods Phys. Res. A 316 (1992) 333.
[8] N. Jovančević, M. Krmar, Appl. Rad. Isot. 69 (2011) 629–635.
[9] N. Jovančević, et al., Nucl. Instrum. Methods Phys. Res. A 612 (2009) 303–308.
[10] G. Heusser, Background in ionizing radiation detection, in: M. Garcia-Leon, R. Gracia-Tenorio (Eds.), Low-Level Measurements of Radioactivity in the Environment, Word Scientific, Singapore, 1994, pp. 69–112.

[11] C. Chund, Y.R. Chen, Nucl. Instrum. Methods Phys. Res. A 301 (1991) 328–336.
[12] J.E. Naye, Nucl. Instrum. Methods Phys. Res. A 368 (1996) 832–846.
[13] G. Fehrenbacher, et al., Nucl. Instrum. Methods Phys. Res. A 372 (1996) 239.
[14] D. Knežević , N. Jovančević, M. Krmar, J. Petrović, Modeling of neutron spectrum in the gamma spectroscopy measurements with Ge-detectors, Nucl. Instrum. Methods Phys. Res. A, 833 (2016), p. 23-26.
[15] C.W. Reich, W. Mannhart, T. England, IAEA Technical Report INDC(NDS)220/L, p.305, IAEA, Vienna (1989).
[16] International Reactor Dosimetry and Fusion File, IAEA Data, https://www-nds.iaea.org/IRDFF.
[17] T. Siiskonen, H. Toivonen, Nucl. Instrum. Methods Phys. Res. A 540 (2005) 403.
[18] ROOT cern, ⟨https://root.cern.ch⟩.
[19] B. Anđelić, D. Knežević, N. Jovančević, M. Krmar, J. Petrović, A.Toth, Ž. Medić, J. Hansman, Presence of neutrons in the low-level background environment estimated by the analysis of the 595.8 keV gamma peak, Nucl. Instrum. Methods Phys. Res. A, 852 (2017), p. 80–84.
[20] A. Trkov, V. Radulović, J. Radioanal. Nucl. Chem. 304 (2015) 763–778.
[21] The ENDF, Evaluated Nuclear Data File, ⟨https://www-nds.iaea.org/exfor/endf.htm⟩.

DETERMINATION OF NEUTRON ENERGY SPECTRA PRESENCE IN GAMMA SPECTROSCOPIC MEASUREMENTS USING GE-DETECTORS

Nikola JOVANČEVIĆ[1], David KNEŽEVIĆ[1,2], Miodrag KRMAR[1], Jovana NIKOLOV[1], Nataša TODOROVIĆ[1], Jovana PETROVIĆ[1]

1) *University of Novi Sad, Faculty of Sciences, Department of Physics, Novi Sad, Serbia, nikola.jovancevic@df.uns.ac.rs*

2) *Institute of Physics, Pregrevica 118, University of Belgrade, Belgrade, Serbia*

ABSTRACT

Determination of neutron spectra in the Ge-detector during low-level gamma spectroscopy measurements is of great importance. Thus, in this paper we analyzed the method for the determination of neutron energy spectra present during measurements with HPGe detectors. This method is based on using the deconvolution procedure. It requires the knowledge of neutron induced gamma activities of Ge isotopes and the cross section data for the neutron reactions of interest. This approach was tested with measurements that used the fission neutron source ^{252}Cf placed in proximity of the HPGe detector. Results show that this method can provide reliable data about the shape of neutron energy spectrum during gamma spectroscopy measurements.

ISSN 1063-7788, Physics of Atomic Nuclei, 2017, Vol. 80, No. 2, pp. 237–250. © Pleiades Publishing, Ltd., 2017.
Original Russian Text © D.C. Vu, A.M. Sukhovoj, L.V. Mitsyna, Sh. Zeinalov, N. Jovancevic, D. Knezevic, M. Krmar, A. Dragic, 2017, published in Yadernaya Fizika, 2017, Vol. 80, No. 2, pp. 113–126.

NUCLEI
Theory

Representation of Radiative Strength Functions within a Practical Model of Cascade Gamma Decay

D. C. Vu[1),2)*, A. M. Sukhovoj[1), L. V. Mitsyna[1)***, Sh. Zeinalov[1)****, N. Jovancevic[3)*****, D. Knezevic[3)******, M. Krmar[3)*******, and A. Dragic[4)********

Received June 14, 2016; in final form, August 24, 2016

Abstract—A practical model developed at the Joint Institute for Nuclear Research (JINR, Dubna) in order to describe the cascade gamma decay of neutron resonances makes it possible to determine simultaneously, from an approximation of the intensities of two-step cascades, parameters of nuclear level densities and partial widths with respect to the emission of nuclear-reaction products. The number of the phenomenological ideas used is minimized in the model version considered in the present study. An analysis of new results confirms what was obtained earlier for the dependence of dynamics of the interaction of fermion and boson nuclear states on the nuclear shape. From the ratio of the level densities for excitations of the vibrational and quasiparticle types, it also follows that this interaction manifests itself in the region around the neutron binding energy and is probably different in nuclei that have different parities of nucleons.

DOI: 10.1134/S1063778817020260

INTRODUCTION

At any excitation energy, parameters of the cascade gamma decay of an arbitrary high-lying nuclear level are determined exclusively by the level density ρ and the partial widths Γ with respect to electric and magnetic dipole transitions. The intensity of cascades that involve purely quadrupole transitions is negligible at nuclear-excitation energies above several MeV units. For either parity, the spins of levels that are excited by primary transitions lie in the range of $2 \leqslant \Delta J \leqslant 4$. Investigation of the gamma-decay process is of interest, first of all, for studying the dynamics of interaction of fermion and boson states of nuclear matter. Reliable information on the subject is also necessary for more precisely describing the fission process. According to [1], the distribution of the energy between excited fission fragments depends on their level densities. However, the level densities calculated on the basis of existing models [2] deviate strongly from the most recent experimental data [3]. The reason behind this discrepancy may only be that experiments that detect the cascade of reaction products provide more information than any procedure for obtaining spectra of single gamma rays or nucleon products without employing a coincidence mode.

Since one-step gamma-ray spectra and reaction cross sections depend on the product $\rho \times \Gamma$, it is absolutely impossible to determine simultaneously reliable values of ρ and Γ from such data. This was done only in experiments that study cascades involving two sequential gamma transitions whose intensities carry information both about the nuclear excitation energy and about the energy of the emitted photon (nucleon). Only such experiments may reduce the total error in the values determined for ρ and Γ to a few tens of percent.

Since all individual levels and probabilities for transitions between them cannot be determined with the aid of modern spectrometric detectors, information about nuclear superfluidity is extractable from indirect experiments exclusively. In that case, both the level density ρ and the partial widths Γ are unknown functions in any nucleus.

1)Joint Institute for Nuclear Research, ul. Joliot-Curie 6, Dubna, Moscow oblast, 141980 Russia.
2)Institute of Physics, Vietnam Academy of Science and Technology, 10 Dao Tan, Ba Dinh, Ha Noi, Viet Nam.
3)Department of Physics, Faculty of Sciences, University of Novi Sad, Trg Dositeja Obradovića 3, 21000 Novi Sad, Republic of Serbia.
4)Institute of Physics Belgrade, Pregrevica 118, 11080 Zemun, Republic of Serbia.
*E-mail: vuconghnue@gmail.com
**E-mail: suchovoj@nf.jinr.ru
***E-mail: mitsyna@nf.jinr.ru
****E-mail: zeinal@nf.jinr.ru
*****E-mail: nikola.jovancevic@df.uns.ac.rs
******E-mail: david.knezevic@df.uns.ac.rs
*******E-mail: krmar@df.uns.ac.rs
********E-mail: dragic@ipb.ac.rs

1. POTENTIAL OF THE PRESENT-DAY EXPERIMENT AND OF ITS MODEL SIMULATION

At a fixed primary-transition energy E_1, the intensities $I_{\gamma\gamma}(E_1)$ of two-step cascades connecting a neutron resonance (or some other compound state) λ and some group f of low-lying nuclear levels and proceeding through arbitrary intermediate levels i are described by the set of equations

$$I_{\gamma\gamma}(E_1) = \sum_{\lambda,f}\sum_{i}\frac{\Gamma_{\lambda i}}{\Gamma_{\lambda}}\frac{\Gamma_{if}}{\Gamma_{i}} \quad (1)$$
$$= \sum_{\lambda,f}\frac{\Gamma_{\lambda i}}{\langle\Gamma_{\lambda i}\rangle m_{\lambda i}} n_{\lambda i}\frac{\Gamma_{if}}{\langle\Gamma_{if}\rangle m_{if}},$$

where $m_{\lambda i}$ is the number of levels excited by primary transitions in the ranges between the energy of the initial level λ and the energy of an intermediate level i, m_{if} is the number of levels excited by secondary gamma transitions in the ranges between the energy of an intermediate level i and the energy of the final level f, and $n_{\lambda i}$ is the number of intermediate levels of cascades in narrow ranges of primary-transition energies. From the set of Eqs. (1), which relates the unknown number of levels, n (or m), to unknown partial widths, Γ, one determines the set of parameters p and q of the model functions $\rho = f(p_1, p_2, \ldots)$ and $\Gamma = \varphi(q_1, q_2, \ldots)$ with an error originating from the inconsistency of the existing theoretical ideas with experimental results. The analysis performed earlier in [4] revealed that one can even include in the model the possible relation between the values of the level density and strength functions in some narrow excitation-energy interval. Thus, we see that, at any densities of the levels λ and i, one can determine parameters of the sought functions ρ and Γ from the spectra of two-step cascades.

The analysis in [3] of experimental data on cascade intensities over the mass-number range of $28 \leqslant A \leqslant 200$ showed that experimental level densities could not be reproduced to an experimental precision on the basis of models that ignore the existence of bosonic branches of nuclear-matter states (on the basis of those where the inclusion of this branch was insufficiently correct).

The procedure developed by our group does not require invoking hypotheses not tested experimentally (such as the Porter–Thomas hypothesis [5] on the distribution of widths with respect to the emission of nuclear-reaction products, the Axel–Brink hypothesis [6, 7] that radiative-width values are independent of the energy of an excited level, or the Bohr–Mottelson hypothesis [8] on the correctness of employing the optical model of the nucleus to determine the probability for the emission of nucleon reaction products). The Dubna model of the cascade gamma decay of compound nuclear states whose excitation energies lie in the range of $E_{\rm ex} \approx 5$–10 MeV is based on a model of the density of n-quasiparticle levels, the balance of the changes in the entropy and energy of quasiparticle levels [2, 9, 10], and tested ideas about the shape of the energy dependence of radiative strength functions.

The systematic error of any experimental procedure for obtaining the functions ρ and Γ is always determined by large coefficients of the transfer of the errors in the measured spectrum, δS, or in the reaction cross section, $\delta\sigma$, to the errors $\delta\rho$ and $\delta\Gamma$ in the parameters being determined. The error in question may grow sizably upon the increase in the energy of the level that decays in the reaction under study. This error and the direction in which the model concepts of $\rho = f(p_1, p_2, \ldots)$ and $\Gamma = \varphi(q_1, q_2, \ldots)$ should be corrected can only be estimated by comparing various versions of the description of the level densities and radiative strength functions. For example, a comparison of several versions of our practical model [3, 11, 12] made it possible to reveal that the rate of the change in the vibrational level density specified phenomenologically in [11, 12] is determined partly or fully by the pairing energy Δ_0 of the last nucleon in the nucleus being considered. In all of the implemented versions of the practical model, the accuracy of the approximation of intensities remains unimpaired as one gradually reduces the number of fitted parameters; therefore, we do not present here the ultimate approximations of the spectra $I_{\gamma\gamma}$.

In contrast to what was done in [3], the proposed model version employs, instead of two parameters (the rate of the change in the nuclear entropy and the rate of the change in the energy of quasiparticle states) in the phenomenological expression for the coefficient of the collective level-density enhancement, $C_{\rm coll}$ [3, 10], only one fitted parameter, E_u; that is,

$$C_{\rm coll} = A_l \exp(\sqrt{(E_{\rm ex} - U_l)/E_u} - (E_{\rm ex} - U_l)/E_u) + \beta, \quad (2)$$

where A_l are the parameters of the vibrational level density above the point of break of each lth Cooper pair and U_l are the energy thresholds for the break of Cooper pairs. For deformed nuclei, the parameter $\beta \geqslant 1$ may differ from unity.

The effect of shell inhomogeneities in the single-particle spectrum [2, 10] was taken into account in terms of the excitation-energy-dependent level-density parameter a,

$$a(A, E_{\rm ex}) = \tilde{a}(1 + ((1 - \exp(\gamma E_{\rm ex}))\delta E/E_{\rm ex})), \quad (3)$$

or in terms of the parameter $g = 6a/\pi^2$ for n-quasiparticle states in the vicinity of the Fermi surface [9]. The asymptotic value of $\tilde{a} = 0.114A + 0.162A^{2/3}$ and the value of $\gamma = 0.054$ were taken from [2, 10]. The shell correction δE calculated [2] on the basis of mass-defect data within the liquid-drop model of the nucleus was slightly modified for the mean spacing between resonances, D_λ, to remain unchanged [3].

2. ENERGY DEPENDENCE OF STRENGTH FUNCTIONS

In the model of cascade gamma decay, the shape of the energy dependence of partial radiative widths should be specified to a high degree of precision for any excited levels and energies of emitted gamma rays.

On the basis of existing models, the strength function for a nucleus of mass number A is defined as $k = \Gamma/(A^{2/3}E_\gamma^3 D_\lambda)$, where E_γ is the gamma-transition energy. The absolute value of the sum of radiative widths for primary $E1$ and $M1$ cascade transitions (total radiative width) can usually be determined from measured reaction cross sections. The most probable form of this sum can be obtained from purely phenomenological considerations or from an extrapolation of some theoretical models to the excitation-energy range of $E_d < E_{\rm ex} < B_n$ {here, E_d is the point of transition in Eq. (1) from known levels [13] to the level-density concept, while B_n is the neutron binding energy in the nucleus}.

It was found experimentally that a precise reproduction of cascade intensities leads to supplementing the energy dependence of the function $k(E1, E_\gamma) + k(M1, E_\gamma)$ with several peaks that have various areas, positions of the center, and shape asymmetries. But the main term in this energy dependence can be represented by a smooth distribution of strength functions from models of the type in [14] but with allowance for additional parameters whose variation generates a set of functions describing $E1$ and $M1$ transitions and taking values over a broad region (see [11, 12]). The shape of the extra peaks can be revealed and specified only empirically. For example, a description of each such peak in terms of two exponentials (as in an earlier version of our model [3, 11, 12]) is convenient in solving the set of nonlinear equations in (1), even though these exponentials are not used in the model formalism based on theoretical concepts [2].

In order to describe the shape of the peaks in the $E1$ and $M1$ strength functions, Breit–Wigner or Lorentzian functions are used. An asymmetric Breit–Wigner function was applied in theoretically analyzing the regularities of fragmentation of quasiparticle states for their various positions with respect to the Fermi surface [15]. In employing this function, we were unfortunately unable to choose a set of parameters that would be appropriate for approximating the most probable values of $\rho = f(p_1, p_2, \ldots)$ and $\Gamma = \varphi(q_1, q_2, \ldots)$.

The use of an asymmetric Lorentzian curve in describing local peaks in the strength functions proved to be more straightforward. For each ith peak its parameters, such as the position of the center, E_i; the width, Γ_i; the amplitude, W_i; and the asymmetry parameter, $\alpha_i = CT^2$, are similar to their counterparts in the model employed in [14]. The expression $\alpha_i(E_\gamma - E_i)/E_\gamma$ increases linearly as the excitations energy $B_n - E_i$ grows from zero at the center of the respective peak to the maximum value at B_n and decreases as the nuclear excitation energy becomes lower. Thus, the peaks of the $E1$ and $M1$ strength functions are represented in the form

$$k = W\frac{(E_\gamma^2 + (\alpha_i(E_i - E_\gamma)/E_\gamma))\Gamma_i^2}{(E_\gamma^2 - E_i^2)^2 + E_\gamma^2\Gamma_i^2}. \qquad (4)$$

In approximating Lorentzian functions that describe the decay of a highly excited level, the convergence of the respective iterative process sharply becomes poorer, which creates a serious problem. Upon fitting all parameters of the functions in Eq. (4), the widths Γ_i decrease indefinitely within some segments of the iterative-process trajectory.

The need for taking into account the effect of a sharp local change in the level density on strength functions was revealed at the stage of a model-free determination of the set of random functions ρ and Γ [16]. For this purpose, the strength functions to be determined were multiplied in [4] by the ratio

$$M = \rho_{\rm mod}/\rho_{\rm exp}, \qquad (5)$$

where $\rho_{\rm exp}$ is the best approximation for the iteration being considered and $\rho_{\rm mod}$ is a smooth model dependence that reproduces both the density of neutron resonances and the cumulative sum of known levels for which $E_{\rm ex}$ is lower than E_d. In order to determine $\rho_{\rm mod}$, we have chosen the back-shifted Fermi gas model. In the present version of our analysis, we have employed the constraint $1 \leqslant \rho_{\rm mod}/\rho_{\rm exp} \leqslant 10$ [11].

3. RESULTS

Difficulties in solving the set of Eqs. (1) arise both because of a strong nonlinearity of the sought functions ρ and Γ and because of their anticorrelation. There is a probability for arriving at a spurious minimum of χ^2, and this may lead to a sizable systematic error in the resulting values of ρ and Γ.

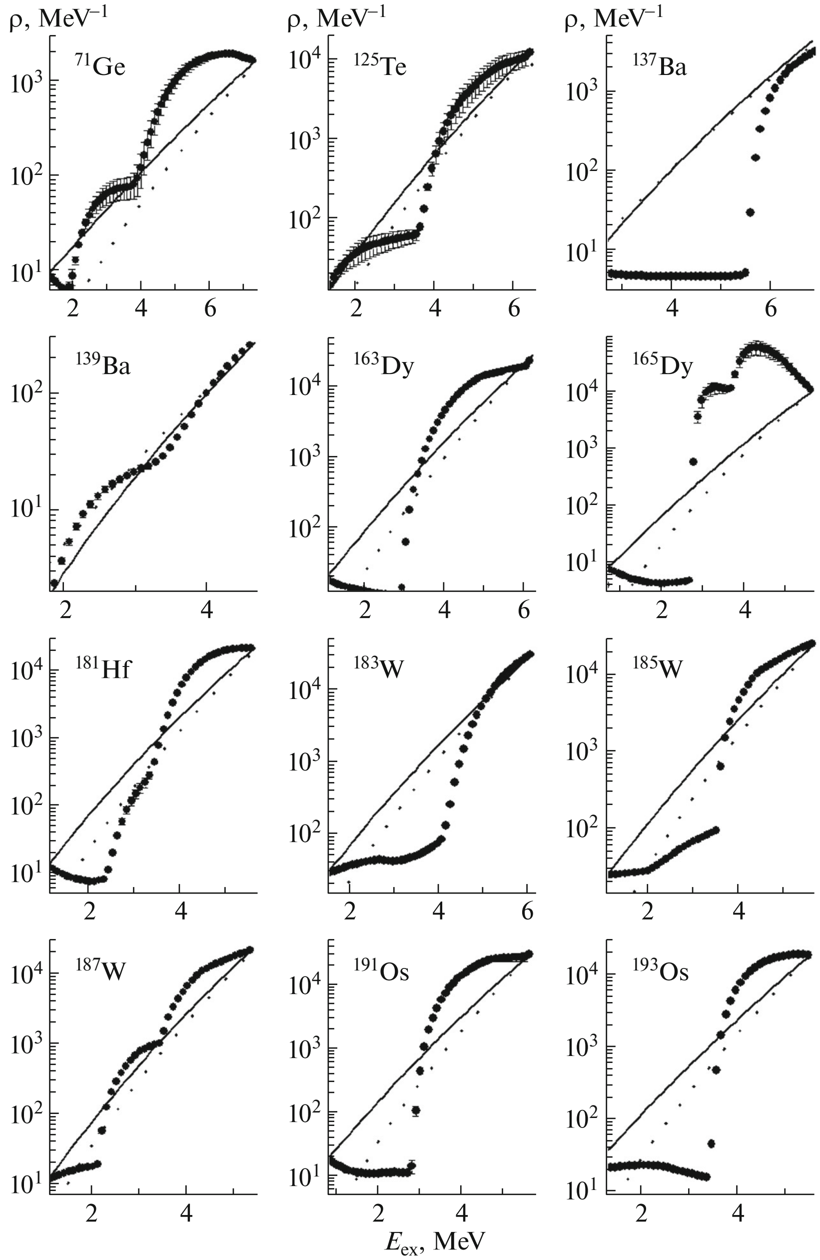

Fig. 1. Excitation-energy dependence of the mean densities of intermediate levels in two-step cascades (points with error bars) for even–odd nuclei (lowest χ^2 fits): (solid lines) data calculated in [17] and (dotted lines) results of the calculations based on the model proposed in [10].

A comparison of the results obtained within the present version of our model and within its earlier versions showed that we reached a fairly high accuracy in describing the densities of intermediate cascade levels. The discrepancies are the greatest for ^{137}Ba and ^{182}Ta. Most likely, a large error for ^{137}Ba stems from the preceding approximation version [3]. For ^{182}Ta, the energy thresholds for the break of the second and third Cooper pairs are 1.6 and 5.8 MeV within the present version; in [3], the values of the same thresholds are 1.6 and 4.0 MeV. It follows that, even in the worst case of ^{182}Ta, the data obtained for the level density yield a picture where the uncertainties are due to the imperfections in the present-day ideas of the gamma-decay process.

One can reach the highest accuracy and reliability of the results on the basis of experiments where it is possible to single out not less than about 99% of the intensities of primary transitions among the whole array of gamma-ray cascades of the decay of the

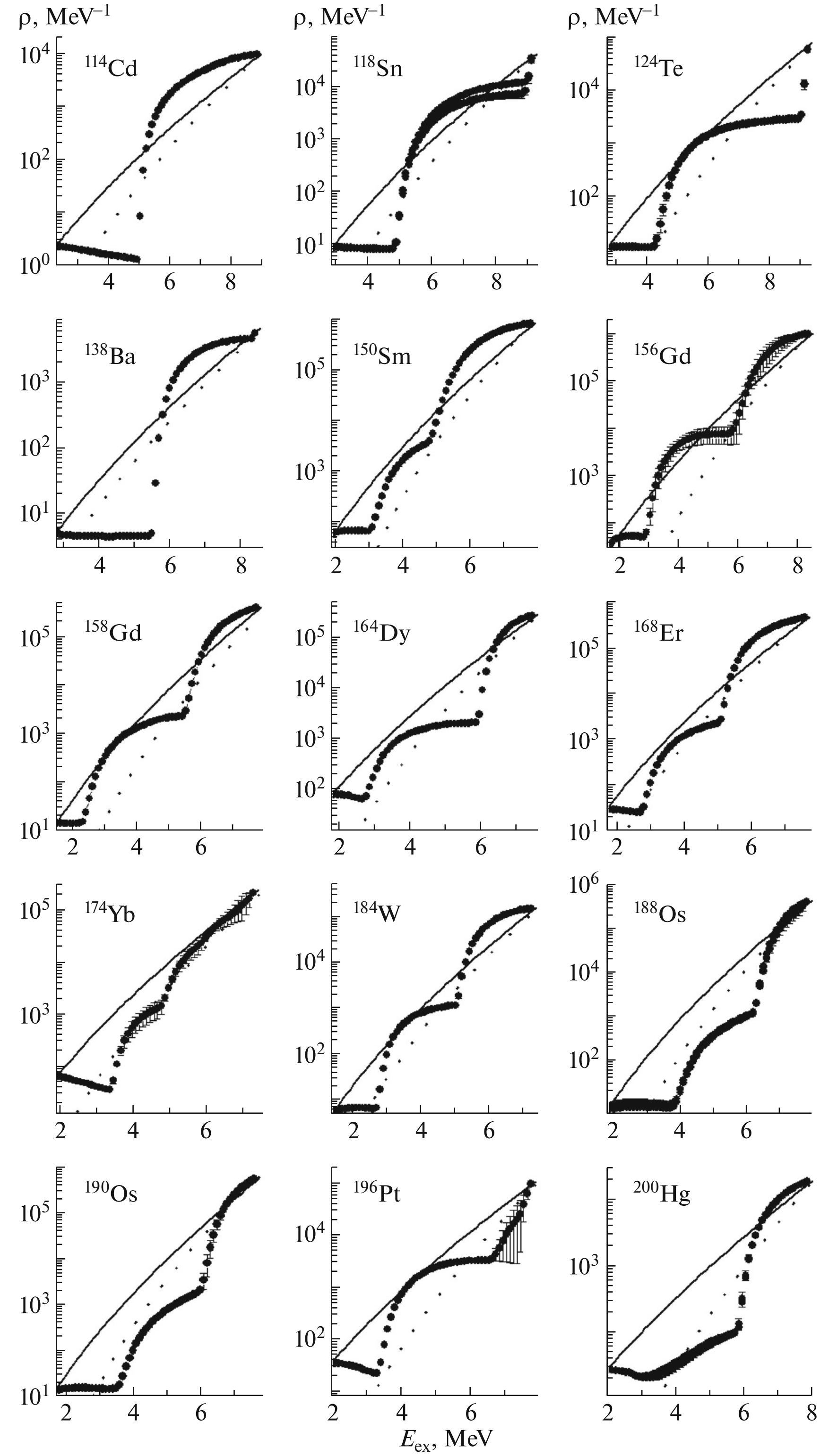

Fig. 2. As in Fig. 1, but for even–even nuclei.

compound state of any nucleus. Nevertheless, reliable information about the most probable level density and about strength functions for dipole gamma transitions can be extracted even from the convolution of the spectrum of primary products of the decay of the compound state and the gamma-transition branching fractions depending on the energy of the interme-

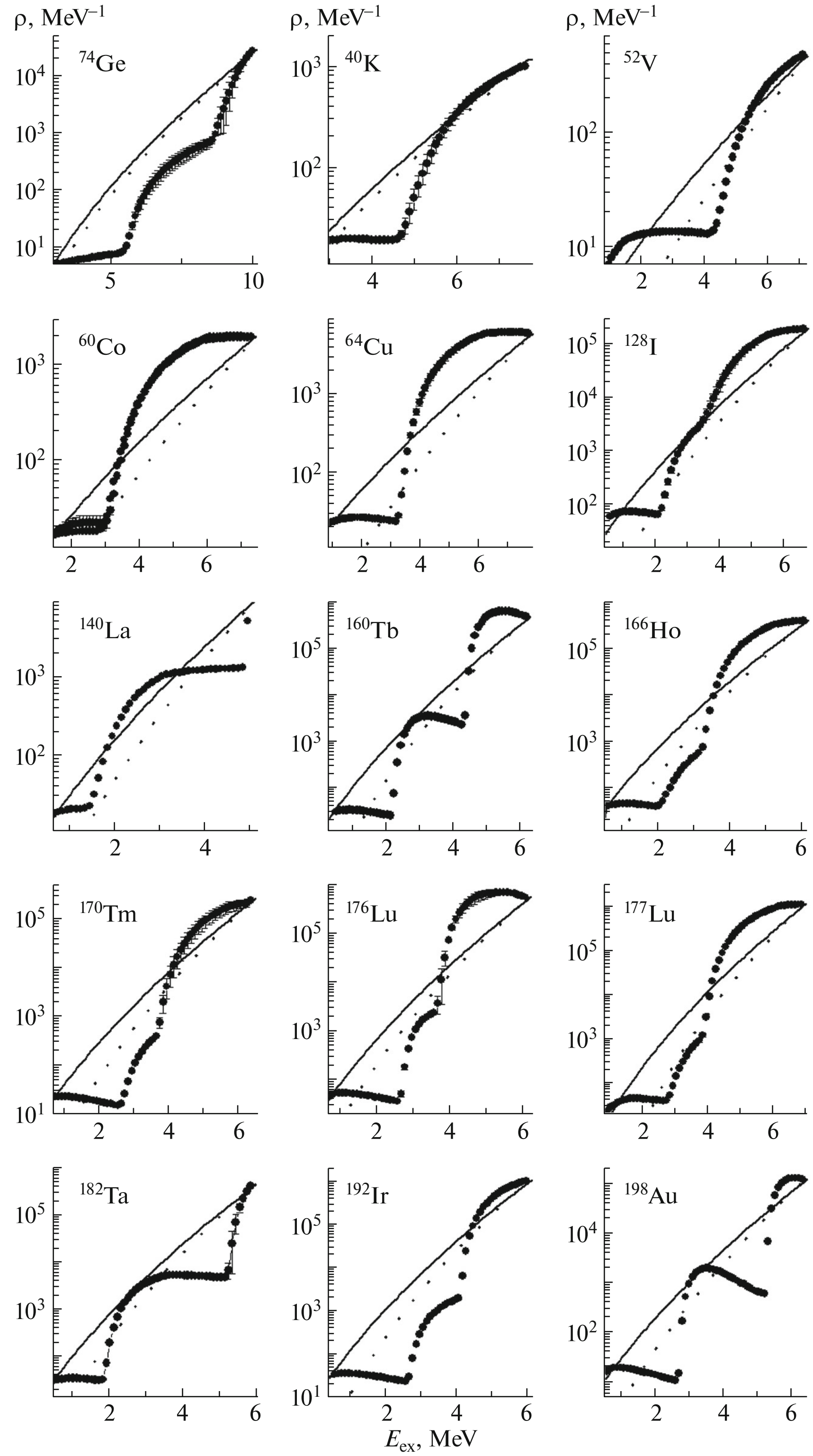

Fig. 3. As in Fig. 1, but for ^{74}Ge, ^{177}Lu, and odd–odd nuclei.

diate cascade level. This follows from a comparison of the thresholds determined for the break of three to four Cooper pairs by employing different versions of the energy dependence of ρ and Γ. In the most recent versions of the practical model, these results change only slightly.

The level densities from the back-shifted Fermi gas model [17] and those from the model that takes

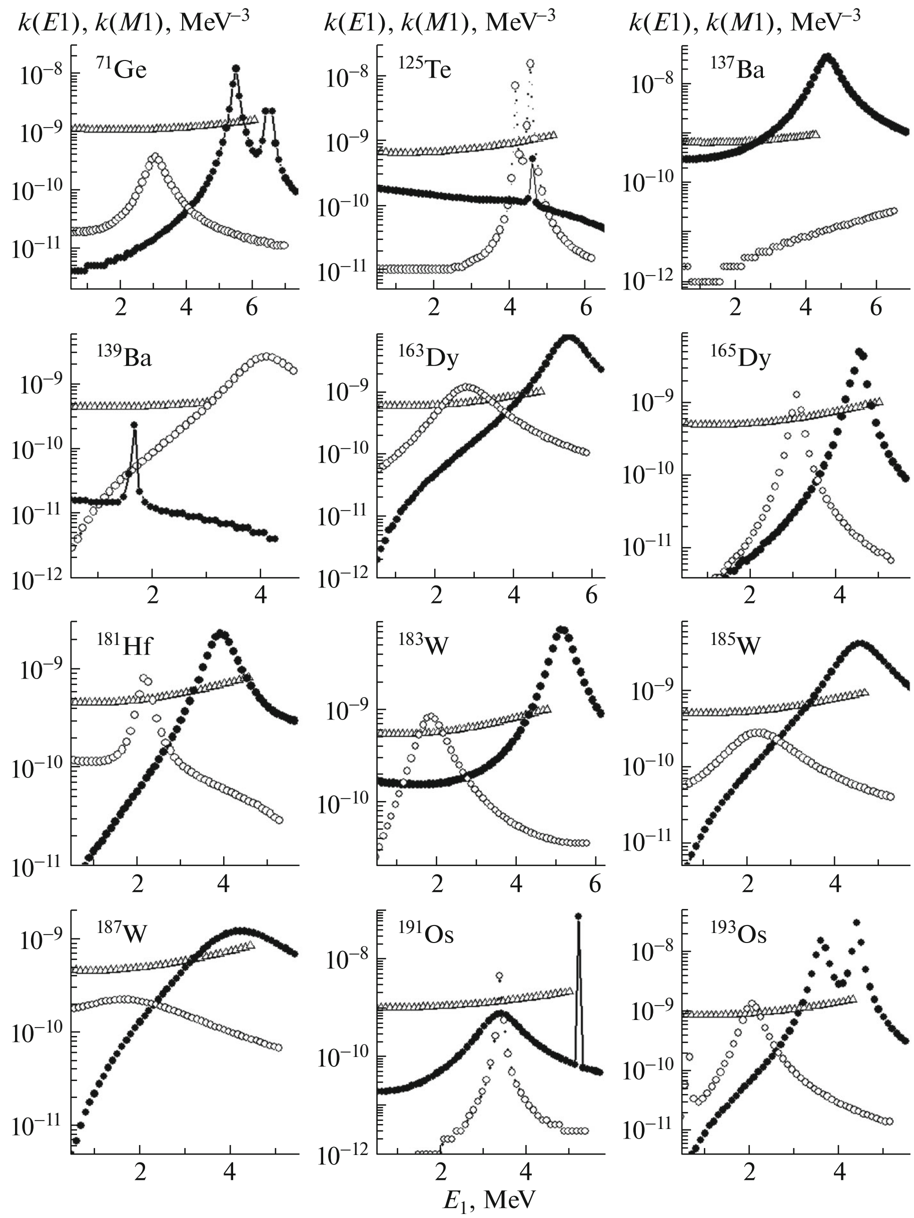

Fig. 4. Strength functions for $E1$ (closed circles) and $M1$ (open circles) transitions for even–odd nuclei versus the primary-transition energy. The open triangles stand for the sum of the values calculated on the basis of the model used in [14] and $k(M1) = \text{const}$ in the energy range of $0 < E_1 < B_n - E_d$.

into account the shell-inhomogeneities in the single-particle spectrum [10] are given in Figs. 1–3. One can see that the model from [10] reproduces the derivative $d\rho/dE_{\text{ex}}$ to a higher degree of precision than the model from [17]; however, the level densities calculated on the basis of both models deviate markedly from the respective experimental results.

The results presented for the $E1$ and $M1$ radiative strength functions (Figs. 4–6) and their sums (Figs. 7–9) do not exhibit drastic distinctions from those published earlier in [18–20], but there remains the unresolved problem of unambiguously describing the shape of the observed peaks in the electric and magnetic strength functions in those cases where the use of exponential functions [3] and the modified Lorentzian function (3) leads to close values of χ^2.

It is worth noting that the data in Figs. 4–9 do not require including any additional pygmy resonance in the strength functions being considered. In order to interpret the process in question, it is sufficient to develop theoretical ideas of the coexistence of vibrational and quasiparticle levels in any nucleus and their fragmentation as E_{ex} grows.

In many nuclei (see Fig. 7–9), the sum of the

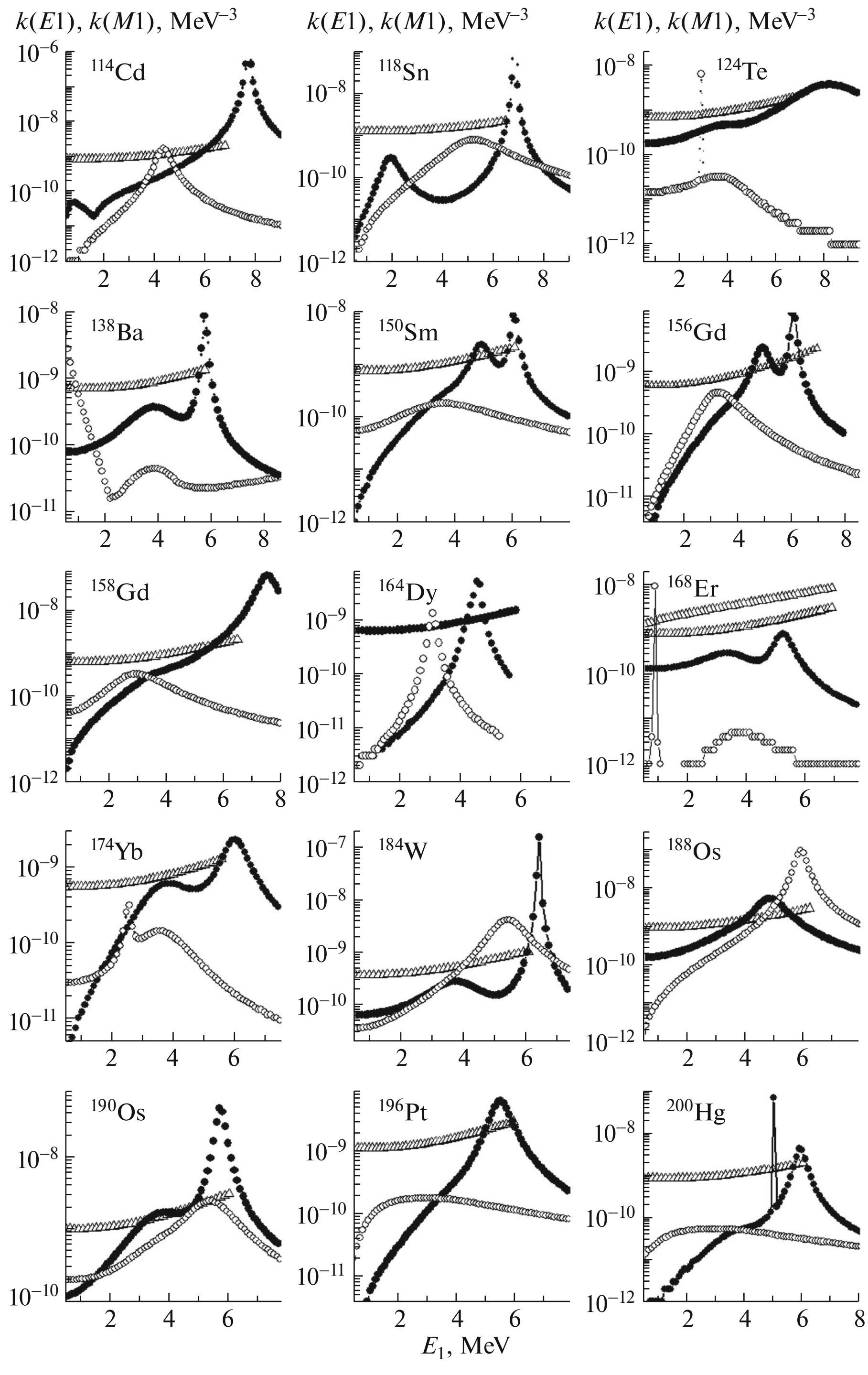

Fig. 5. As in Fig. 4, but for even–even nuclei.

strength functions for $E1$ and $M1$ transitions develops a plateau that agrees with the sum of the values calculated within the model used in [14] and $k(M1) = \text{const}$ normalized to the experimental ratios $k(M1)/k(E1)$. The strength functions for primary transitions whose energy lies in the range of $E_1 < 0.5B_n$ decrease regularly as the energy becomes lower. A significant decrease in the sum $k(M1) + k(E1)$ for moderately small gamma-transition energies is observed for all versions of the description of radiative strength functions. At the same time, there are no asymptotic zero values of the sums of strength functions [14]. We cannot rule out the possibility of a sizable increase in the $E1$ or $M1$ strength functions in the vicinity of and above B_n because of the fragmentation of n-quasiparticle nu-

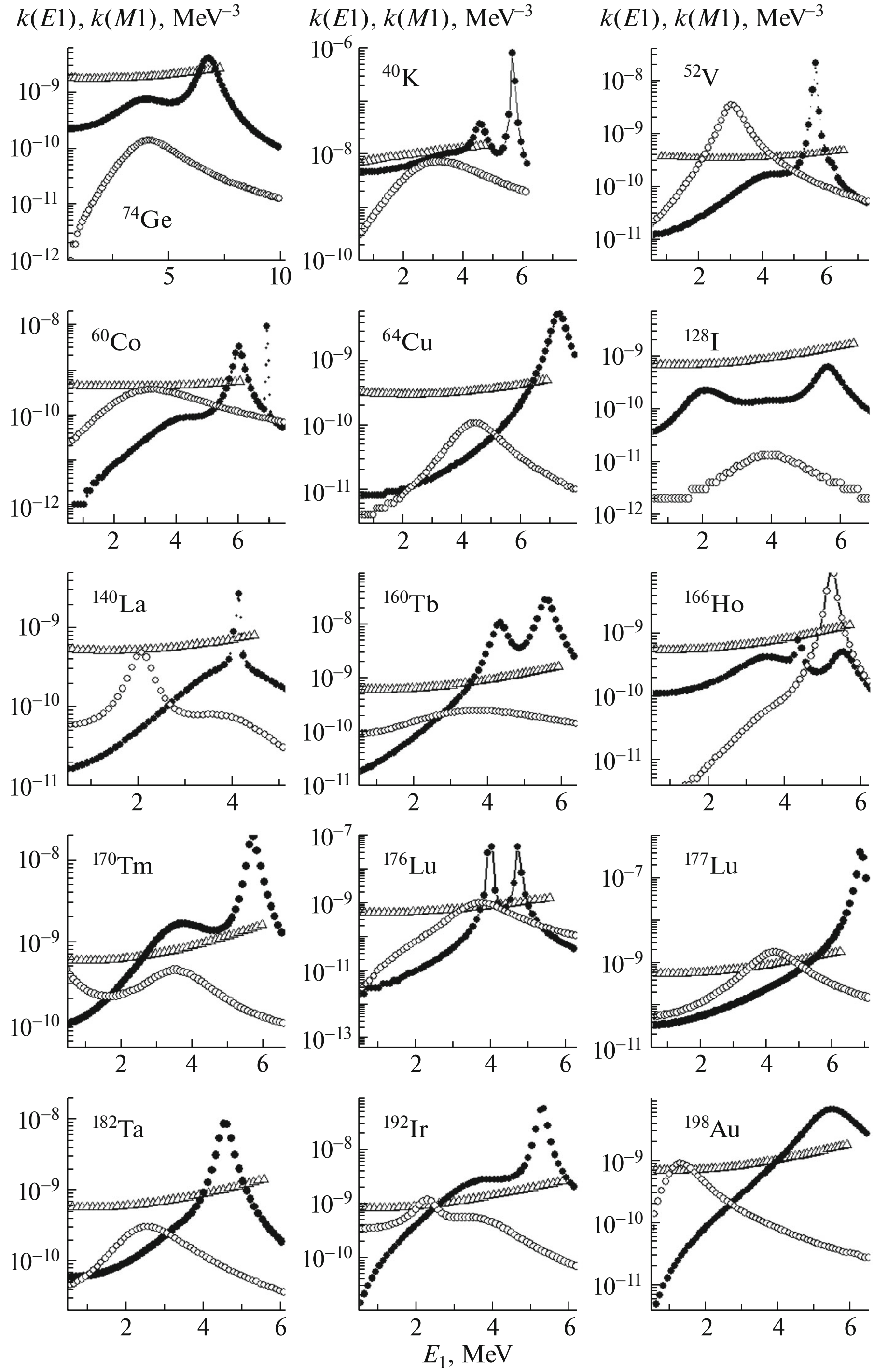

Fig. 6. As in Fig. 4, but for ^{74}Ge, ^{177}Lu and odd–odd nuclei.

clear states if the threshold for the break of a Cooper pair lies in the region of the neutron binding energy. Therefore, the radiative strength functions cannot be a mere extrapolation of giant resonances. This contradicts radically the Axel–Brink hypothesis [6, 7], which is used in dealing with gamma spectra.

Figure 10 gives the mass-number dependence of the energy thresholds for the break of the second and third Cooper pairs. Since these quantities are different for nuclei in which the numbers of nucleons have different parities and depend on the mean pairing energy, they are shown separately in this figure and are compared with B_n/Δ_0 (in just the same way as in [3]). One can see that the thresholds for the break of

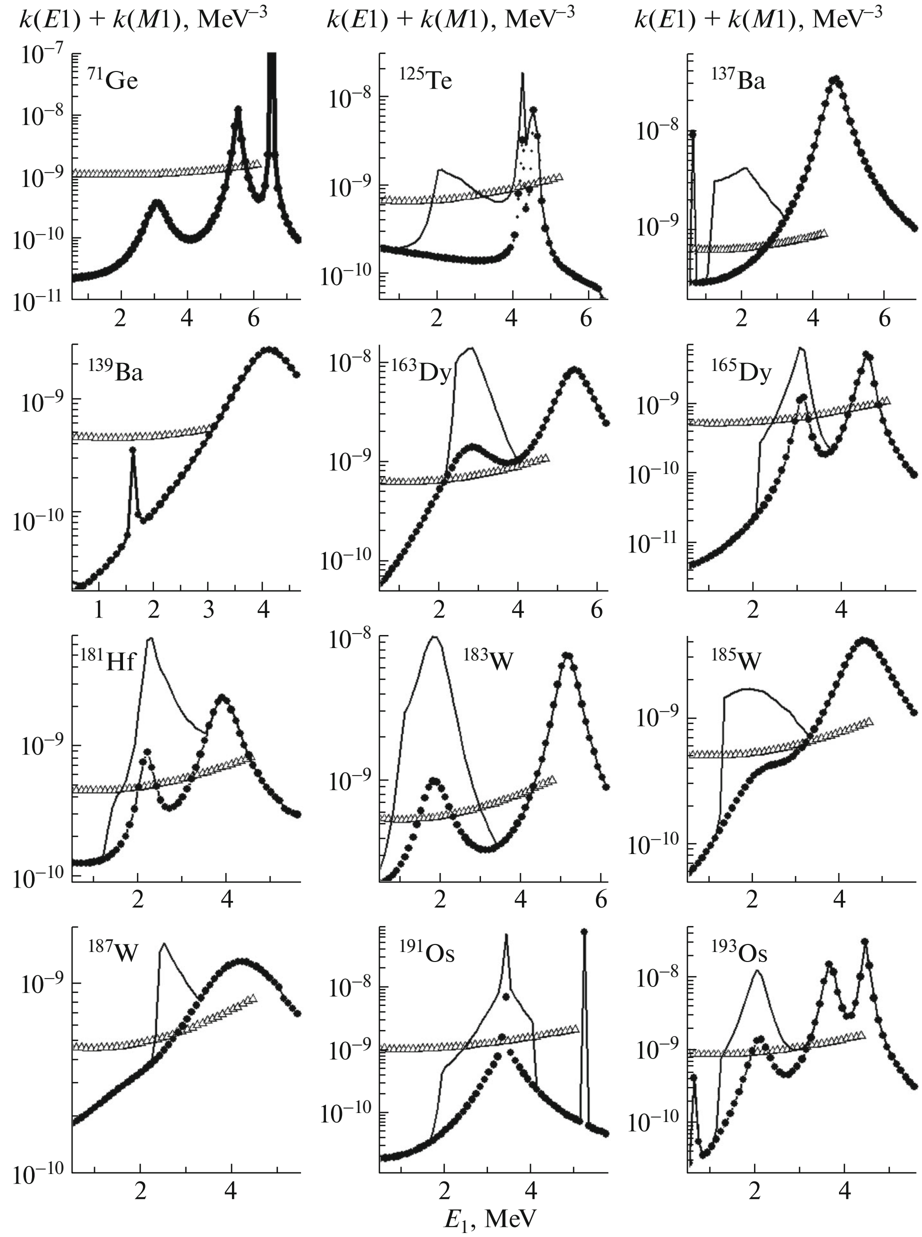

Fig. 7. Sums of strength functions for $E1$ and $M1$ transitions (closed circles) for even–odd nuclei versus the primary-transition energy. The solid lines represent the results fitted with allowance for the correction in Eq. (5). The open triangles stand for the sum of the values calculated on the basis of the model used in [14] and $k(M1) = \text{const}$ in the energy range of $0 < E_1 < B_n - E_d$.

pairs depend only slightly on the shape of the strength functions. This means that, in experiments detecting two-step cascades, the actual correlation of ρ and Γ is insignificant.

Figure 11 shows the results obtained by approximating the parameter E_u. Its values almost perfectly comply with the mean pairing energy Δ_0 of the last nucleon for approximately 30 nuclei. The spread of the remaining values of E_u may be due to the errors in the normalization of experimental values of $I_{\gamma\gamma}$ because of the fact that the model used in [11, 12] disregards the possibility of the break of proton pairs simultaneously with or instead of the break of neutron pairs, the inaccuracy of the phenomenological part of the model, or fluctuations of the experimental values of Δ_0 [21]. In addition, we cannot rule out the possibility of different weights of quasiparticle and phonon components in the wave function for the resonance that determines the cross section for thermal-neutron capture by any stable (long-lived) target nucleus.

In currently used models [2], the total level density is represented as the sum of the level densities for

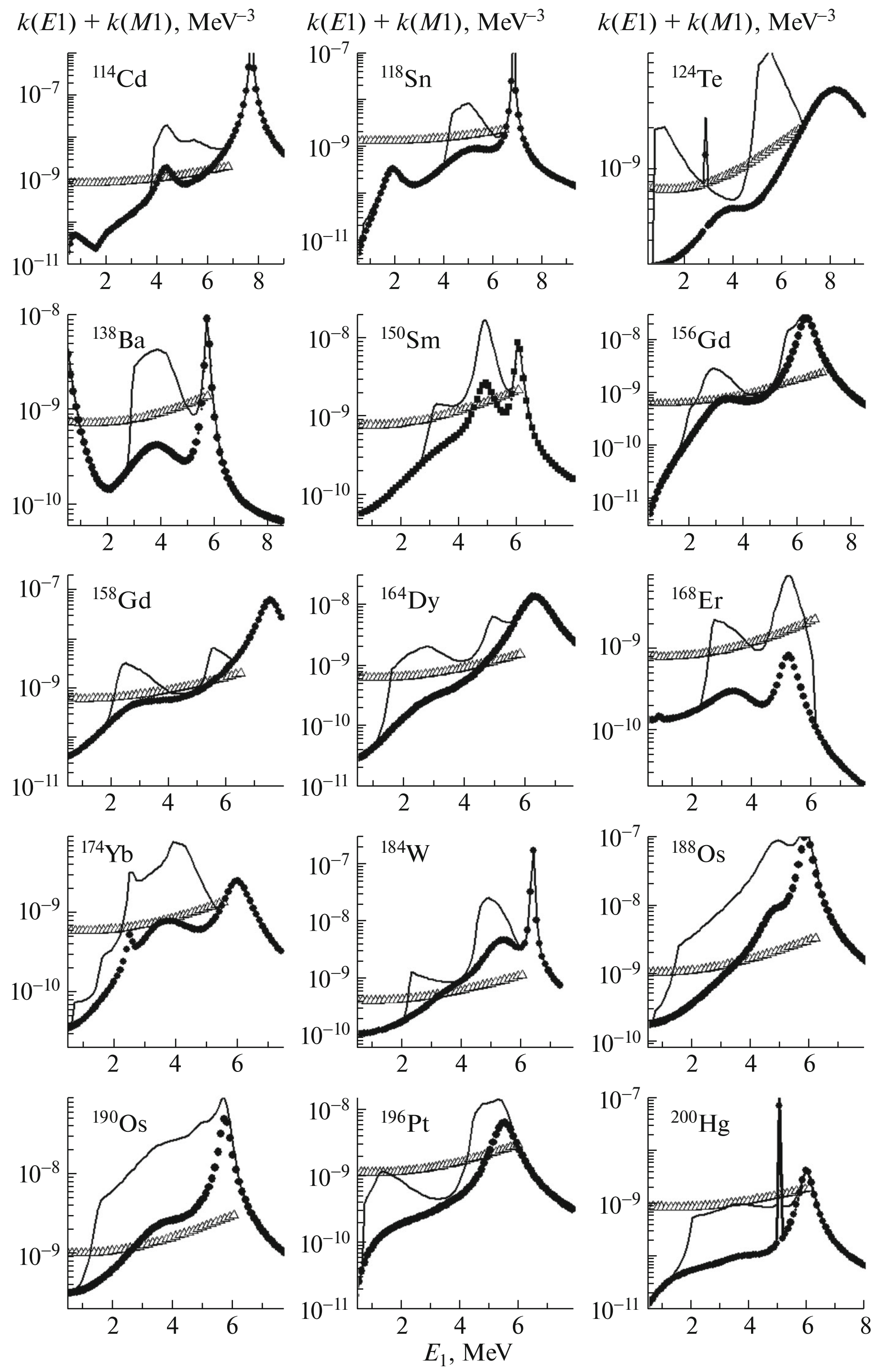

Fig. 8. As in Fig. 7, but for even–even nuclei.

quasiparticle and collective excitations. Figure 12 gives the ratio of the collective (only vibrational in actual practice) level density to the total level density. In the region around B_n, this ratio has close values for nuclei in which the numbers of nucleons have different parities, but, at the energy E_d, the ratio in question is substantially smaller for even–even nuclei than for even–odd and odd–odd ones. No version of the Dubna model gives grounds to assume the presence of sharp changes in the nuclear structure at the point $E_{\text{ex}} = B_n$. On the basis of the data in Fig. 12, it would be legitimate to assume that neutron resonances may preserve various types of the wave-function structure (dominated by quasiparticle or phonon components)

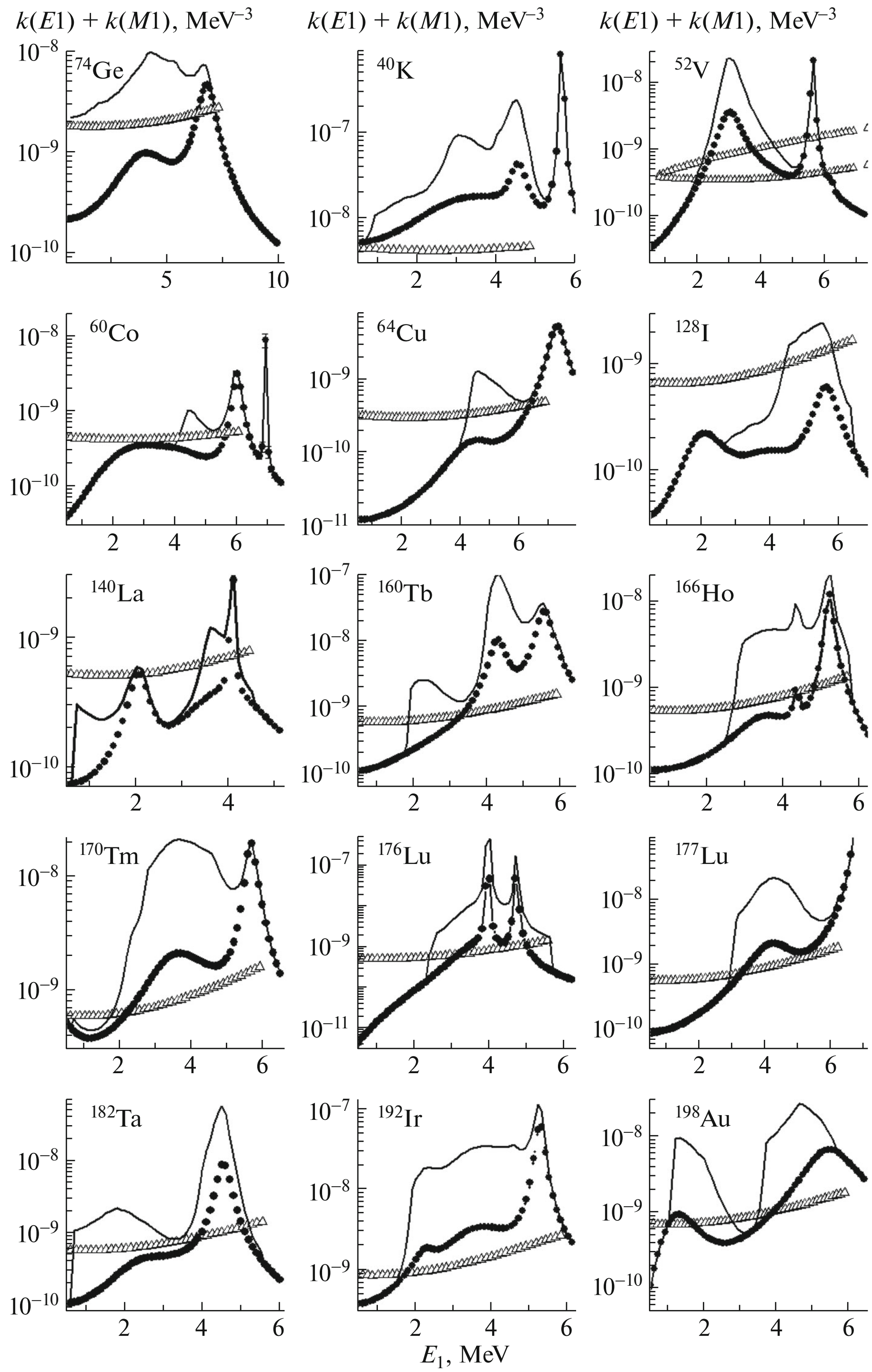

Fig. 9. As in Fig. 7, but for ^{74}Ge, ^{177}Lu, and odd–odd nuclei.

and belong to several different distributions of reduced neutron and total radiative resonance widths.

The distribution of reduced neutron and total radiative widths of neutron resonances were approximated in [22]. In the respective analysis, it is assumed that the experimental set of these widths is represented as the sum of several (up to four) distributions whose widths and peak positions are varied. For the total radiative widths in nuclei featuring not less than 170 resonances, the mean fractions of two distributions that are the most intense are 44 and 34% of the summed distribution of total radiative widths (this is close to a 40% fraction of vibrational levels). Thus, two experiments that are methodologically indepen-

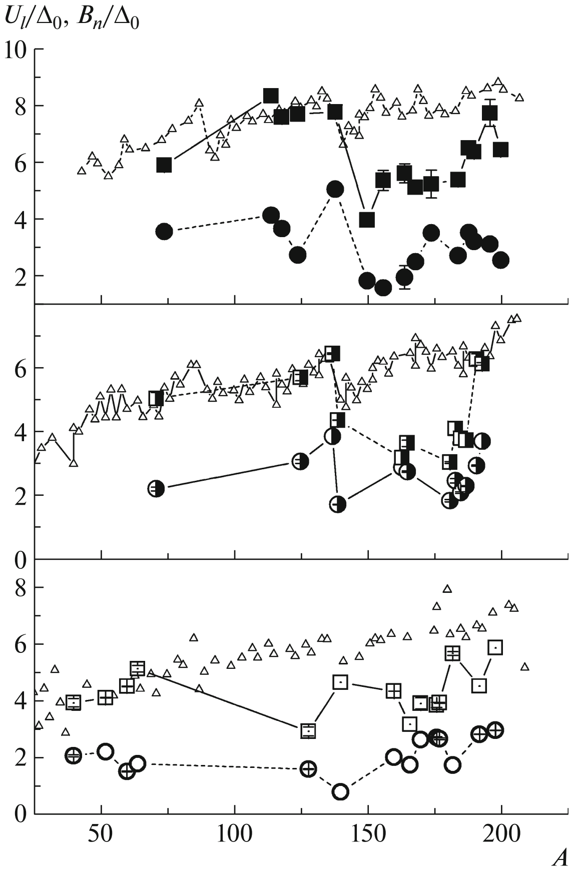

Fig. 10. Mass-number dependence of the energy thresholds for the break of the (circles) second and (boxes) third Cooper pairs. The closed, half-closed, and open symbols represent these results for, respectively, even–even, even–odd, and odd–odd compound nuclei. The open triangles correspond to the mass-number dependence of B_n/Δ_0.

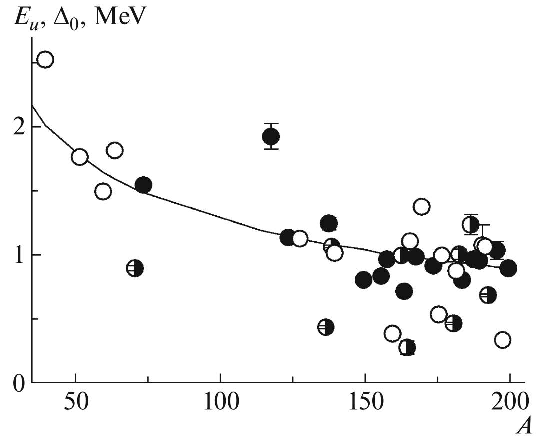

Fig. 11. Mass-number (A) dependence of the parameter E_u (2) for (closed circles) even–even, (half-closed circles) even–odd, and (open circles) odd–odd compound nuclei. The curve represents the mean pairing energy Δ_0 of the last nucleon in a nucleus of mass number A [21].

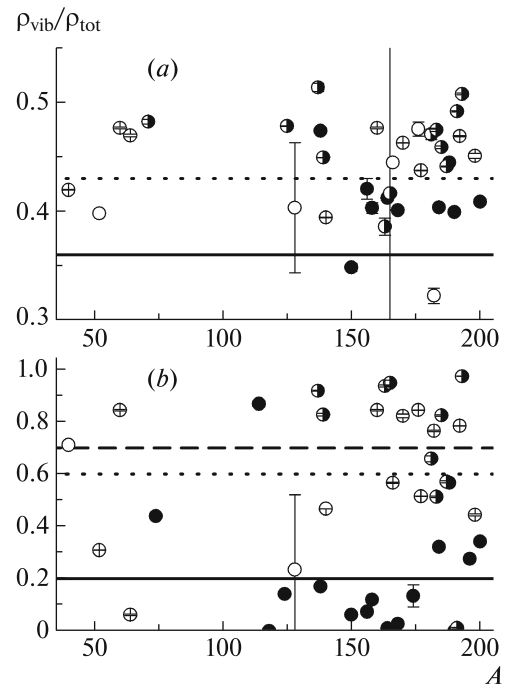

Fig. 12. Ratio of the vibrational level density to the total level density in the region around the neutron binding energy B_n (a) and at the point E_d (b). The closed, half-open, and open circles represent these results for, respectively, even–even, even–odd, and odd–odd nuclei. The solid, dashed, and dotted lines stand for the mean values in, respectively, even–even, even–odd, and odd–odd nuclei.

dent are indicative of the difference in the structure of the wave functions for neighboring levels over a broad range of stable target nuclei up to an energy of or somewhat higher than B_n.

There is some discrepancy between the values obtained here for the $E1$ and $M1$ strength functions (see Fig. 4–9) and the results reported in [3], which is due most likely to different degrees of the effect that the shape of the partial widths of the additional peaks (4) in the strength functions exert on χ^2 values in the region of small values of the energy dependences used. The observed variations in the shape of the sums of $E1$ and $M1$ strength functions (see Fig. 7–9) cannot be interpreted as their unquestionable distinction without ruling out the possible existence of levels of different structure at excitation energies of about 5 to 10 MeV.

4. CONCLUSIONS

We have obtained experimental information about the dynamics of the break of three to four Cooper pairs of nucleons. The systematic error in determining the break thresholds does not exceed a value of about 1 MeV for the bulk of nuclei that are accessible to study.

The set of data obtained by employing (i) the model of the density of n-quasiparticle levels from [9] for describing the sequential break of three to four Cooper pairs at an energy not higher than 5 to 10 MeV above the ground state of the nucleus being considered; (ii) the phenomenological concepts specified by Eq. (2), which concern the energy dependence of the vibrational level density in the same energy range; and (iii) combinations of phenomenological and/or theoretical ideas of the shape of the energy dependences of widths with respect to gamma-ray emission gives sufficient grounds to assume that the dynamics of the interaction of fermion and boson nuclear-matter states depends on the shape of the nucleus being studied.

REFERENCES

1. K. H. Schmidt and B. Jurado, Phys. Rev. C **83**, 014607 (2011).
2. *Reference Input Parameter Library RIPL-2, Handbook for Calculations of Nuclear Reaction Data*, IAEA-TECDOC (IAEA, 2002).
3. A. M. Sukhovoj, L. V. Mitsyna, N. Jovancevic, Phys. At. Nucl. **79**, 313 (2016).
4. N. Jovancevich, A. M. Sukhovoj, W. I. Furman, and V. A. Khitrov, in *Proceedings of the 20th International Seminar on Interaction of Neutrons with Nuclei, Dubna, May 2012,* Preprint JINR No. E3-2013-22 (Joint Inst. Nucl. Res., Dubna, 2013), p. 157. http://isinn.jinr.ru/past-isinns.html.
5. C. F. Porter and R. G. Thomas, Phys. Rev. **104**, 483 (1956).
6. P. Axel, Phys. Rev. **126**, 671 (1962).
7. D. M. Brink, PhD Thesis (Oxford Univ., Oxford, 1955).
8. A. Bohr and B. R. Mottelson, *Nuclear Structure*, Vol. 1: *Single-Particle Motion*, (Benjamin, New York, 1969).
9. V. M. Strutinsky, in *Proceedings of the International Congress on Nuclear Physics, Paris, France, 1958,* p. 617.
10. A. V. Ignatyuk, Report INDC-233(L) (IAEA, Vienna, 1985).
11. A. M. Sukhovoj, Phys. At. Nucl. **78**, 230 (2015).
12. A. M. Sukhovoj and L. V. Mitsyna, in *Proceedings of the 22nd International Seminar on Interaction of Neutrons with Nuclei, Dubna, May 2014,* Preprint JINR No. E3-2015-13 (Joint Inst. Nucl. Res., Dubna, 2015), p. 245. http://isinn.jinr.ru/past-isinns.html.
13. http://www-nds.iaea.org/ENDSF.
14. S. G. Kadmenskiĭ, V. P. Markushev, and V. I. Furman, Sov. J. Nucl Phys. **37**, 165 (1983).
15. L. A. Malov and V. G. Solov'ev, Sov. J. Nucl. Phys. **26**, 384 (1977).
16. E. V. Vasilieva, A. M. Sukhovoj, and V. A. Khitrov, Phys. At. Nucl. **64**, 153 (2001).
17. W. Dilg, W. Schantl, H. Vonach, and M. Uhl, Nucl. Phys. A **217**, 269 (1973).
18. A. M. Sukhovoj and V. A. Khitrov, Preprint JINR No. E3-2005-196 (Joint Inst. Nucl. Res., Dubna, 2005).
19. A. M. Sukhovoi and V. A. Khitrov, Phys. Part. Nucl. **36**, 359 (2005).
20. A. M. Sukhovoj and V. A. Khitrov, Phys. Part. Nucl. **37**, 899 (2006).
21. V. A. Kravtsov, *Atomic Masses and Nuclear Binding Energies* (Atomizdat, Moscow, 1965) [in Russian].
22. A. M. Sukhovoj and V. A. Khitrov, Phys. At. Nucl. **76**, 68 (2013).

Journal of Research in Physics Vol. 39, No. 1, 47 - 63 (2018)

doi:10.2478/jrp-2018-0005

Testing the modified dependence of the radiative strength function on different excitation energies in the light nucleus ^{28}Al

[1]D. Knezevic, N. Jovancevic[1], A. M. Sukhovoj[2], L.V. Mitsyna[2]
[1] *University of Novi Sad, Faculity of Science, Department of Physics, Novi Sad, Serbia*
[2] *Joint Institute for Nuclear Research, Dubna, 141980, Russia*
E-mail: nikola.jovancevic@df.uns.ac.rs

Received: *December 29, 2017*

Abstract

The spectrum of random functions of level density as well as radiative strength functions of dipole E1- and M1-transitions of ^{28}Al were determined. Obtained functions can reproduce very precisely the intensity of the two-step cascade following the radiative capture of thermal neutrons for a given energy of the primary transitions. The density of the observed intermediate levels can be reproduced correctly using the mean value of these functions. In this work we proposed a new hypothesis about the dependence of radiative strength functions for gamma-transitions in heated nucleus on the energy of excited levels. The results provide a solid basis that this new hypothesis allows to get realistic estimation on the parameters of nuclear structure in any nucleus, including the light ones.

Key words: Neutron resonance, two step gamma cascades, level density, radiatve strength function.

1. Introduction

The determination of accurate values for the excited nuclei level density and radiative strength functions is one of the most important tasks in low energy nuclear physics. Trustable experimental values of these parameters are necessary for the study of the fundamental properties of the nuclear structure. For example, the step-like structure in the level density provides information about the phase transitions in heated nuclei and the influence of different type of resonance wave functions on radiative strength function for the γ decay process. Moreover, accurate experimental values of the level density and the radiative strength function are very important for applications as the analysis of astrophysical reactions, the production of medical isotopes, reactor technology, the production of rare isotope beams, etc.

The development of theoretical models needs a set of experimental information for the excited levels density (with given quantum numbers) and for the values of the partial radiative widths of all possible decay channels. If those data are available, the theoretical calculations can give a correct interpretation of the dynamics of the nuclear transitions, in a broad variety from the simple low-lying levels (e.g., quasiparticle or phonon structure) to the very complex compound-states.

The quality of the model-based description of all the parameters for the neutron resonance gamma-decay, for example, depends entirely on the precision of the experimental data. Hence, it is very important to minimize the overall experimental uncertainty and, accordingly, to minimize the possible misrepresentation in analysis of the observed process, mostly as a result of the use of certain assumptions and the related hypothesis. The ability to get an accurate solution substantially increases when in the measurement are employed nuclear spectrometers, having $FWHM \ll D_\lambda$ for all energy spaces D between the initial nuclear levels λ.

In this situation a fundamental experimental problem is to search for the connection between the emission probability Γ of the reaction product and the excited levels densities ρ. The sum of the branching ratios B_r ($B_r = \Gamma_{\lambda i}/\Gamma_\lambda$) for partial $\Gamma_{\lambda i}$ and total widths Γ_λ (if there are no competing processes) is equal to one and does not depend on the absolute values of the levels density ρ and the partial widths Γ. However, branching ratios of any level are determined by the sum of the partial widths and consequently they are dependent on the level density. So, to give an accurate description of the dependence between the measured values (intensity of the emitted spectrum of particles observed in the reaction), the excited levels density and the partial radiative widths is one of the most important tasks in the process of estimation of those parameters values.

In this work we proposed a new and a modified form of the dependence for the radiative strength function of the excited level density, based on the analysis of the experimental data and the existing models of the level density as well as the partial gamma-widths. This new approach was tested experimentally by the estimation of the most probable mean values of the level density and the radiative strength function of ^{28}Al compound-state gamma-decay. To accomplish this task, the Dubna two-step gamma cascade method was used [1, 2].

2. Theoretical considerations

2.1. Current state of the experiments designed for the determination of Γ and ρ

The information about the properties of the excited nuclei can be extracted only by the measurement of the spectra (cross-sections) S of the observed reaction product, and the subsequent analysis based on some existing functional dependencies between S and the parameters Γ and ρ ($S = \Psi(\Gamma, \rho)$). Such experiment can be performed measuring the reaction products spectra with a single detector ("one-step" reaction [3]), or by coincidences between two detectors ("two-step" reaction [4, 5]).

The first of these two experimental techniques was used up to now for the analysis of the spectra and the cross-sections of evaporative nucleons [3, 6] and full gamma spectra [7, 8]. The second one was applied in the spectroscopy measurements of two photons [3, 4] successively emitted after the neutron capture. Comparison of the Γ and ρ values obtained in the analysis of the experimental data collected in one- and two-step reactions, makes possible to identify the main sources of the systematic experimental uncertainties, to estimate the uncertainty values and to compare them if different methods were applied in the study of the same nucleus.

2.1.1. Spectra of evaporative nucleons

The level density can be obtained from the evaporative nucleons spectra by the use of this method only if the value of Γ is known. The numerical value of the parameter Γ was calculated until now from the relativly rudimentary optical model. The agreement between the calculated cross-section and the experimentally determined one can be used for the validation of the obtained results. However, this method does not take into consideration that the experimentally measured cross-section (spectrum) is determined only by the absolute value of the product $\Gamma \cdot \rho$, and not by the absolute values of the individual terms Γ and ρ. One of the consequences (as can be seen comparing the data measured by this method [3, 8] with the two-step reaction analysis [4, 5]), is that the obtained values for the level density in the energy range around the threshold of the second gap for nucleons Cooper pairs are overestimated at least by 5-10 times [9].

2.1.2. Spectra of the primary quanta of cascades depopulating different energy exited states

The total intensity of the spectra of the first generation of cascade quanta [7] does not depend on the absolute values of Γ and ρ. Moreover, the absolute value of the function describing the dependence of the mentioned parameters Γ and ρ on the energy of the gamma-quanta and the energy of the excited level has no significant influence on the total gamma spectra (the sum of the gamma energies of cascade photons depopulating some level is absolutely independent from Γ and ρÏĄ). The mean quadratic variation of the different forms of the full gamma-spectra calculated employing various realistic representations of $\Gamma = f(E_\gamma)$ and $\rho = \varphi(E_{ex})$ does not exceed 30 %, in the best case, [10] (where E_{ex} is the exited level energy).

Fig. 1 shows the gamma rays spectra [11] following the inelastic scattering of ^{3}He on the ^{45}Sc isotope. The intensive and well-resolved low energy peaks registered in the "first generation" and the in "higher-generation" spectrum are produced, in most cases, only by second or higher cascade quanta [11]. These gamma peaks appear in the "first generation" spectra only due to an error of the specific techniques used. Specifically, this is a consequence of the non-compliance of the basic condition of the used technique [7]. The spectrum of the gamma radiation emitted after the decay of the levels for a given excitation energy is initialized by the beam of the charged particles and described by the one particular set of quantum numbers. This spectrum should be exactly the same as the spectrum measured in the experiment where observed levels are populated by the transitions from the high-lying energy levels. As a result, the systematic error of the "first generation" spectra can exceed 100 % in low energy photon region. The increase of E_γ can reduce this error by some unknown degree. This fact is not mentioned in the evaluation [12] of the error appearing in this approach [8].

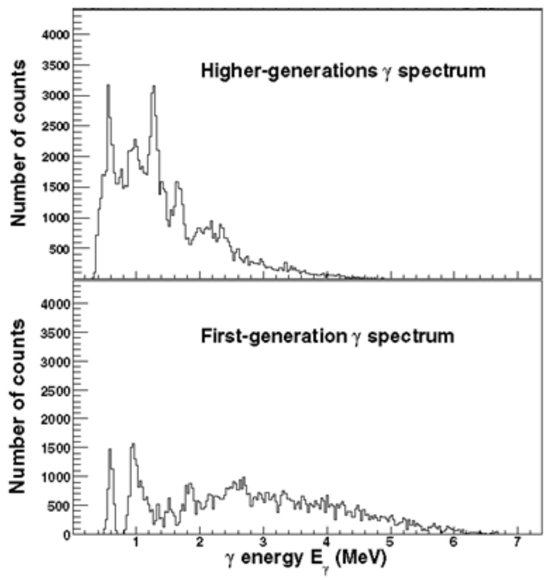

Figure 1: Gamma-ray spectra in the ^{45}Sc(^{3}He,^{3}Heγ)^{45}Sc reaction [11] for the first and next cascade quantum.

2.1.3. Two-step cascade quanta

The absolute intensity of the cascades $I_{\gamma\gamma} = \Psi(\Gamma, \rho)$, which can be measured by ordinary HPGe-detectors for a limited number of final levels, is defined by the inverse absolute value of the level density and by the form of the strength function $K = f(E_\gamma)$ [13]. Thereby, the relationship between the experimental values of $I_{\gamma\gamma}$ and the unknown functions Γ and ρ is always nonlinear, for all intervals of the excitation energy. The current experimental methods allow to determine only an interval for the possible values of Γ and ρ reproducing the measured intensity of the cascades $I_{\gamma\gamma}$. Even in the limit of zero statistical errors of the experimental values, Γ and ρ could not be unequivocally determined [14].

All the methods listed above have also common sources of systematic errors.

1. There is no practical model of the decay of the nuclear excited levels, for both nucleon and radiation channel, suitable for the analysis of the experiment. Such a model should be able to take into account explicitly the coexistence and the interactions of the boson and the fermion components of the nuclear matter.

2. It is necessary that the model considers the dependence of the partial widths Γ on the wave function for both the initial and the final level when the reaction product of a specified energy is emitted.

All the three techniques listed above, without exception, requires an additional, methodically independent, experiment. That experiment should produce a non-degenerate system of equations which can describe the relation between the measured spectrum and the values of the parameters Γ and ρ.

The influences of the mentioned sources of systematic errors, which are most significant for one-step reactions, can be essentially reduced in the two-step reaction experiment. Therefore, it is necessary to develop a modern model able to describe and predict possible changes of the nuclear properties caused by different excitation energies. This model would require data from two-step reaction experiments.

2.2. Status of the current models of the level density and the partial gamma-widths

In modern theoretical views, for example for the quasiparticle-phonon model of the nucleus, the partial emission width is determined by the coefficients of the wave function components for both decayed and excited level [15]. The actual values of the partial widths are specified by the degree of the fragmentation for the different nuclear states with a fixed number of quasiparticles and phonons. The level density directly determines it, since the ρ value is defined by the degree of the fragmentation of all the possible states of the nucleus having energy lower than the excitation one.

Currently,the radiation strength function of the dipole gamma transitions for a nucleus with mass A can be expressed as:

$$k_{standard} = \Gamma_{\lambda i}/(E_{\gamma}^{3} A^{3/2} D_{\lambda}) \quad (1)$$

where E_γ is the energy of the emitted gamma quanta, A is the atomic mass, D_λ is the density of the decaying level and $\Gamma_{\lambda i}$ represents the partial width of the nucleus transition from the λ to the i-th level.

The expression above takes into account the dependence of the partial radiative widths only from the density $\rho_\lambda = D_\lambda^{-1}$ of the decayed high-energy levels, such as the neutron resonances. However, the possibility that the partial radiative widths can be a function of the density of the intermediate levels of the heated nucleus having sufficiently high energy is not taken into consideration by Eq. 1. The modern two-step reaction $(n_{th}, 2\gamma)$ experiment revealed the existence of such a kind of dependence [16].

It was observed the smooth form of the function describing the energy spectra of the evaporated nucleons for the composite ^{181}W nucleus for several different initial excitation energies [17]. But, analysis [18] indicates that in the excitation energy near the threshold of the second gap of the Cooper pair of nucleons, the partial widths of the nucleon emission increase many times, compared with the partial widths in neighboring excitation energies of the residual nucleus. This tendency does not change (or shows just a moderate variation) when the energy of the incident protons in the (p, n) reaction is changed [18]. This can be explained only if the partial width of a nucleon emission is strongly dependent on the excitation energy of the residual nucleus and if the Strutinsky model for the level density [19] is used for the reproduction of the evaporate spectra. The set of parameters in the Strutinsky model approximation for the masses $40 \leq A \leq 200$ is derived from the level density obtained by $(n_{th}, 2\gamma)$ reaction. This means that, even for the different excitation energies of the produced nucleus ^{182}W, the product $\Gamma{\cdot}\rho$ preserves it's form. Moreover, in the case of (p, n) reactions the wave function of the excited levels of the target nucleus (neutron resonance) changes significantly through the decay when evaporated neutron appears.

Therefore, it is possible to obtain the correct form of the energy dependence of the $\Gamma \cdot \rho$ product and, accordingly, the cross-section, for fixed nucleus excitation energy and for different energies of charged particles beam, even if the calculated values of Γ and ρ

are not correct.

2.3. Principles of the proposed modified model of radiation strength functions

In the previous section we mentioned the effect on dependence of the partial width for a nucleon emission on the excitation energy of the residual nucleus. This effect opens a possibility for a modification of the standard form of the relation between the radiative strength function and the excited level density. The modified expression Eq. 1 describing the radiation strength of the gamma transitions between an arbitrary compound state λ and any low-lying level i, can be written in the following form [20]:

$$k_{modif} = k_{sandard}/D_i = (\Gamma_{\lambda i}/(E_\gamma^3 A^{3/2} D_\lambda))/D_i \qquad (2)$$

This modification takes into account the fact that the radiative strength function is dependent on the average spacing D_i between the low-lying levels i.

In practice, in order to maintain continuity with Eq. 1, the following modification is suitable:

$$k_{modif} = k_{sandard}\frac{D_{asim}}{D_i} = \frac{\Gamma_{\lambda i}}{E_\gamma^3 A^{3/2} D_\lambda}\frac{D_{asim}}{D_i} \qquad (3)$$

In Eq. 3 D_{asim} is the asymptotic spacing between the levels of a heated nucleus treated as a pure fermion system (defined, for example, by non-interacting Fermi gas model) and D_i is the maximum possible expected space between the intermediate levels for a given excitation energy. The specific value D_i is the outcome of the coexistence and the interaction of the quasiparticle and the phonon types of excitations in the nucleus. Considering that the degree of fragmentation of some nuclear states is minimal at it's initial energy and grows up with energy increase [21], it can be expected that $D_{asim} \leq D_i$ and $k_{modif} \geq k_{standard}$ for the highest number of gamma transitions.

3. Measurement of the two-step gamma cascade intensity of ^{28}Al

The ^{28}Al compound state gamma decay was measured in order to test the new modified model describing the dependence of the radiative strength function on the level density. The two-step gamma cascade method was used for this purpose.

It is commonly believed that the mechanism of neutron capture in light nuclei, for example, is significantly more dependent on the structure of the wave function of the excited level than in the neutron capture reaction in medium and heavy mass nuclei. Therefore, there is a modest practical interest for the average parameters of cascade gamma decay of neutron resonance in light nuclei. However, it can be important for the estimation of the reliability of the radiation strength functions for the gamma transitions between the levels of the heated nucleus obtained by the use of modified model Eqs. 2 and 3.

The spectroscopic analysis data were already published and all details can be found in reference [22]. In this paper we present just a short description of the measurement procedure and the analysis of the spectroscopic information.

3.1. Experimental set-up

The two-step cascades emitted after thermal neutrons capture in the ^{27}Al target were measured at the LWN-15 reactor in Rež, Czech Republic. Gamma-gamma coincidences were registered by two HPGe detectors with 28 % and 25 % relative efficiency, respectively, which have the standard energy resolution for this type of detectors. The time resolution was better than 10 ns. The optimal count rate for the gamma-gamma coincidence detection of the ordinary fast-slow coincidences scheme was $100 - 200\,\mathrm{s}^{-1}$. This count rate is a trade-off between two demands: to get the maximal possible values of the photopeak underlying background intensity ratios and to collect at least several tens of thousand events for the most intensive peaks. The required result can be achieved if the duration of the experiment is about several days at least and if the mass of the target ranges from hundreds of milligrams to several grams.

3.2.Spectroscopic information

The coincidence events were analyzed with the standard method [1, 2] based on the sum coincidence principle. Fig. 2 presents the most informative part of the measured spectrum.

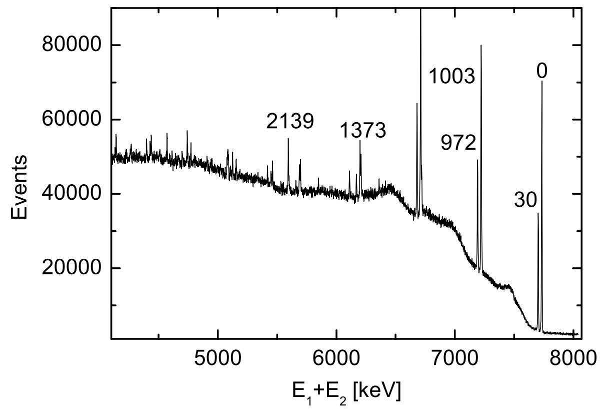

Figure 2: The main part of the sum coincidence spectrum of ^{28}Al. Full-energy peaks are labeled with the energy (in keV) of the final cascades levels.

Using the procedure described in [23], the intensity distributions of the cascades were obtained for some selected primary transition energy. For example, Fig. 3 shows the half of the measured intensity spectra of the cascades with energy of 7.725 MeV populating the ground state of the ^{28}Al nucleus (for $E_\gamma < 0.5B_n$). The other half is mirror symmetric [24]. The transition energy and the intesity of about 250 cascades were obtained using 13 collected spectra, similar to the one presented in Fig. 2. The positions and the area of the peaks in the spectrum are uniquely identified by the cascade parameters.

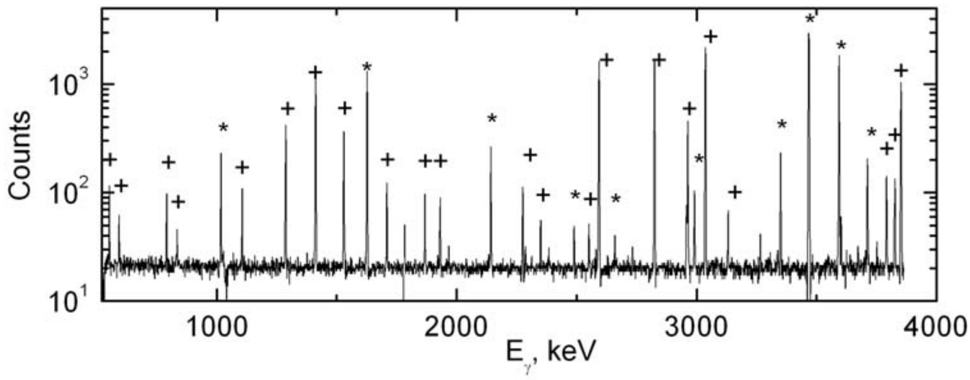

Figure 3: Half of the intensity distribution of the two-step cascades with energy 7.725 MeV populating the ground state. The primary transition of the ^{28}Al cascades are marked by crosses, whereas asterisks are the secondary one's. (The spectrum is shifted up to 20 counts due to the logarithmic scale.)

The order of the quanta in the cascades was determined by an algorithm [25]. This algorithm is based on a fact: the primary gamma transition has some energy in different two-step cascades and the second cascade photon energies have shifted on a difference for the final cascade level energies.

After the quanta sequence and the intermediate level energy were determined, almost all detected cascades were exactly placed into the decay scheme up to the energy of $\approx B_n - 520$ keV. This method of two-step gamma cascades gives the posibility to provide the most complete level scheme for an investigated nucleus. The total number of levels observed with this method in ^{28}Al is close to hundred; file of evaluated data [26] contains about 45 levels identified up to now. It should be emphasized that in the two-step cascade spectrum registered after the thermal neutron capture, the number of observed excited levels is always noticeably higher than the number of levels found in any other nuclear spectroscopy method.

In order to extract the values of the level density and of the radiative strength function by the analysis of the experimental data, it is required to transform the relative intensities of the resolved peaks into absolute values (in % per decay). This was done by normalization to the absolute intensities i_1 [27] of some primary transitions, multiplied by the branching ratios B_r of the corresponding secondary transitions. B_r was determined from the standard data treatment of the same measurement set of $\gamma - \gamma$ coincidence.

The dependence of the absolute intesity of the two-step gamma cascades on the energy of the primary gamma transition, was obtained as final spectroscopic result. This result is crucial for the determination of the level density and of the radiative strength function. Fig. 4 presents the absolute intensity of the two-step gamma cascades on the two first excited levels and the ground level [22]. The values of the level density and of the radiative strength function for ^{28}Al were obtained by the fitting procedure described in references [2, 20] and the spectroscopic results are presented on Fig. 4.

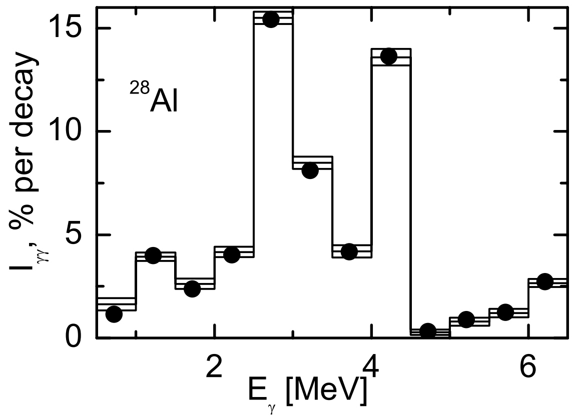

Figure 4: Histogram - distribution of the intensity of the two - step gamma cascades of the ^{28}Al to the ground, the first and the second excited level as functions of their primary transition energy. The approximated values $I_{\gamma\gamma}$ obtained by one of the variants defining the random radiative strength and the level density functions are noted by dots.

3.3.The levels density and the radiation strength functions of the ^{28}Al nucleus

The unambiguous determination of ρ and Γ from the measured spectra is impossible, even in principle, because the functional dependence of the two-step gamma cascade intensity on the level density and on the radiative strength function is nonlinear and degenerated:

$$I_{\gamma\gamma}(E_1) = \sum_{\lambda,f}\sum_{i}\frac{\Gamma_{\lambda i}}{\Gamma_\lambda}\frac{\Gamma_{if}}{\Gamma_i} = \sum_{\lambda,f}\frac{\Gamma_{\lambda i}}{\langle\Gamma_{\lambda i}\rangle\, m_{\lambda i}}n_{\lambda i}\frac{\Gamma_{if}}{\langle\Gamma_{if}\rangle\, m_{\mathrm{i}f}} \tag{4}$$

where $\Gamma_{\lambda i}$ and Γ_{if} are the partial radiative widths corresponding to the primary and to the secondary transition; $n_{\lambda i} = \rho_\lambda \Delta E_i$ is the number of the excited intermediate levels in a certain interval of the excitation energy ΔE_i; $\langle\Gamma_{\lambda i}\rangle$ and $\langle\Gamma_{if}\rangle$ are the average values of the corresponding intervals of the nucleus excitation energy widths; $m_{\lambda i}$ and m_{if} are the number of levels in the same intervals.

However, the form of the functional relation for the parameters appearing in Eq. 4 limits the region of their possible parameter values. For this reason N values of the experimental cascade intensities always can be converted in $\sim 2N$ values of ρ and Γ, satisfying the conditions:

$$\begin{aligned}\rho_1 \le \rho \le \rho_2\\ \Gamma_1 \le \Gamma \le \Gamma_2.\end{aligned} \tag{5}$$

With the use of an iterative technique it is possible to obtain a random function of the level density and of the radivative strength function which can reproduce, with high precision, the experimental values of $I_{\gamma\gamma}$. Hence the measurement of the two-step gamma cascades provides a good possibility to determine the most probable values for these parameters.

The approximated values of the measurement $I_{\gamma\gamma}$ (obtained by the iterative method based on Eq. 4) are presented by the dots in Fig. 4. These values correspond to any of the single random functions of the level density and of the radiative strength function. In Fig. 5 the thin lines represent the obtained random functions for the level density and by the dots are shown the average value of these random functions. The most probable region of the level density is presented on Fig. 6.

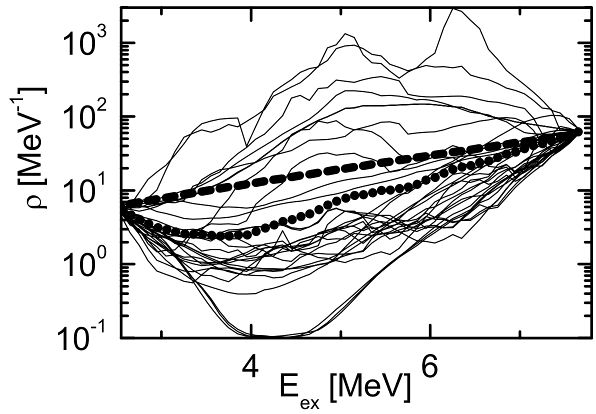

Figure 5: A set of random functions describing level densities able to reproduce data presented on Fig. 4 with a very close and small χ^2 values (thin lines). The average value of the entire set of random functions is presented by dots. Dashed line - model value for ρ [29].

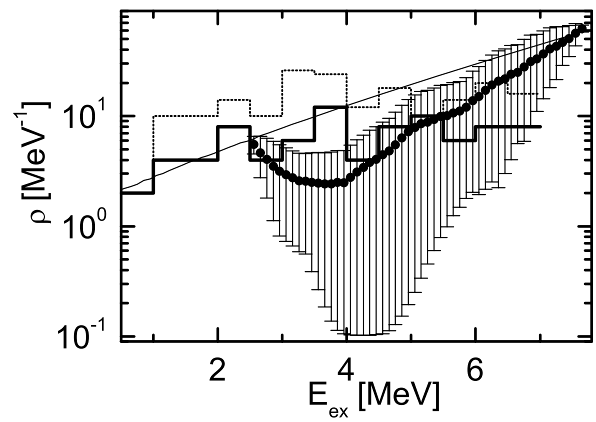

Figure 6: Thick line - model value for ρ [29]. Solid histogram presents density of the ^{28}Al levels from [26], dotted histogram - from processing spectra [22] similar to those shown in Fig. 1. Dots with error bars are the results of this study (same as in Fig. 5).

Two different forms of the radiative strength function dependence on the level density (Eq. 1 and 3) were used in the fitting procedure. In this way, the modified dependence in

Eq. 3 is tested in comparison with the standard one in Eq. 1 on the set of experimental data presented in Fig. 4. In Figs. 7 and 8 are presented the obtained random functions and the most probable region of the radiation strenght function when using Eq. 1. The same results are shown in Figs. 9 and 10, but here Eq. 3 was used. The difference between the obtained values of the radiative strength function, as presented in Figs. 8 and 10, provides the information about the influence of the collective enhancement for the level density on the radiative strength function.

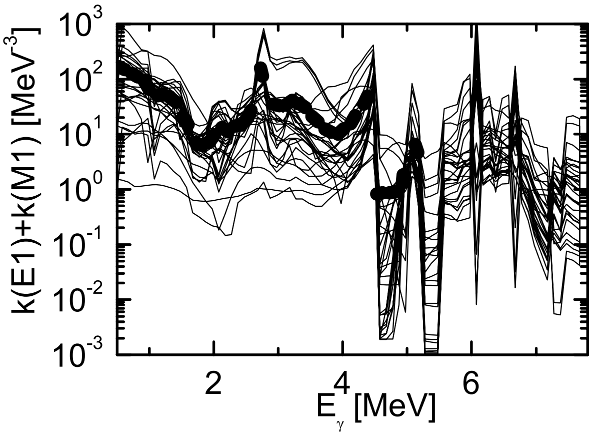

Figure 7: Thin lines - set of random functions (obtained by interative process)describing the radiation strength function in standard definition Eq. 1 able to reproduced data presented on Fig. 4. Dotted line - average for sum of strength function E1- and M1- transition.

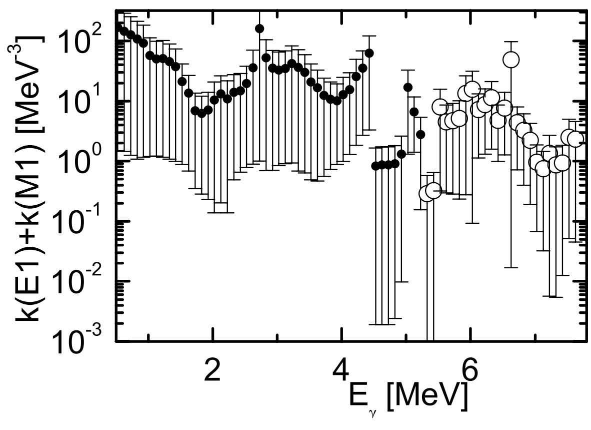

Figure 8: Values for the radiation strenght function in standard definition Eq. 1. Dark dots - sum of M1- and E1-transition. Open dots - data only for M1-transition.

The values of the radiative strength functions for the $E1 + M1$ transition (dotted line) and the values for only the $M1$-transition are presented in Figs. 7 and 8. In the energy region above 3.465 MeV are present only M1- transitions. The positive parity of the ^{28}Al neutron resonances and of all the known low-lying levels define practically only $M1$ multipolarities of the primary transitions. Hence, the information on the $E1$ radiative strength functions for $E_\gamma > 4260$ keV cannot be obtained from the two-step cascade intensity.

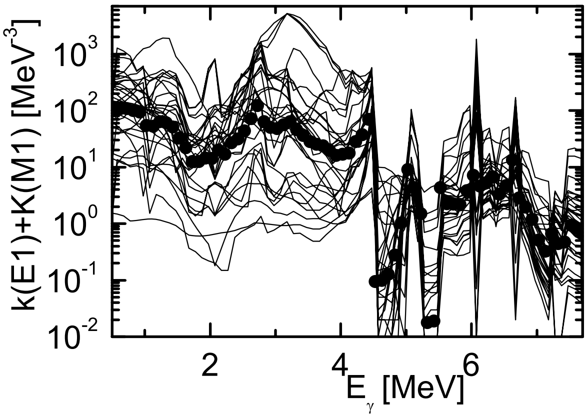

Figure 9: The same as in Fig. 7 for the modified model of the radiation strength function Eq. 3. Dotted line is average values.

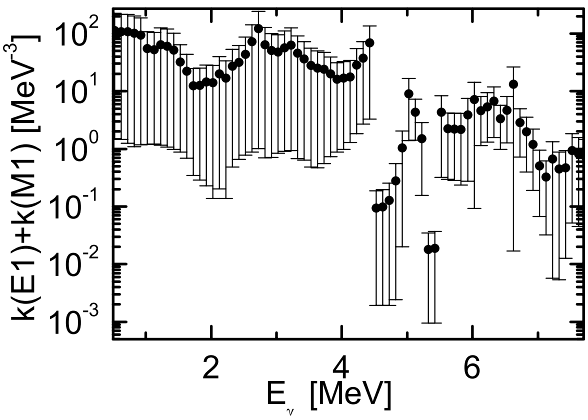

Figure 10: Average values of radation strenght function with error bars in case of modified model Eq. 3.

The thermal neutrons capture cross sections for this nucleus is determinated by the resonances with spins 2 and 3. The dominant dipole type of the primary gamma-transitions limits the spin window for the intermediate levels to the interval $1 \le J \le 4$. The level density in this spin interval, calculated from the schemes evaluated from file [26, 27] in Fig. 5 is compared with similar data obtained from the two-step cascades. The corresponding data, together with the density of the neutron resonances are always used for the normalization of the relative level density in both the one- and the two-step reactions. Unfortunately, the independent analysis [18] of the accuracy for the values D_λ showed that the possible systematical error may underestimate the density of the neutron resonances, even by one order of magnitude.

The influence of the mentioned error of the level density in all excitations can be accounted by a simple change of the normalization parameters for the set of random chosen functions describing the level density and the radiative strength. However, no data related to the real errors on the neutron resonances densities, identified in [28], are available in the literature until now.

4. Discussion

The unknown values of Γ and ρ correspond to each interval of the excitation energy for the intermediate levels (two-step cascades, in particular). In the general case, the inequality of the radiative strength functions for the primary and the secondary gamma transitions should be taken into account, even if they have the same energy and multipolarity. In principle, these circumstances make degenerated any system of nonlinear equations which connect the spectra intensity and unknown gamma-decay parameters. However, even in such case it can be defined a region Eq. 5 of the possible values for the level density and for the radiation strength functions. Authors of [2] showed that this can be done with acceptable precision if a sufficiently large set of values of the random functional dependencies for ρ and Γ on the energy gamma-transition are provided for excitation of nuclei. This is true in the frame of the postulate that the difference between the average of the random values and true unknown real value always tends always to minimum. Therefore, the value obtained in the two-step gamma cascads experiment [2] can be considered as a valid results, with the corresponding uncertainty of the level density and the radiation strength functions values.

The very significant difference of the ^{28}Al low-lying levels density in the region from $\rho \approx 4\,\mathrm{MeV}^{-1}$ up to $\rho \approx 20\,\mathrm{MeV}^{-1}$ (Fig. 5, solid and dotted histogram), can explain the skepticsm related to the contemporary experiment. This includes as well the occurrence of the possible methodical errors in the determination of the values of Γ and ρ. However, the hypothesis in Eq. 3 can be taken as a first approximation of the model description for the radiative strength functions in any heated nucleus. As a special case, this hypothesis includes the existing assumption that the radiative strength functions and the level density for any nucleus are independent from the structure of the excited levels. This possibility should be checked on a large set of experimental data.

The practical absence of the negative-parity levels below 3.3 MeV does not allow to obtain the strength function of the $E1$-transition in this interval for ^{28}Al excitation energies. It is also not possible to obtain a satisfactory approximation for the intensity distribution in the range of the primary cascade energies from $E_1 \approx 0.5$ MeV to $E_1 \approx 1$ MeV. The increase of the strength functions in this interval, which can be observed in Fig. 8 and 10, can be explained as a consequence of the absence of secondary cascade transitions enhancement in this interval of energies. The corresponding increase in the strength functions can be qualitatively explained only by the presence of the collective type of primary transitions in the region of B_n and the corresponding vibration enhancement of the level density. This might be possible if the breaking threshold of the next Cooper pair falls randomly in the region of nuclear excitation near B_n.

In Fig. 11, we show the potential effectiveness of the technique presented in this work. In Fig. 11a, the level density was determined by model [29], whereas in Fig. 11b the level density was obtained with the approximation similar to the one presented on Fig. 5 but assuming equality of ρ for the levels of positive and negative parity. The main result of this exercise is to show that an independent experiment, able to determine the level density, will make possible to obtain a precise information on the radiation strength function. In the same way an experiment designed to determine the radiative strength function can provide the values of the level density.

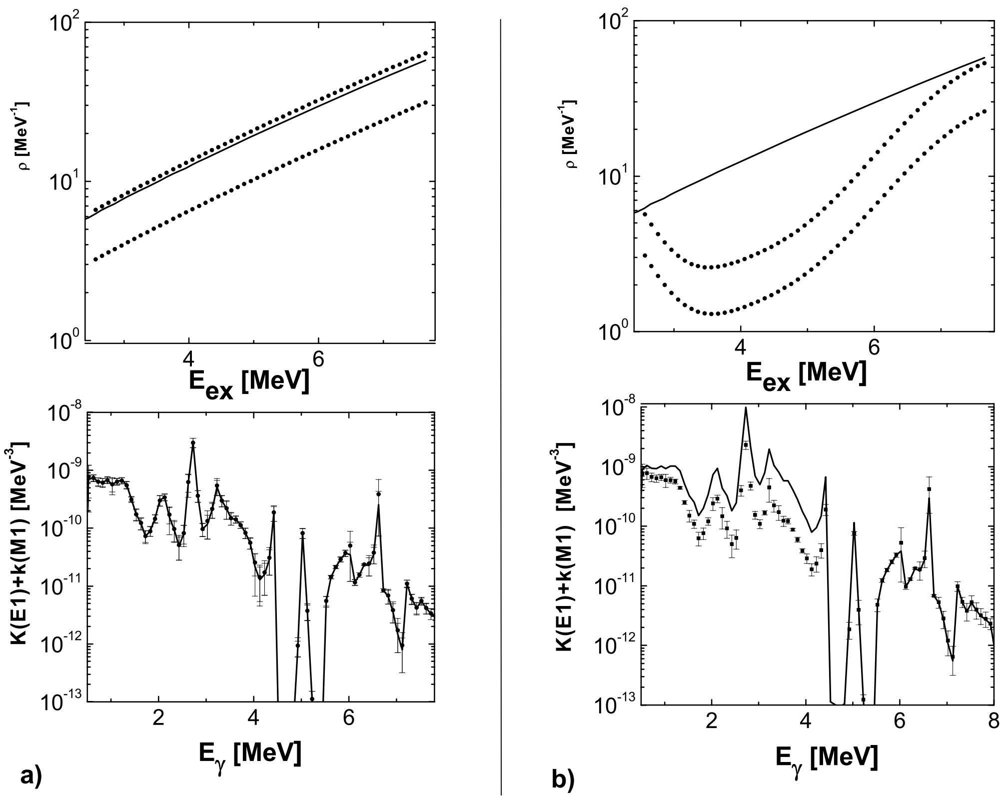

Figure 11: a) Top row: fixed to the level density of ^{28}Al (dots and line) from model [29]. Bottom row: the best approximation of the radiative strength functions for fixed level density. Points with error bars: standard presentation of the radiation strength function; line: strength function in the Eq. 3. b) Top row: level density from model [29] (line) and approximated level density (dots). Bottom row: points with error bars: standard presentation of the radiation strength function; line: strength function in the Eq. 3.

Searching the solution of a degenerate nonlinear systems of equations can always give as a result both the real function and a local maximum likelihood function. Methods good enough to identify and solve such systems have already been developed. The data in Fig. 4, presenting the worst version for the fitting process of the experimental data at $I_{\gamma\gamma}$, has been used to determine Γ and ρ. Hence, the number of iterations required to achieve a minimum disagreement between the experimental and the approximation values for the cascade gamma decay of the neutron resonances on ^{27}Al nucleus usually exceeds 10^5 for each variant of the calculation. Here, as in many other cases, it is convenient that the first iteration includes in source data specific values of the strength functions for the most intensive gamma-transition "spread" under appropriate intervals of the primary gamma-transition energy.

5. Conclusion

In this work we proposed Eqs. 2 and 3 as new hypothesis for the energy dependence form of the radiative strength function for the excited level density of the residual nuclei. This hypothesis was experimentally tested on the light nuclei ^{28}Al. The spectrum of the random functions for the level density as well as the radiative strength functions of the dipole $E1$- and $M1$-transitions were determined for ^{27}Al. The obtained functions can reproduce very precisely the intensity of the two-step cascade following the radiative capture of thermal neutrons for a given energy of primary transitions. The density of the intermediate levels corresponding to all the energetically resolved cascades observed (including those firstly established in reaction$(n_{th}, 2\gamma)$) can be reproduced correctly using the mean value of the obtained functions for the level density. In this work, for the first time, we obtained the information about the influence of the collective enhancement of the level density on the radiative strength function.

The results of the ^{28}Al two-step cascades experiment show that the hypothesis given by Eq. 2 can ensure the maximum precision for the description of the spectra and of the cross sections in a broad region of nuclear masses [20] (including light nuclei). Unfortunately, the determination of the density for the low-lying levels and the neutron resonances in a custom nucleus, with acceptable precision, still remains an unsolved problem. For this reason the dynamic model of the interaction of superfluid and normal states of nuclei, in the transition region from levels with a simple wave function to extremely complex compound-states, can not be identified and described correctly.

Further experiments are indispensable to accomplish this task. This can be done through the implementation of multi-step reactions. The most promising technique is the measurement of the intensity for a sequence of three or more cascade photons [30] in the radiation capture of nucleons and light nuclei reactions, as well as measuring the intensities of the cascades, containing nucleon products of nuclear reactions [9], in coincidences with photons.

The improvement of the process for the determination of the radiative strength function and the level density can be achieved also by the development of new models. These models should introduce the dependence of both the radiative strength function and the level density on the same fitting parameters. The first of all these parameters should be the threshold gap for the Couper pair and the mutually connected coefficients for vibration and collective enhancement of the levels density. This should be done for the radiative strength functions at decay of the levels with large enough components of the phonon type in the structure of their wave functions. For example, it can be expected that the models of this type will be able to easily reproduce the intensity of the cascades primary transition in the $\approx 0.5 - 1\,\mathrm{MeV}$ energy range (Fig. 2) for ^{28}Al, as well as, for large number of other nuclei. Under favorable conditions (a small number of parameters), it can be expected a rather uniquely determination of the radiative strength functions and of the level density even without fixing one of those parameters.

References

[1] S. T. Boneva, E. V. Vasileva, Yu. P. Popov, A. M. Sukhovoj and A. Khitrov, Sov. J. Part. Nucl. **22**, 232 (1991).

[2] S. T. Boneva, E. V. Vasileva, Yu. P. Popov, A. M. Sukhovoj and V.A. Khitrov, Sov. J. Part. Nucl. **22**, 698 (1991).

[3] H. Vonach, Phys. Rev. C **38**, 2052–2062 (1988).

[4] E. V. Vasilieva, A. M. Sukhovoj and V. A. Khitrov, Phys. At. Nucl. **64**, 153 (2001).

[5] A. M. Sukhovoj and V. A. Khitrov, Phys. Particl. and Nuclei **36**, 359 (2005).

[6] B. V. Zhuravlev, Bull. Rus. Acad. Sci. Phys. **63**, 123 (1999).

[7] G. A. Bartholomew, E. D. Earle, A. J. Ferguson, J. W. Knowles and M. A. Lone, Advances in nuclear physics **7**, 229 (1973).

[8] A. Schiller, L. Bergholt, M. Guttormsen, E. Melby, J. Rekstad and S. Siem, Nucl. Instrum. And Methods A **447**, 498 (2000).

[9] A.M. Sukhovoj and V. A. Khitrov, Nucl. Instrum. Phys. At. Nucl. **73**, 1635 (2010).

[10] A. M. Sukhovoj and V. A. Khitrov, In Proc. of the XVII International Seminar on Interaction of Neutrons with Nuclei, Dubna (2009).

[11] A. C. Larsen, M. Guttormsen, R. Chankova, F. Ingebretsen, T.Lonnroth, S. Messelt, J. Rekstad, A. Shiller, S. Siem, N. U .H. Syed and A. Voinov, Phys. Rev. C **76**, 044303 (2007).

[12] A. C. Larsen, M. Guttormsen, M. Krtcka, A. Betak, A. Burger, A. Gorgen, H. T. Nyhus, J. Rekstad, A. Schiller, S. Siem, H. K. Toft, G. M. Tveten, A. V. Voinov and K.Wikan, Phys. Rev. C **83**, 034315 (2011).

[13] A. M. Sukhovoj, V. A. Khitrov and W. I. Furman, Phys. At. Nucl. **72**, 1759 (2009).

[14] V. A. Khitro,v and Li Chol and A. M. Sukhovoj, Proceedings of the XII International Seminar on Interactions of Neutrons with Nuclei, Dubna, **E3-2004-9**, (2004).

[15] V. G. Soloviev, Sov. Phys. Part. Nuc. **3**, 390 (1972).

[16] A. M. Sukhovoj and V. A. Khitrov, Phys. Particl. and Nuclei **37**, 899 (2006).

[17] V. G. Pronyaev et al., Sov. J. Nuc. Phys. **30**, 310 (1979).

[18] A. M. Sukhovoj and V.A. Khitrov, Phys. At. Nucl. **73**, 1507 (2010).

[19] V. M. Strutinsky, Proceedings of the International Congress on Nuclear Physics, Paris, 617 (1958).

[20] N. Jovancevic, A. M. Sukhovoj, W. I. Furman and V. A. Khitrov, Proc. XX International Seminar on Interaction of Neutrons with Nuclei, Alushta (2012).

[21] L. A. Malov and V. G. Solovev, Yad. Phys. **26**, 729 (1977).

[22] J. Honzatko, V.A. Khitrov, A.M. Sukhovoj and I. Tomandl, Fizika B **12**, 299 (2003).

[23] S. T. Boneva, V. A. Khitrov and A. M. Sukhovoj, Nucl. Phys. A **12**, 199 (1995).

[24] A. M. Sukhovoj and V. A. Khitrov, Instrum. Exp. Tech. **27**, 1071 (1984).

[25] Yu. P. Popov et al., Bull. Acad. Sci. USSR Phys. Ser. **48**, 53 (1984).

[26] NNDC, *Evalueted Nuclear Structure Data File* (2013), URL **http://www.nndc.bnl.gov/nndc/ensdf**

[27] IAEA, *Evalueted Gamma-ray Activation File* (2013), URL **http://www-nds.iaea.org/pgaa/egaf.html**

[28] A. M. Sukhovoj and V.A. Khitrov, XVIII International Seminar on Interaction of Neutrons with Nuclei, Dubna (2011).

[29] W. Dilg, W. Schantl, H. Vonach and M. Uhl, Nucl. Phys. A **217**, 269 (1973).

[30] K. Furutaka, M. Oshima, A. Kimura, Y. Toh, M.Koizumi, T. Kin and J.Goto,In Proceedings of the International Conference on nuclear data for science and technology 2007, Nice, 517 (2007).

Available online at www.sciencedirect.com

ScienceDirect

Physics Procedia 59 (2014) 56 – 62

Physics Procedia

Gamma-2 Scientific Workshop on the Emission of Prompt Gamma Rays in Fission and Related Topics

Studies of the low-energy gamma background

K. Bikit, D. Mrđa*, I. Bikit, J. Slivka, M. Veskovic, D. Knezevic

Department of Physics, Faculty of Sciences, University of Novi Sad, Trg Dositeja Obradovica 4, 21 000 Novi Sad, Serbia

Abstract

The investigations of contribution to the low-energy part of background gamma spectrum (below 100 keV) and knowing detection efficiency for this region are important for both, a fundamental, as well as for applied research. In this work, the components contributing to the low-energy region of background gamma spectrum for shielded detector are analyzed, including the production and spectral distribution of muon-induced continuous low-energy radiation in the vicinity of high-purity germanium detector.

In addition, the detection efficiency for low energy gamma region is determined using the GEANT 4 simulation package. This technique offers excellent opportunity to predict the detection response in mentioned region. Unfortunately, the frequently weakly known dead layer thickness on the surface of the extended-range detector, as well as some processes which are not incorporated in simulation (e.g. charge collection from detector active volume) may limit the reliability of simulation technique. Thus, the 14, 17, 21, 26, 33, 59.5 keV transitions in the calibrated ^{241}Am point source were used to check the simulated efficiencies.

Selection and peer-review under responsibility of Guest Editor: Mr. Stephan Oberstedt - stephan.oberstedt@ec.europa.eu

Keywords: background gamma spectrum; low-energy spectral region; Compton scattered events; X-ray fluorescence; cosmic-ray muons; Bremsstrahlung; nuclei recoils

* Corresponding author: Tel.: +381 21 485 2815.
Email-address: mrdjad@df.uns.ac.rs.

Selection and peer-review under responsibility of Guest Editor: Mr. Stephan Oberstedt - stephan.oberstedt@ec.europa.eu
doi:10.1016/j.phpro.2014.10.009

1. Introduction

Some of the examples in fundamental and applied research, where the exploration of background events in low-energy gamma region is necessary, are given below:

a) The predicted weakly-interacting massive particles (WIMPs), which are the best candidates for dark matter, should cause nuclei recoils in detector active volume of up to 100 keV (Sisti; 1999)
b) Weak low-energy nuclear transitions
c) Many radionuclides in environmental samples (^{238}U, ^{210}Pb) emit gamma rays with energies of several tens of keV, which are used for determination of their activity concentrations

In order to obtain quantitative results of measurements, the efficiency calibration of gamma detector should be performed. However, the determination of the low-energy efficiency of high-purity germanium (HPGe) detectors is the most difficult task in detector calibration.

2. The contributing components to the low-energy gamma background

The contribution of environmental radioactivity to the low-energy spectral part of gamma spectra can be significantly reduced by passive shielding of germanium detector with dense materials, such as lead. In Fig.1, the comparison between low-energy parts of gamma spectra (below 500 keV) for unshielded and lead-shielded HPGe detector (100% relative efficiency, 380 cm^3 of detector active volume) is presented (Mrđa et al., 2007).

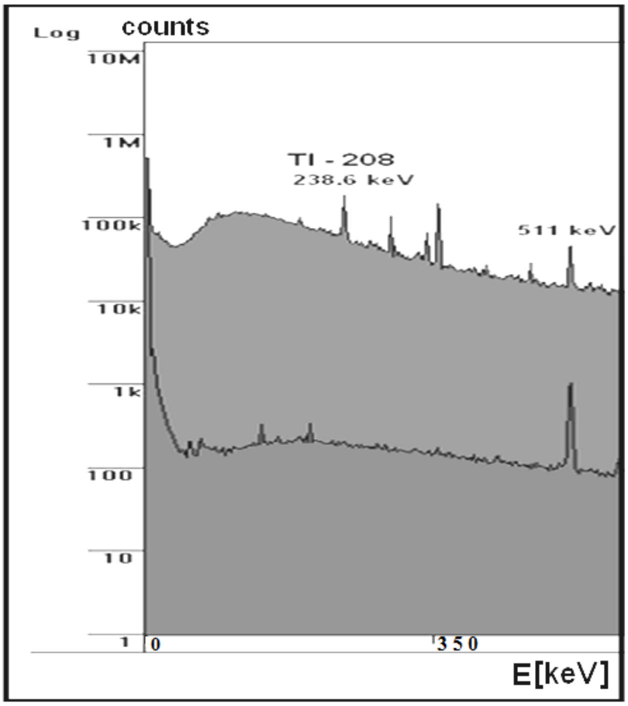

Fig. 1. The low-energy regions of unshielded (upper spectrum) and lead shielded HPGe detector (lower spectrum). The ratio of spectral intensities for the energy interval 20 keV-350 keV is about 380.

Several components contribute to the low-energy region of background gamma spectrum for the shielded detector:

- The Compton scattered events of high-energy gamma rays (^{40}K, ^{208}Tl)
- X-ray fluorescence from materials in detector vicinity (Bikit et al., 2009)
- Continuous radiation distribution induced by cosmic-ray muons in materials from detector surroundings (active shielding necessary for further background reduction)
- Bremsstrahlung from ^{210}Pb present in detector lead-shield
- Nuclei recoils in detector active volume due to elastic and inelastic neutron scattering

2.*1. The Compton scattered events*

The expected effects of Compton scattering of 2.6 MeV gamma rays emitted outside of lead shield, on detected gamma spectrum are presented in Fig. 2. In order to avoid all other contributions, which can be involved in real experimental conditions, this spectrum is obtained by GEANT4 simulation toolkit (Geant 4 Collaboration, 2012). As a result of Compton scattered high-energy gamma rays within lead shield and gamma detector, the approximately uniform distribution of deposited energies over wide energy interval is obtained, including the low-energy interval.

2.2. Pb X-ray fluorescence

The intensity of Kα and Kβ X-fluorescence rays from lead can be very strong if appropriate inner lining for lead shield is not applied. Very often the cadmium layer with 1 mm thickness is used as a lining material. However, since Cd has a relatively high cross section for thermal neutron capture, the corresponding gamma lines from ^{113}Cd (n,γ)^{114}Cd reaction may be present in background spectrum (558.4 keV, 805.9 keV).
The other possibility is to use tin and copper layers. In figure 3 the reduction of Pb X-rays by a 1 cm thick Cu layer is shown for an “extended range” HPGe detector.

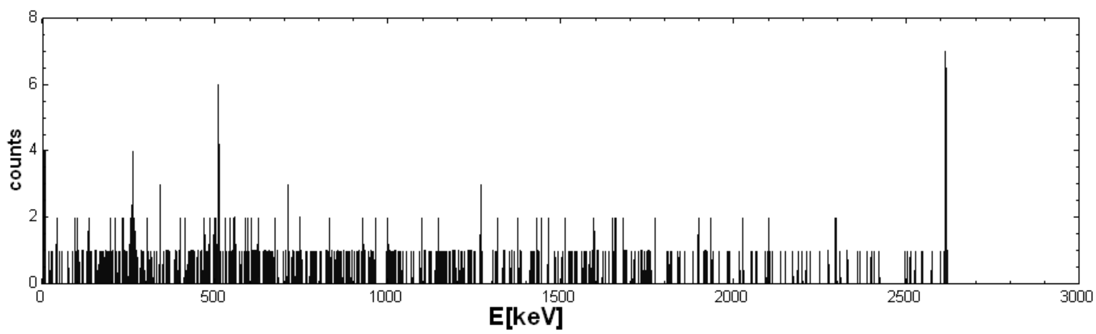

Fig. 2. The simulated gamma spectrum of events registered by the detector as a consequence of mono-energetic 2.6 MeV gamma rays emitted outside of a 10 cm thick lead shield.

2.3. Continuous radiation distribution induced by cosmic-ray muons

Although the presence of thick layers of materials in the vicinity of HPGe detector (such as thick copper layer) is efficient for Pb X-ray fluorescence reduction, this also causes the increase in intensity of low-energy continuous radiation, produced by cosmic ray muons. The coincidence measurements based on plastic scintillation detectors and germanium detector can be used for investigation of mentioned continuous spectral distribution arising from detector surrounding material, including determination of effective cross-sections for low-energy continuum production (Bikit et al., 2013).

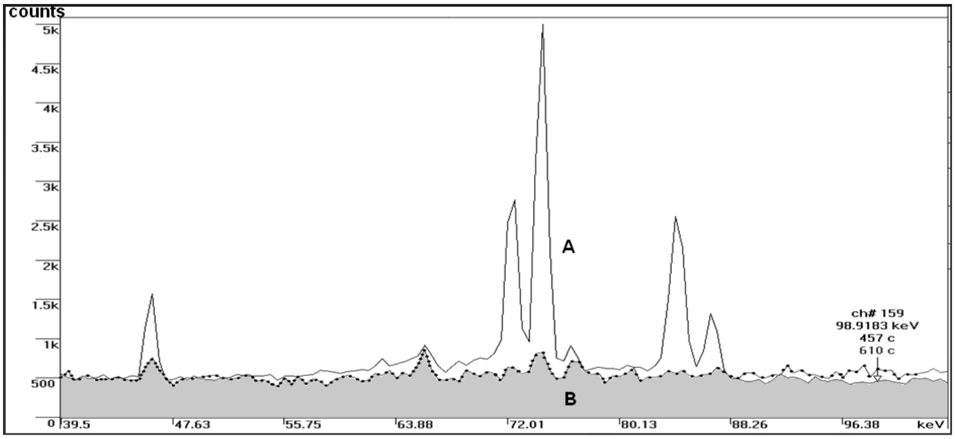

Fig. 3. The low energy regions of background gamma spectra (A- without inner lining of lead shield, B- with 1cm thick Cu lining)

2.4. Bremsstrahlung induced by ^{210}Pb in lead shield

The isotope ^{210}Pb emits only a weak (4.05%) low energy γ-ray at 46.5 keV, while its daughter ^{210}Bi is an almost pure β-emitter ($E_{\beta max}$ = 1.16 MeV). We used a semi-empirical method, for the estimation of bremsstrahlung intensity, induced by ^{210}Pb, in the background of the GMX type “ORTEC” HPGe spectrometer with nominal efficiency of 32%. The ^{210}Pb content in the lead shield is measured to be 25 ± 5 Bq/kg. In figure 4 the calculated bremsstrahlung distribution compared with the measured background spectrum is presented.

We found that the bremsstrahlung contribution to the spectral intensity in the region up to 500 keV is about 20% for our surface based detector (Mrđa D. et al. 2007).

2.5. Nuclei recoils in detector active volume

As an example of inelastic scattering of neutrons in germanium crystal, the 68.7 keV line from ^{73}Ge (n, n') ^{73}Ge is analysed by coincidence circuit of germanium detector and plastic scintillator. The changes in the intensity and shape of the 68.7 keV line for different selected intervals of the time spectrum were observed Thus, the fine broadening of the selected time interval toward faster events led to a more prominent tail of this line, due to the fact that faster neutrons (i.e., more energetic neutrons) cause larger recoils of germanium nuclei (Mrđa et al., 2013).

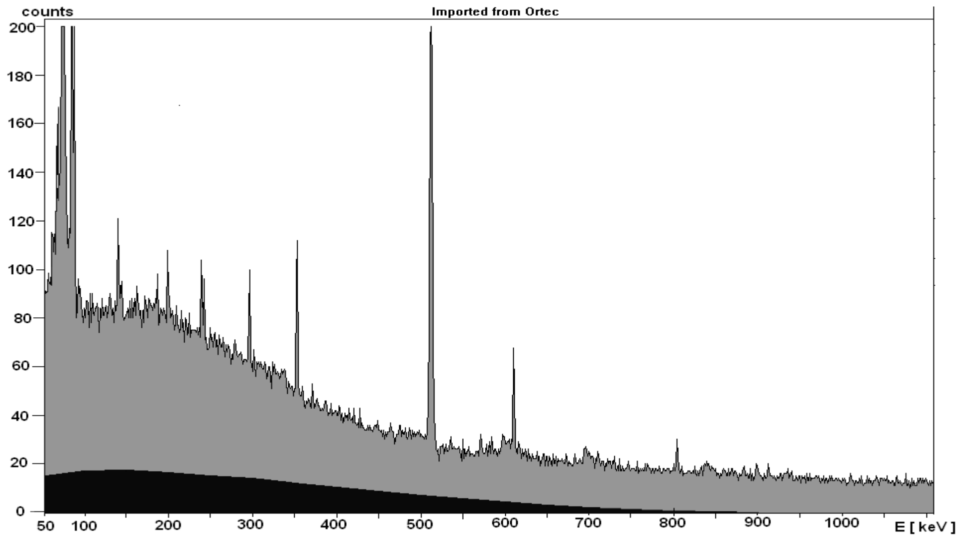

Fig. 4. The bremsstrahlung contribution (black area) to the measured background spectrum

3. Determination of detection efficiency for low-energy region

We compared the results of efficiency calibration (below 60 keV) for extended range HPGe detector, obtained by experimental approach (using ^{241}Am point source), with efficiencies determined by GEANT4 simulation software. The schematic view of experimental setup for determination of detection efficiency and the corresponding source-detector geometry from GEANT-4 simulation are given in Fig. 5.

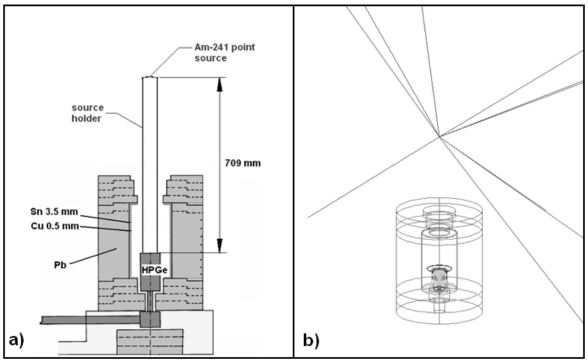

Fig. 5. The experimental setup (a) and source-detector geometry from GEANT-4 simulation (b), for determination of detection efficiency for low-energy region

The 13.9, 17.6, 21.0, 26.3, 59.5 keV transitions in the calibrated 432(15) kBq activity ^{241}Am point source were used to check the simulated efficiencies. The comparison of experimental data with GEANT4 results is presented in Fig. 6, while the relative differences between measured and simulated efficiency values are summarized in Tab. 1.

The possible origin of these differences can be caused by the fact that the manufacturer not exactly specified the layer thicknesses, necessary for simulating the detector. However, our efficiency simulations for other detectors (which are not of extended-range type), do not show such discrepances compared to experimental values.

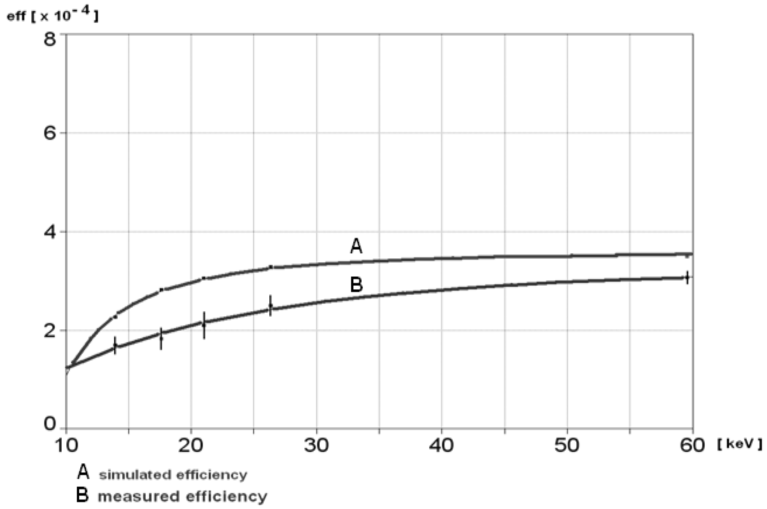

Fig. 6. Comparison of the detector efficiency obtained from experiment and using GEANT4 simulation software

Table 1. The relative differences between measured and simulated efficiencies for low-energy region

Energy [keV]	Relative differences
13.9	34
17.6	55
21.0	46
26.3	31
59.5	14

4. Concluding remarks

Many factors influence the low-energy background in gamma spectrometry and their contributions should be carefully analyzed for each specific situation (experiment). The reduction of low-energy spectral contribution can be achieved by selecting the proper surrounding materials for gamma detector, as well as by active shielding.

Monte-Carlo simulations in combination with measured results are the most effective approach for investigation of low-energy background components.
The determination of detection efficiency for low-energy region is a difficult task in case of various source types and source-detector geometries. Thus the significant discrepancies can be expected between measured and simulated results.

Acknowledgements

The authors acknowledge the financial support of the Ministry of Education, Science and Technological Development of Serbia, within the projects No.171002 and No.43002**.**

References

Bikit I., Mrđa D., Anicin I., Veskovic M., Slivka J., Krmar M., Todorovic N., Forkapic S., Nucl. Inst. and Meth. A606 (2009) 495
Bikit K., Mrđa D, Bikit I., Veskovic M., 2013. Investigation of cosmic-ray muon induced processes by MIREDO facility, ICRM 2013: 19th International Conference on Radionuclide Metrology and its Applications , Antwerp, Belgium , P-156
Geant4 Collaboration, 2012. Geant4 User's Guide for Application Developers, Version: geant4 9.6.0, http://geant4.web.cern.ch/geant4/UserDocumentation/UsersGuides/ForApplicationDeveloper/html/
Mrđa D., Bikit I., Veskovic M., Forkapic S., Todorovic N., Harissopulus S., J. of Res. in Phys. 31, No. 2 (2007) 157.
Mrđa D., Bikit I., Vesković M., Forkapić S., Nucl. Inst. and Meth. A572 (2007) 739.
Mrđa D. et al., Astropart. Phys. 42 (2013) 103-
Sisti M., 1999, CRESST - a Cryogenic Experiment for Dark Matter Search, Hieronymus, München, ISBN 3-89791-050-0, p.12

PRIRODNO-MATEMATIČKI FAKULTET
Univerzitet u Novom Sadu

FACULTY OF SCIENCES
University of Novi Sad

TRG DOSITEJA OBRADOVIĆA 3, 21000 NOVI SAD, SRBIJA (SERBIA)
tel +381.21.455.630 **fax** +381.21.455.662 **e-mail** dekanpmf@uns.ac.rs **web** www.pmf.uns.ac.rs
PIB 101635863 **MB** 08104620

Uverenje br.: 482/2019
Broj dosijea: 73d/12

Na osnovu čl. 29 st. 1 Zakona o opštem upravnom postupku ("Službeni glasnik RS" br. 18/2016) i po molbi Knežević (Radenko) Davida od 31.01.2019. godine izdaje se

U V E R E NJ E

kojim se potvrđuje da je Knežević (Radenko) David, rođen 03.06.1988. godine u mestu Knin, opština Knin, država Republika Hrvatska student koji se sam finansira. Upisan je na 3. godinu (5. put) doktorskih studija Prirodno-matematičkog fakulteta Univerziteta u Novom Sadu, na Departmanu za fiziku, na studijskom programu Doktorske studije - Fizika, školske 2018/2019. godine.

Knežević (Radenko) David upisan je prvi put školske 2012/2013. godine, na Departmanu za fiziku, na studijskom programu Doktorske studije - Fizika.

Uverenje se izdaje na lični zahtev imenovanog.

Stručnotehnički saradnik za studije i studentska pitanja

Novi Sad, 31.01.2019.

Katica Šoškić-Knežević

РЕПУБЛИКА СРБИЈА

УНИВЕРЗИТЕТ У НОВОМ САДУ
ПРИРОДНО-МАТЕМАТИЧКИ ФАКУЛТЕТ, НОВИ САД

Оснивач: Република Србија
Аутономна Покрајина Војводина

Дозволу за рад 106-022-00644/2009-01 од 22. 12. 2009. године је издала Аутономна Покрајина Војводина, Покрајински секретаријат за образовање

ДИПЛОМА

Давид (Раденко) Кнежевић

рођен 03. 06. 1988. године у Книну, општина Книн, Република Хрватска, уписан школске 2011/2012. године, а дана 30. 10. 2012. године завршио је мастер академске студије другог степена на студијском програму ФИЗИКА обима 124 (сто двадесет четири) бодова ЕСПБ са просечном оценом 9,93 (девет и 93/100).

На основу тога издаје се ова диплома о стеченом високом образовању и академском називу

МАСТЕР ФИЗИЧАР

Број дипломе: 866-М-508m/11, 24. 09. 2014. године
У Новом Саду

ДЕКАН
Проф. др Неда Мимица-Дукић

РЕКТОР
Проф. др Мирослав Весковић

UNS08MA02102

РЕПУБЛИКА СРБИЈА

УНИВЕРЗИТЕТ У НОВОМ САДУ
ПРИРОДНО-МАТЕМАТИЧКИ ФАКУЛТЕТ, НОВИ САД

Оснивач: Република Србија
Аутономна Покрајина Војводина

Дозволу за рад 106-022-00644/2009-01 од 23.12.2009. године је издала Аутономна Покрајина Војводина, Покрајински секретаријат за образовање.

ДИПЛОМА

Давид (Раденко) Кнежевић

рођен 03.06.1988. године у месту Книн, општина Книн, Република Хрватска, уписан школске 2007/08 године, а дана 21.09.2011. године завршио је Основне академске студије првог степена на студијском програму ФИЗИКА обима 183 (стоосамдесеттри) бодова ЕСПБ са просечном оценом 10,00 (десет и 00/100). На основу тога издаје се ова диплома о стеченом високом образовању и стручном називу:

ФИЗИЧАР

Број дипломе: 619-455/07, 25.05.2012. године
У Новом Саду

ДЕКАН
Проф. др Неда Мимица-Дукић

РЕКТОР
Проф. др Мирослав Вескови

UNS08BC00

Природно-математички факултет
Универзитет у Новом Саду

Трг Доситеја Обрадовића 3, 21000 Нови Сад, Србија
тел 021.455.630 факс 021.455.662 e-mail dekan@pmf.uns.ac.rs web www.pmf.uns.ac.rs
ПИБ 101635863 МБ 08104620

Број: 0603-5L
Датум: 09.01.2019.

ПОТВРДА

Којом се потврђује од стране Природно-математичког факултета у Новом Саду да је **КНЕЖЕВИЋ ДАВИД,** дана 01.11.2016. године пријавио тему докторске дисертације под насловом: **„Експериментално одређивање параметара нуклеарне структуре активационим техникама".**

Наставно-научно веће факултета прихватило је тему на 25. седници одржаној 23.02.2017. године. Сенат Универзитета у Новом Саду на 23. седници одржаној 23.03.2017. године дао је сагласност на предложену тему.

Израда докторске дисертације је у току.

Потврда се издаје на лични захтев именованог.

Самостални стручнотехнички сарадник за студије
и студентска питања – руководилац службе

Тамара Зорић, дипл.правник